THE INVESTIGATION, DEVELOPMENT AND CHARACTERISATION OF NOVEL ZIRCONIUM-BASED TANNING AGENTS

SUBMITTED IN FULFILMENT OF THE REQUIREMENTS FOR THE DEGREE OF

DOCTOR OF PHILOSOPHY

IN THE

DEPARTMENT OF CHEMISTRY
FACULTY OF SCIENCE
RHODES UNIVERSITY

BY

JEFFRY JAMES GUTHRIE-STRACHAN
OCTOBER 2005

TABLE OF CONTENTS

ACKNOWLEDGEMENTS

I would like to thank the following:

Rhodes University: Dr Gary Watkins, who embarked on this rollercoaster ride as my supervisor. Prof. Perry Kaye, Prof. Mike Brown, Dr Cheryl Sacht, and the rest of the staff in the Chemistry Department, who have been like family and helped, supported and educated me privately and professionally for a large proportion of my life. My laboratory colleagues in L5, Emmanuel Lamprecht and Gerardo Medina, who are the most intelligent and entertaining people I have ever met.

Mintek: for their financial support, and in particular, Dr Ernst Giesekke and Dr Bob Tate, for setting me on my current path.

UNISA: Prof. Sylvia Paul, for her uncomplicated assistance with Raman spectroscopy.

ISTT: Dr Clive Jackson-Moss, Karl Flowers and Leona Barnard, for the years of friendship and support.

My South African, Portuguese, Mexican, Swazi, and UK family and friends, and Russian and Frankfurter, who are part of the fabric of my life.

The University of Northampton: Prof Geoff Attenburrow, for his support.

Dr Edith Antunes: for her unwavering help, support and confidence in my abilities.

Most importantly, my wife, Paula. Without you I would not be where and who I am today. The world has opened up and for this I will be eternally grateful. This thesis is a testament to your love and support. Thank you.

ABSTRACT

Various oxygen- and nitrogen-donor ligands were investigated as potential zirconium masking agents in zirconium tanning. α-Hydroxycarboxylic acid ligands were identified as effective zirconium(IV) chelators in acidic aqueous solution. Glycolic acid, lactic acid, mandelic acid, 4-hydroxymandelic acid, 4-chloromandelic acid and 4-bromomandelic acid complexes were synthesised, isolated and characterised using a range of analytical techniques. Linear Free Energy Relationships were examined to optimise the stability of the zirconium complexes. Hammett σ plots and Yukawa-Tsuno modified σ plots of the mandelate ligand and zirconium complex series indicated that inductive effects dominate within the benzene ring, however, mesomeric effects are significant outside the ring.

Zirconium 4-hydroxymandelate complex solutions were identified as the most effective tanning agents and achieved shrinkage temperatures of 80 and 97ºC for hide powder and goatskin, respectively. The zirconium and 4-hydroxymandelic acid interact synergistically to yield leather equivalent to combination tanned leather in one step. Tanning was performed similarly to vegetable tanning processes with a pickle pH of approximately 5 and fixation was achieved upon acidification. Pilot-scale tanning of goatskin produced white tanned leathers and crust leathers which were physically and aesthetically comparable to matched chromium tanned material.

LIST OF ABBREVIATIONS

ATR	attenuated total reflectance
BSLT	British School of Leather Technology
°C	degrees Celcius
cf.	compared
Conv.	conventional
DFT	Density Functional Theory
dik	β-diketonate
DSC	differential scanning calorimetry
EDTA	ethylenediaminetetraacetate
EDXA	energy dispersive X-ray analysis
e.g.	for example
ER	endoplasmic reticulum
et al.	and others
etc.	etcetera
FOSKOR	Phosphate Development Corporation
g	gram
Gly	glycine
HOMO	highest occupied molecular orbital
Hyp	hydroxyproline
ICP	inductively coupled plasma
i.p.	in-plane
IR	infrared
IRE	internal reflection element
K	Kelvin
kg	kilograms
kgf	kilogram force
kJ	kilojoules
kt	kilotons
lit.	literature
M	is an alkali, alkaline earth, divalent transition metal, or lanthanide cation, or the conjugate acid of a nitrogen base
m	meter
M	Molarity
M_{eff}	effective molecular mass
MO	molecular orbital
mol	moles
m.p.	melting point
MPa	megapascals
MS	mass spectroscopy

N	Newton
nm	nanometers (10^{-9} m)
NMR	nuclear magnetic resonance
o.o.p.	out-of-plane
PC	personal computer
pm	picometers (10^{-12} m)
PMC	Palabora Mining Company
ppt	precipitate
Pro	proline
RBM	Richards Bay Minerals
RH	relative humidity
RT	room temperature
SEM	scanning electron microscopy
syntan	synthetic tanning agent
T_D	denaturation temperature
TG	thermogravimetry
T_m	melting temperature
T_s	shrinkage temperature
UCT	University of Cape Town
UPE	University of Port Elizabeth
viz.	namely
XRD	X-ray diffraction
XRPD	X-ray powder diffraction

LIST OF FIGURES

CHAPTER 1

CHAPTER 2

CHAPTER 3

LIST OF TABLES

CHAPTER 1

CHAPTER 2

CHAPTER 3

CHAPTER 1:
INTRODUCTION

And the Lord God made clothes out of animal skins for Adam and his wife, **Genesis** 4:20

The use of hides and skins, tanned or untanned, as useful articles has been with us for thousands of years. The Oxford Dictionary refers to leather as "a material made from the hide or skin of an animal by tanning." Tanning, in simple terms, refers to the treatment of raw hides and skins with tanning substances to render the material immune to bacterial attack, *i.e.*, to produce leather.[1] Additional changes introduced in the process of tanning are secondary and are related to the tanning and retanning chemicals used.

There are hundreds of different leather types and tens of thousands of different chemicals to choose from when producing these leathers. The most important chemicals in the tanning process are the tanning agents as they define the process of leather manufacture as a whole. In this modern day and age, tanners will choose tanning chemicals based on price, convenience of use, environmental issues, and by matching the physical and aesthetic properties introduced by the tanning chemicals to the desired leather properties of the end product. A basic knowledge of (i) the general processes involved in leather production, (ii) the tanner's true raw material, *i.e.*, collagen, (iii) the pretanning, tanning and retanning chemicals used in the production of leather, and (iv) the mechanistic interaction of tanning chemicals, are all factors which are important in order to appreciate just part of the intricate process of leather manufacture.

1.1. THE TANNING PROCESS

Hides and skins are primarily composed of water, protein and fatty materials as indicated by **Figure 1.1**. The most important protein in the production of leather is collagen, which makes up approximately 29% of the mass of a freshly flayed hide.

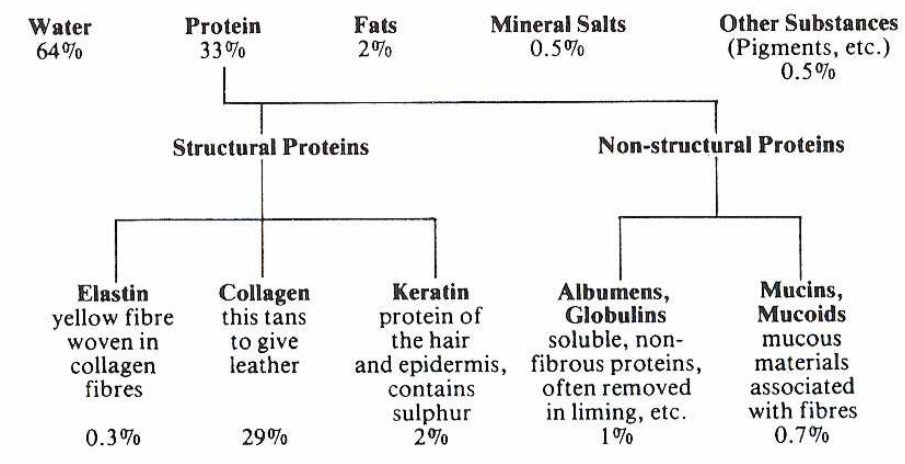

Figure 1.1: The approximate composition of a freshly flayed hide.[2]

The collagen desirable for tanning is found in the grain and reticular layers where it is "intimately woven" in a three-dimensional mesh that is thin and tightly woven in the grain and coarser and stronger in the reticular layer (**Figure 1.2**).[2]

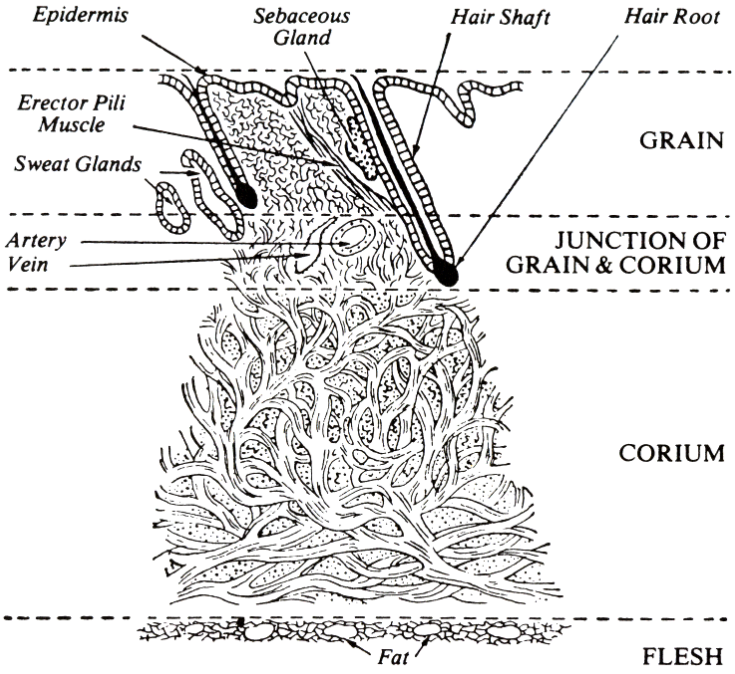

Figure 1.2: A general cross-section of a calf skin.[2]

After slaughter, hides and skins must be temporarily preserved for shipment and storage prior to tanning. The most common commercial method of preservation is to cure the hides and skins using salt to produce a dehydrated wet-salted or dry-salted material (**Table 1.1**).

Table 1.1: An approximate comparison of the composition of raw and cured hides.[2]

Raw Material	Composition	Parts by Weight	Hide Shrinkage
Green Hide	65% moisture 35% protein + fat	65 35 (100)	0%
Wet-Salted Hide	44% moisture 14% salt 42% protein + fat	37 12 35 (84)	16%
Dry-Salted Hide	15% moisture 22% salt 63% protein + fat	8 12 35 (55)	45%
Dried Hide	10% moisture 90% protein + fat	4 35 (39)	61%

The majority of leather (almost 90%) is tanned with chromium and is therefore commonly used as the basic format when trying to understand leather production.[3] **Figure 1.3** shows a basic flow diagram of the production of chromium tanned shoe upper leather. Other methods of tanning will have significantly different production flow diagrams, although if the material to be produced is without hair, wool or scales, the preparation and isolation of the collagen in the beamhouse processes[4] will remain largely similar. The diagram also indicates the use of drums as process vessels but paddles, pits and mixers are also common. Leather manufacture is usually divided into three or four zones but this may vary slightly according to processing and the perspective from which it is viewed. **Figure 1.3** is divided into Beamhouse, Tanyard, Dyehouse and Finishing.

1.1.1. PREPARATION OF THE RAW PELT FOR TANNING

Tanning primarily involves the reaction of tanning chemicals with collagen and as can be seen from **Figure 1.1** and **Table 1.1**, raw hides contain a number of undesirable components, which are commonly removed prior to tanning. Buljan[5] showed that approximately 75% of the mass purchased as raw material is removed as polluting solid

or liquid waste. Preparation of the raw pelt includes the processes from soaking to pickling.[6]

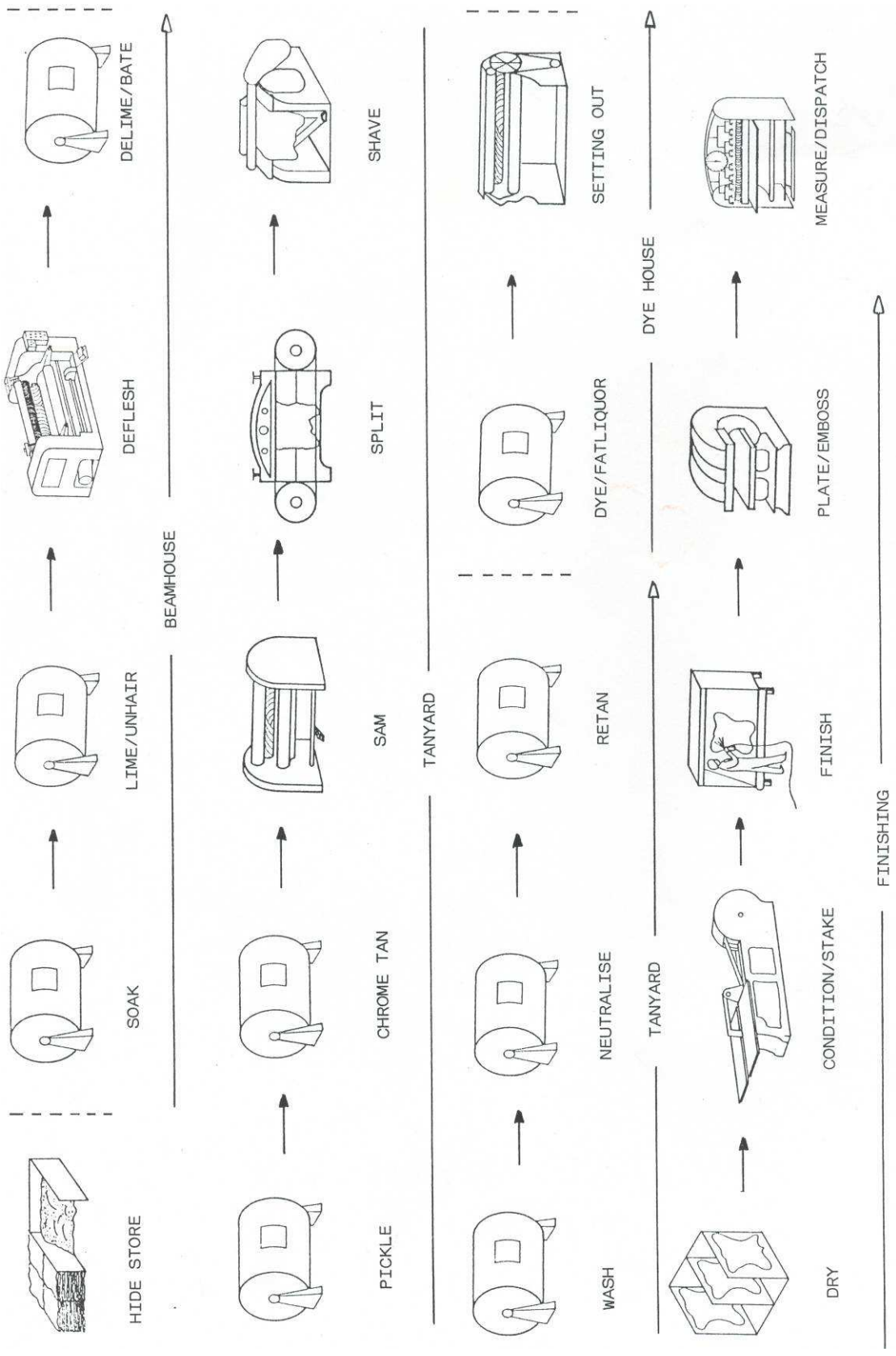

Figure 1.3: A basic flow diagram showing the production of chromium tanned shoe upper leather.[2]

1.1.1.1. Soaking

Soaking is usually the first process encountered in the tannery, as the previously dehydrated raw material must be carefully rehydrated before it can be subjected to extended mechanical action. Water is also the vehicle for both chemical penetration and removal, and is a necessary prerequisite for most of the processes to follow. Soaking also assists in the removal of curing agents, non-structural proteins and fats. The flesh layer (**Figure 1.2**) is removed mechanically to aid an even and full penetration of the chemicals to follow. Fleshing is commonly done after slaughter, after soaking, or after liming.[2]

1.1.1.2. Unhairing and Liming

The majority of leathers produced are treated in order to remove the hair or wool to leave the characteristic pattern of the grain surface (analogous to wood grain). Conventionally, the hides or skins are treated with sodium sulfide and hydrated lime to destroy the keratinous material of the epidermis and hair or wool. Fats are hydrolysed due to the increased pH and the skin structure swells as water is drawn into the fibre network to form a turgid, open-structured, translucent, jelly-like material.[7]

1.1.1.3. Deliming and Bating

Weak acids are used to lower the pH and to reduce swelling which causes the water to flush out many impurities with it. The skin becomes flaccid and is treated with proteolytic bating enzymes to clean the grain and make the pelt smooth and silky.[4]

1.1.1.4. Pickling

The bated pelts are finally treated with acid (commonly sulfuric and/or formic acid) to obtain the desired pH for optimal penetration of the tanning agent, and with salt, to suppress swelling when the acid is added. At this stage, the isolated collagen, termed the pickled pelt, is ready for a pretannage or main tannage.[2]

1.1.2. PRETANNING, TANNING AND RETANNING

This includes processes from pretanning and tanning through to retanning *via* samming, splitting, shaving and neutralisation as a preparation for the dyehouse.

1.1.2.1. Pretanning (See **Section 1.3**)

The pickled pelt may be lightly tanned prior to the main tannage to improve the penetration and distribution of the tanning chemicals to follow, to add specific properties into the leather or to stabilise it for mechanical operations such as shaving.[8]

1.1.2.2. Tanning (See **Section 1.3**)

The main tannage has the primary function of producing an utilisable material resistant to microbial attack. The most common chemicals used in tanning are chromium tanning salts, vegetable tannins and more recently, glutaraldehyde. After the tanning agent has penetrated the collagen structure and distributed satisfactorily, it must be irreversibly bound to the collagen (*e.g.*, a process called basification, in which the pH is raised, is used to bind chromium and glutaraldehyde tanning agents to the collagen).[9]

1.1.2.3. Mechanical Operations

At some point during production, the leather is split longitudinally to yield an upper grain split and a lower flesh split of desired thickness. In the production of chromium tanned leathers, this process is most commonly performed after basification and samming. The material is then shaved to give a more accurate and even thickness depending on the requirements for the end products, *e.g.*, shoe upper (1.8 mm ± 0.2 mm), garment (0.9 mm ± 0.2 mm) or upholstery leathers (1.1 mm ± 0.2 mm).[10]

1.1.2.4. Neutralisation

The mechanical operations generally squeeze water out of the leather, so prior to further treatment a wetting back and washing process is used to rehydrate the leather and to

remove dirt, shavings or grease that may have been picked up. The majority of the chemicals still to be added to the leather are anionic in nature, whereas the tanned collagen at low pH tends to be cationic in nature. Neutralisation is a process in which the pH is raised and chemicals are added to reduce the astringency of the leather to anionic chemicals such as retanning agents, dyes and fatliquors.[7]

1.1.2.5. Retanning (See **Section 1.3**)

The tanned leather is subjected to additional tannages with similar or new tanning materials.[1] These agents may be used to lighten the colour of the leather, to produce a feeling of fullness and to aid in the penetration of dyes, *etc*.[11]

The choice of pretanning, tanning and retanning chemicals is dependent on the properties desired in the final leather, and therefore, on the properties required in the final leather product.

1.1.3. DYEING, FATLIQUORING AND DRYING

This stage includes preparing the retanned material for finishing by processing through to dried crust.

1.1.3.1. Dyeing

Chromium tanned leather is blue in colour and must be dyed to obtain the desired colour. The dye acts as a base colour for finishing, and the depth of dye penetration and leather colour are of great importance.[4]

1.1.3.2. Fatliquoring

Chromium tanned material dries out hard and crusty and is unsuitable for most purposes.[2] Small quantities of oil, present as emulsions known as fatliquors, make a significant difference to the handle, *i.e.*, the fullness, softness and flexibility, among other factors.[12]

1.1.3.3. Drying

The retanning, dyeing and fatliquoring chemicals are allowed to penetrate and distribute within the collagen fibre structure before the pH is lowered and the astringency causes them to "fix" to the tanned material. The final binding of chemicals is encouraged by the drying process. Batches of leather are commonly toggle dried on frames in heated tunnels for four to six hours or are vacuum dried individually for two to ten minutes. Drying is usually followed by buffing, conditioning and staking or milling. The resultant crust material is resistant to microbial attack and contains all the leathering properties desired of leather and is ready for finishing.[10]

1.1.4. FINISHING

A finish process and finishing chemicals must be carefully designed and "married" with the production of the crust to ensure compatibility. The finish may be required to hide defects, to contribute to the leather beauty and properties and to provide fashion effects. Resins, pigments, dyes, handle modifiers, fillers, dullers and other chemicals are added in layers to the surface of the leather by spraying, roller-coating, curtain-coating or by hand. Heated hydraulic or roller presses are used to produce smooth or patterned leathers, depending on customer requirements.[10]

Finishing finally completes the leather manufacturing process and the area is then measured and the leather sent for dispatch to a product manufacturer to be turned into shoes, clothing or upholstery.[13]

1.2. COLLAGEN

Collagen is an insoluble fibrous protein which plays a major structural role in extracellular and connective tissues, and is the single most abundant protein in the animal kingdom.[14] The name, collagen, is derived from the Greek “kolla” (glue) and “genes” (born of), and describes its link to gelatine as gelatine was used as glue and is produced when collagen is boiled for extended periods of time.[15] There are at least twenty seven different types of collagen[16] which all contain three-stranded helical segments of similar

structure but all of which are unique, due to differing segments that interrupt the triple helix and fold it into a variety of three-dimensional structures.[14] Collagen types may be described by: (i) variations in the length of the triple helix, (ii) variations in the charge profile along the helix, (iii) interruptions in the integrity of the triple helix, (iv) variations in the size and shape of the terminal globular domains, (v) variations in the cleavage or retention of the latter in the supramacromolecular aggregate, and (vi) variations in post-translational modifications.[17]

Classified, according to the nature of the aggregate structure, collagens may be (i) fibrous, (ii) non-fibrous, (iii) filamentous, or (iv) fibril associated (**Table 1.2**). Other proteins may contain short sections of the collagen triple helix but are not classified as collagens due to their lack of the collagen-linked supramacromolecular structure and function.

The most abundant collagens are Types I, II and III, which fall within the classification typically associated with collagen, *i.e.*, the fibre forming collagens. Each fibre forming collagen molecule possesses a 300 nm triple helix in the quarter stagger arrangement with the N- and C-globular domains partially removed.[18] The structure and development of a typical collagen fibre may be exemplified by considering Type I collagen.

1.2.1. TYPE I COLLAGEN

Type I collagen is abundant in tendon-rich tissues which makes it easy to isolate and it was consequently the first collagen to be characterised. Type I collagen molecules are long (300 nm), thin (1.5 nm in diameter) and consist of three coiled subunits. Each subunit contains precisely 1050 amino acids with three amino acids per turn, further wound around each other in a characteristic right handed triple helix (**Figure 1.4**).

1.2.1.1. Structure of Type I Collagen

Many regions of the collagen subunits are composed of the repeating amino acid sequence Gly-Pro-X, where X can be a variety of amino acids, frequently hydroxyproline. Glycine (Gly), the smallest amino acid, occurs approximately every third residue in the collagen subunit to limit steric interactions within the crowded interior of the collagen triple helix.

Table 1.2: The types, composition, structural details and representative tissues of select collagens.[14,16,17]

Fibre Forming Collagens

Type	Molecule Composition	Structural Details	Representative Tissues
I	$[\alpha1(I)]_2[\alpha2(I)]$ $[\alpha1(I)]_3$	300 nm, large 67 nm banded fibrils	Skin, tendon, bone, dentin, muscles, aorta, placenta, nerves, liver fetal form in skin, other tissues
II	$[\alpha1(II)]_3$	300 nm, small 67 nm banded fibrils	Cartilage, spinal discs, vitreous humor
III	$[\alpha1(III)]_3$	300 nm, small 67 nm banded fibrils, frequently together with Type I collagen	Skin, muscle, blood vessels, placenta, lung, liver
V	$[\alpha1(V)]_3$ $[\alpha1(V)]_2[\alpha2(V)]$ $[\alpha1(V)][\alpha2(V)][\alpha3(V)]$	390 nm, N-terminal globular domain; frequently together with Type I collagen	Cell cultures, fetal tissues, liver, fetal membranes, skin, bones, placenta, most intestinal tissues, tendon, muscle, lung, kidney, cornea
XI	$[\alpha1(XI)][\alpha2(XI)][\alpha3(XI)]$	300 nm, small fibres; frequently together with Type II collagen	Cartilage

Non Fibrous Collagens

Type	Molecule Composition	Structural Details	Representative Tissues
IV	$[\alpha1(IV)]_2[\alpha2(IV)]$ other forms	400 nm, two dimensional crosslinked network	All basal laminas, lens capsule, kidney glomeruli, capillaries
VII	$[\alpha1(VII)]_3$	450 nm, dimeric; globular domains at each end	Epithelia (anchors skin basal lamina to underlying stroma), placenta, cervix
VIII	Not Known	Regular triangular lattice	Endothelial cells; Descement's membrane (separating corneal epithelial cells from the stroma)
X	$[\alpha1(X)]_3$	150 nm, C-terminal globular domain	Growth plate (mineralising cartilage forming bone)

Filamentous Collagens

Type	Molecule Composition	Structural Details	Representative Tissues
VI	$[\alpha1(VI)][\alpha2(VI)][\alpha3(VI)]$	150 nm, N- and C-terminal globular domains; microfibrils banded every 100 nm; associated with Type I collagen	Most interstitial tissues, skin, tendon, cartilage, muscles

Fibril Associated Collagens

Type	Molecule Composition	Structural Details	Representative Tissues
IX	$[\alpha1(IX)][\alpha2(IX)][\alpha3(IX)]$	200 nm, N-terminal globular domain; bound glycosaminoglycan; associated with Type II collagen	Cartilage, vitreous humour
XII	$[\alpha1(VII)]_3$	Large N-terminal domain; cross-shaped molecule; interacts with Type I collagen	Embryonic tendon and skin, bone

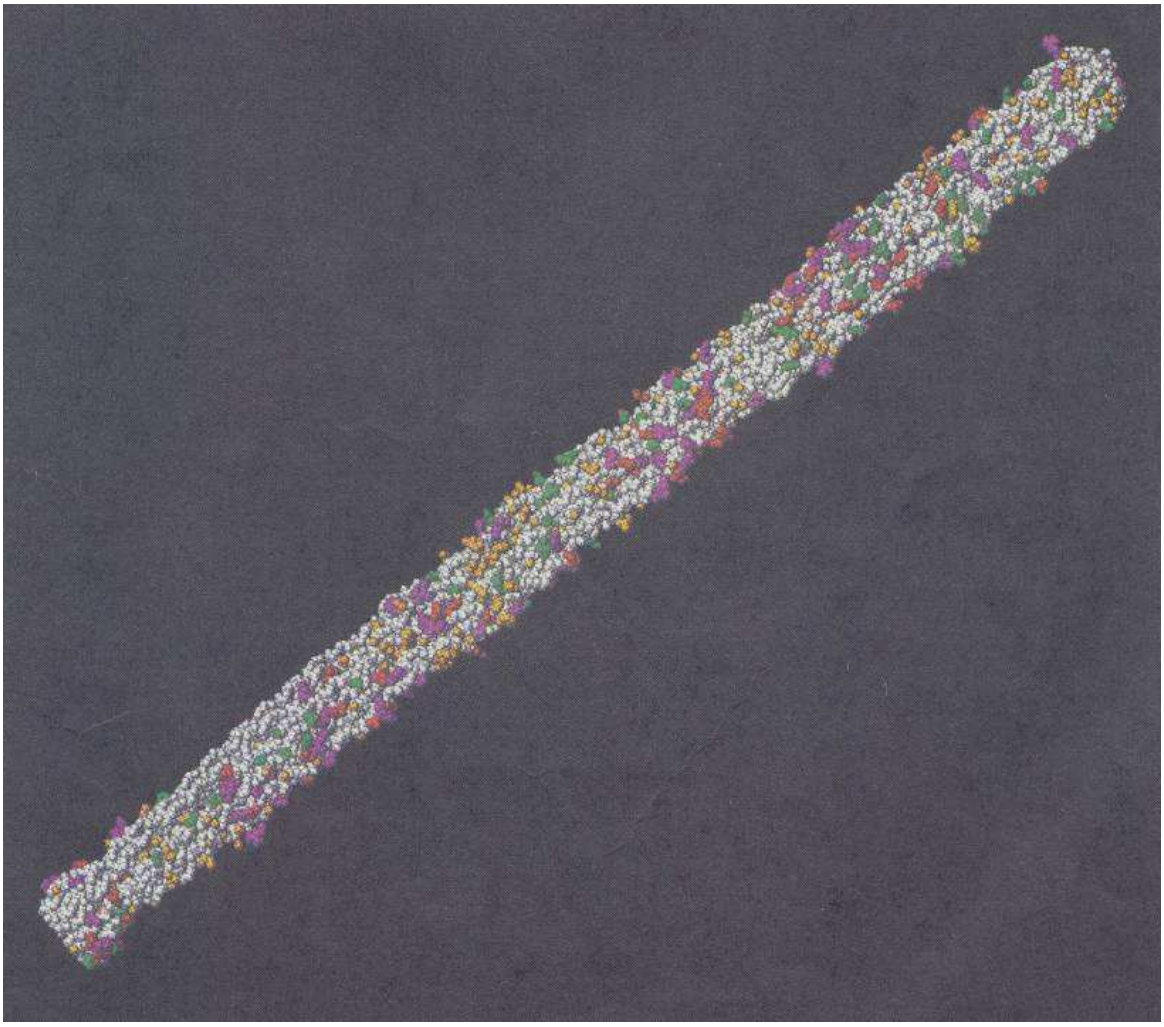

Figure 1.4: A representation of the collagen triple helix in a Smith microfibril [19]. The helix is represented by 5[3(Gly-Pro-Hyp)**105**].

Figure 1.5 shows the α-carbon atom of the glycine residue (labelled G) and how the chains are able to approach one another closely due to the small H-atom side chain. The closeness of the strands to one another allows the formation of many strong hydrogen bonds (represented by ···) which link the peptide NH of a glycine residue with a peptide carbonyl, C=O, in an adjacent polypeptide, and hold the three chains together. The direction of the hydrogen bond is transverse to the long axis of the collagen rod. Note the pyrrolidine rings of the proline residues are also found almost every third residue of each subunit facing outwards. Interestingly, although the rigid, fixed angle of the C-N peptidyl-proline bond disrupts the packing of amino acids in an α-helix, they stabilise the rigid three-stranded collagen helix.[20] Few other proteins show the amino acid sequence regularity of collagen or the presence of hydroxyproline and hydroxylysine (**Table 1.3**).

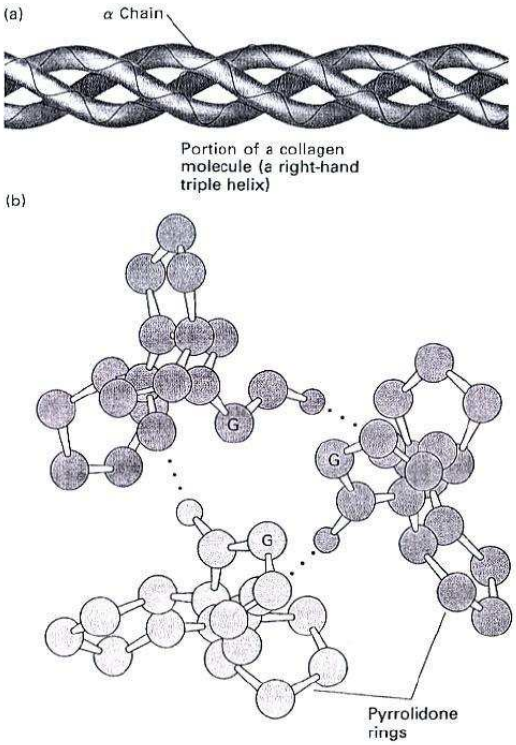

Figure 1.5: A cross-section of a model of collagen showing glycine residues.[15]

Table 1.3: Amino acid composition of bovine tendon collagen.[21]

Amino Acid	Amino Acid Composition (%)	Amino Acid	Amino Acid Composition (%)
Glycine	32.7	Valine	1.8
Proline	22.1[a]	Threonine	1.6
Alanine	12.0	Phenylalanine	1.2
Glutamic Acid and Glutamine	7.7	Isoleucine	0.9
Arginine	5.0	Methionine	0.7
Aspartic Acid and Asparagine	4.5	Tyrosine	0.4
Lysine	3.7[b]	Histidine	0.3
Serine	3.4	Tryptophan	0
Leucine	2.1	Cysteine	0

[a] about 39% of this is hydroxyproline
[b] about 14% of this is hydroxylysine

Proline residues are hydroxylated by prolyl hydroxylase at the C-4 carbon if situated on the amino side of a glycine residue. Hydroxylation sometimes occurs at the C-3 carbon of proline but only if the proline is situated on the carboxyl side of glycine residues. This hydroxylation does not occur on the free amino acid but rather on relatively large polypeptide strands before they become helical. Lysine may also be hydroxylated at C-5

by the action of lysyl hydroxylase.[15] Lysine residues modified in this manner are always found on the amino side of glycine residues.

The importance of hydroxylated collagen is emphasised by the disease scurvy. Scurvy is caused by the dietary deficiency of ascorbic acid (vitamin C), which is necessary as the reducing agent in maintaining the active form of the hydroxylating enzymes. Collagen synthesised in the absence of ascorbic acid is abnormal and cannot form fibres properly, causing the skin lesions and blood vessel weakness inherent with scurvy.

1.2.1.2. Synthesis of Type I Collagen Fibres

Collagen subunits are synthesised as longer precursors called procollagens and are transported into the lumen of the rough endoplasmic reticulum (ER) of fibroblasts where the chains are modified and assembled into triple helices (**Figure 1.6**). All three subunits in immature Type I collagen contain 150 more amino acids at the N-terminus and 250 more at the C-terminus than are present in mature Type I collagen. These propeptides constitute the globular domains mentioned in **Table 1.2** and may vary dramatically between different collagen types.

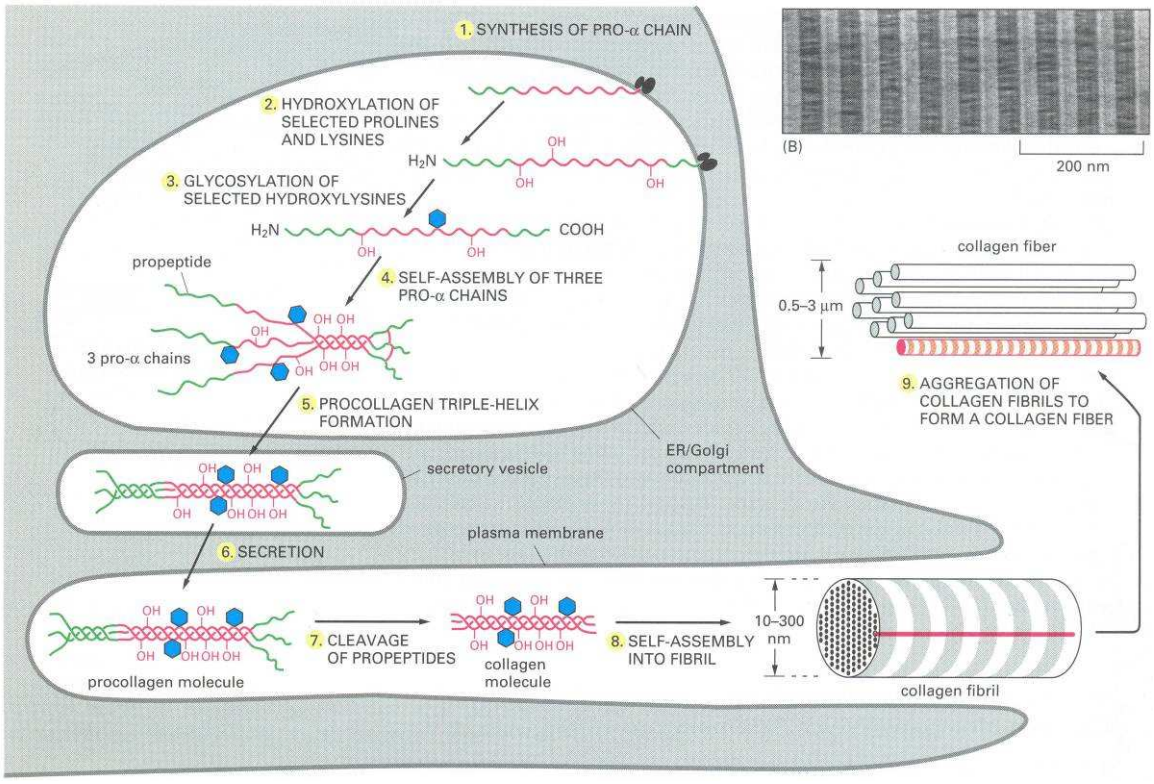

Figure 1.6: A diagrammatic representation of the synthesis of collagen fibres.[14]

In Type I collagen, both the propeptides contain intrachain disulfide bonds and, in addition, the C-terminal propeptides contain five interchain disulfide bonds connecting all three procollagen chains. The interchain disulfide bonds are important in producing in-register alignment of the three chains prior to the formation of the triple helix. It is believed that the interchain disulfide bonds form first followed by the "zipping" together of the three chains in the C→N direction to form the triple helix. The hydroxylated proline is thought to be instrumental in the twisting of the chains into the triple helix at physiological conditions.[16] Glycosylation of procollagen occurs in the rough ER where glucose and galactose residues are added to hydroxylysine residues, and long oligosaccharides are added to certain asparagine residues in the propeptides.

Type I procollagen molecules are thought to undergo proteolytic cleavage by extracellular procollagen peptidases during or following exocytosis to remove the N- and C-terminal propeptide chains forming tropocollagen.[14] This is supported by the fact that Type I collagen does not contain cysteine (**Table 1.3**), the amino acid involved in inter- and intrachain disulfide bonds (although disulfide bonds may be present in other collagens). Microfibrils consist of five strands of collagen molecules displaced against each other which pack together to form Type I collagen fibrils (typically 50 nm in diameter) according to the "Smith" microfibral model.[20] The fibrils aggregate together side by side in parallel bundles to form collagen fibres (**Figure 1.7**).[16]

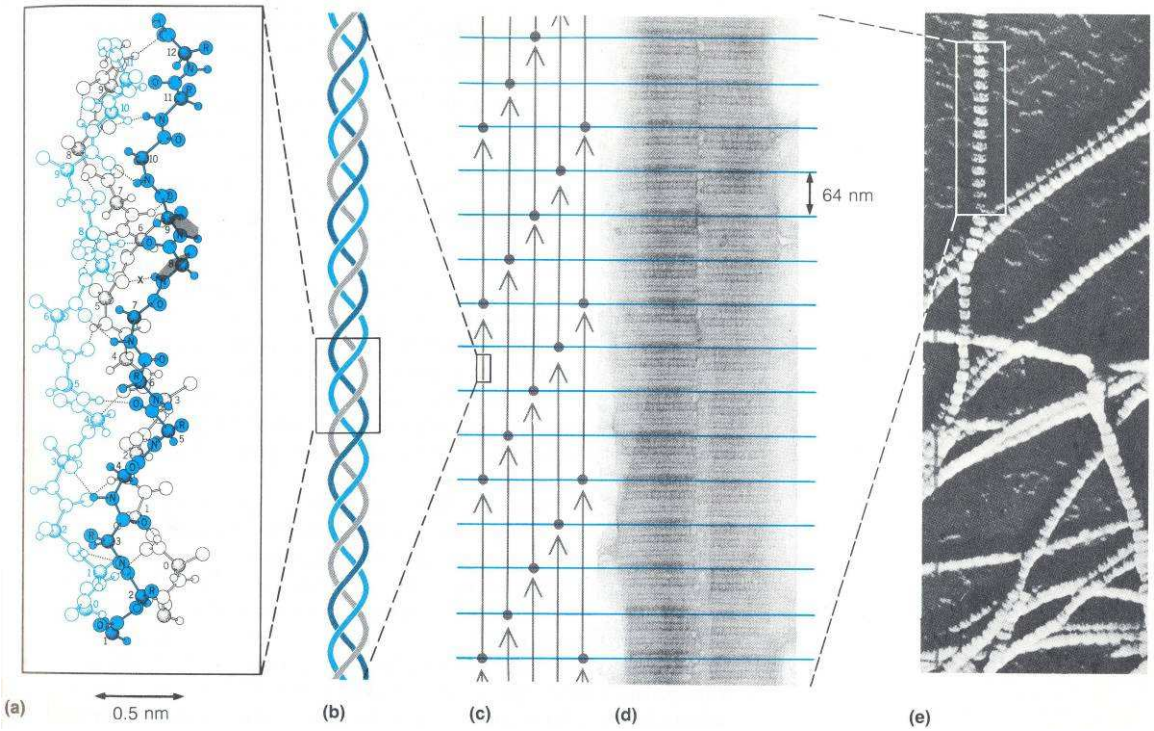

Figure 1.7: A diagrammatic representation showing the quarter stagger arrangement (c and d) of collagen microfibrils.[16]

These Type I collagen fibrils form by the spontaneous aggregation of tropocollagen (300 nm triple helix rods, staggered by about 64 nm) followed by covalent crosslinks between two chains to stabilise the staggered array and contribute to fibril strength. The presence of collagen in tissues such as skin, tendon, bone, cartilage, *etc*., may be ascribed to its high tensile strength fibres with a load of at least 10 kg required to break a Type I collagen fibre 1 mm in diameter,[15] and is gram for gram stronger than steel.[14] In embryonic and immature animals Type I collagen, consisting of three α1(I) chains, has few covalent crosslinks and the fibrils are less rigid. The $[\alpha 1(I)]_3$ is more sensitive to degradation by tissue proteases than is the more mature $[\alpha 1(I)]_2[\alpha 2(I)]$ collagen, essential for the remodelling of bones and tendons as animals grow. The crosslinking process continues throughout life and encourages the loss of elasticity in bones, tendons and skin. Wrinkles and brittle bones and tendons are some of the signs of old age associated with this simple crosslinking process (See **Section 1.2.2**).[21]

1.2.2. NATURAL CROSSLINKING OF COLLAGEN

Nonpolar and salt-bridge interactions are believed to control the side by side aggregation of tropocollagen molecules in collagen fibrils.[22] Once assembled, intra- and intermolecular covalent crosslinking occurs almost immediately (**Figure 1.8**). The bonds formed appear to be unique to collagen and to elastin.

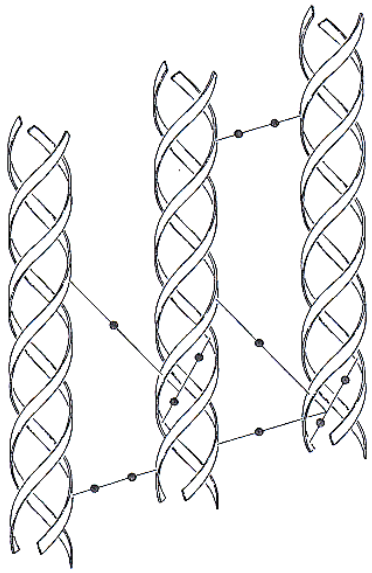

Figure 1.8: Intramolecular and intermolecular crosslinks in collagen.[15]

The characteristic Gly-Pro-X sequence of collagen results in the equally characteristic triple helix but there may be sections that lack this sequence. Even in Type I collagen, globular polypeptide sequences called telopeptides occur at the N- and C-terminals, *viz.*,

sixteen and twenty five amino acids respectively in the α1(I) chain. Lysine residues, commonly found as the fifth[15] or ninth[16] amino acid from the N-terminus and the seventeenth amino acid from the C-terminus in the telopeptides, are instrumental in intra- and intermolecular crosslinks of the α1(I) chain. The flexibility of the telopeptide portion may facilitate the formation of the crosslink.

Figure 1.9 (a) shows the oxidation, by lysyl oxidase, of the lysine side chain amino group to an aldehyde residue called allysine. Lysine residues may react with an allysine to form a Schiff base, or imine. The imine products are susceptible to hydrolysis but stabilise with age as they are reduced, as shown in **Figure 1.9 (b)**.[16] It was initially believed that two allysine aldehydes underwent an aldol condensation reaction to form an aldol crosslink[15] which has previously been detected (**Figure 1.9 (c)**), but the conditions required are not practical and this more likely forms *via* another pathway. Further crosslinking may occur as histidine residues may react with the Schiff base. In addition, some collagens, *e.g.*, Type III and IV have disulfide cystine bridges as crosslinks.[16]

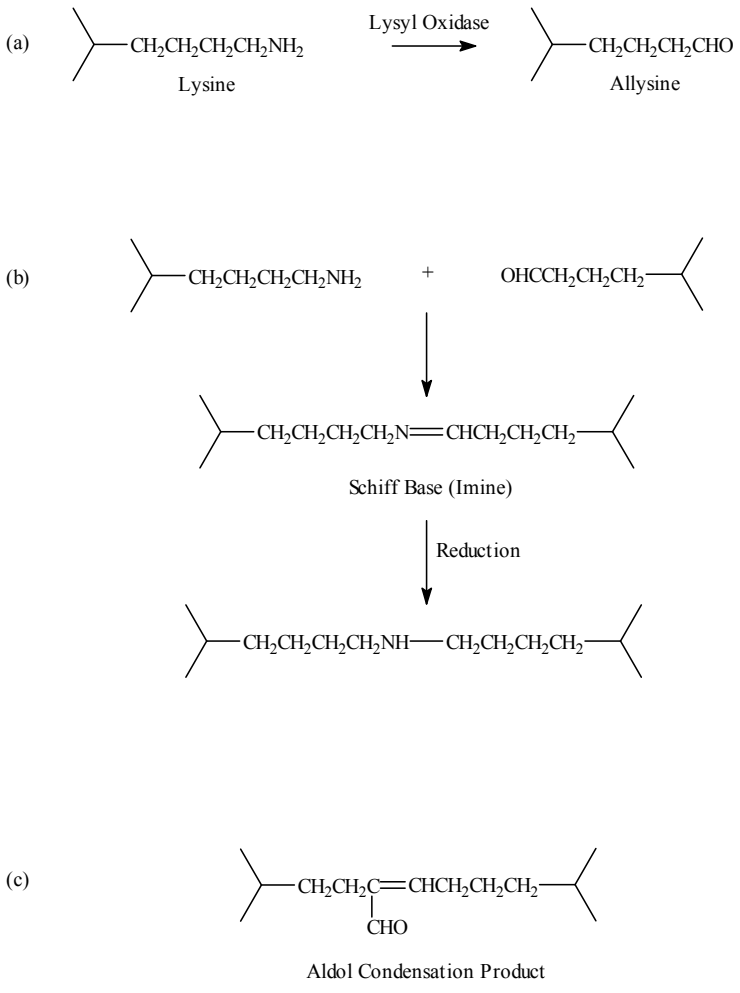

Figure 1.9: Proposed synthetic pathways of natural crosslinks in Type I collagen.[16]

Reconstituted collagen, as a biomaterial in the tissue engineering field, requires crosslinking to restore the high tensile strength and proteolytic resistance of naturally crosslinked collagen. When reconstituted collagen is used as films, fibres or sponges, the rate of degradation may also need to be customised and recognised chemical crosslinkers employed are diisocyanates, polyepoxides, azides, carbodiimides or aldehydic in nature.[23, 24] A great deal of current research targets the identification of new crosslinking agents which are not considered toxic.

1.2.3. COLLAGEN WATER

Collagen, like many other proteins loses its flexibility upon drying. If dehydration proceeds below a threshold value it may result in irreversible conformation "breakdown"[25] and the flexibility cannot be fully recovered by rehydration. The dead-dried collagen tends to be brittle, hard callousy and unpleasant to the touch and the properties are no longer those of the hydrated or native state. Extreme dehydration causes the denaturation of collagen by destroying the local conformation although it results in an increase in the number of intra-molecular hydrogen bonds.[26]

Water in collagen behaves as a plasticiser and in leather processing it is employed as a medium and reaction partner. Collagen has five degrees of hydration according to Bienkiewicz[25] which are summarised in **Table 1.4**. The boundaries are not likely to be definitive but reflect the retention lifetime of water as bound or unbound.

Hydroxylated lysine and proline residues act as cluster centres for the bonded and "crosslinking" water molecules and these are therefore central to the stability of collagen as a whole. There are more than 600 hydrogen bonds per 1000 amino acid residues in one collagen molecule, and water molecules play a significant role in the formation of many of them. For stereochemical reasons, two or more water molecules are involved in an hydrogen bond bridge. Kopp *et. al.*[27] determined that covalent crosslinking (which includes tanning) of collagen causes less water to bind but that which is bound is more thermostable.

Crust leather generally has a moisture content of 14-16% (dependent on atmospheric humidity) and shoe upper leathers may absorb up to 40% moisture without being wet to the touch.[25] Water is an integral part of collagen, leather-making and leather.

Table 1.4: Degrees of collagen hydration.[25]

g Water/ g Collagen	Water Bonding	Type of Bonding	Freezing Temperature (K)	Measurement
0 ↓	strongly bound "immobile water"	bound within triple helix by 3 H bonds	does not freeze	detected by Fischer Method
0.02 ↓		bound to collagen by 2 H bridges		removed by drying at 105°C or P_2O_5 under vacuum
0.07 ↓		bound to collagen by 2 H bonds	180	
0.25 ↓		bound to functional groups by 1 H bond	265	
0.35 ↓	weakly bound "mobile water"	ordering action through water chains of up to 10 links		
0.50 ↓	weakly bound "swelling water"		266	removed mechanically
2.0 ↓	unbound "bulk water"	unbound "bulk water"	273	

1.2.4. THE THERMAL SHRINKAGE OF COLLAGEN

The dislocation of interchain crosslinks of collagen fibrils may be induced by heating and this causes, (i) changes in the physical properties of collagen solutions, *e.g.*, altered optical rotatory properties and increased viscosities, and (ii) contraction or shrinkage of the collagen fibre; indicating that the helical, rod-like structure of the individual strands has been destroyed. The structural changes are analogous to the melting of a crystal and indicate the loss of a highly ordered structure. If this phase change occurs abruptly over a narrow temperature range, as it does with collagen, it indicates that the triple helix is stabilised by cooperative interactions.[16]

The temperature at which half of the helical structure is lost is called the melting temperature (T_m) and is reflective of soluble collagens, *e.g.*, tropocollagen. In many circles, T_m may also be referred to as denaturation temperature, T_D.[9] Shrinkage temperature (T_s) is the comparable index for intact collagen fibres. Thermal stability varies between collagen types and animal species and is commonly correlated to the locking effect of proline and hydroxyproline residues as indicated by **Table 1.5**.

The importance of hydroxyproline (Hyp) is further indicated by T_m values of synthetic polypeptide models, *i.e.*, 24 and 58°C for poly-(Pro-Pro-Gly) and poly-(Pro-Hyp-Gly),

respectively.[15] The hydrothermal stability of collagen is commonly attributed to the ability of collagen-water to "crosslink" adjacent hydroxyproline residues *via* hydrogen bonds but this theory has recently been questioned[28] and hydrothermal stability may rely on "previously unappreciated inductive effects."[29]

Table 1.5: A comparison of thermal stability to the proline and hydroxyproline content of various collagen sources.[15]

Source	Proline plus Hydroxyproline (per 1000 residues)	Thermal Stability (°C)		Body Temperature (°C)
		T_s	T_m	
Calf Skin	232	65	39	37
Shark Skin	191	53	29	24-28
Cod Skin	155	40	16	10-14

Shrinkage temperature values of collagen are influenced by pH values, the addition of solvents and detergents,[16] crosslinking and water content[9] and therefore standard methods of analysis are adhered to.[30]

Hydrothermal treatment of mammalian skin or tendon causes it to shrink to approximately a quarter of its original length without changing the elementary composition, acid binding capacity or water content.[31] The denatured collagen does, however, feel like glue, shows rubber-like elasticity and lowered tensile strength, while losing its original resistance to trypsin. This denatured collagen partially regenerates to form gelatine (**Figure 1.10**).

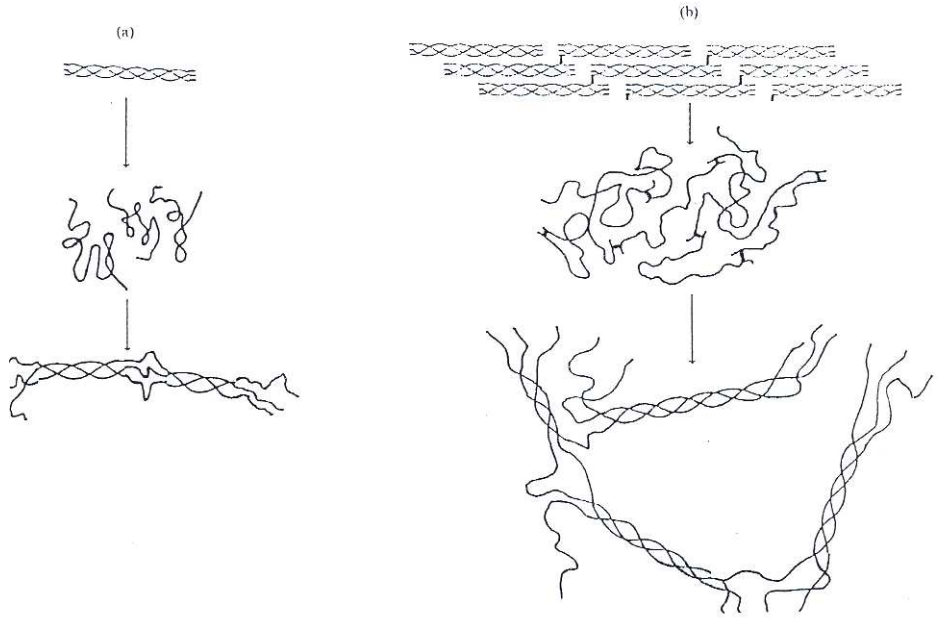

Figure 1.10: The denaturation of collagen to form gelatine in (a) uncrosslinked, and (b) crosslinked collagen.[17]

A wide range of analytical techniques are currently being used in an attempt to shed more light on the changes that occur when heating collagen. Thermal transitions are commonly investigated using differential scanning calorimetry (DSC), thermogravimetry (TG) and dynamic mechanical thermal analysis (DMTA).[32-35] Nuclear magnetic resonance (NMR),[33] Raman spectroscopy[36] and X-ray diffraction have also been utilised in the study of the thermal denaturation processes of collagen recently.

1.2.5. COLLAGEN IN HIDES AND SKINS

The collagen of importance in leather manufacture is found in the corium layer and is isolated *via* the beamhouse processes. Type IV and VII collagen are associated with the basement membrane of the grain-epidermis junction and are removed during liming (**Table 1.6**). Type I collagen is the dominant collagen type in the corium and contributes more than 98% of the total collagen in a mature hide by mass.[29]

The grain layer is composed of thin, individual fibres packed and woven so tightly that a smooth surface is revealed after the removal of the hair and epidermis with a characteristic pattern (called the grain surface and which is analogous to wood grain). The grain network contains a relatively large proportion of Type III collagen fibres with Type I and V. Type III collagen fibres are usually associated with tissues that require flexibility, such as growing skin. These fibres are later replaced by larger Type I fibres as the animal grows. Type V collagen forms small fibrils with close structural relationships to Type I and III. Type V collagen is a relatively minor but widespread component of virtually all non-cartilaginous tissues and bone which contain Type I and III collagen fibres (**Table 1.6**).

Table 1.6: Collagen types in bovine hides.[17]

Region of Hide	Collagen Type	Fibre Type
Grain-Epidermis Junction	Type IV	Non-Fibrous Structure
	Type VII	Anchoring Fibrils
Grain Layer	Type I	Fine Banded Fibrils
	Type III	Fine Banded Fibrils
	pro Type I / pro Type III	Microfibrils
Reticular Layer	Type I	Thick Banded Fibres
	Type III	Fine Banded Fibres
	Type V	Fine Banded Fibres
	Type VI	Filamentous Structure

In the reticular layer the fibres are coarser and stronger. The fibre bundles are surrounded by a sheath of fine fibrils split longitudinally into finer fibres to create the characteristic three dimensional woven fibre structure. The reticular layer is primarily Type I collagen[37] although Type III, V and VI are all closely associated in minor amounts. Type VI collagen has disulfide bridges and is therefore highly likely to be damaged and even removed during the liming process. This is thought to be instrumental in the "opening-up" of the fibre structure during liming.[17]

1.2.6. COLLAGEN PROPERTIES IN HIDES AND SKINS

The network of collagen fibres is a polyelectrolyte with ionisable, crosslinking and hydrogen bonding side chains. The functional groups on the side chains are activated or deactivated in various processes of leather manufacture by changing the pH and the ionic strength of the tanning float. The functional groups have water molecules assembled around them and therefore this associated water is the first contact a substance will have when approaching the collagen.[9]

Acids, alkalis and lyotropic agents cause collagen to swell. This swelling is limited by the presence of crosslinks, which also makes mature collagen insoluble in water. Swelling is indicated by an increase in thickness and plumpness and by a decrease in compressibility. There are two kinds of swelling according to Bienkiewicz,[9] *viz.*, osmotic and lyotropic swelling.

Osmotic swelling occurs outside the pH 4-8 range, *i.e.*, away from the isoelectric point, where swelling can increase ten-fold. The greatest swelling occurs at pH 2 and 12 (**Figure 1.11**) and this is reversible by changing the pH or increasing the salt concentration. Osmotic swelling results when side chains on the collagen backbone become ionised (anionic at high pH and cationic at low pH) and the charge is fixed and cannot migrate. Water moves into the collagen structure in an attempt to reduce the charge imbalance, this causes swelling and the fibres develop a glassy, translucent look.

Lyotropic swelling is caused by neutral salts that decrease the cohesion of the fibres by breaking hydrogen bonds and is not completely reversible. The volume and length increase is smaller than in osmotic swelling and the collagen maintains its natural silky look. Lyotropic anions and cations are ordered in a Hofmeister's series according to their swelling power: *e.g.*, anions,

$$F^- < Cl^- < CH_3COO^- < NO_3^- < Br^- < SCN^- < SO_4^{2-},$$

and cations,

$$K^+ < Mg^{2+} < Na^+ < Cs^+ < Li^+ < Ca^{2+}$$

The salts may be further divided into three groups according to their interaction with collagen. Firstly, salts that decrease the shrinkage temperature and cause collagen to swell, *e.g.*, $CaCl_2$ and KSCN; secondly, salts that have little influence on the shrinkage temperature and swelling, *e.g.*, NaCl; and finally, salts that decrease the shrinkage temperature and cause swelling at low concentrations but act in the reverse way at high concentrations, *e.g.*, Na_2SO_4 and $(NH_4)_2SO_4$.[38]

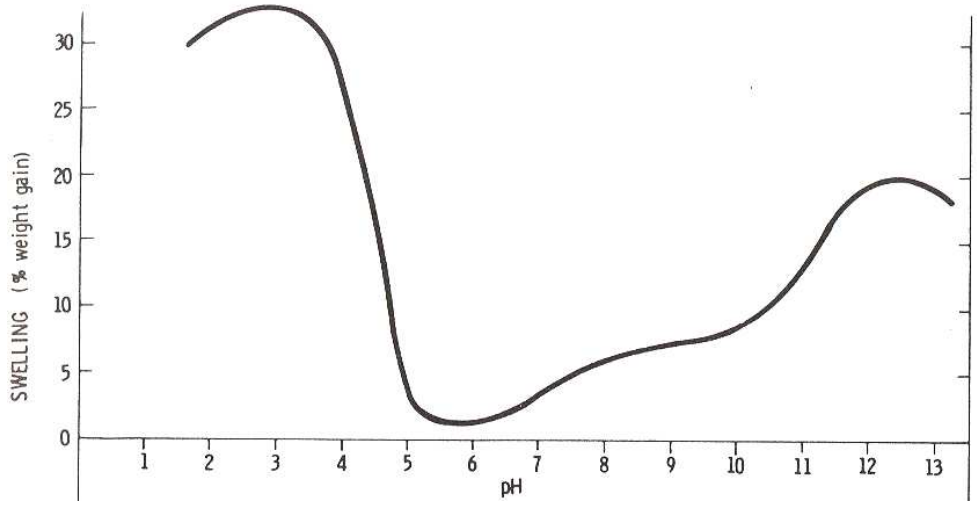

Figure 1.11: The relationship between pH and swelling of pelt.[39]

1.3. TANNING CHEMISTRY

Collagen is relatively inert to chemical and biological attack but to increase both the mechanical strength and ability to resist deterioration, hides are stabilised by tanning agents.[17]

1.3.1. PRETANNING, TANNING AND RETANNING AGENTS

The physical properties of leather is dependent on the type of tannage, the quantity of tanning agents fixed, drying techniques, and other modifications such as the application of fats, oils and retanning agents. Pretanning usually involves the use of a tanning agent different to that used as the main tannage. Pretanning may be performed to (i) reduce the astringency of the main tannage for collagen, *e.g.*, in vegetable tannages, (ii) to increase the shrinkage temperature so that the material is not damaged during shaving or in

degreasing during which temperatures higher than 60°C can easily be reached, and (iv) to produce a stabilised material for short-term preservation.[40]

Retanning is the treatment of previously tanned material with additional tanning agents to add or modify leather properties. Material retanned with one or more agents different to the main tannage is described as having undergone a "combination tannage." Material tanned with vegetable tannins followed by a chromium retannage is referred to as "semi-chrome", while chromium tanning followed by organic retannages is referred to as "chrome retan."[1]

There is a wide range of chemicals used as pretanning, tanning and retanning agents and these may be classified according to their origin, functional groups or method of synthesis.[41] Five classifications are commonly used in one form or another and include mineral, vegetable, syntan, aldehyde and resin/polymer tanning agents.

1.3.1.1. Mineral Tanning Agents

As the name implies, mineral tanning agents are inorganic in nature and usually involve the interaction of metal ions with collagen. Mineral tanning agents include chromium, aluminium,[42-45] zirconium,[9,16] titanium,[46,47] iron[48,49] and some novel rare earth metals,[16] usually as basic sulfates, and silicates.[9] In general, the initial fixation is by dative or coordination bonds with carboxylate side chains of the collagen triple helix. Convention dictates that bound water is displaced and the metals form aggregate or bridging complexes that stabilise the skin structure, thereby increasing the shrinkage temperature. This may, however, vary considerably as may be shown by zirconium (See **Section 1.4.5**). The individual chemistries of each element will dictate the extent of penetration into, and fixation with, collagen. This, in turn, influences the pickle and basification pHs when processing with mineral salts (**Table 1.7**).

Table 1.7: A comparison of general pickle and basification pHs for chromium and zirconium tanning processes.[9]

Tanning Agent	Pickle pH	Basification pH
Basic Zirconium Sulfate	1.0-2.0	2.0-4.0
Basic Chromium Sulfate	2.5-3.0	3.8-4.2

Penetration of the metal cations may be assisted by the use of "masking agents."[50] Masking agents partially stabilise the tanning salts by forming a tanning complex with a lower astringency for collagen and which is also less sensitive to pH variations.[39] This allows masking agents to be used to manipulate pickling and basification pHs. The masking agents may contribute properties of their own to the leather or improve others, such as, fullness, increased shrinkage temperature, grain pattern or smoothness, modification of handle, improvement of tanning agent distribution and lightening of the leather colour (unless the leather is already white). Masking agents are typically anions with varying affinities for metal ions, *e.g.*, nitrate < chloride < sulfate < sulfite < formate < acetate < sulfophthalate < succinate < tartrate < glycolate < phthalate < sulfosalicylate < malonate < lactate < citrate < oxalate < hydroxide show an increasing complex affinity with chromium, where each anion is able to displace the one before it. There is also a limit where the masked tanning complex may become stabilised to a degree where it will have no affinity for collagen.[12]

1.3.1.2. Vegetable Tannins

Vegetable tannins are extracted from plant sources such as leaves, nuts, bark and wood. They consist of large, sometimes acidic, polyphenolic structures with molecular masses from 500 to 20 000 $g.mol^{-1}$ which form numerous hydrogen bonds[51] with collagen's side chains and peptide backbone.[52,53] They are used as the main tannage and frequently as retanning agents.[54] There are two main types of vegetable tannins recognised, *viz.*, hydrolysable and condensed (**Figure 1.12**).

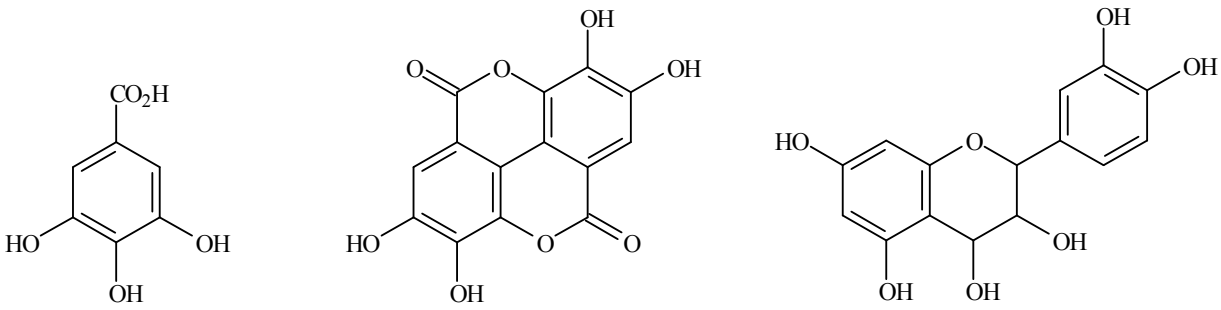

(a) Gallic Acid (a) Ellagic Acid (b) Leucoanthocyanidin

Figure 1.12: Basic structures associated with (a) hydrolysable and (b) condensed vegetable tannins.[55]

Hydrolysable tannins may undergo hydrolysis and consist of esters of gallic acid, called gallotannins (*e.g.*, Sumach and Tara), or contain modified hexahydroxydiphenic acid (ellagic acid), called ellagitannins (*e.g.*, Chestnut, Valonea, Myrabolams and Divi Divi).[55] Condensed tannins occur widely and consist of complex forms of leucoanthocyanidins, with Mimosa and Quebracho as examples.[2] The vegetable tannins are all derived from the amino acid synthesising Shikimate pathway and may be sulfited to reduce astringency and increase solubility, and so improve penetration.[55]

1.3.1.3. Syntans

"Synthetic tannins" or syntans are a diverse group and technically incorporate any tanning agent that is synthesised, including aldehydes, resins and polymers.[56] The term syntans, for the purpose of this study, will only include conventional syntans (from an historical perspective) *viz.*, auxiliary, replacement, combination and mineral syntans.[16]

Auxiliary syntans are usually based on aromatic sulfonic acids (**Figure 1.13**) and assist processes such as tanning and dyeing (dispersing agents), while having little to no inherent tanning ability.[57]

Replacement syntans were originally synthesised to replace and mimic vegetable tannins and are typically phenolic in nature.[58] Replacement and combination syntans may be employed as the sole tannage or as pretanning and retanning agents.[59,60] The monomers are commonly polymerised using formaldehyde to yield methylene condensed resins although additional linkages are also used with increasing light-fastness in the order -CHR- < $-CH_2NHCONHCH_2-$ < $-CR_2-$ < CO_2- < $-SO_2NH-$.[9]

Combination syntans (**Figure 1.13**) make use of the blending and/or polymerisation of phenolic and aromatic sulphonic acid monomers to give tanning agents with multiple structures and a hybrid of properties and uses. Syntans are commonly sulfited to improve solubility, penetration and colour and are therefore generally anionic in nature.[54] The ionised sulfonic acid group has a strong ionic attraction for the cationic amino functional groups on the collagen side chains, while the phenolic structures bind similarly to vegetable tannins, *i.e.*, *via* hydrogen bonds.[61]

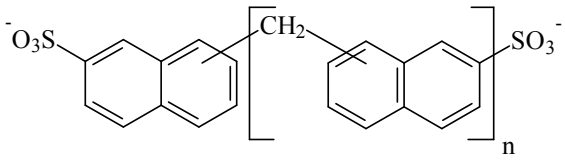

(a) Condensation product of naphthalene sulfonic acid

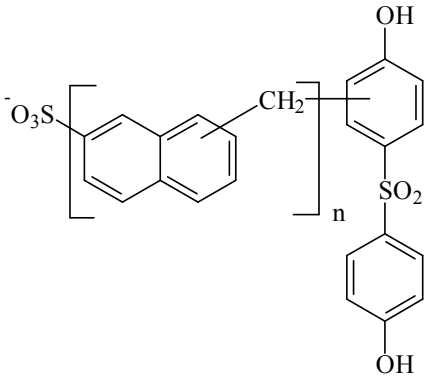

(b) Condensation product of 4,4'-dihydroxydiphenylsulfone with naphthalene sulfonic acid

Figure 1.13: Structures associated with (a) auxiliary and (b) combination syntans.[54,61]

Mineral syntans may be produced in two main ways: (i) by blending mineral and syntan agents, where conventional masking occurs *in situ*, and (ii) by forming a cation-syntan complex with hybrid properties where the "masking" may be considered permanent and a new, neutral or often anionic, tanning agent is produced.[62] In this way, tanning agents may be produced or synthesised with variable astringency, penetration power, colour, and filling properties.[54]

1.3.1.4. Aldehydes

The aldehyde functional group forms covalent bonds when it reacts with nonionised amino side chains of collagen. The aldehydic tanning chemicals include formaldehyde,[2] glutaraldehyde,[63,64] dialdehyde starches, and oxazolidines. If not fatliquored, aldehyde tannages tend to yield hard and thin leathers. Glutaraldehyde has shown to be the most versatile and widely used, especially in automotive upholstery leathers.[54] Oxazolidines are heterocyclic derivatives obtained from the reaction of aminohydroxy compounds with aldehydes but remain aldehydic in nature and are alternatives to true aldehydes (**Figure 1.14**).[54,65,66]

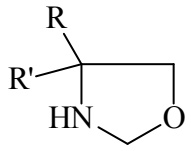

Figure 1.14: A basic structure of oxazolidines.[66]

1.3.1.5. Polymers and Resins

This is a large and disparate group including acrylics,[67] polyurethanes, and formaldehyde resins of melamine, urea and dicyandiamide.[68] All are predominantly used as retanning agents, with little to no influence on the shrinkage temperature, to improve cutting yields by selectively filling the more open structured parts of hides and skins with "polymer deposits" and for tightening the grain.[7]

Significant work has also been done on combination tannages involving the crosslinking of polyphenolics with mineral agents.[50,69-72] Synergistic effects are also exploited in the search for mineral-free tannages of the future.[73]

1.3.2. TANNING MECHANISMS

It has long been accepted that collagen is stabilised by hydrogen bonding and that heating of collagen results in shrinking due to the breaking of these bonds.[74] Bailey and Miles[75] have shown that shrinking occurs in hydroxyproline poor areas of the collagen chain which supports Weir and Carter's[76] suggestion that shrinking is initiated at a "shrinking nucleus." The sudden shrinkage occurs at temperatures that are characteristic of the tannage (**Table 1.8**) and such shrinkage temperatures were first used as a qualitative and diagnostic tool by Povarnin.[9]

Tanning changes at least one of the essential properties of collagen.[9] This, according to Covington,[38] may affect: (a) rendering the collagen non-putrescible, (b) changes in physical appearance and properties, *e.g.*, opacity and handle, (c) an increase in shrinkage temperature, and (d) the irreversibility of the above properties. Covington continues that all four criteria are required to define tanning.

Table 1.8: Tanning agents and characteristic shrinkage temperature ranges.[38]

Tannage Type	Tanning Agent	Shrinkage Temp. Range (°C)
Raw Hide or Pelt	None	60-65
Mineral	Chromium	100-115
	Zirconium	90-98
	Aluminium	70-80
	Titanium	70-80
Vegetable	Condensed Tannins	80-85
	Hydrolysable Tannins	75-80
Syntan	Auxiliary	60-70
	Replacement	70-80
	Combination	70-80
Aldehyde	Formaldehyde	75-80
	Glutaraldehyde	70-80
Polymers and Resins	All	60-70

"Leathering" generally provides the qualities desired for the production of useful articles but a definition based on this is difficult to measure from a scientific perspective.[2] The increase in shrinkage temperature is generally used as a scientific measure of the tanning ability of a chemical but it does not give an indication of leathering. Vegetable, aldehyde, oil, brain, tawing and smoke tanning yield usable leathers after tanning alone, however, chromium and zirconium tanning yield hard leathers which need additional processes (retanning and fatliquoring) to provide the properties commonly associated with leather.[38] Oil, brain and smoke tanning[77] do not increase the shrinkage temperature and tawing is reversible and therefore these do not fulfil Covington's criteria for tanning. Tanning, based on shrinkage temperature, falls into four zones as shown in **Table 1.9**.

Table 1.9: The four tannage zones based on shrinkage temperature.[38]

Tanning Zone	Shrinkage Temperature (°C)
Negative Tannages	30-60
Moderate Stability Tannages	60-85
Combination Tannages	80-100
High Stability Tannages	100-130

There is a concerted thrust towards uncovering a unified theory for tanning within the leather science fraternity. The ability to predict the effects of new tanning agents and

processes without trial-and-error is highly desirable. This could lead to a giant leap forward for "environmentally friendly" processing, high thermal stability and composite collagen materials.

Approaches which have been adopted in this quest include: (a) identification of protein binding sites with tanning systems, (b) types of interactive forces, (c) protein charge variations, (d) changes in shrinkage temperature, (e) evidence for intermolecular crosslinking, and (f) changes in collagen hydration.[78]

Tanning does not change the shrinking mechanism but merely stabilises it as the thermal degradation of tanned material involves the breaking of hydrogen bonds and not the tannin-collagen interactions.[79] Tanning agents interact with sites on the collagen and thereby vary collagen hydration, resulting in increased crosslinks and an increase in the shrinkage temperature.[80] Covington is at the forefront of a unifying thermodynamic view of the shrinking mechanism.[38,73,79]

Covington treats the shrinkage reaction as a normal chemical reaction with a reactant, referred to as a "cooperating unit." The "cooperating unit" controls the kinetics of the process and determines the observed shrinking temperature. The shrinking transitions are as follows:

$$\text{intact collagen} \rightleftarrows \text{dissociating collagen} \rightarrow \text{shrunk collagen}$$

The Gibbs energy for the first step may be defined as follows:

$$\Delta G^\circ = -RT \ln K = -RT \ln (k_1/k_{-1}) = -RT \ln k_1 + RT \ln k_{-1}$$

At the conventionally measured shrinkage temperature, $k_1 >> k_{-1}$,therefore:

$$\Delta G^\circ \approx -RT \ln k_1$$

The Gibbs energy of the transition state complex may be defined as follows:

$$\Delta G^\dagger = \Delta H^\dagger - T\Delta S^\dagger$$

According to the Hammond postulate[81] for an endothermic process the transition state complex is more like the products than the reactants and therefore Covington makes the assumption that $\Delta G^{\dagger} \approx \Delta G°$. So,

$$-RT \ln k_1 \approx \Delta H° - T\Delta S° \approx \Delta H^{\dagger} - T\Delta S^{\dagger}$$

and,

$$-\ln k_1 \approx \Delta H^{\dagger}/RT - \Delta S^{\dagger}/R$$

Covington makes a further assumption that changes to collagen impact directly on the rate of shrinking and the shrinking temperature. This allows for the analysis of tanning reactions in terms of the known chemistries of reaction where the shrinkage temperature depends on enthalpic and entropic contributions (**Table 1.10**). To increase the shrinkage temperature would require an increase in the enthalpy and/or a decrease in the entropy of the system.

Table 1.10: Activation parameters at 333K for different tannages.[38]

Tannage	$\Delta G^{\dagger}$ (kJ/mol)	Tannage	$\Delta H^{\dagger}$ (kJ/mol)	Tannage	$\Delta S^{\dagger}$ (kJ/mol)
bated pelt	104	aluminium	343	aluminium	0.73
aluminium	104	uranium	427	uranium	0.97
vanadium	105	formaldehyde	473	formaldehyde	1.1
iron	106	vanadium	493	iron	1.2
uranium	106	iron	498	vanadium	1.2
formaldehyde	121	zirconium	573	zirconium	1.3
zirconium	147	bated pelt	673	bated pelt	1.7
chromium[a]	151	chromium[a]	1350	chromium[a]	3.6

[a]0.6% Cr_2O_3 offer

The overall increase in shrinkage temperature correlates to the increase in $\Delta G^{\dagger}$ from bated pelt to chromium tannage. The contribution to $\Delta H^{\dagger}$ is proposed to be related to structure whereas the entropic contribution is related to order.[79] Chromium is the only tannage which imposes rigidity to the structure of bated pelt but also creates more disorder. This disorder is thought to be related to the solvation shell of collagen.[38] As the range of entropic contributions is small (0.73-1.3 kJ/mol) the enthalpy may be concluded to be the controlling parameter for shrinkage temperatures in lower stability tannages.

The imposed structure may be correlated to a "cooperating unit" or theoretical molecular weight of reactant (tanned collagen) in the shrinking reaction and has been measured experimentally from the rate of shrinking. Plotting the theoretical molecular mass of the "cooperating unit" versus the shrinkage temperature of various tannages (**Figure 1.15**) suggests two different mechanisms of stabilisation. The first correlates with Covington's thermodynamic explanation where the shrinkage temperature increases with an increase in the size of the cooperating unit, *i.e.,* increase in enthalpy, and includes tannages that produce relatively simple covalent crosslinks. The second population of results, where the increase in shrinkage temperature is independent of the size of the cooperating unit, includes tannages that rely on multiple interactions between the crosslinker and collagen and suggest a different mechanism.[38]

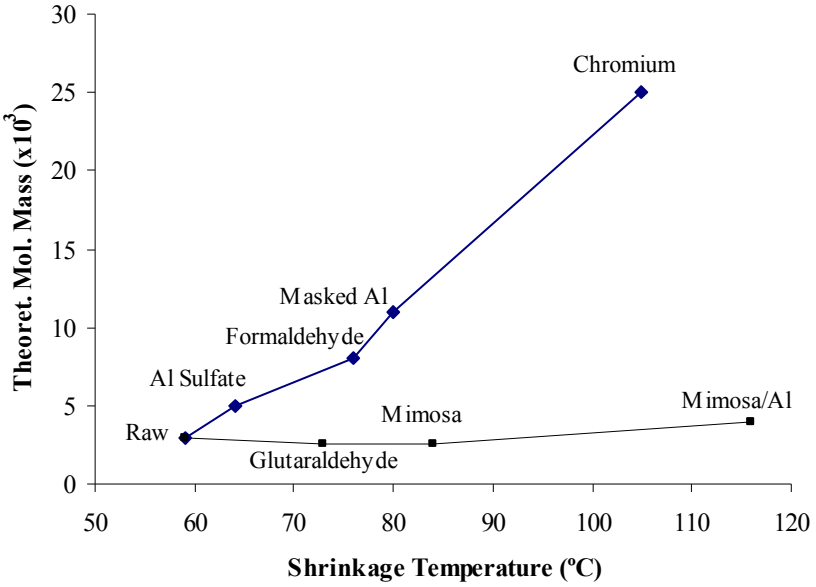

Figure 1.15: The relationship between the theoretical molecular mass of the cooperating unit and shrinkage temperature.[38]

The enthalpic tanning mechanism requires an imposed structure. To impose structure, the tanning agent must form high energy, non-labile bonds, which may be covalent or multiple hydrogen bonds. The tannage must optimise the size (molecular mass) of the "cooperating unit" by crosslinking. If the crosslinking is covalent, the linking must be rigid and short. Multiple hydrogen bond crosslinking requires a rigid matrix where the tannin has a greater affinity for the collagen than for itself.

Negative tannages correspond to salts or compounds that are known hydrogen bond breakers, *e.g.,* lithium chloride. Moderate hydrothermal stability arises from tannages

that impose structure but which neither reduce the amount of supramolecular water nor create a substantial compensating stabilising environment. The high stability tannages (100-130°C) also require a stable, rigid matrix around collagen, however, this is achieved by displacing supramolecular water from collagen but may incorporate some water as part of the matrix structure. Combination tannages are a mixture of moderate and high stability tannages.[38]

The development of a universal mechanism for tanning is not just an academic exercise but can have far reaching consequences. Industrially, an understanding could improve the efficiency of processes, temperatures and chemical use; tanning chemicals could be modelled, predicted and developed to tackle a range of problems including environmental issues such as replacements for chromium, or high specification tannages with high shrinkage temperatures.

1.4. ZIRCONIUM

Zirconium most likely derives its name from the Arabic “zerk” (a precious stone) or the Persian “zargon” (gold-coloured). Klaproth, in 1789, proved that the "imperfect diamonds" he studied were distinct mineral species containing a distinguishing oxide he named *Zirkonerde* or zirconia. It was only in 1824 that J. J. Berzelius produced an impure elementary zirconium. In 1922, it was recognised that all naturally occurring zirconium contains a small proportion of hafnium as an impurity, commonly between 0.5 and 2%, because the elements are extraordinarily alike. Zirconium's atomic mass was correctly calculated at 91.22, in 1923.[82]

Zirconium comprises 0.016% of the earth's crustal rocks and is fourth most abundant of the transition metals after iron (6.2%), titanium (0.63%) and manganese (0.106%), respectively. Zirconium is a type-a metal (or a hard metal) and commonly exists as silicates and oxides in many silicaceous materials which are resistant to weathering and often accumulate in beach deposits.[83] Zirconium's most important minerals are zircon and baddeleyite found principally in Australia, Russia and South Africa (**Section 1.4.1**).[84]

Zirconium is a lustrous, silvery metal with a high melting point (**Table 1.11**) and is not considered a "good" conductor of heat and electricity in comparison with most other metals. Zirconium typically has a metallic hexagonal close packing (hcp) structure that transforms to body centred cubic (bcc) at 870°C. Traces of oxygen, nitrogen and carbon have an embrittling effect and makes metal production difficult.[85]

At high temperature zirconium metal reacts directly with most non-metals, particularly hydrogen and oxygen. The metal is pyrophoric when finely divided but the main feature of zirconium is that at room temperature it is extremely resistant to corrosion due to the formation of a dense, adherent, self-sealing oxide film. Mineral acids have little effect, except for hydrofluoric acid, unless hot, and oxidising agents, *e.g.*, nitric acid, reduce the reactivity by contributing to the protective oxide film.[83]

Table 1.11: Properties of zirconium.[83]

Property	Zirconium
Atomic Number	40
Number of Naturally Occurring Isotopes	5
Atomic Weight	91.22
Electronic Configuration	$[Kr]4d^2 5s^2$
Electronegativity	1.4
Metal Radius (pm)	160
Ionic Radius Zr(IV) 6-Coordinate (pm)	72
Melting Point (°C)	1857
Boiling Point (°C)	4200
Density ($g.cm^{-3}$, 25°C)	6.51

1.4.1. ZIRCONIUM MINERALS

Zirconium is widely distributed in the earth's crust and is present in many minerals, two of which are currently of commercial significance, *i.e.*, zircon sand ($ZrSiO_4$ or $ZrO_2.SiO_2$, typically 65-66% ZrO_2 + HfO_2) and baddeleyite, a form of zirconium dioxide (ZrO_2). Zircon varies from a translucent yellow colour, through red, brown or grey to green. It occurs as stubby, prismatic or dipyramidal crystals or as irregular granules. Baddeleyite may be colourless to yellow, brown or even black.[86] The naturally occurring radioactive elements, uranium and thorium are present in both minerals.

Though zircon is a common accessory mineral in igneous, metamorphic and sedimentary rocks, commercial quantities are rarely found in consolidated rocks. With the exception of small quantities of baddeleyite which are extracted from primary deposits, all of the world's zircon production at present is obtained from alluvial, mainly beach sand deposits, where it is recovered as a by-product of the titanium-bearing minerals, ilmenite and rutile.[86] Most of South Africa's zircon is produced from the mining of sand dunes along the KwaZulu-Natal north coast by Richards Bay Minerals (RBM) and by Namakwa Sands Ltd on the west coast between Alexander Bay and Lambert's Bay. Worldwide baddeleyite sources are dwindling and South Africa's source was found in the Phalaborwa Complex in the Northern Cape under the control of the Phosphate Development Corporation (FOSKOR) and Palabora Mining Company (PMC), as a by-product of copper and apatite mining.[86,87] In 1995 South Africa exported 272 kt of zircon sand and 15 kt of baddeleyite (down from 22.5 kt in 1993) and contributed to approximately 29% of the world's zirconium minerals. Russia is presently the sole producer of baddeleyite[88] and South Africa produces some 31% of the world zirconium minerals as zircon.[84]

1.4.2. ZIRCONIUM(IV) COMPOUNDS

The dominant oxidation number of zirconium is +4 which when combined with a relatively small size, leads to an extensive hydrolysed aqueous chemistry with a largely covalent nature. Donor ligands containing oxygen, nitrogen and chloride are especially stable, commonly creating complexes with coordination numbers of seven, eight and higher. The relatively small, highly charged ion with a d^0 spherical symmetry configuration allows for a variety of stereochemistries.

High coordination numbers (seven and eight) are characteristic of zirconium complexes and the ligands are normally labile which results in the great variety of stereochemistries. The complexes are typically diamagnetic (to be expected for the d^0 configuration) and hydrolysis is common, resulting in polymeric species with -OH- or -O- bridges.[83]

1.4.2.1. Halogens as Donors

The most important zirconium halides are the tetrahalides which are well characterised. The tetrahalides are high melting crystalline white solids which readily sublime between 320 and 430°C, except for the fluorides, which are nonvolatile. α-ZrF_4 (dodecahedra) and β-ZrF_4 (square antiprism) have extended three-dimensional structures linked together by sharing F atoms. $ZrCl_4$ and $ZrBr_4$ consist of infinite zigzag chains of ZrX_6 octahedra. ZrI_4 forms a helical chain structure where the ZrI_6 octahedra share non-opposite edges. All the tetrahalides behave as Lewis acids, are hygroscopic and hydrolyse easily.[89] The tetrafluorides form stable hydrates, $ZrF_4(H_2O)_n$ (n = 1 or 3), whereas the other tetrahalides react with water to give oxyhalides.[90]

Zirconium forms a vast array of complex fluorometallates, $M_xZr_yF_z$, where M is an alkali, alkaline earth, divalent transition metal, or lanthanide cation, or the conjugate acid of a nitrogen base. The number of fluorine atoms per zirconium atom is commonly eight, seven, six or five but non-integral ratios are also found reflecting zirconium centres with different coordination numbers (**Table 1.12**).

Table 1.12: Selected fluorometallates of zirconium.[91]

Coordination Number	Fluorometallate Compound
8	Li_4ZrF_8
7	Na_3ZrF_7
6	Na_2ZrF_6
5	$NaZrF_5$
Non-Integral	$Na_3Zr_2F_{11}$
Non-Integral	$Na_7Zr_6F_{31}$

Nearly all of the known chloro-, bromo- and iodometallates are salts that contain the simple, octahedral $[ZrX_6]^{2-}$ anion. The M_2ZrX_6 compounds are moisture sensitive, high-melting, white (X = Cl or Br) or yellow (X = I) crystalline solids that decompose at elevated temperatures to solid MX and gaseous ZrX_4.[92]

1.4.2.2. Nitrogen as a Donor

Compounds of the type $ZrCl_4.nNH_3$ (n = 8, 4 or 2) are prepared by the reaction of the tetrahalides with gaseous ammonia. Thermal decomposition of $ZrCl_4.8NH_3$ in argon gives stepwise formation of $ZrCl_4.6NH_3$, $ZrCl_4.4NH_3$ and finally $ZrCl_4$. Studies indicate that $ZrCl_4.8NH_3$ is a mixture of $ZrCl_3(NH_2).6NH_3$ and NH_4Cl. The same products are obtained when reacting liquid ammonia with M_2ZrCl_6 (M = NH_4, Rb or Cs).[91]

Zirconium(IV) halides form adducts with a variety of monodentate and polydentate amines. These compounds are air- and moisture-sensitive white (Cl and Br) or yellow (I) solids, thermally stable and insoluble in most organic solvents. Tertiary amines yield ZrX_4L_2 or ZrX_4L complexes, depending on the steric bulk of the substituents on the nitrogen atom. Tertiary and secondary amines form simple adducts whereas aminolysis takes place with primary amines, yielding $ZrX_2L_2.L$ and $ZrX_3L.L$.[92]

Diamines such as ethylenediamine and tetramethylethyldiamine yield 1:1 adducts with zirconium(IV) halides, consistent with an octahedral *cis* structure.[91]

There is a world-wide interest in the design and synthesis of zirconium(IV) complexes using imido, amido and Schiff base ligands as catalysts for polymerisation reactions, enantioselective processes, kinetic resolution, Diels-Alder cycloadditions and hydrosilylation.[93-101]

1.4.2.3. Oxygen as a Donor

The main oxide is zirconia, ZrO_2, with a 7-coordinate zirconium (**Figure 1.16**). The ignited ZrO_2 is unreactive, has a very high melting point (2710 ± 25°C), and has a low coefficient of thermal expansion and is therefore a useful refractory material.[83] A problematic phase change at 1100°C is avoided by using CaO or MgO in the ZrO_2 to retain the cubic fluorite structure throughout the temperature range.[102] ZrO_2 has also been produced in fibrous form and coupled with its chemical inertness, refracticity and apparent lack of toxicity, is used as an insulator and for the filtration of corrosive liquids.

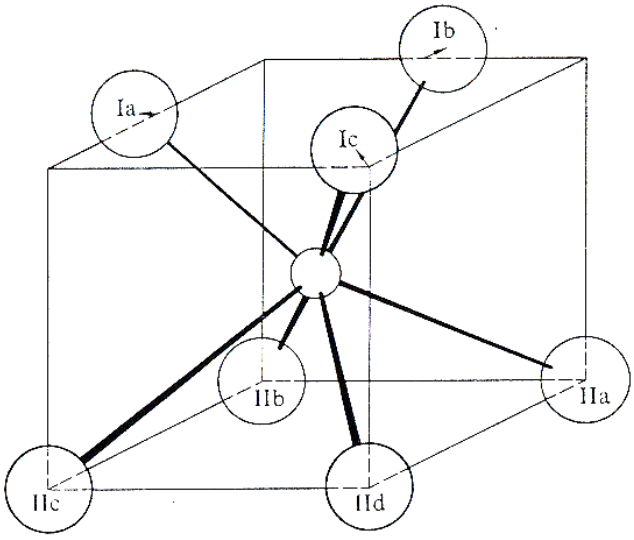

Figure 1.16: The coordination of zirconium(IV) in zirconia, ZrO_2.[92]

Very little data is available for zirconium complexes that contain oxo ligands. The only X-ray evidence for the existence of the zirconyl group, $Zr{=}O^{2+}$, comes from a structural study of K_2ZrO_3. This compound contains chains of ZrO_5 square pyramids that share basal edges. MacDermott[103] stated that "there is no doubt that the zirconyl group as a persistent species in solution is mythical." Planalp and Anderson[104] have, however, reported the presence of centrosymmetric oxo-bridged dinuclear complexes with a linear Zr-O-Zr bridge.

At high temperatures ZrO_2 reacts with metal oxides, metal hydroxides or metal carbonates to form so-called zirconates, $M^{II}ZrO_3$. There is no evidence for the existence of discrete zirconate anions, ZrO_3^{2-}, and the metal zirconates are best described as macromolecular mixed metal oxides.[92]

The constitution of the gelatinous precipitates obtained by the addition of hydroxyl ions to solutions of zirconium has caused much controversy.[105,106] Zaitsev[107] claims that three distinguishable hydroxides exist. The α-hydroxide is obtained as the freshly precipitated $Zr(OH)_4(H_2O)_n$ and is formulated as $Zr_4{}^{b}(OH)_8{}^{t}(OH)_8(H_2O)_x$ with bridging (b) and terminal (t) hydroxo-groups. This compound ages to the γ-hydroxide, $ZrO(OH)_2(H_2O)_m$, better formulated as $Zr_4O_4{}^{t}(OH)_8(H_2O)_y$ with oxo-bridges instead of hydroxo-bridges. The intermediate β-hydroxide, $Zr_4O_2{}^{b}(OH)_4{}^{t}(OH)_8(H_2O)_z$ was obtained by precipitation

from methanolic solutions of zirconium oxychloride. It was suggested that a number of the "basic" salts could be rationalised in terms of structures based on the hydroxides with some of the terminal hydroxo-groups being replaced by other ligands.

Direct evidence for the existence of tetranuclear hydroxo complexes comes from X-ray diffraction (XRD) studies of the zirconium oxyhalides, $ZrOX_2.8H_2O$ (X = Cl or Br). These compounds contain the $[Zr_4(OH)_8(H_2O)_{16}]^{8+}$ cation (**Figure 1.17**) in which four zirconium atoms are connected by double hydroxo bridges. Each zirconium atom is also attached to four water molecules, resulting in an eight-coordination distorted dodecahedron. Concentrated aqueous solutions are consistent with a similar structure.[108] Dilution of zirconium solutions (from 10^{-2} to 10^{-4} *M*) with an increase in perchloric acid (from 0.5 to 2-4 *M*) converts the tetranuclear species to a mononuclear ion, $[Zr(H_2O)_8]^{4+}$.

X-ray diffraction studies have established the presence of coordinated water molecules and bridging hydroxo ligands in normal and basic zirconium salts and in certain neutral and anionic complexes.[109] Water and hydroxo-containing compounds that consist of discrete complexes are listed in **Table 1.13**.

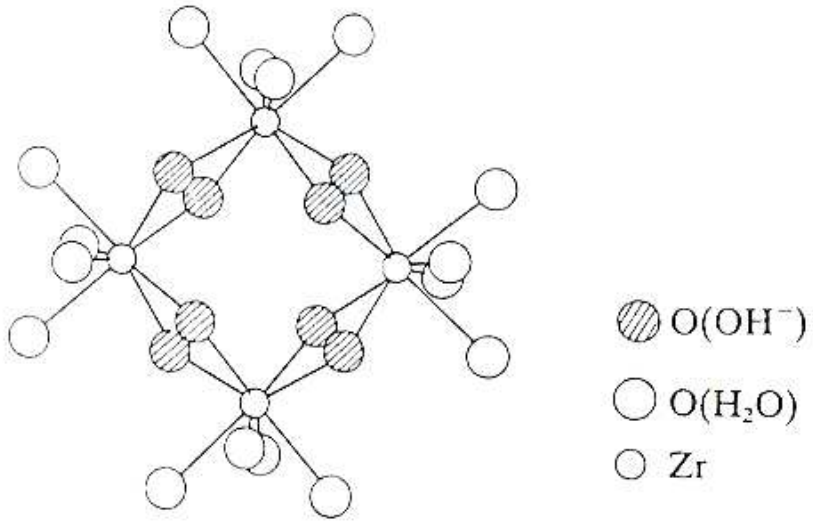

Figure 1.17: Structure of the $[Zr_4(OH)_8(H_2O)_{16}]^{8+}$ cation.[91]

Table 1.13: Aqua and hydroxo complexes of zirconium.[91]

Structural Formula	Coordination Polyhedron
$[Zr(OH)_8(H_2O)_{16}]Cl_8.12H_2O$	dodecahedron
α-$[(H_2O)_4(SO_4)Zr(SO_4)_2Zr(SO_4)(H_2O)_4].2H_2O$	dodecahedron
β-$[(H_2O)_4(SO_4)Zr(SO_4)_2Zr(SO_4)(H_2O)_4].2H_2O$	dodecahedron
$[(H_2O)_4(SO_4)Zr(SO_4)_2Zr(SO_4)(H_2O)_4].6H_2O$	dodecahedron
$K_4[(H_2O)_2(SO_4)_2Zr(SO_4)_2Zr(SO_4)_2(H_2O)_2]$	dodecahedron
$K_6[(CO_3)_3Zr(OH)_2Zr(CO_3)_3].6H_2O$	dodecahedron
$[NH_4]_6[(CO_3)_3Zr(OH)_2Zr(CO_3)_3].4H_2O$	dodecahedron
$[(H_2O)_3F_3ZrF_2ZrF_3(H_2O)_3]$	dodecahedron
$[NMe_4]_2[(H_2O)F_4ZrF_2ZrF_4(H_2O)]$	pentagonal bipyramid
$[Zr(edta)(H_2O)_2].2H_2O$	dodecahedron

1.4.2.4. Oxyhalides (See **Section 1.4.2.1** and **Section 1.4.2.3**)

Zirconium oxyhalides, $ZrOX_2.8H_2O$ (X = Cl or Br), are formed when tetrahalides react with water and may also be isolated from highly acidic aqueous solutions. Much of the understanding of aqueous zirconium chemistry has been based on the study of zirconium oxychloride solutions, previously called zirconyl chloride due to the incorrect interpretation of the existence of the zirconyl ($Zr{=}O^{2+}$) group.[103,110]

1.4.2.5. Sulfates

Due to the high ionic charge to radius ratio, normal salts are extremely difficult to prepare from aqueous solution and may only be isolated if sufficiently acidic.[111] The sulfate ion has a strong affinity for zirconium(IV) and besides normal discrete sulfates, *e.g.*, α-$Zr(SO_4)_2(H_2O)_5$, ε-$Zr(SO_4)_2(H_2O)_5$ and $Zr(SO_4)_2(H_2O)_7$, forms many anionic complexes and basic salts containing 7- or 8-coordinate zirconium. The dodecahedral configuration occurs in the basic sulfate, $Zr_2(OH)_2(SO_4)_3(H_2O)_4$, in which each zirconium is bonded to two hydroxo-groups, two water molecules and four sulfates. In another basic sulfate, $Zr(OH)_2SO_4$ the zirconium has a square antiprismatic configuration with infinite zigzag chains of $[Zr(OH)_2]_n$ which are bridged by sulfato-groups. Basic zirconium sulfates are unlikely to contain discrete complexes.[89,111,112]

Numerous complex sulfates of the type $M_2Zr(SO_4)_3(H_2O)_x$, $M_4Zr(SO_4)_4(H_2O)_x$ and $M_6Zr(SO_4)_5(H_2O)_x$ (M = Na, K, Rb, Cs, or NH_4) have been isolated from aqueous sulfuric acid solutions.[111] X-ray studies show that these complex sulfates can have mono-, di- or polynuclear structures. Cation exchange, solvent extraction and Raman spectroscopic studies of highly acidic zirconium sulfate solutions suggest that these solutions contain a mixture of solution species having from one to four sulfate ligands per zirconium atom.[92]

1.4.2.6. Carbonates

Normal carbonates of zirconium have not been identified although numerous basic carbonates are known. The X-ray structure of $K_6[Zr_2(OH)_2(CO_3)_6(H_2O)_6]$ shows that carbonate groups are covalently bonded to zirconium and infrared (IR) studies on a larger number of basic carbonates suggest that the carbonato-group is always bidentate or bridging but not ionic.[112-114]

1.4.2.7. Alkoxides

Zirconium tetraalkoxides, $Zr(OR)_4$, zirconium chloride alkoxides, $ZrCl_3(OR).nROH$, and mixed alkoxides, *e.g.*, $Zr(OR)(OCMe_3)_3$ and $Zr(OR)_2(OCMe_3)_2$ (R = Me or Et) have been synthesised *via* a number of methods.[115,116] Zirconium tetraalkoxides are highly reactive compounds. They react with water, alcohols, silanols, hydrogen halides, acetyl halides, Lewis bases, aryl isocyanates and other metal alkoxides. With chelating hydroxylic compounds, such as β-diketones, carboxylic acids and Schiff bases, they give complexes of the type $ZrL_n(OR)_{4-n}$. Partial hydrolysis of zirconium alkoxides yields polymeric oxozirconium alkoxides and complete hydrolysis affords hydrated zirconium dioxide.[92]

1.4.2.8. Carboxylates

Zirconium carboxylates include normal, mixed-ligand and basic carboxylates.[117] Normal carboxylates, $Zr(O_2CR)_4$ have been prepared by reaction of $ZrCl_4$ with an excess of hot, anhydrous carboxylic acid.[118] Temperature control appears to be an important factor as intermediate products are obtained at low temperature and thermal decomposition occurs at high temperatures.[119] The tetrakis(carboxylates) rapidly hydrolyse in moist air and

thermally decompose to oxocarboxylato compounds at elevated temperatures.[120] As these compounds are insoluble in most organic solvents they have been assumed to be polymeric, however, molecular weight measurements on some compounds indicate that they are monomeric.[91] Infrared data also suggests that some ligands are chelating rather than bridging.[114,121] Basic carboxylates of the type, $ZrO(O_2CR)_2(H_2O)_x$, $Zr(OH)_3(O_2CR)$, $Zr_2O(O_2CR)_6$ and $Zr_2O(OH)(O_2CR)_5(H_2O)_x$ are also known. They are generally obtained from reactions of zirconium oxychloride with carboxylic acids or acyl chlorides.[122] Dicarboxylic acids precipitate zirconium(IV) from aqueous zirconium oxychloride solutions at pH 2-3 yielding polymeric complexes of composition, $Zr(OH)_3(O_2CRCO_2H)$ {R = CH=CH, C_6H_4, or $(CH_2)_n$ where n = 1,2 or 4}.[123,124]

The best characterised oxalato complex of zirconium is the $[Zr(C_2O_4)_4]^{4-}$ ion, which has been isolated in alkali, alkaline earth, cadmium and lead salts. X-Ray studies have shown that the $[Zr(C_2O_4)_4]^{4-}$ ion has a slightly distorted dodecahedron structure in which the bidentate oxalato ligands span the polyhedral edges.[91] Tris- and pentakis(oxalato) complexes of the type $M_2Zr(C_2O_4)_3.nH_2O$, $M_3H_3Zr(C_2O_4)_5.nH_2O$ and $M_6Zr(C_2O_4)_5.nH_2O$ have also been reported with bidentate and monodentate oxalato ligands.[125] Zaitsev and Bocharev[126] have prepared basic oxalates and have suggested that these complexes may have tetranuclear structures based on the $[Zr_4(OH)_8(H_2O)_{16}]^{8+}$ structure. Divalent metal basic oxalates are of interest as precursors for the preparation of ceramic materials.[125]

1.4.2.9. α-Hydroxycarboxylates

α-Hydroxycarboxylic acids such as glycolic, lactic, malic, tartaric, trihydroxyglutaric and citric acids form stable complexes with zirconium, even in strongly acidic solutions. The complexing ability of the hydroxy acids is attributed to the formation of five-membered chelate rings (**Figure 1.18**).[127] Hydroxoglycolato complexes of composition $Zr_2O(OH)_2(CH_2OHCO_2)_4.nH_2O$ and $Zr(OH)(CH_2OHCO_2)_3.nH_2O$ (n = 3-7) were isolated by mixing 1 *M* solutions of $ZrOCl_2.8H_2O$ and glycolic acid in 1:1, 1:2, 1:3 and 1:4 molar ratios. Infrared spectra indicate that the carboxylate and hydroxyl oxygen atoms are attached to the metal atom, but the detailed structures of these compounds are unknown. The lactato complexes $Zr(CH_3CHOHCO_2)_4$ and $Zr(OH)(CH_3CHOHCO_2)_3$ have been

obtained from 3-5 *M* hydrochloric acid solutions, however, $Zr(CH_3CHOHCO_2)_4$ is easily hydrolysed.

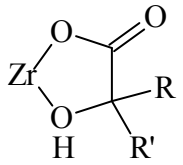

Figure 1.18: The five-membered chelate ring attributed to form when zirconium reacts with α-hydroxycarboxylic acids.[91]

Compounds of composition $Zr(C_4H_2O_6).2H_2O$ and $Zr(C_5H_4O_7).3H_2O$ have been isolated from tartaric and trihydroxyglutaric acid, respectively, and citric acid yielded a mixture of $Zr(C_6H_4O_7).4H_2O$ and $Zr_2(OH)_4(C_6H_4O_7).2H_2O$. Infrared studies of the tartrate and citrate complexes suggest that complex formation involves both the carboxylate and the hydroxyl groups and is accompanied by loss of the hydroxyl protons.[91]

Mandelic acid and its derivatives have long been used as gravimetric analytical reagents for the determination of zirconium and hafnium.[128] The tetrakis(mandelate), $Zr\{(\alpha)\text{-}PhCHOHCO_2\}_4$, is precipitated when a solution of mandelic acid is added to a hot (80-90°C) 5 *M* hydrochloric acid solution of zirconium oxychloride.[129] Larsen and Homeier[121] proposed that the complex has a polymeric structure in which eight-coordinate zirconium atoms are linked by pairs of bridging mandelate ligands (**Figure 1.19**).

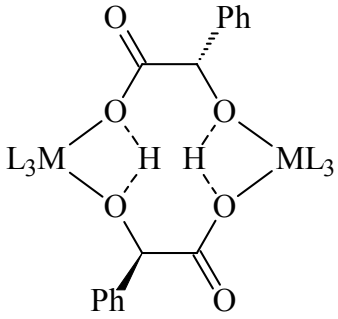

L = $PhCHOHCO_2^-$

Figure 1.19: Polymeric eight-coordinate zirconium atoms linked by bridging (±)-mandelate ligands.[121]

The stability of this complex was attributed to short hydrogen bonds involving the hydroxyl protons and the carboxylate oxygen atoms, only possible when a (±) pair of ligands is present in the bridge. Evidence also includes: (i) the very low solubility and

lack of volatility of the complex, (ii) the presence of broad O-H···O infrared bands centered at 2600, 2300 and 1850 cm^{-1}, and (iii) the fact that the complexes could only be prepared when the ligand was (±)-mandelate. Attempts to prepare Zr{(+)-$PhCHOHCO_2$}$_4$ and Zr{(-)-$PhCHOHCO_2$}$_4$ yielded basic mandelates, $Zr(OH)_x(PhCHOHCO_2)_{4-x}$.[121]

Zr{(±)-$PhCHOHCO_2$}$_4$ precipitates dissolve in solutions of weak bases such as ammonia, organic amines and sodium bicarbonate. The dissolution reaction has been attributed to the salt formation, $[Zr\{(\pm)\text{-}PhCH(O)CO_2\}_4]^{4-}$, by Hahn and Weber[129] due the increased acidity of the OH groups in a chelate structure.

1.4.2.10. β-Diketonates (dik)

A large number of β-diketonate derivatives have been described. These compounds are of the type $[Zr(dik)_4]$, $[Zr(dik)_3X]$, $[Zr(dik)_2X_2]$ and $[Zr(dik)X_3]$ (dik = β-diketonate anion; X = Cl, Br, I, NO_3, or alkoxide) and include acetylacetonate (acac) as the β-diketonate.[130-135]

1.4.3. AQUEOUS ZIRCONIUM CHEMISTRY

There is abundant evidence that zirconium(IV) species are polymerised in aqueous solution.[136] The aqueous chemistry of zirconium is largely based on the species identified in aqueous zirconium oxyhalides (See **Section 1.4.2**). The hard metal nature of zirconium is characterised by hydrolysis and results in a great variety of basic salts as evidenced in zirconium sulfate compounds (See **Section 1.4.2.5**). Studies concur that the most likely discrete aqueous zirconium species to be found are the mono-, $[Zr(H_2O)_8]^{4+}$ and tetranuclear, $[Zr_4(OH)_8(H_2O)_{16}]^{8+}$, species under strongly acidic conditions.[108,109,128] Hydrolytic polymerisation of these species is readily encouraged by ageing, heating, or by reducing the acidity, to precipitate zirconium hydroxides at approximately pH 2. The rate at which polymerisation occurs is important in determining whether gelatinous or easily handleable solid zirconium chemicals are produced. Generally, randomly structured gelatinous products are obtained by the addition of base and are made more ordered and easily hand able chemicals by heating.[92] When the chloride anion is replaced by nitrate or

perchlorate the solution chemistry remains qualitatively the same, however, with sulfates, considerable differences exist, *viz.*, the presence of neutral and anionic complexes.[91] This is attributed to the ability of sulfate to bind strongly with zirconium.[137] The tendency for inorganic ligands to form complexes with zirconium can be summarised by the following two series where it is clear that oxygen is the most important ligand donor atom in the chemistry of zirconium.[89]

$$OH^- > F^- > PO_4^{3-} > CO_3^{2-} > SO_4^{2-} > NO_3^- > Cl^- > ClO_4^-$$

lactate > citrate > glycolate > malate > tartrate

To summarise, in solution the species are invariably polymeric in nature and may be cationic, anionic or neutral with labile ligands.

1.4.4. USES OF ZIRCONIUM AND ITS COMPOUNDS

The use of zirconium metal and its compounds is wide and ever expanding. Approximately 95% of all zirconium consumed is in the form of zirconium compounds, predominantly as zirconia.[138] In the production of pure zirconium chemicals, basic zirconium sulfate is the most important compound due to control over the form in which it is precipitated. It is used for the production of zirconium hydroxide and basic zirconium carbonate, which are precursors for the production of zirconia and a variety of other chemicals.[139,140]

Examples of uses of zirconium compounds may be summarised by **Table 1.14** which demonstrates the variety and versatility of the element and its compounds. Zirconium metal and alloys are used in the chemical industry as components in heat exchangers, acid concentrators, tank shafts, valves, pump housings, fan wheels, high speed agitators, electrode assemblies, steam jet exhausts, tubing, pipes and fittings, spinnerets, and crucibles. Zirconium adds strength, ductility and corrosion resistance to many alloys. Zirconium metal also has low thermal neutron absorption, low radioactivity after exposure, and transparency to thermal neutrons when hafnium-free. High-purity metal and alloys are therefore used as a structural material for nuclear reactors employing pressurised water heat exchangers.[92]

Table 1.14: Uses of zirconium chemicals.[88,138,141-143]

Zirconium Chemical	Uses
Zircon	refractories (bricks, cements), foundry moulds, glaze opacifiers, alkali resistant glass, abrasives
Zirconia	refractories, abrasives, ceramic colours (tiles, sanitary ware), piezoelectrics (spark ignitors, sonar devices, ultrasonics), capacitors, pyroelectrics (fire alarms), ceramics (furnace linings, crucibles, nozzles, extrusion dies), ceramic heating elements, thermal barrier coatings, ceramic fibres, solid electrolytes (oxygen sensors, fuel cells), glass (optical glasses, photochromic lenses, glass polishing), gemstones, catalysts
Zirconium oxy- and hydroxychloride	oil industry (thixotrophic cements, clay stabilisation), wool flameproofing, antiperspirants
Zirconium acetate	wax emulsion water repellents (textiles, paper), photography (gelatin hardening), refractory binding
Ammonium zirconium carbonate	paper (binder insolubiliser), textiles (fungicidal treatment), adhesives (water resistence), floor polishes, emulsion paints, non-wovens, metal conversion coatings
Potassium zirconium carbonate	thixotrophic paints
Zirconium sulfates	leather (tanning), photography, pigment coating (titania)
Zirconium phosphates	kidney dialysis, ion exchange, catalysis
Potassium fluorozirconates	wool flameproofing, metal conversion coatings, metallurgical (alloys)
Basic zirconium sulfate and carbonate	zirconium 'soaps' (paint driers), preparation of other zirconium chemicals
Zirconium tetrachloride	production of zirconium metal, zirconium oxides

1.4.5. ZIRCONIUM TANNING

A report on the tanning properties of molybdenum and tungsten (as the phospho-tungstic acid) was presented in 1928 and it was also common knowledge that salts of silicon, titanium and cerium had some tanning properties. This prompted Somerville[144] to investigate the use of zirconium salts in 1931. It was later discovered that in 1907 Garelli had previously made observations that the nitrates of zirconium and thorium had an affinity for hide powder. Somerville's aim was to produce a white leather without bleaching, which was stable to washing (unlike alum tannages). Somerville discovered that the basic zirconium sulfate was most suitable over the chloride and nitrate salts and that the tanned material was lightfast and he began the development of the tannage on a tannery scale.[144-150]

Sufficient tanning was shown to occur under strongly acidic conditions with offers from 3-10% ZrO_2. The tannage was basified to pH 3 or higher to produce mellow, full leather

especially in the flanks.[9] It was further demonstrated that combination tannages with zirconium as a main or retannage did not adversely affect other tanning agents. The leathers were found to be stable and washable with shrinkage temperatures up to 95°C and they showed satisfactory tensile strength. The use of zirconium results in a good resistance to water and the plumpness lends itself to excellent buffing properties to provide a short, fine, velvety nap.[16] Leathers tanned with zirconium have little stretch and the grain remains fine, while the white colour allows for the production of leathers with pastel colours or brilliant shades with high fastness.[151]

1.4.6. ZIRCONIUM TANNING MECHANISMS

Somerville[144-150] believed that zirconium tanning occurred *via* a cationic species, analogous to chromium tannages, with the interaction on carboxylate groups. Ranganathan and Reed[152-154] demonstrated the error of Somerville's assumption and the importance of anionic and non-ionic species, especially with sulfate ligands. Lassere[155] proposed that fixation of zirconium is independent of carboxyl and amino groups because it does not reach a maximum. The studies were based at pH 4 and no masking agents were present so the hide powder was likely to have retained unfixed hydrous zirconium oxide and this proposal is likely to be flawed.[156]

Ranganathan and Reed[152-154] experimented on deaminated and methylated hide powder to final pH's of 1 and 3. They concluded that the amino groups are indeed likely to take part since only about one third of the normal amount of ZrO_2 was taken up with the corresponding lower shrinkage temperature. The carboxylate groups appear unlikely to participate in binding as esterification and pretanning with chromium did not affect the amount of zirconium taken up, and pretanning with zirconium did not affect the amount of chromium taken up. The presence of citrate as a masking agent decreased the amount of zirconium fixation by either inhibiting the coordination of zirconium with collagen, or by inhibiting zirconium precipitation, or by a combination of the two. More zirconium was fixed at pH 3 than at pH 1 when masked with citrate and if this is not attributed to conventional precipitation then some other pH-dependent process must be at work. Hydrogen bonding or other interactions between complex zirconium ions and collagen were also proposed. However, Hock[157] cautioned that most of Ranganathan and Reed's

work was carried out with such high proportions of chloride ions that their conclusions which related to pure sulfates could be "ill-founded."

Williams-Wynn[158-163] determined that tanning chromium-pretanned material with zirconium oxychloride does not remove any chromium but does lower the shrinkage temperature. Similar material tanned with zirconium oxysulfate removes almost one third of the chromium but leaves the shrinkage temperature unimpaired while citrate masking causes additional loss of chromium with both zirconium salts. The amount of zirconium deposited on chromium pretanned material was found to be significantly reduced and this contrasts directly with the conclusions of Ranganathan and Reed. Williams-Wynn contradicts the latter's findings further by stating that an increase in zirconium fixation resulted from citrate masking. Williams-Wynn reported three different types of tannage depending on the basification pH, (i) a zirconium salt tannage, said to occur at pH values below 1.0 giving shrinkage temperatures of 88-90°C; (ii) a zirconium complex tannage in the pH range 1.6-2.4, producing shrinkage temperatures of 94-98°C; and (iii) a colloidal tannage with hydrated zirconia in the pH range 5.5-6.0 giving a shrinkage temperature of 82-83°C.

Babich and Shapilskaya[164] proposed the zirconium tanning mechanism to be analogous with vegetable tanning and that zirconium tannage was essentially anionic in nature with interaction with cationic amino groups. This electrostatic bonding is later changed to hydrogen bonding, but how and when was not explained.

Hock[157] reconciles the results of others by accepting three mechanisms likely to explain the true tannage of collagen by zirconium:

(i) electrostatic bonding of anionic sites of zirconium species with cationic amino groups,
(ii) electrostatic bonding of cationic sites of zirconium species with anionic carboxylate groups, and
(iii) covalent bonding between zirconium species and oxygen donor atoms present in collagen.

The possibility of further bonding between oxygen atoms of collagen and complex hydrous zirconium hydroxides and oxides cannot be dismissed. The mechanisms can co-exist but individual prominence would depend on the tanning environment.

1.5. A RENEWED INTEREST AND AIMS OF THE PRESENT INVESTIGATION

Environmental concerns regarding the presence of chromium in solid and liquid tannery waste as well as the final disposal of chromium-containing leather goods, has generated a constant search for suitable tanning replacements. There have been few motivations, from a tanner's point of view, to change from the versatile, simple and low cost chrome tannage, however, the lucrative automotive industry's demand for chromium free leather has driven much of this change.

The substitution of chromium by zirconium has not been possible due to the higher price of zirconium tanning salts and more particularly, the plumpness of the leather produced. The use of zirconium is further inconvenienced by the necessity for extremely low pickle pHs due to hydrolysis and precipitation of zirconium salts above pH 2.[16] Despite this a relatively recent resurgence on the use of zirconium is being experienced as the search for "environmentally friendly" tannages continues. New "expensive" technologies become viable as the cost of chrome waste treatment and disposal increases and the public are educated in the dangers of chromium containing materials.

Montgomery[165] described a novel basic chromium-zirconium sulfate complex which yields shrinkage temperatures in excess of 100°C, and Poletaev *et al.*[166] used sodium and ammonium sulfate to increase the dissolution of zirconium. Gaidau *et al.*[167] investigated the use of an aluminium-zirconium-magnesium metal heterocomplex tanning agent. Recently Raghava Rao and coworkers[168-170] have mistakenly assumed that their research, using zirconium oxychloride and ligands such as citrate, tartrate, formate, malate, oxalate and adipate, was new; however, much of this had previously been examined by Somerville and others and dismissed in favour of the use of zirconium sulfates.

The use of reactive chelators to produce alternative mineral tanning agents, considered by Holmes,[171] has been utilised in the development of Organozir by the Central Leather

Research Institute, in India.[172,173] Organozir, is a polymeric ligand-masked zirconium complex, *i.e.*, a mineral syntan, which resists hydrolysis up to pH values of 5 and reaches shrinkage temperatures of 90°C.

The aim of the current investigation included the identification of novel zirconium masking agents that would lower the astringency of the zirconium salts but would not affect the overall uptake of zirconium. Such novel masking agents should also allow the use of zirconium tanning salts within the conventional chrome tanning pH range of 2.5 to 6.7. They should facilitate the use of lower zirconium offers (currently 10% ZrO_2) while improving or maintaining the shrinkage temperatures associated with zirconium tanned material. A process, utilising conventional zirconium tanning salts with novel masking agents, should be optimised to produce leathers that have properties similar to chrome tanned material.

The goal is that processes and chemicals identified should be simple, convenient, easy to implement, and cost effective.

CHAPTER 2:

AN INVESTIGATION OF MASKING AGENTS AND POTENTIAL ZIRCONIUM SYNTANS

A desire to add value to raw materials mined in South Africa has led to a renewed interest in the use of zirconium in the tanning process. The aqueous solution chemistry of zirconium is dominated by hydrolysis, even at low pH. Any attempt to manipulate the pickle, tanning pH and/or the leather properties obtained from zirconium tanning, should logically begin with an investigation of known masking agents (**Section 2.2.1**), followed by an attempt to identify new ones (**Section 2.2.2**). A range of zirconium-based complexes were synthesised and characterised (**Section 2.2.3**) using ligands identified in **Section 2.2.1** and **Section 2.2.2** and their applicability as tanning agents was investigated in **Chapter 3**.

2.1. EXPERIMENTAL

2.1.1. GENERAL METHODS

2.1.1.1. Infrared Spectroscopy (IR)

Infrared spectra were recorded on a Perkin-Elmer Spectrum 2000 FT-IR spectrometer. Mid infrared spectra, using a KBr splitter and a DTG detector, were recorded in the region 4000 to 400 cm^{-1} with typically 16 scans being co-added and averaged at a resolution of 4 cm^{-1}. Samples were run on KBr windows or as KBr mulls.

2.1.1.2. Raman Spectroscopy

Raman spectra were obtained using a Bruker RFS100 FT-Raman Spectrophotometer (UNISA, Pretoria, South Africa) with a Nd:YAG air-cooled laser (1064 nm radiation) and a liquid nitrogen cooled Ge detector. Samples were measured in a powdered form in small aluminium holders or in a small capillary tube. The laser excitation power ranged from 3 to 30 mW, depending on the fluorescence of the sample. This fluorescence also necessitated a larger number of scans; either 512 or 1064 scans were co-added and averaged. The spectra were recorded at a resolution of 4 cm^{-1} with a zero filling factor of 2 in the region 4000 to 100 cm^{-1}.

2.1.1.3. Differential Scanning Calorimetry (DSC)

Differential Scanning Calorimetry was performed using a Perkin-Elmer DSC7 Differential Scanning Calorimeter equipped with a Perkin-Elmer TAC7 PC Instrument Controller. A Sartorius MC5 microbalance was used for the weighing of samples. Samples were measured under nitrogen in open aluminium pans between 25 and 450°C with a heating rate of 10°C per minute.

2.1.1.4. Thermogravimetric (TG) Analysis

Thermogravimetric analysis was performed using a Perkin-Elmer TGA 7 Thermogravimetric Analyzer equipped with a Perkin Elmer TAC7 PC Instrument Controller. Samples were measured under nitrogen in a platinum pan between 50 and 600°C with a heating rate of 10°C per minute.

2.1.1.5. Atomic Absorption (AA) Spectroscopy

Zirconium analyses were attempted using a GBC 909AA spectrophotometer with varying acetylene/nitrous oxide ratios and standards were prepared from a 1000 mg/L zirconium atomic absorption solution (Wirsam, South Africa) and diluted accordingly. The analyses proved irreproducible, necessitating the employment of ICP-MS.

2.1.1.6. Inductively Coupled Plasma Mass Spectrophotometry (ICP-MS)

A Perkin-Elmer Sciex ELAN 6100 Inductively Coupled Plasma Mass Spectrophotometer (UPE, Port Elizabeth) was used for quantitative zirconium measurements. Three isotopes of zirconium were measured (89.904, 90.905 and 93.906). Two standard curves were required and prepared from a 1000 mg/L zirconium atomic absorption solution (Wirsam, South Africa) and diluted accordingly, corresponding to zirconium concentrations below 1 ppm and for concentrations between 1 and 5 ppm. Standard curves were run after every ten samples measured.

2.1.1.7. Microanalysis

Carbon, hydrogen and nitrogen combustion microanalyses were performed using a Fisons Elemental Analyser 1108 CHNS-O (UCT, Cape Town, South Africa).

2.1.1.8. Mass Spectrophotometry (MS)

Low resolution mass spectra were obtained using a Finnigan Mat LCQ ion trap mass spectrometer equipped with an electrospray ionisation source.

2.1.1.9. Nuclear Magnetic Resonance Spectroscopy (NMR)

All ^{1}H and ^{13}C NMR spectra were run in $CDCl_3$ on an Avance Bruker AMX 400 MHz spectrometer using solvent reference peaks (δ_H 7.25 and δ_C 77.0 ppm).

2.1.1.10. X-Ray Powder Diffraction (XRPD)

X-Ray Powder Diffraction was measured at RT using a Seifert JSO-DEBYEFLEX 1001 power supply and CuK_α radiation (λ = 1.54Å) with a Zn filter. The samples were packed in an aluminium plate to a depth of 1 mm and were scanned over a 2θ range of 65°. The diffractometer was a Phillips PM8000 with a scintillation counter.

2.1.1.11. pH

A Mettler Toledo MP 225 pH meter was used for all pH measurements.

2.1.1.12. Chemicals

All chemicals with chiral centres were used as racemic mixtures unless stated otherwise. Zirconium oxychloride octahydrate was obtained from BDH Chemicals Ltd (Poole, UK). All other chemicals were obtained from Sigma-Aldrich (St Louis, USA).

2.1.2. INVESTIGATION OF COMMON MASKING AGENTS[152]

Zirconium oxychloride (0.30g, 0.93 mmol) was dissolved in water (10 mL) and masking agent (0.93 mmol) was added with stirring to obtain a masking agent:zirconium ratio of 1:1. Solutions were then titrated with 0.2 ***M*** NaOH and the pH value at which precipitation was observed was recorded.

2.1.3. SYNTHESIS OF SELECTED 4-SUBSTITUTED MANDELIC ACIDS[174,175]

4-Chloro- and 4-bromomandelic acids were synthesised according to the synthesis outline in **Figure 2.1**. Attempts to synthesise amino-, carboxy-, nitro- and aldehydic 4-substituted mandelic acids in a similar manner were unsuccessful as polymerisation of the substituted benzaldehydes occurred during the addition of sodium bisulfite. Nitration of mandelic acid was attempted using nitric acid[176] but oxidation of the secondary alcohol occurred, to produce 4-nitrobenzoic acid.

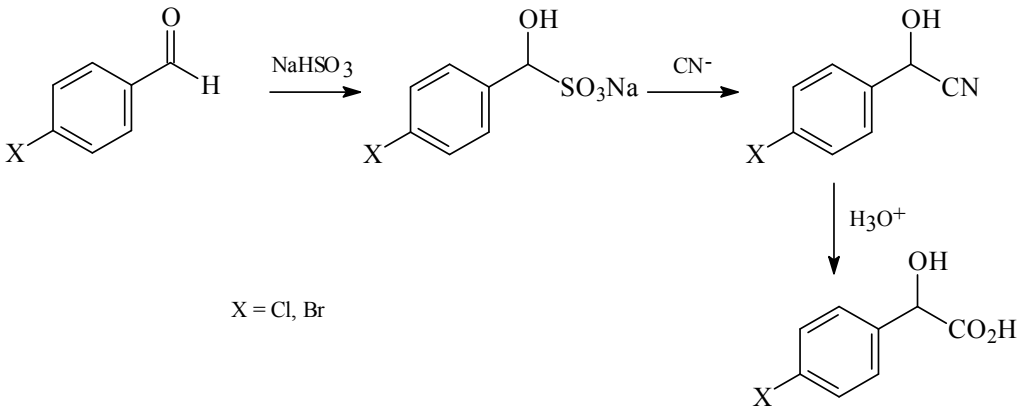

Figure 2.1: Synthesis outline of 4-chloro- and 4-bromomandelic acid.

2.1.3.1. 4-Bromomandelic Acid

A saturated sodium bisulfite solution was added to 10 mL aqueous 4-bromobenzaldehyde solution (4.00 g, 21.6 mmol) in an erlenmeyer flask (100 mL) and stirred until precipitation was complete. The resultant adduct was filtered, washed with water and dried. The adduct was dissolved in the minimum amount of water with stirring and 5 mL potassium cyanide solution (1.41 g, 21.7 mmol) was added over ten minutes. The crude 4-bromomandelonitrile was isolated using a separating funnel and placed in a 12 cm evaporating dish. The aqueous phase was extracted using toluene, the toluene evaporated, and the residual crude 4-bromomandelonitrile added to the main portion in the evaporating dish.

Concentrated hydrochloric acid (32%) was added to the evaporating dish and hydrolysis was allowed to proceed in the cold for twelve hours, after which the mixture was heated on a steam bath to dryness. The product was cooled and allowed to air-dry for one day. The mixture was washed twice with hot toluene. The toluene extract was cooled in ice and the 4-bromomandelic acid crystals filtered under vacuum. Further amounts of 4-bromomandelic acid were obtained when the toluene solution was concentrated under vacuum and cooled in ice. Pure white crystals of 4-bromomandelic acid were obtained after recrystallisation from toluene (2.89g, 58%), m.p. 117.1°C (lit.,[177] 117-119°C); ν_{max}/cm^{-1} 1715 (C=O); δ_H 5.22 (1H, s, C*H*OH), 7.32 and 7.54 (4H, 2xd, ArH); δ_C 72.33 (CHOH), 123.29, 128.65, 132.25 and 136.91 (ArC) and 176.20 (C=O); *m/z* 232 (M^+) and 185 (100%).

2.1.3.2. 4-Chloromandelic Acid

A saturated sodium bisulfite solution was added to 10 mL aqueous 4-chlorobenzaldehyde solution (4.00 g, 28.5 mmol) in an erlenmeyer flask (100 mL) and stirred until precipitation was complete. The resultant adduct was filtered, washed with water and dried. The adduct was dissolved in the minimum amount of water with stirring and 5 mL potassium cyanide solution (1.86 g, 28.6 mmol) was added over ten minutes. The crude 4-chloromandelonitrile was isolated using a separating funnel and placed in a 12 cm evaporating dish. The aqueous phase was extracted using toluene, the toluene

evaporated, and the residual crude 4-chloromandelonitrile added to the main portion in the evaporating dish.

Concentrated hydrochloric acid (32%) was added to the evaporating dish and hydrolysis was allowed to proceed in the cold for twelve hours, after which the mixture was heated on a steam bath to dryness. The product was cooled and allowed to air-dry for one day. The mixture was washed twice with hot toluene. The toluene extract was cooled in ice and the 4-chloromandelic acid crystals filtered under vacuum. Further amounts of 4-chloromandelic acid were obtained when the toluene solution was concentrated under vacuum and cooled in ice. Pure white crystals of 4-chloromandelic acid were obtained after recrystallisation from toluene (2.77g, 52%), m.p. 124.5°C (lit.,[177] 122-123°C); ν_{max}/cm^{-1} 1720 (C=O); δ_H 5.22 (1H, s, C*H*OH), 7.34 and 7.39 (4H, 2xd, ArH); δ_C 71.91 (CHOH), 127.95, 128.92, 134.77 and 135.93 (ArC) and 176.30 (C=O); *m/z* 185 (M^+) and 141 (100%).

2.1.4. GENERATION OF SOLUTIONS FOR THE INVESTIGATION OF POTENTIAL ZIRCONIUM MASKING AGENTS (LIGANDS)

Zirconium oxychloride (0.30 g, 0.93 mmol) was dissolved in water (3 mL) and conc. HCl (1 mL) was added with stirring. Ligand (3.72 mmol, a 4:1 ligand:zirconium ratio) was dissolved in water (3 mL) and both solutions were warmed to approximately 80°C. The ligand solution was added to the zirconium slowly (5 min) and allowed to age for 48 h at RT. Mixing of the two solutions and ageing resulted in the formation of either a clear solution or a precipitate.

2.1.4.1. Treatment of Clear Solutions

The zirconium:ligand solution was titrated in duplicate with 0.2 ***M*** NaOH. The average precipitation pH was recorded.

2.1.4.2. Treatment of Precipitates

The zirconium:ligand precipitates were filtered and washed with ethanol. The precipitates were allowed to air dry at RT and then dried further in a vacuum desiccator.

The precipitates were then characterised using infrared spectroscopy and DSC to determine if complexation had occurred.

Zirconium:ligand precipitation solutions (excluding those shown to be starting material only) were generated as before and titrated using 0.2 ***M*** NaOH. The pHs at which the precipitates redissolved were recorded as a range.

2.1.5. Synthesis of Zirconium Complexes for Characterisation

Zirconium oxychloride (0.30 g, 0.93 mmol) was dissolved in water (3 mL) and conc. HCl (1 mL) was added with stirring. Ligand (3.72 mmol for a 1:4 zirconium:ligand ratio and 1.81 mmol for a 1:2 zirconium:ligand ratio, respectively) was dissolved in water (3 mL). The zirconium and ligand solutions were warmed to approximately 80°C. The ligand was added drop-wise to the zirconium solution (5 min) with stirring; cooled and allowed to age for 48 h at RT. The gelatinous amorphous precipitates were filtered using a Buchner funnel with cellulose-acetate filters (50 mm diameter, 0.45 μm pore size), washed with ethanol and dried in a vacuum desiccator over silica.

2.2. Results and Discussion

The results and discussion which follow include the initial investigation of common masking agents (**Section 2.1.1**), followed by an extensive investigation of potential masking agents (**Section 2.1.2**) and, finally, the synthesis, isolation and characterisation of a series of potential zirconium-based tanning complexes and precursors (**Section 2.1.3**).

2.2.1. An Investigation of a Selection of Common Masking Agents

In order to lower the astringency of mineral tanning agents and to raise the pH at which precipitation occurs, masking agents are commonly used. The inclusion of organic acids into a mineral tanning process results in a less cationic complex and this decreases the affinity of the mineral for collagen. The desired requirement of a masking agent is to raise the pH of the onset of precipitation to allow the direct reaction of the tanning agent

with collagen instead of precipitating within the structure. This "softens" the astringency of the tanning reaction and allows better penetration and distribution of the tanning chemical.[7]

The most common masking agents are formic acid/sodium formate and acetic acid/sodium acetate which are used extensively for chromium tanning.[16] Zirconium, however, does not respond well to these masking agents and hydroxycarboxylic acids, *e.g.*, lactic and citric acid and their conjugate bases, are favoured.[9] The present study confirmed previous reports that the molar ratio of masking agent to metal does have an effect on the precipitation pH and a ratio of 1:1 was utilised for the comparative precipitation experiments as the ratio falls within the ratios generally utilised (0.5-2:1).[9]

Solutions were prepared and treated according to **Section 2.1.2**. The results show a correlation with the literature values (**Table 2.1**) and corroborate the common use of lactic and citric acid as masking agents for zirconium tanning. The results also indicate the dramatic effect the sulfate ion may play in tanning and masking.

Table 2.1: Experimental zirconium precipitation pHs for selected masking agents and related literature values.

		Present Work: $ZrOCl_2.8H_2O$		**Literature**
Masking Agent	**K_{a1} (x 10^{-4})**	**Initial pH**	**Precipitation pH 1:1**	**Precipitation pH* 1:1**
none	-	1.53	1.71	1.5[9] **2.35**[152]
formic acid	1.77	1.41	1.80	1.7[9] **2.85**[152]
acetic acid	0.176	1.45	1.85	1.92[9] **2.70**[152]
glycolic acid	1.48	1.35	7.45	11.4[152]
lactic acid	1.48	1.39	5.07	5.7[152]
citric acid	7.45	1.28	no ppt	no ppt[152]

* Literature values in bold refer to the use of zirconium sulfates

The effect may be demonstrated by the higher precipitation pH values achieved by Ranganathan and Reed,[152] as zirconium sulfate was utilised as the source of zirconium, compared to the results from Bienkiewicz[9] and the current investigation, which both made use of zirconium oxychloride. The sulfate ion complexes zirconium more strongly

than chloride, nitrate or perchlorate and has also been shown to displace hydroxy groups from hydrolysed zirconium(IV) species and to form sulfate bridges between zirconium ions.[178] The addition of the sulfate ion causes a disproportionate increase in the number of neutral and anionic species and is instrumental as a masking agent in zirconium tanning.[128]

Ranganathan and Reed[154] postulated that carboxylic acids with an "available" hydroxyl group are necessary for complexation with zirconium, as experiments with hydracrylic acid (**Figure 2.2**) showed no masking ability. β-Hydroxycarboxylic acids are known to be more stable as the lactone.

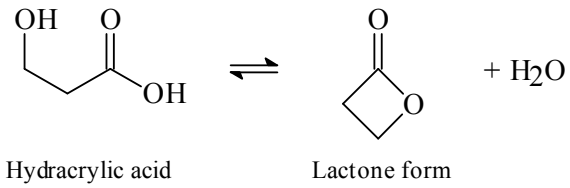

Figure 2.2: Hydracrylic acid and its lactone.

Glycolic, lactic and citric acid showed promise as masking agents for zirconium but the increased stability of the complexes formed is known to lower the uptake of the zirconium by the pelt.[16] The uptake of zirconium varies according to the complexing strength of the masking agent in question. It is commonly accepted that approximately 70% of the conventionally masked chromium added in the tanning process complexes with the pelt and the remainder is lost to the effluent plant.[2] Conventional zirconium tannages result in a 95% uptake of the zirconium.[9] The precipitation pHs were elevated, however, indicating that hydroxide ion displacement of the ligands was hindered and masking had taken place.

A thorough investigation of potential masking agents (ligands) was undertaken (**Section 2.2.2**) in an attempt to identify new masking agents for zirconium tanning and to determine the type and location of functional groups most suitable to complex zirconium(IV) in aqueous solution.

2.2.2. INVESTIGATION OF POTENTIAL ZIRCONIUM MASKING AGENTS

Normally the visual indicators of transition metal complexation are the formation of a precipitate and/or a colour change as ligands displace coordinated water. Zirconium(IV) compounds have a d^0 configuration and therefore produce white precipitates or colourless aqueous solutions. Consequently, a colourless solution neither indicates nor denies the formation of a complex. A precipitate does indicate complexation although the complex would appear to be ineffective as a tanning agent if it is insoluble in water. The formation of a precipitate does, however, give an indication of the functional groups that are important for complexation and therefore highlights potential ligands for use as masking agents.

The literature[91,92] indicates the prevalence of oxygen, nitrogen and chlorine donor atoms in zirconium coordination chemistry. Zirconium is a type-a (or hard) acid and in aqueous solution oxygen ligands dominate zirconium chemistry. Consequently, the functional groups focused on in the present investigation were alcohols (**Section 2.2.2.2**) and carboxylic acids (**Section 2.2.2.3**), including hydroxy- and amino-substituents.

2.2.2.1. Generation of Zirconium-Ligand Solutions for Investigation

Zirconium oxychloride was used for all experiments to limit the influence of the anion. A number of complexation methods were attempted but due to the hard acid nature of zirconium, a method based on the gravimetric determination of zirconium with mandelic acid was used to minimise hydrolysis of the zirconium. A zirconium to ligand ratio of 1:4 was used to maximise the effect of the masking agent under investigation. Solutions were prepared and treated according to **Section 2.1.4**.

2.2.2.2. Potential Alcohol Ligands

The alcoholic compounds were selected (**Figure 2.3**) in an attempt to encompass a range of bonding possibilities with zirconium. Ethanol and phenol are monodentate ligands and ethylene glycol, catechol, L-ascorbic acid, D-glucose and D-galactose were selected as potential di- and polydentate ligands. The ligands incorporated 1,2- and 1,3-diols with

free and/or restricted rotation about the C-C axis, and di- and polyols with fixed orientations.

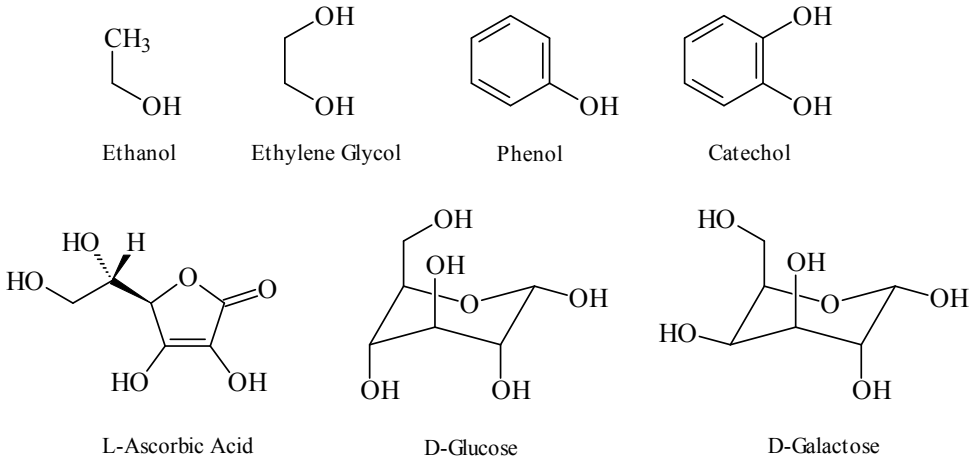

Figure 2.3: Potential alcohol ligands investigated.

The results of the pH investigation are shown in **Table 2.2**. All hydroxy compounds can act as ligands, however, the selected hydroxy compounds showed little to no effect on the precipitation pH. In alcohol solutions, metal ions may be solvated just as in water, but the likelihood is that the alcohol ligands are displaced by water in aqueous solution and have little to no interaction with the zirconium. Alcohols, like water, are both weak Brønsted acids and weak Lewis bases and have very small K_a values, *e.g.,* 1×10^{-18} for ethanol.[179]

Table 2.2: Precipitation pHs of zirconium-alcohol solutions.

Ligand	K_{a1}	Initial pH	Precipitation pH
None	-	0.93	1.70
ethanol	1×10^{-18}	0.69	1.73
ethylene glycol	6.03×10^{-15}	0.55	1.78
phenol	1.28×10^{-10}	0.81	1.83
catechol	3.98×10^{-10}	0.78	1.78
L-ascorbic acid	7.94×10^{-5}	0.53	2.59
D-glucose	1.35×10^{-13}	0.62	2.14
D-galactose	3.55×10^{-13}	0.87	2.39

The precipitation pHs for D-glucose and D-galactose were considerably higher than the remainder of the alcohols, although not significantly enough to be considered as a desirable masking agent (**Section 1.5**). Glucose is known to increase the solubility of

calcium in lime liquors and a similar interaction may be responsible for the increase in precipitation pH of zirconium.[180]

2.2.2.3. Potential Carboxylic Acid Ligands

Hydrogen bonding is responsible for the high water solubility of the simple carboxylic acids with less than five carbons. Even though the carboxylic acids are weak acids, they are many orders of magnitude stronger than the corresponding alcohols, *e.g.*, the K_a of acetic acid is 10^{11} times larger than that of ethanol. The stabilisation energy of the carboxylate anion is substantially greater than that of the acid because the anion is a resonance hybrid of two energetically equivalent structures, whereas the acid is represented by a hybrid of nonequivalent structures (**Figure 2.4**).[179]

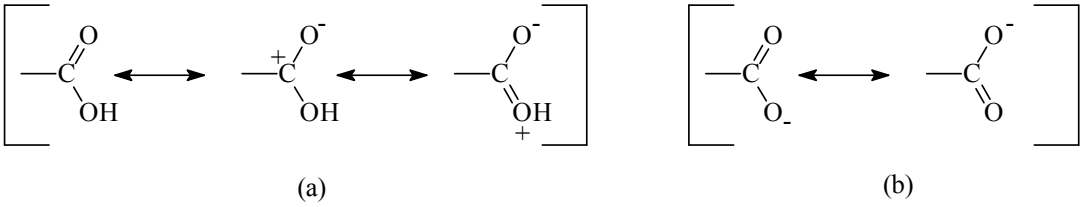

Figure 2.4: Resonance structures of (a) carboxylic acids and (b) the carboxylate anion.

Substituent groups can have a profound effect on acid strength (reflected in K_a) by inductive and resonance effects. The inductive effect of one carboxyl group enhances the acidity of the other in dicarboxylic acids, $HO_2C\text{-}(CH_2)_n\text{-}CO_2H$, where $n<5$. The second acid dissociation constant of the small dicarboxylic acids is smaller than the K_a for acetic acid, except in the case of oxalic acid.[179]

The carboxylates are a very important class of ligands with the most common forms of bonding being unidentate, symmetrical chelate and symmetrical *syn-syn* bridging (**Figure 2.5**).[181]

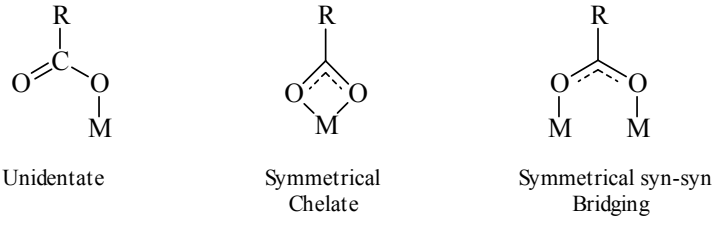

Figure 2.5: The most common forms of carboxylate bonding.[181]

Carboxylic acid ligands were selected in an attempt to encompass as many bonding possibilities with zirconium as possible. Ligand groups investigated include: (i) mono- and dicarboxylic acids (**Section 2.2.2.3.1**), (ii) hydroxycarboxylic acids (**Section 2.2.2.3.2**), and (iii) aminocarboxylic acids (**Section 2.2.2.3.3**).

2.2.2.3.1. Mono- and Dicarboxylic Acid Ligands

The potential ligands investigated include aliphatic and aromatic mono- and dicarboxylic acids (**Figure 2.6**).

The results of the pH investigation are shown in **Table 2.3**. Oxalic, phthalic and terephthalic acid cause precipitation upon mixing with zirconium solutions. Infrared and DSC were utilised to show that the phthalic and terephthalic acid precipitates consisted of free ligand only. The low pH of the reaction solution was likely to have decreased the solubility of the aromatic dicarboxylic acids to such an extent that they precipitated upon mixing.

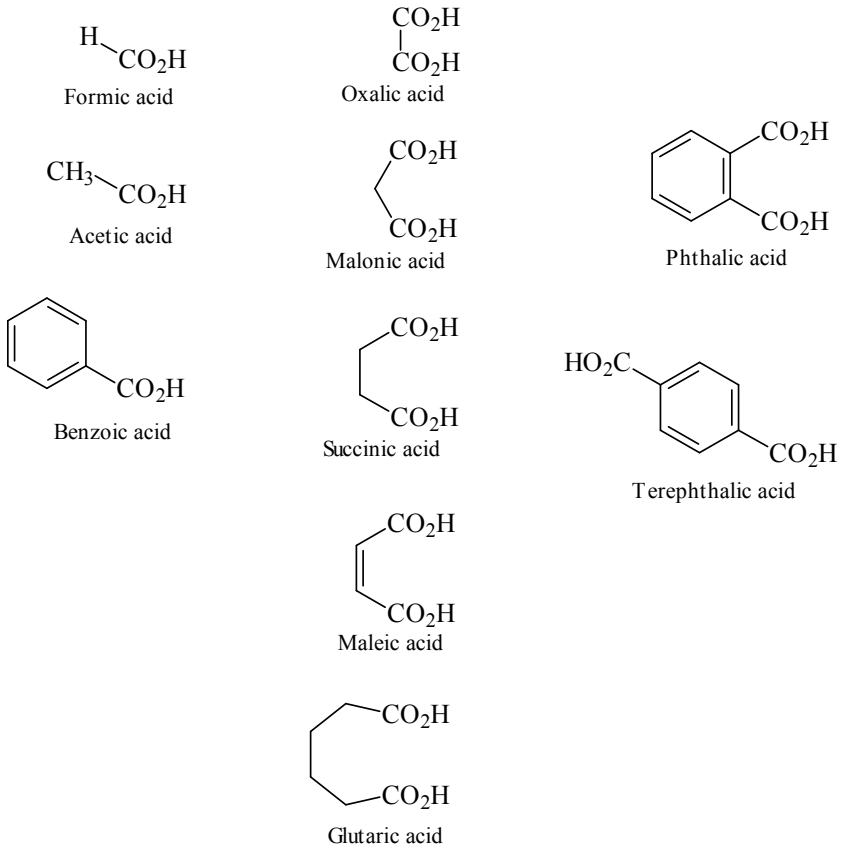

Figure 2.6: Potential mono- and dicarboxylic acid ligands investigated.

Table 2.3: Precipitation pHs of zirconium-carboxylic acid solutions.

Ligand	K_{a1}	Initial pH	Precipitation pH
None	-	0.93	1.70
Formic Acid	1.77×10^{-4}	0.52	2.01
Acetic Acid	1.76×10^{-5}	0.43	1.99
Benzoic Acid	6.46×10^{-5}	0.90	1.93
Oxalic Acid	5.90×10^{-2}	0.69	0.69
Malonic Acid	1.49×10^{-2}	0.77	2.22
Succinic Acid	6.89×10^{-5}	0.94	1.94
Maleic Acid	1.42×10^{-2}	0.75	2.18
Glutaric Acid	4.58×10^{-5}	0.81	1.98
Phthalic Acid	1.30×10^{-3}	0.90	0.90
Terephthalic Acid	3.10×10^{-4}	0.95	0.95

Malonic acid increased the precipitation pH to 2.22 and this may be attributed to its relatively large K_a value and to its ability to chelate *via* a six-membered ring. Maleic acid has a similarly large K_a value to malonic acid but would chelate to form a seven-membered ring and increased the precipitation pH to a similar value of 2.18. Succinic acid, which could also form seven-membered rings upon chelation, has a smaller K_a than maleic acid and only achieved a precipitation pH of 1.94. Oxalic acid forms five-membered chelate ring structures and has a relatively large K_a (similar to malonic and maleic acid) and is known to produce complexes with zirconium. This suggests that the acidity of the ligand (ability to form an anion) and ability to form a five-membered chelate are important to achieve a zirconium-ligand interaction in aqueous solution.

2.2.2.3.2. Potential Hydroxycarboxylic Acid Ligands

Hydroxycarboxylic acids combine the complexing ability of the hydroxy and carboxylic acid functionalities. The hydroxycarboxylic acids tested were divided into three groups: (i) hydroxybenzoic acids, (ii) α-hydroxycarboxylic acids, and (iii) β-hydroxycarboxylic acids.

2.2.2.3.2.1. Potential Hydroxybenzoic Acid Ligands

Hydroxybenzoic acids are well known chelators of metals,[182,183] and historically gallic and tannic acid were complexed with iron(II) to produce iron gall ink.[184] The hydroxybenzoic acids presently investigated are shown in **Figure 2.7**.

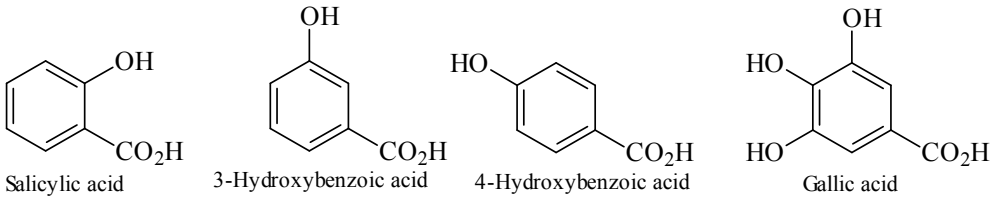

Figure 2.7: Potential hydroxybenzoic acid ligands investigated.

Table 2.4 indicates the lack or limited ability of the hydroxybenzoic acids to complex to zirconium under the conditions used. Precipitations that occurred upon the addition of ligand to zirconium solutions were shown using infrared and DSC to consist of free ligand only, and included the 3- and 4-hydroxybenzoic and salicylic acids.

Gallic acid did not precipitate upon the addition of zirconium solution and the resulting solution was titrated with 0.2 ***M*** sodium hydroxide solution. The onset of precipitation was measured at a pH of 2.11 (**Table 2.4**).

Table 2.4: Precipitation pHs of zirconium-hydroxybenzoic acid solutions.

Ligand	K_{a1}	Initial pH	Precipitation pH
None	-	0.93	1.70
Salicylic Acid	1.07×10^{-3}	0.83	0.83
3-Hydroxybenzoic Acid	8.7×10^{-5}	0.85	0.85
4-Hydroxybenzoic Acid	3.3×10^{-5}	0.74	0.74
Gallic Acid	3.9×10^{-5}	0.67	2.11

The use of hydroxybenzoic acids as masking agents for zirconium tanning was not considered further.

2.2.2.3.2.2. Potential α-Hydroxycarboxylic Acid Ligands

The α-hydroxycarboxylic acids are a class of ligands extremely effective at chelating metals.[185] They are an important group of biogenic ligands which take part in many basic biochemical processes, *e.g.*, the Krebs cycle, the Cori cycle and photorespiration.[186] The acids investigated (**Figure 2.8**) include mono-, di- and tricarboxylic acids.

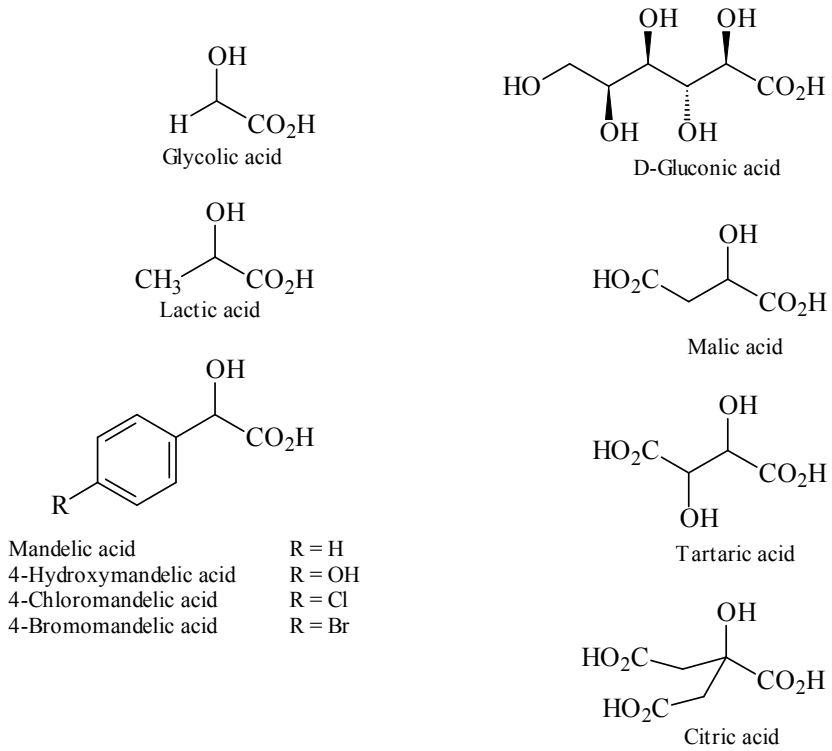

Figure 2.8: Potential α-hydroxycarboxylic acid ligands investigated.

The results of the precipitation pH studies of the α-hydroxycarboxylic acids are shown in **Table 2.5**. Precipitation occurs during the generation of the zirconium-ligand solutions for many of the ligands. The complexes produced cannot be used for tanning under these circumstances as the pH is extremely low and the complexes insoluble.

Table 2.5: Precipitation pHs of zirconium-α-hydroxycarboxylic acid solutions.

Ligand	K_{a1}	Initial pH	Precipitation pH
None	-	0.93	1.70
Glycolic Acid	1.48×10^{-4}	0.76	0.76
Lactic Acid	1.48×10^{-4}	0.41	0.41
Mandelic Acid	1.40×10^{-4}	0.88	0.88
4-Hydroxymandelic Acid	3.09×10^{-4}	0.50	0.50
4-Chloromandelic Acid	7.24×10^{-4}	0.61	0.61
4-Bromomandelic Acid	7.24×10^{-4}	0.53	0.53
Malic Acid	3.90×10^{-4}	0.30	-
Citric Acid	7.45×10^{-4}	0.44	-
D-Gluconic Acid	4.46×10^{-4}	0.74	-
L-Tartaric Acid	1.04×10^{-3}	0.84	-

The only α-hydroxycarboxylic acids that did not precipitate on complexation with zirconium have one or more hydrophilic hydroxy- or carboxylic acid functional group in addition to the chelating α-hydroxycarboxylic acid moiety. Complexation of the malic, D-gluconic, L-tartaric and citric acids with zirconium was confirmed by the ability of these ligands to resist the precipitation of zirconium to pHs in excess of 11 (**Table 2.5**). The water solubility of the malic, D-gluconic, L-tartaric and citric acid complexes shows great potential for their use as masking agents for zirconium and lactic and citric acid are already in use as masking agents.[16]

The α-hydroxycarboxylic acid:zirconium precipitates were also titrated with 0.2 ***M*** sodium hydroxide and were discovered to dissolve at elevated pHs (**Table 2.6**) similarly to the behaviour of zirconium α-hydroxycarboxylates treated with ammonia.[129,187] The latter amorphous gelatinous products were believed to lead to hydrolytic polymerisation and salt formation as pH is increased. The dissolution of these structures in alkali solutions has been attributed by Hahn and coworkers[129,187] to the formation of a soluble salt due to the removal of the α-OH proton according to:

$$Zr\{PhCHOHCO_2\}_4 + 4OH^- \rightarrow [Zr\{PhCH(O)CO_2\}_4]^{4-} + 4H_2O$$

Table 2.6: pH range where zirconium-α-hydroxycarboxylate precipitates dissolve upon basification.

Zr:Ligand Complex	K_a	Soluble pH
Glycolate	1.48×10^{-4}	5.0 - 5.5
Lactate	1.48×10^{-4}	7.5 - 8.0
Mandelate	1.40×10^{-4}	8.0 - 8.4
4-hydroxymandelate	3.09×10^{-4}	6.0 - 7.0
4-chloromandelate	7.24×10^{-4}	8.5 - 10.0
4-bromomandelate	7.24×10^{-4}	8.5 - 10.0

Attempts, by Larsen and Homeier,[121] to find a solvent to recrystallise the zirconium complexes were unsuccessful and this was attributed to the presence of polymeric zirconium mandelate structures synthesised in aqueous media. Larsen and Homeier also found that zirconium mandelates produced from $ZrCl_4$ and racemic mandelic acid in acetonitrile produced a water soluble seven coordinate tetrakis structure where one of the mandelate ligands is monodentate and does not coordinate *via* the OH (See **Section 1.4.2.9** and **Section 3.2.1**).

2.2.2.3.2.3. Potential β-Hydroxycarboxylic Acid Ligands

β-Hydroxycarboxylic acids are commonly used as starting materials for the production of chiral compounds.[188] Many aliphatic β-hydroxycarboxylic acids cyclise to form the lactone and may not be effective chelators. The ligands investigated include a straight chain aliphatic, *viz.*, 3-hydroxybutyric acid, and two alicyclic carbohydrate ligands, *viz.*, D-glucuronic and D-galacturonic acid (**Figure 2.9**) which cannot form the lactone.

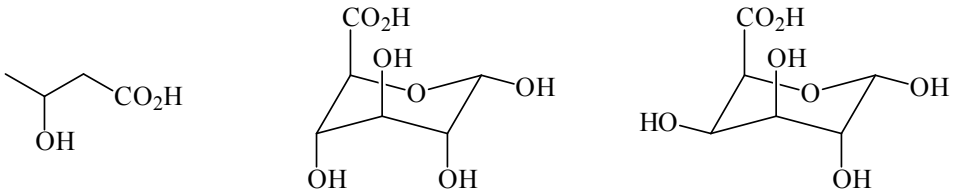

3-Hydroxybutyric acid D-Glucuronic acid D-Galacturonic acid

Figure 2.9: Potential β-hydroxycarboxylic acid ligands investigated.

3-Hydroxybutyric acid had no observable effect on the precipitation pH of zirconium as straight chain β-hydroxycarboxylic acids are likely to be more stable as the cyclic lactone. The precipitation pHs of D-glucuronic and D-galacturonic acid were relatively high compared to the majority of the ligands studied but still result in precipitation well below the desired pH range for effective masking agents (**Section 1.5**).

Table 2.7: Precipitation pHs of zirconium-β-hydroxycarboxylic acid solutions.

Ligand	K_a	Initial pH	Precipitation pH
None	-	0.93	1.70
3-Hydroxybutyric Acid	1.9×10^{-5}	0.86	1.78
D-Glucuronic Acid	5.01×10^{-4}	0.90	2.36
D-Galacturonic Acid	5.01×10^{-4}	0.64	2.43

2.2.2.3.3. Potential Aminocarboxylic Acid Ligands

α-Aminocarboxylic acids (amino acids) are the building blocks of proteins, and therefore of collagen. Zirconium has shown an affinity for nitrogen donor atoms although this is predominantly in the absence of water.[91] Zirconium has shown a tendency to complex with α-hydroxycarboxylic acids and the substitution of hydroxy groups for amino groups was a logical progression for the investigation.

A representative group of aminocarboxylic acids was investigated (**Figure 2.10**) with glycine, glutamic acid and anthranilic acid selected as aminocarboxylic acid equivalents of glycolic, malic and salicylic acid, respectively.

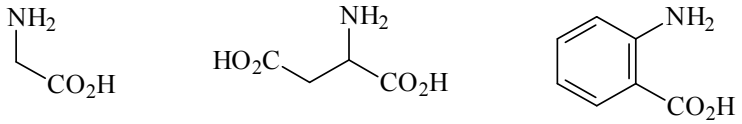

Glycine Glutamic acid Anthranilic acid

Figure 2.10: Potential aminocarboxylic acid ligands investigated.

The results in **Table 2.8** indicate that precipitation did occur upon the addition of anthranilic acid, but similarly to salicylic acid, this was shown through use of DSC and infrared to be free ligand only. The elevation of the precipitation pH of zirconium with glycine and glutamic acid was insignificant and complexation with zirconium was unlikely as amino groups are protonated at low pH and therefore lack the available lone pair of electrons necessary to participate in complexation.

Table 2.8: Precipitation pHs of zirconium-aminocarboxylic acid solutions.

Ligand	K_a	Initial pH	Precipitation pH
None	-	0.93	1.70
Glycine	1.67×10^{-10}	0.83	1.88
Glutamic Acid	7.41×10^{-3}	0.79	1.90
Anthranilic Acid	1.07×10^{-7}	0.65	0.65

The results of the investigation of potential zirconium masking agents are summarised in **Section 2.2.2.4**.

2.2.2.4. Summary of the Investigation of Potential Zirconium Masking Agents

The investigation of potential masking agents may be summarised according to **Figure 2.11**. The ligands that precipitated without coordinating with zirconium were identified by infrared and melting points (using DSC), and include salicylic acid, 3-hydroxybenzoic acid, 4-hydroxybenzoic acid, phthalic acid, terephthalic acid and anthranilic acid, and were consequently not investigated further.

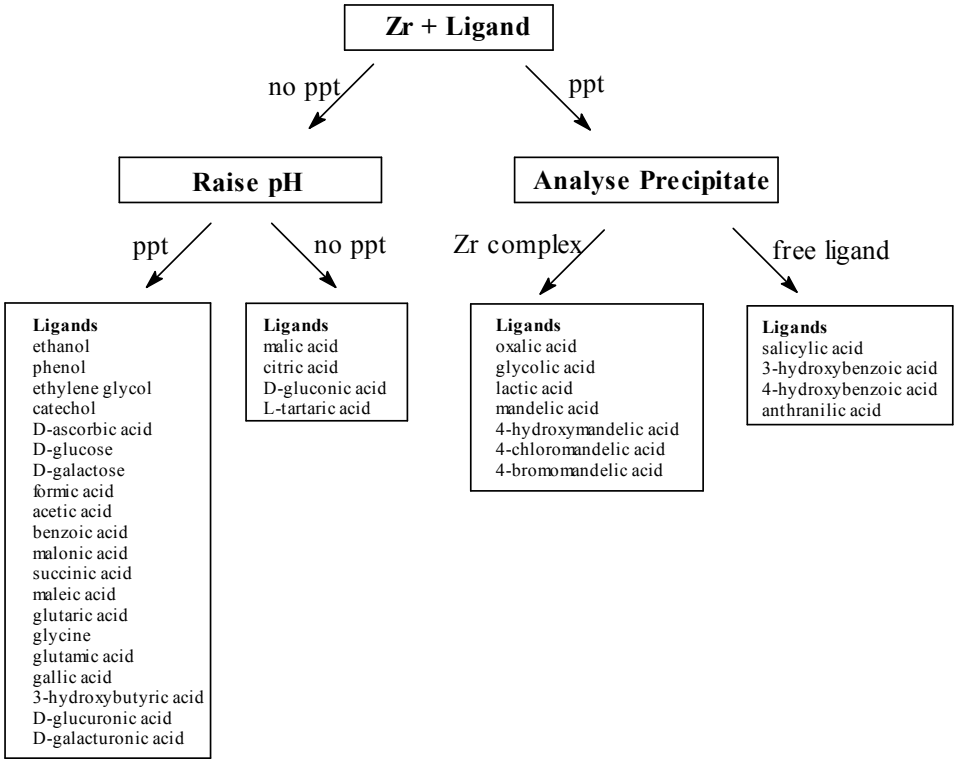

Figure 2.11: A summary of the investigation of potential masking agents.

The ligands which did not precipitate on mixing but precipitated upon titration with sodium hydroxide showed limited masking ability. **Figure 2.12** shows a plot of precipitation pHs versus pK_a of the respective ligands. **Series 1** represents the alcohol and hydroxycarboxylic acid ligands and **Series 2** represents the carbohydrate ligands. It is evident that as the pK_a of the ligands decrease, the precipitation pH is increased and the masking ability is improved.[189] The increased acidity of the ligands favours the stability of the carboxylate anion, which is responsible for complexation. This is supported by the fact that previously trifluoroacetic acid (pK_a = 5.9 x 10^{-1}) was tentatively shown to precipitate zirconium from solution.[119]

There were two exceptions to **Series 1** and they have been identified independently as: (i) 3-hydroxybutyric acid (♦), which stabilises zirconium(IV) in solution to a lesser degree than its pK_a would predict, but as mentioned previously (**Section 2.2.1**), it is more likely to exist as the lactone and is therefore unlikely to complex zirconium, and (ii) gallic acid (*), which increases the precipitation pH of zirconium to a greater extent than expected of its pK_a due to the presence of three hydroxyl groups in addition to the carboxylic acid group.

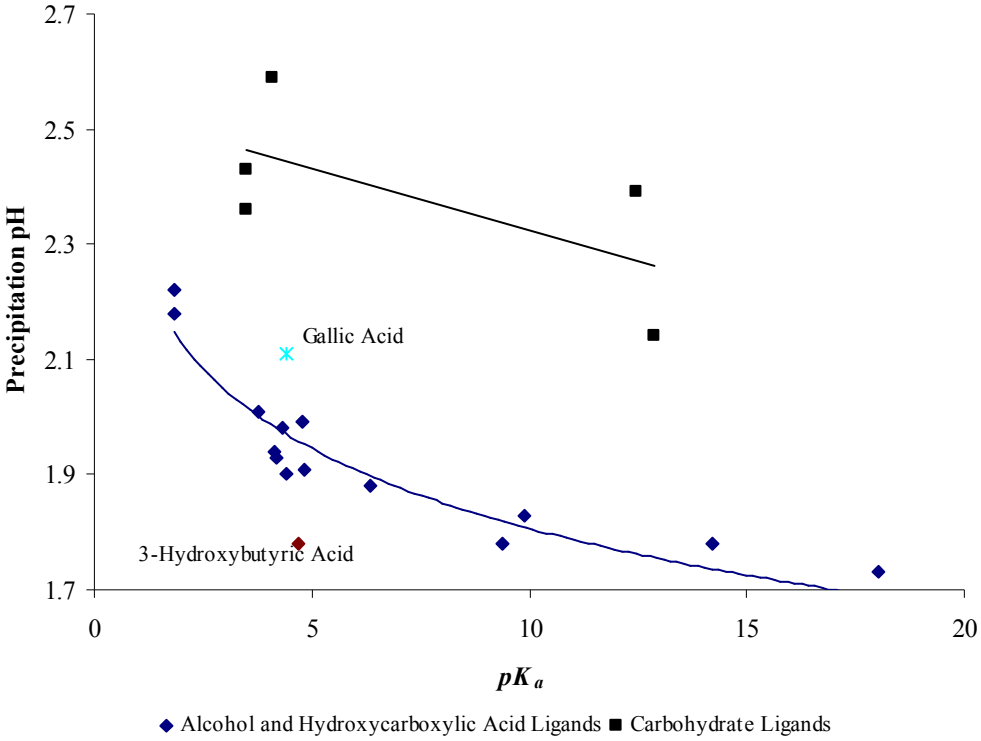

Figure 2.12: Graph showing precipitation pH versus ligand pK_a when complex solutions were titrated with 0.2 ***M*** NaOH.

The carbohydrates (D-glucose, D-galactose, D-glucuronic acid and D-galacturonic acid) and L-ascorbic acid (**Series 2**) fall outside the general trend described above and stabilise zirconium significantly, relative to the other ligands, but not enough to be considered as effective masking agents for zirconium (**Section 1.5**).

Citric, malic, L-tartaric and D-gluconic acid did not result in a precipitate when added to zirconium solutions; and on titration with sodium hydroxide, precipitation did not occur. This indicated firstly, that complexation was likely to have occurred and secondly, that the zirconium:ligand bond is strong enough to resist hydrolysis and displacement by hydroxide ions.

The final series of results to be discussed involves the ligands that precipitated zirconium upon complexation. Oxalic acid is a short chain dicarboxylic acid and was the only ligand investigated to precipitate zirconium that was not an α-hydroxycarboxylic acid. It is likely to be a combination of the relatively low pK_{a1} and pK_{a2} values and the ability to form a five membered ring upon chelation that led to oxalic acid's ability to form stable

zirconium complexes. The high oxidation state of zirconium and its small ionic radius is likely to favour chelation *via* five-membered rings over six-membered rings.

The resistance to precipitation by citrate, malate, L-tartarate and D-gluconate zirconium complexes and the precipitation of zirconium as complexes with glycolic, lactic, mandelic and 4-substituted mandelic acids, indicated the strong affinity zirconium has for α-hydroxycarboxylic acids. The ability to chelate *via* the α-hydroxy and carboxylic acid moieties results in five-membered rings similarly to oxalic acid. These ligands, however, do not appear to meet the desired criteria of masking agents, as complexation may be deemed to be so successful that precipitation was either prevented completely (indicating the likelihood that the complex is so stable that interaction with collagen would be diminished) or occurred at pHs below the desired pH range of 2.5 - 6.7 (**Section 1.5**).

The complexes were insoluble in all common solvents at low pH. However, dissolution of the zirconium α-hydroxycarboxylate precipitates, as the pH was increased, occurred over a pH range (5.5 - 10.0), which overlaps the upper end of the desirable tanning pH range. The zirconium containing complexes are recognised to hydrolyse and dissolve at high pH and then slowly depolymerise and possibly precipitate as the pH is lowered.[128] The target of finding a masking agent was therefore shifted to investigate the potential of a series of zirconium α-hydroxycarboxylate syntans which can dissolve and penetrate the collagen matrix at an elevated pH and potentially bind to collagen as the pH is lowered and the complex depolymerises.

2.2.3. Synthesis and Characterisation of Selected Zirconium α-Hydroxy-carboxylate Complexes

The precipitation of zirconium α-hydroxycarboxylate complexes and their potential use as tanning agents necessitated the synthesis of complexes (**Section 2.2.3.1**) for the purpose of characterisation (**Section 2.2.3.2**).

2.2.3.1. Synthesis of Zirconium α-Hydroxycarboxylate Complexes

Zirconium(IV) compounds commonly have a coordination number of six, seven or eight, and eight-coordinate ZrL_4 complexes are well established where L is a bidentate

ligand.[91,92] These compounds are coordinatively saturated and therefore unlikely to bind further ligands, hence, two series of zirconium complexes were produced according to **Section 2.1.5**; the first was the potentially coordinatively saturated complex using a metal to ligand ratio of 1:4, the second was a coordinatively unsaturated complex using a metal to ligand ratio of 1:2.

The α-hydroxycarboxylic acid ligands investigated further included: glycolic, lactic, mandelic, 4-hydroxymandelic, 4-chloromandelic, 4-bromomandelic, citric, malic and D-gluconic acids.

Precipitation of zirconium glycolates only occurred after ageing for 48 h. The 1:2 zirconium:glycolic acid reaction formed an extremely small quantity of a fine suspension that could not be suitably isolated and was therefore not characterised further. Precipitation with lactic acid occurred relatively quickly (within 2 h) and the precipitate was filtered. Precipitation with mandelic acid and the substituted mandelic acids occurred immediately and produced thick pastes when filtered. Drying under vacuum produced fine white powders suitable for characterisation for all the complexes isolated.

Complexation reactions with citric acid resulted in the formation of a precipitate from a ligand to zirconium ratio of approximately 0.5 to 0.9 after which the addition of citric acid resolubilised the precipitate to produce clear solutions at ratios of 1:2 and 1:4.

Malic and D-gluconic acid resulted in clear solutions at all times although the D-gluconic acid solutions were slightly yellow. Initial attempts to isolate and characterise these complexes were unsuccessful and the analysis of the precipitates was prioritised.

2.2.3.2. Characterisation of Zirconium α-Hydroxycarboxylate Complexes

Characterisation of the zirconium α-hydroxycarboxylate complexes was undertaken with the aid of the techniques listed in **Section 2.1.1**.

2.2.3.2.1. Quantitative Determination of Zirconium

Generally, the application of spectrometric methods based on the formation of coloured chelates of zirconium ions is limited due to the low selectivity of the chromogenic agents.[128] Analytical alternatives include differential colourimetric methods based on the specific behaviour of metal ions under different acidic conditions or in the presence of specific masking agents.[190] Zirconium(IV) has been extracted and measured spectrophotometrically as its ferron complex,[191] a 1:2 water soluble 4-(2-Pyridylazo)resorcinol complex,[192] and *via* spectroflourimetric methods using salicylic acid or N-phenylanthranilic acid with Rhodamine B.[193]

Atomic absorption (AA) spectroscopy was developed in the 1960s and is a rapid, accurate, reproducible and convenient method for the quantitative and qualitative analysis of many metals.[194] Zirconium, however, forms very stable oxides with ease and this makes the quantitative determination of zirconium using AA spectroscopy extremely difficult. Attempts to reproducibly measure a series of zirconium AA standards with varying acetylene/nitrous oxide ratios were unsuccessful and the use of AA spectroscopy for the quantitative determination of zirconium was abandoned.

Zirconium in the leather industry is commonly determined *via* a back-titration with excess EDTA[195] due to difficulties attributed to hydrolysis in direct titrations. A direct EDTA titration method,[196] designed to avoid hydrolysis and polymerisation, was utilised and compared to the results obtained with a more convenient, Inductively Coupled Plasma-Mass Spectrometry (ICP-MS) spectroscopic method (**Table 2.9**).

ICP-MS was found to yield satisfactory results when compared with the titration method for a standard solution of zirconium oxychloride, and the results are shown in **Table 2.9**.

Table 2.9: A comparison of a direct titration using EDTA and the use of ICP-MS for the quantitative determination of zirconium in zirconium oxychloride.

Method	Direct EDTA Titration	ICP-MS	Theoretical
% Zr	28.0	28.198	28.307

The direct titration and ICP-MS methods were shown to be useful and sufficiently accurate in the determination of zirconium. Due to the convenience and ease of use, ICP-

MS was used for all further zirconium determinations. The quantitative determination of zirconium in the complexes isolated is summarised in **Table 2.10**.

2.2.3.2.2. Carbon, Hydrogen and Nitrogen Microanalysis

The amount of carbon and hydrogen corresponding to the α-hydroxycarboxylic acid ligand was measured using combustion analysis. **Table 2.10** summarises the zirconium, carbon and hydrogen quantitative analysis of the zirconium α-hydroxycarboxylate precipitates and suggests the most likely formulae of the dry precipitate isolated. **Table 2.10** clearly shows that the precipitated products are identical for the different synthesis ratios used.

Table 2.10: Summary of the quantitative analysis of precipitated zirconium α-hydroxycarboxylate complexes.

Ligand	Zr:Ligand Synthesis Ratios	Proposed Formula of Product	Zirconium (%)		Carbon (%)		Hydrogen (%)		Yield (%)
			Found	Calc.	Found	Calc.	Found	Calc.	
Glycolate (G)	1:2	no ppt	-	-	-	-	-	-	-
	1:4	$Zr_2O(OH)_2G_4$	34.276	34.254	18.065	18.039	3.275	2.650	27
Lactate (L)	1:2	$Zr(OH)L_3$	24.285	24.298	28.295	28.791	4.685	4.296	14
	1:4	$Zr(OH)L_3$	24.362	24.298	28.471	28.791	4.524	4.296	63
Mandelate (M)	1:2	ZrM_4	12.731	13.111	55.735	55.238	3.865	4.057	26
	1:4	ZrM_4	12.703	13.111	55.370	55.238	3.900	4.057	97
4-Hydroxy-	1:2	$Zr(hM)_4$	12.028	12.007	50.060	50.585	3.755	3.715	21
mandelate (hM)	1:4	$Zr(hM)_4$	12.104	12.007	50.000	50.585	3.590	3.715	83
4-Chloro-	1:2	$Zr(cM)_4$	10.631	10.944	46.279	46.108	2.800	2.902	27
mandelate (cM)	1:4	$Zr(cM)_4$	10.863	10.944	46.315	46.108	2.860	2.902	98
4-Bromo-	1:2	$Zr(bM)_4$	9.087	9.019	37.700	38.002	2.175	2.392	29
mandelate (bM)	1:4	$Zr(bM)_4$	8.733	9.019	38.210	38.002	2.315	2.392	99

2.2.3.2.3. Thermal Analysis

The thermal decomposition of the zirconium α-hydroxycarboxylate complexes was studied using DSC and TG under a nitrogen atmosphere according to **Section 2.1.1**. DSC measurements of the complexes showed a broad endotherm (ΔT = 30 to 70°C) between 200 and 320°C (**Figure 2.13**). This was likely to be the decomposition of the zirconium α-hydroxycarboxylate complexes to zirconium oxycarbonates[120] and was supported by TG analysis.

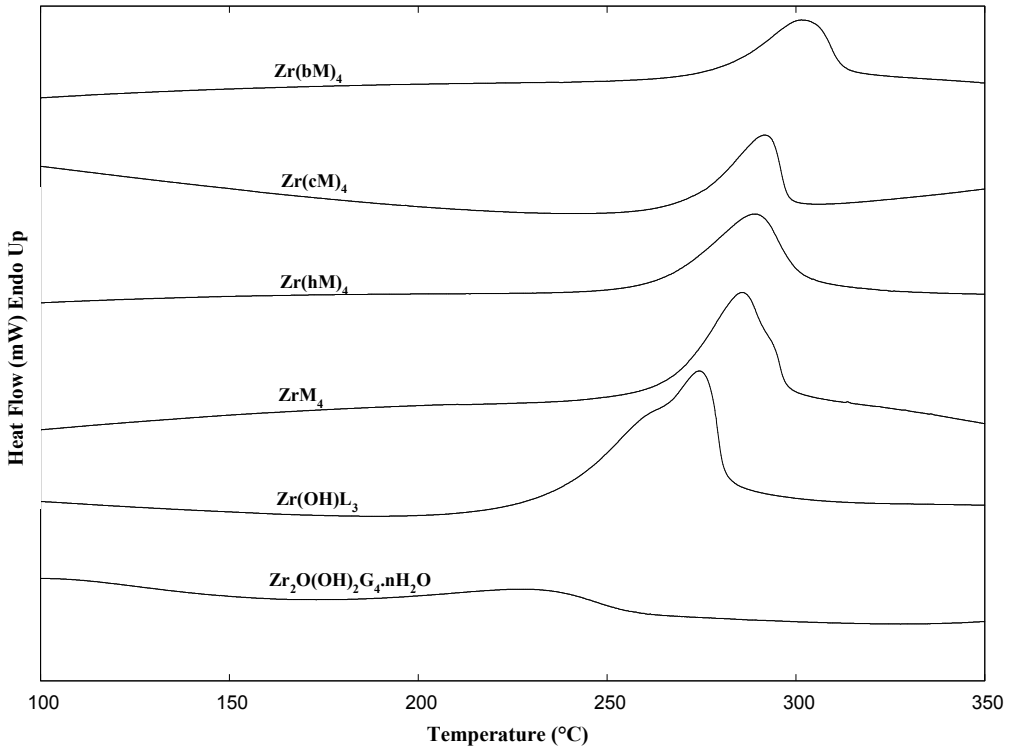

Figure 2.13: DSC endotherms of selected zirconium α-hydroxycarboxylate complexes.

The zirconium lactates and mandelates showed two distinct decomposition phases using TG analysis, with the first corresponding to the DSC endotherm and a second, (likely to overlap with the end of the first) slower decomposition corresponding to the loss of CO_2 to yield ZrO_2. The zirconium mandelate complex was used to illustrate this point in **Figure 2.14** and indicates the decomposition of ZrM_4 (100%) to $ZrO(CO_3)_2$ (32.7%) and finally ZrO_2 (17.7%). The lack of endothermic transitions at the free ligand melting point indicated that complexation had occurred and the lack of endotherms between 50 and 200°C further suggests that there was no coordinated or lattice water present. The zirconium contents determined by ICP-MS were supported by TG analysis.

DSC spectra of the zirconium glycolate complex showed an additional broad endotherm which peaked at 98°C and indicated the presence of lattice water.[112] The TG curve was similar to that of mandelic acid except weight loss started from about 50°C and was almost linear until 350°C, corresponding to water loss and the decomposition to the oxycarbonate. A rapid mass loss from 350°C to 450°C and a further mass loss above 550°C were accepted to be due to the loss of water derived from hydroxo ligands and the

decomposition of the oxycarbonate to ZrO_2.[112] Microanalysis suggested a zirconium glycolate complex formula of $Zr_2O(OH)_2G_4$, however, TG and DSC results indicated that the complex was hydrated. The $Zr_2O(OH)_2G_4$ complex has been previously identified as a hydrate (**Section 1.4.2.9**).[91] Microanalysis samples were stored over silica gel and under vacuum prior to analysis whereas the TG and DSC runs were performed on freshly prepared samples. DSC runs performed later on the dried glycolate samples showed no water of hydration endotherm.

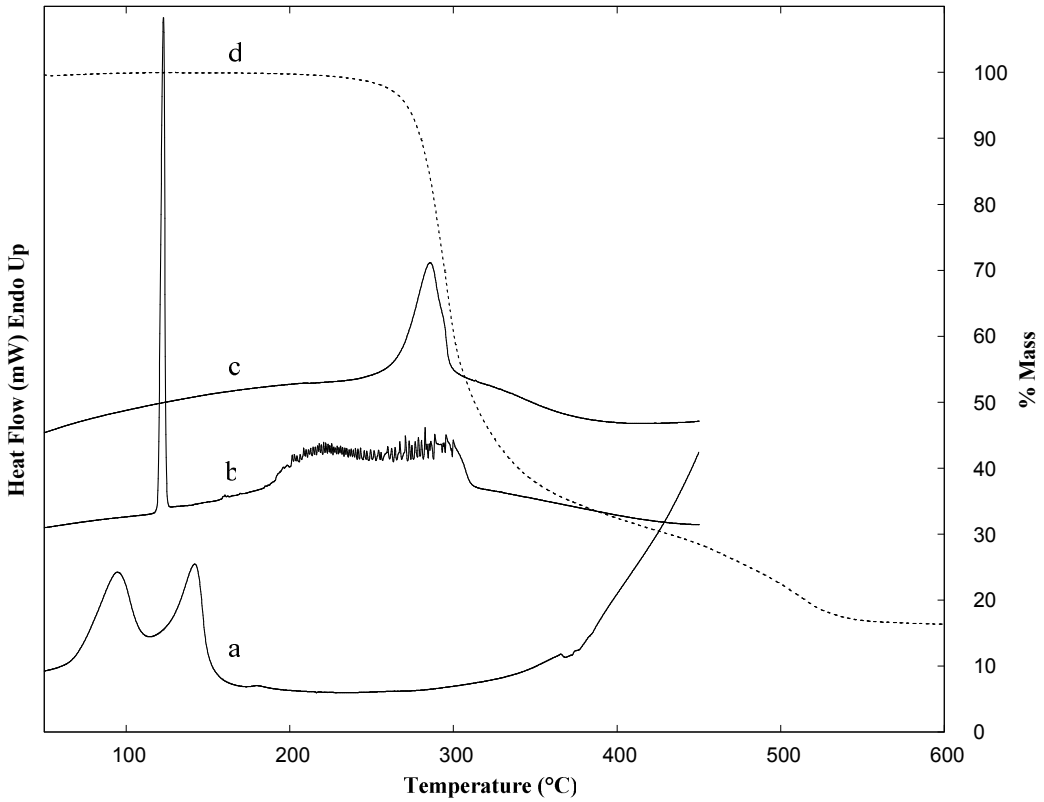

Figure 2.14: DSC thermograms for (a) zirconium oxychloride, (b) mandelic acid, and (c) zirconium mandelate, with the TG spectrum of (d) zirconium mandelate.

Powder X-ray diffraction showed all the zirconium complexes to be amorphous.

Microanalysis indicated that the complexes isolated from the 1:2 and 1:4 zirconium:ligand synthesis solutions are the same for each ligand, excluding glycolate. It must be noted that the species existing in solution are not necessarily the same as those that precipitate out. For a metal ion (M) complexing with a ligand (L) in aqueous solution, the following equilibria are expected:

$$
\begin{array}{lcll}
M\,(aq) + L\,(aq) & \rightleftarrows & ML\,(aq) & K_1 \\
ML\,(aq) + L(aq) & \rightleftarrows & ML_2\,(aq) & K_2 \\
ML_2\,(aq) + L\,(aq) & \rightleftarrows & ML_3\,(aq) & K_3 \\
 & \downarrow & & \\
ML_{n-1}\,(aq) + L\,(aq) & \rightleftarrows & ML_n\,(aq) & K_n
\end{array}
$$

with an overall equation:

$$M(aq) + nL(aq) \rightleftarrows ML_n(aq);$$

and an overall equilibrium constant:

$$\beta = [ML_n]/[M][L]^n \qquad \beta = K_1 \times K_2 \times K_3 \ldots\ldots K_n$$

The solids were isolated by lowering the pH, which caused the less soluble metal species to precipitate out at the given pH. Even if the concentration of ML_4 were insignificant, precipitation would shift all the individual equilibria (Le Chatelier's Principle) to the right. In the case of a 1:2 molar ratio solution some ML_2 would dissociate to liberate ligand for the formation of more of the insoluble ML_4. This would continue to occur until there is no more ML_2 left to be sacrificed for the liberation of additional free ligand. At which point the dominant species in solution would be the solvated metal ion, or in the case of zirconium, a hydrated or hydroxylated species. The only species characterised were in the insoluble form.

2.2.3.2.4. Infrared and Raman Spectroscopy

The analysis and interpretation of the infrared and Raman spectra was made using standard analytical spectroscopic texts,[185,197-202] with particular interest in the vibrational spectra of benzene derivatives for the mandelates.[201]

The wide use of spectroscopy as an analytical tool in carboxylate chemistry is based on the characteristic group frequencies of the asymmetric C=O stretch (ν_aC=O), the symmetric C=O stretch (ν_sC=O) or the magnitude of distance between them (ΔCO_2^-). Most work makes use of infrared spectra rather than Raman spectra because of the intensity and characteristic broadness of the ν_aC=O vibration (found between 1840 and 1540 cm^{-1} for the free ligand and between 1700 and 1550 cm^{-1} for metal complexes)

which occurs in a region devoid of many alternative fundamentals. In the Raman spectrum its intensity is much reduced, and the absorption is medium to weak, depolarised.

The candidates having the greatest potential to cause a misassignment using infrared spectroscopy are the ν_sC=O stretch and the δO-H bend. The bend can easily be identified since it is extremely weak and often absent in the Raman. For the free ligand the ν_sC=O is found as a weak infrared band between 1440 and 1210 cm^{-1}. In the Raman the absorption is polarised, but of variable intensity ranging from very strong to weak. For metal complexes the intensity of the vibration is enhanced in the infrared spectrum as a result of the increased dipole change on coordination, with the band being characteristically broad of medium to strong intensity, and found between 1460 and 1315 cm^{-1}. Unlike the asymmetric stretch, ν_sC=O occurs in a region with a number of alternative fundamentals, and in a vibration rich spectrum (such as the mandelic acids in this work) the potential for misassignment is high. Working with more than one vibrational technique and with systems of known, well-behaved spectral activity reduces this danger. It is for this reason that the present study employed both infrared and Raman spectral studies and, in light of the extensive work by Varsányi[201] on substituted benzenes, why mandelic acid was selected for the substitution study.

The literature establishes several diagnostic indicators regarding ν_aC=O, the magnitude difference involving coordination complex studies, and ν_sC=O. These include that:

i) Both ν_aC=O and ν_sC=O are substituent sensitive.[185]

ii) For the free ligand a ν_aC=O between 1730 and 1700 cm^{-1} indicates a non-ionised carboxyl, while values between 1595 and 1575 indicate an ionised carboxyl group.[185]

iii) For coordination complexes the ν_aC=O frequency increases as the M-O bond becomes more covalent,[185] hence the range of 1650 to 1620 cm^{-1} indicates a covalent coordination complex, the range of 1630 to 1575 indicates an ionic covalent complex.

iv) For coordination complexes, when compared with the free ligand, unidentate coordination is indicated by ν_aC=O shifting to higher frequency while ν_sC=O shifts to lower frequency, increasing ΔCO_2^- (values typically > 200 cm^{-1}).[202]

v) For coordination complexes, when compared with the free ligand, chelate coordination is indicated by $\nu_a C{=}O$ shifting to lower frequency while $\nu_s C{=}O$ shifts to higher frequency, decreasing ΔCO_2^- (values typically ≈ 100 cm^{-1}).[202]

vi) For coordination complexes, when compared with the free ligand, bridging coordination is indicated by both $\nu_a C{=}O$ and $\nu_s C{=}O$ shifting to higher frequency (ΔCO_2^- values typically ≈ 150 cm^{-1}).[202]

Carboxylic acids show a high degree of association through hydrogen bonding because of their strongly polarised O-H bonds and they are able to form hydrogen bonds to the negative oxygen of the carbonyl dipole and therefore they frequently exist as cyclic dimers in the solid and liquid states (**Figure 2.15**).[179]

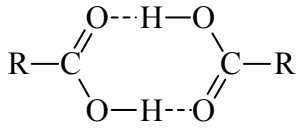

Figure 2.15: Carboxylic acid cyclic dimer.

When a hydroxyl group is in the same molecule with the carbonyl group, or when an acid is dissolved in a solvent containing a hydroxyl group, there exists the opportunity for other types of hydrogen bonding to occur involving hydroxyl-carboxyl bonds as an alternative to carboxyl dimer bonding. When this occurs, symmetry is destroyed and the carbonyl vibrations appear in both the infrared and Raman spectra. When the carbonyl is hydrogen bonded but not dimerised, as in alcohol-carbonyl bonds, a band appears at 1760-1735cm^{-1} in both the infrared and Raman.[197] **Table 2.11** and **Figure 2.16** show that the infrared asymmetric carbonyl stretch in the free ligands falls between 1753 and 1691 cm^{-1}.

The carbonyl stretch at 1691 cm^{-1} for 4-hydroxymandelic acid is expected as the phenyl hydroxy group contributes to more hydrogen bonding and a shift to a lower wavenumber as the double bond character of the carboxyl decreases. Raman spectra of the free ligands (**Figure 2.16**) show the asymmetric carbonyl stretching bands in a similar range to the infrared (1728 - 1670 cm^{-1}), which indicates that the free ligands are not found as dimers.

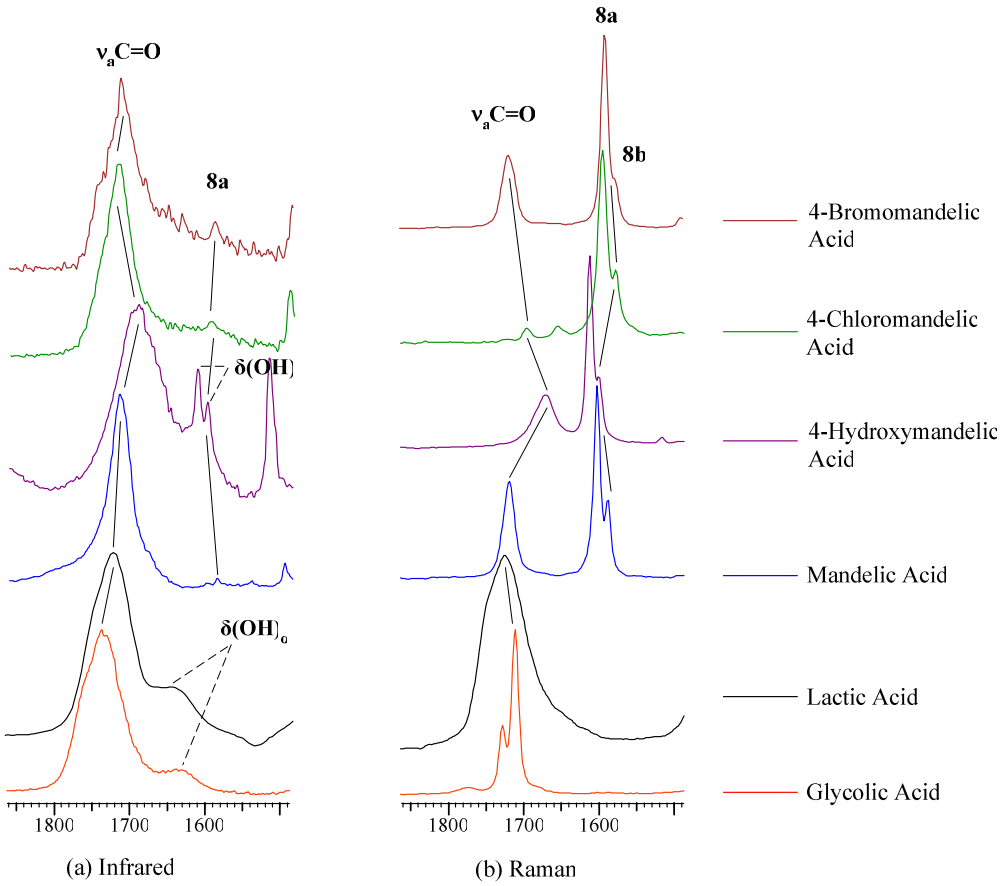

Figure 2.16: (a) Infrared and (b) Raman spectra of the asymmetric CO_2 stretching vibrations (ν_aC=O), and ring stretches (Wilson modes 8a and 8b) of selected α-hydroxycarboxylic acids.

Carboxylic acids are usually characterised in the condensed state by a strongly bonded, very broad OH stretching band centred near 3000 cm^{-1}. While this is superimposed on the CH stretching bands (3100-2800 cm^{-1}) the broad wings of the OH stretch can be seen on either side of the narrow CH bands (**Figure 2.17**).

Distinctive shoulders between 2700 and 2500 cm^{-1} appear regularly and are due to overtones and combinations of the 1300 and 1420 cm^{-1} bands due to interacting C-O stretch and C-C-O(H) deformation vibrations. These bands are especially evident in glycolic, mandelic and 4-hydroxymandelic acids. Monomeric acids absorb weakly and sharply at 3580-3500 cm^{-1}.[197] The OH stretching band becomes broader and shifts to a lower wavenumber due to hydrogen bonding. In the liquid and solid state, alcohols and phenols have a very broad and intense OH absorption in the region 3500-2800 cm^{-1} with the maximum near 3300 cm^{-1}.

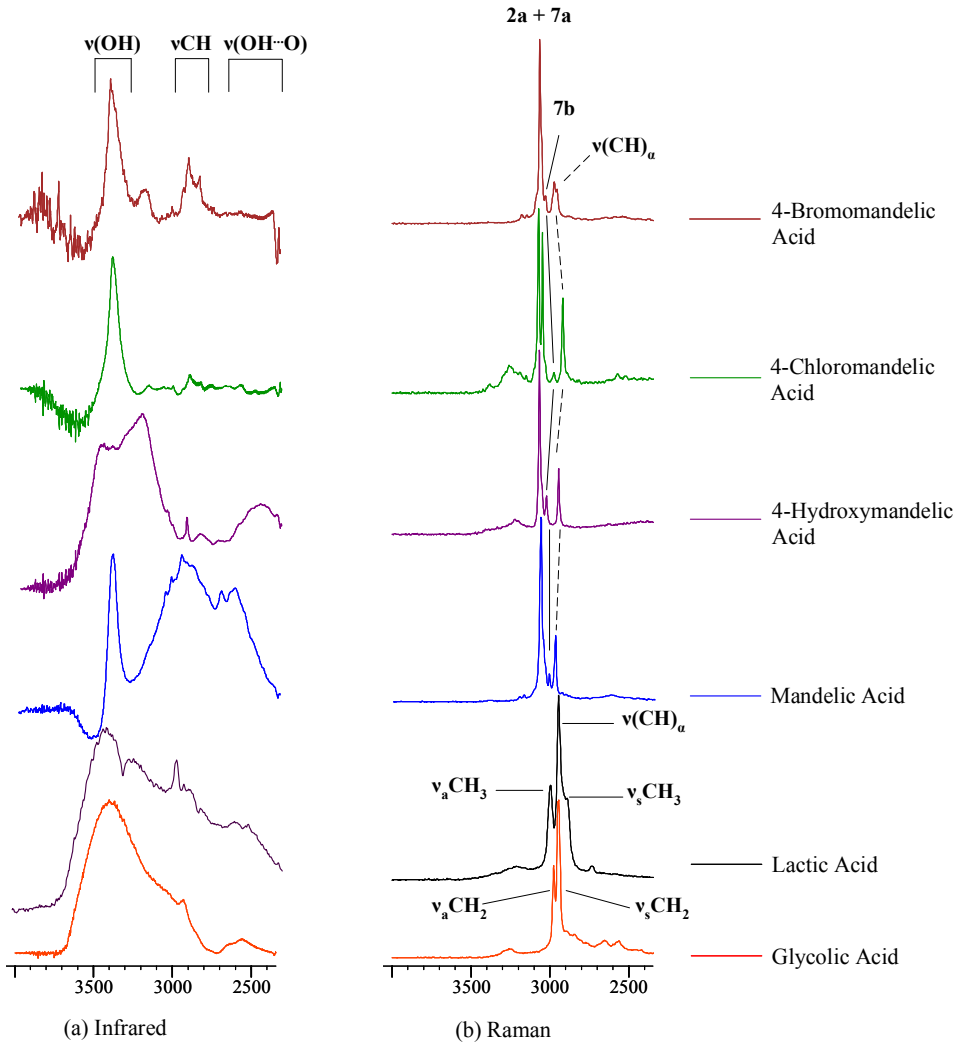

Figure 2.17: (a) Infrared and (b) Raman spectra of: (i) OH stretching bands, ν(OH), (ii) hydrogen bonding bands, ν(OH···O), and (iii) aliphatic CH stretches and aromatic CH stretches (Wilson modes 2, 7a and 7b) of selected α-hydroxycarboxylic acids.

When a salt is made from a carboxylic acid, the C=O and C-O are replaced by two equivalent carbon-oxygen bonds which are intermediate in force constant between the C=O and C-O. These two "bond and a half" oscillators are strongly coupled, resulting in the strong ν_aC=O vibration at 1650-1540 cm^{-1} and the somewhat weaker ν_sC=O vibration at 1450-1360 cm^{-1}. This is observed in **Table 2.11** and **Figure 2.18** and is the most direct evidence of complexation.

Table 2.11: Assignment of important infrared and Raman bands for selected α-hydroxycarboxylic acids and the zirconium complexes isolated.

Assignment	ν(O-H) cm^{-1}		ν_aC=O cm^{-1}		δ(OH) cm^{-1}		ν_sC=O cm^{-1}		δC-C-O(H)/$\delta_r CH_2$ cm^{-1}		ν_aC-C-O(H) cm^{-1}	
Compound	**Infrared**	**Raman**	**Infrared**	**Raman**	**Infrared**	**Raman**	**Infrared**	**Raman**	**Infrared**	**Raman**	**Infrared**	**Raman**
HG	3393 *vsbr*[(a)] masked	 3256 *wbr*[(b)]	1736 *s*	1728 *m* 1711 *s*	1638 *wbrsh*[(d)]	-	-	-	1230 *vsbr*	1228 *m*	1088 *s*	1085 *w*
$Zr_2O(OH)_2G_4$	3417 *vsbr*[(a)]	-	1612 *s*	1637 *wbr*	masked	-	1391 *m*	1384 *wsh*	1309 *m*	1322 *msh*	1083 *wsh*	1096 *wbrsh*
HL^{203}	3426 *mbr* 3289 *mbr*	 3248 *wbr*[(b)]	1719 *s*	1717 *vw*	1642 *wsh*[(d)]	-			1275 *mbrsh*	1286 *wbr*	1122 *s*	1124 *m*
$Zr(OH)L_3$	3395 *mbr*[(a)] masked	 3210 *vw*[(b)]	1610 *s*	1610 *wbr*	masked	-	1407 *m*	1396 *m*	1315 *m*	1321 *m*	1052 *m*	1055 *m*
HM	3402 *s*	-	1716 *s*	1720 *m*	masked	-	-	-	1298 *sbr*	1294 *w*	1061 *s*	1056 *vw*
ZrM_4	3445 *wbr* masked	- -	1623 *sbr*	1605 *m*	masked	-	1352 *s*	1346 *w*	1288 *msh*	1279 *vw*	1048 *m*	1048 *vwbr*
H(hM)	3489 *vsbr*[(a)] 3224 *vsbr*[(c)]	 3217 *vwbr*[(c)]	1691 *sbr*	1671 *wbr*	1648 *msh*[(e)]	-	-	-	1259 *vsbr*	1261 *m*	1073 *s*	1075 *vw*
$Zr(hM)_4$	3332 *sbr* masked	 3213 *wbr*[(c)]	1612 *sbr*	1618 *wbrsh*	masked	-	1356 *s*	1356 *wsh*	1297 *msh*	masked	1052 *m*	1055 *w*
H(cM)	3402 *m*[(a)] 3263 *sbr*[(b)]	- -	1720 *s*	1721 *m*	masked	-	-	-	1268 *mbr*	1278 *w*	1066 *m*	1058 *vw*
$Zr(cM)_4$	3412 *wbr* masked	- -	1623 *s*	1620 *msh*	masked	-	1356 *s*	1360 *w*	1293 *msh*	1296 *w*	1056 *w*	1055 *vw*
H(bM)	3447 *mbr*[(a)] 3194 *wbr*[(b)]	- -	1715 *s*	1718 *m*	masked	-	-	-	1247 *msh*	1247 *wbr*	1057 *s*	1060 *wsh*
$Zr(bM)_4$	-	-	1622 *s*	1620 *msh*	masked	-	1357 *s*	1361 *wbr*	1297 *msh*	1296 *vw*	1058 *wbr*	1052 *w*

Where G = glycolate, L = lactate, M = mandelate, hM = 4-hydroxymandelate, cM = 4-chloromandelate, and bM = 4-bromomandelate
Where *(a)* = $\nu(OH)_{COOH}$, *(b)* = $\nu(OH)_{\alpha}$, *(c)* = $\nu(OH)_{\alpha/para}$, *(d)* = $\delta(OH)_{\alpha}$, and *(e)* = $\delta(OH)_{\alpha/para}$
Where *s* = strong, *m* = medium, *w* = weak, *v* = very, *br* = broad, and *sh* = shoulder.
Where ν = stretch, δ = bend and r = rock

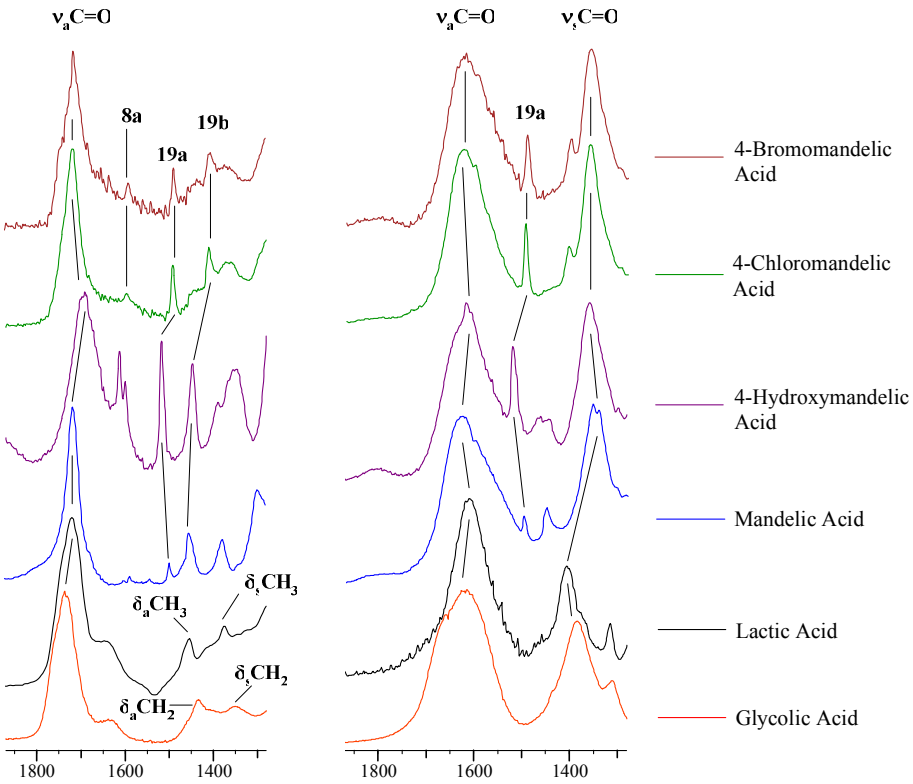

Figure 2.18: Infrared spectra showing the asymmetric (ν_aC=O) and symmetric (ν_sC=O) CO_2 stretching vibrations and ring stretches (Wilson modes 19a and 19b) of (a) selected free α-hydroxycarboxylic acid ligands, and (b) of selected zirconium α-hydroxycarboxylates.

Nakamoto[185] described how the difference in wavenumber between the asymmetric and symmetric ν(C=O) stretches (ΔCO_2^-) might be used to determine the method of coordination between metal ion and carboxylate ligands. Large $\Delta(CO_2^-)$ values (>200 cm^{-1}) (**Table 2.12**) indicate that coordination to zirconium *via* the carboxylate is likely to be unidentate.

Table 2.12: The separation of the asymmetric and symmetric carbonyl stretching vibrations in a selection of zirconium compounds.

Ligand	Compound	$\Delta(CO_2^-)$ cm^{-1}
Acetate (A)	NaA	150
Acetate (A)	ZrA_4	152
Glycolate (G)	$Zr_2O(OH)_2G_4$	221
Lactate (L)	$Zr(OH)L_3$	203
Mandelate (M)	ZrM_4	271
4-Hydroxymandelate (hM)	$Zr(hM)_4$	256
4-Chloromandelate (cM)	$Zr(cM)_4$	267
4-Bromomandelate (bM)	$Zr(bM)_4$	265

Bidentate, ionic and bridging carboxylate ligands exhibit significantly smaller $\Delta(CO_2^-)$ values.[204] Chelation is therefore likely to occur *via* structure (a) in **Figure 2.19**.[205,206] This is understandable as the chelation involves a five-membered ring, which is particularly stable.

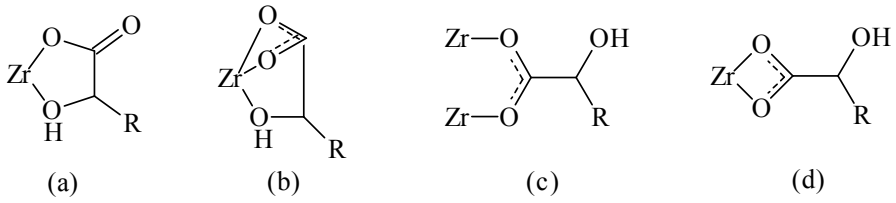

Figure 2.19: Carboxylate complexes of α-hydroxycarboxylates may be (a) unidentate with protonated coordination, (b) bidentate with OH coordination, (c) symmetric syn-syn bridging with unprotonated coordination, and (d) bidentate with unprotonated coordination.

All OH deformation vibrations are strongly coupled with CH wagging and the C-O stretching vibration. Carboxylic acids have a strong band in the region 1315-1200 cm^{-1}. These bands involve stretching of the C-O bond and in-plane (i.p.) deformation of the C-O-H angle, which interact somewhat with $\delta_r CH_2$ so that both bands, to some extent, involve both C-H deformation and C-O stretch, both i.p. and out-of-plane (o.o.p.). In acids this band is normally accepted as predominantly C-O stretching in a wide selection of the literature but is in fact a bending vibration, lifted to the high wavelength by coupling with $\delta_r CH_2$. Consequently, the C-C-O(H) i.p. deformation is strongly coupled with the CH_2 rock ($\delta_r CH_2$) to yield an undefined absorption because it is overlapped by various other C-H deformation bands, and it is mostly insignificant for interpretation.

Goulden[207] indicated that the i.p. deformation band of the OH group in lactate compounds shift from 1275 to 1390 cm^{-1} in the chelated ion. Nakamoto *et.al*.,[208] in studying metal-glycolate complexes, used deuterated ligands to show a shift from ~1250 cm^{-1}, in the free ligand, to 1482 cm^{-1} in the complex. If the metal is more strongly associated with one oxygen of the CO_2 group than the other, that CO will have a little more single bond character and the other a little more double bond character. This shifts the o.o.p. band higher and the in-plane i.p. band lower in frequency than when the CO bonds are equal. What is evident in **Figure 2.20** is the disappearance of the slightly broad bands (1298 - 1230 cm^{-1}) in the free ligand upon chelation, which were tentatively assigned as the coupled C-C-O(H) i.p. deformation vibration.

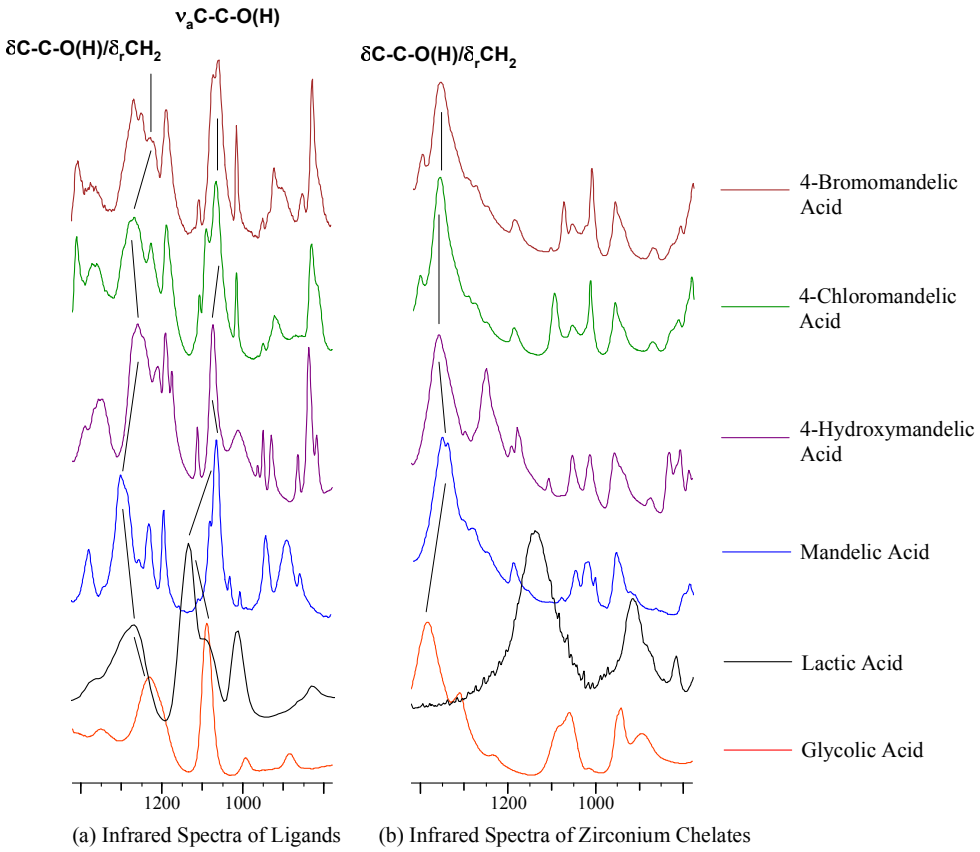

Figure 2.20: Infrared spectra showing the disappearance of the i.p. ν_aC-C-O(H) vibration upon chelation from (a) the free α-hydroxycarboxylic acid ligands, to (b) the zirconium α-hydroxycarboxylates. The δC-C-O(H)/δ_rCH$_2$ coupled vibration is also shown.

The alcohol C-O single bond shows a strong stretching band in the region of 1210-1000 cm^{-1}. This is coupled with neighbouring C-C bonds, resulting in a higher ν_aC-C-O(H) around 1050 cm^{-1}, and a lower ν_sC-C-O(H) around 950 cm^{-1}. The coupling of the C-O vibration with the neighbouring C-atoms is significantly large and α-C substituents affect the C-O band position. Assignment of the ν_sC-C-O(H) was not included in **Table 2.11** as this area is rich in benzene vibrations.

2.2.4. Linear Free Energy Relationship - The Hammett Equation

In an effort to better evaluate the nature of the Zr-O bond, several complexes with various *para* derivatives of mandelic acid were examined to identify any structural activity relationships that may exist. This may assist understanding the potential role of zirconium α-hydroxycarboxylates as tannages in terms of possible binding to collagen, and the stability of the metal complex.

Principles underlying reactivity and free energy relations of a multitude of heterolytic reactions of substituted benzene reactions can be ascribed by the classical Hammett equation defining the structural activity relationship for the rate of hydrolysis of benzoic acid derivatives:

$$XArCOOH \rightleftarrows XArCOO^- + H^+$$

$$\log(k_X \backslash k_H) = \rho\sigma_X$$

where, σ_X is the Hammett substituent parameter for the substituent, X; ρ is the reaction constant, and k_H is the rate of hydrolysis when X = H.[179]

The σ parameter indicates the inductive effect of the substituent. For substituents more electron withdrawing than hydrogen, $(k_X \backslash k_H) > 1$ and σ_X is positive. For substituents more electron donating than hydrogen, $(k_X \backslash k_H) < 1$ and σ_X is negative. After the 1980's the inductive effect has been called the field effect. The literature consequently employs the symbols σ_I and σ_F, respectively. The reaction constant, ρ, is sensitive to polar effects, and by definition $\rho = 1$ for the ionisation of benzoic acid (in H_2O, 25°C). Its value depends on the reactant; $\rho = 1.96$ for ArOH, and $\rho = 0.489$ for $ArCH_2COOH$.

The effects of substituents on chemical reactivities and physical properties are reflected by linear log k vs σ, $\delta^{13}C$ vs σ (NMR), and ν(metal-ligand) vs σ plots (IR). Such linearity holds for *meta* and *para* substituents, but steric effects make the Hammett equation inappropriate for *ortho* substituents.

Failure of Hammett σ plots does occur for some substituents that show a strong resonance interaction between the substituent and the reaction site - either potentially electron withdrawing (NO_2, CF_3) or electron donating (OH, NH_2). Such systems are consistently nonlinear.[209-211] This is also evidenced by comparing the σ_F for the substituents used in the present study in the *para* and *meta* positions. For X = OH, electron donation is more powerful than σ_F predicts, while for X = Cl or Br, electron donation is smaller than σ_F predicts (**Table 2.13**).

Dual substituent parameter relationships such as those of Taft,[212] Swain-Lupton,[213] and Yukawa-Tsuno[214] allow the separation of the influence of inductive (field) and

mesomeric (resonance) effects of substituents on chemical reactivities and physical properties. The degree of success of such treatments bears no simple relationship to theories that connect structure with reactivity.

Table 2.13: Hammett σ_F values for bromo-, chloro- and hydroxy-substituents of benzoic acid in the *meta* and *para* positions.[179]

	σ_F (*meta*)	σ_F (*para*)
Br	+0.391	+0.232
Cl	+0.373	+0.227
OH	+0.121	-0.37
H	0	0

Taft's equation is an extension of the Hammett equation, using appropriate substituents σ_F and σ_R and their contributions ρ_F and ρ_R for the inductive (field) and resonance influences, respectively, on the rate constant k_X:

$$\log(k_X/k_H) = \rho_F\sigma_F + \rho_R\sigma_R.$$

Negative ρ values indicate the positive charge within the ring and positive values indicate resonance stabilisation. In the majority of chemical reactivities and physical properties studied, the signs of ρ_F and ρ_R are the same. In those cases where opposing signs are found, Taft interpreted this as indicating a charge migration on going from reactant to transition state, *e.g.*, positive charge moves closer toward the substituent (ρ_F positive) to quinoidal resonance stabilisation (ρ_R negative). While suitable for *para* derivatives, Taft concluded that available data did not provide a suitable basis for its application to *meta* substituted benzene derivatives. Swain, however, has been able to successfully extend the principle to a series of *meta* substituted benzene derivatives.[213]

The use of infrared frequencies in establishing linear Hammett σ plots is well established, and has been employed in coordination chemistry to establish the degree of the *trans* effect, and the absence or presence of metal to ligand back bonding ($M\rightarrow L$ π bonding).[209,215-218] The latter is established by comparing the slope of the ν(metal-ligand) *vs.* σ plot with that of an internal ligand vibration (such as νC=O) *vs.* σ plot, an inverse relationship indicates back bonding.[219] The Hammett substituent parameter affects the carboxyl group in two ways. Electron donating substituents increase the frequency of the

asymmetric stretch (ν_aC=O) and increase the integrated intensities of the C=O stretching bands.[220]

For the free ligand, a linear Hammett σ plot may be established for the asymmetric stretch (ν_aC=O) as well as for several Wilson modes of the benzene ring that are recognised to be substituent sensitive (**Figure 2.21**).[201] This is illustrated in the region of interest (1800-1350 cm^{-1}) by tangential ring vibrations, modes 8a and 8b. Both are very weak or absent in the infrared, however 8a is very intense in the Raman, with 8b appearing as a medium-weak band (sometimes as a shoulder) at lower energy (**Figure 2.16**). As expected, electron donating substituents increase the frequencies of both modes, however the intensities of the Raman bands are insensitive to the substituent. This is better illustrated in the infrared spectra by the tangential ring vibrations, modes 19a and 19b (**Figure 2.18**).

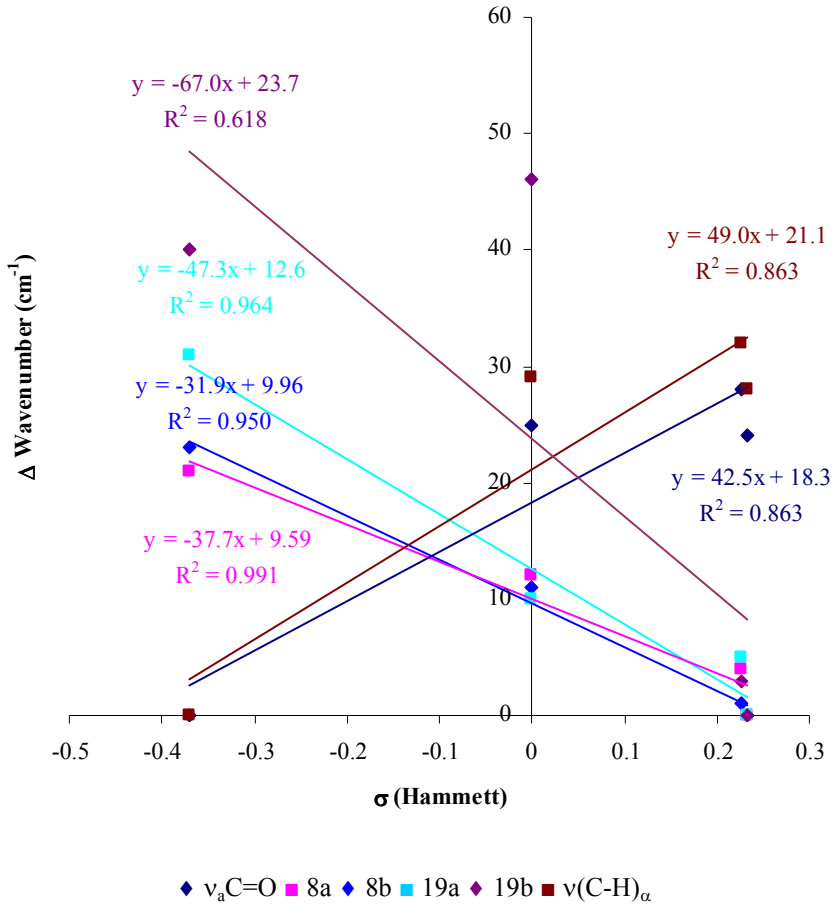

Figure 2.21: Plot of change in wavenumber versus conventional Hammett σ values for selected vibrations in *para* substituted mandelic acid ligands (ρ = 1).

For both modes, electron donating substituents increase both the frequency and intensity of the vibrations: both frequency and intensity are greatest when X = OH. Radial ring

vibrations, ring breathing modes 1, 6a, 6b and 12, tend to be highly substituent sensitive, occurring in a vibrationally rich region and difficulties in peak assignment hindered correlation with Hammett σ values.

The asymmetric carboxyl stretch (ν_aC=O) shows the expected intensity sensitivity with respect to the extent of electron donation. However the linear Hammett σ plot is the inverse of that observed for substituted benzoates. This indicates that as electron donation increases, the double bond character of the carboxyl group surprisingly *decreases*. This supports previous reports that there is an interaction between the proton on the α-OH and the asymmetric carboxylic oxygen.[221] As such, increasing electron donation in the ring favours the ionisation of the nearby alcohol proton over the carboxyl group, with concomitant increased hydrogen bonding of the proton to the carboxyl. It is envisaged that this would be sensitive to polarity of the solvent, based on the polar sensitivity of the reaction constant, ρ, and supporting evidence for such a proposed mechanism may be found in the order of ρ:

$$ArOH > ArCOOH > ArCH_2COOH.$$

For this scenario, the linear Hammett σ plot of νC-OH would be expected to be typical of substituted benzoates and phenols. However, the present assignment of this vibration is tentative due to the spectral complexity in this region and so prevents such conclusions from being made. The typical linear Hammett σ relationship for $\nu(C\text{-}H)_\alpha$ as based on the Raman spectra is, however, additional supporting evidence. Final conclusions regarding the unusual linear Hammett σ relationship of ν_aC=O must await a planned DFT study on this system.

Whereas a fair correlation is obtained for the linear Hammett σ relationship of the free ligand the complexes correlate more poorly with the electronic substituent parameters (**Figure 2.22**). This change on complexation is by no means unprecedented.[222] Such failure of Hammett σ plots can be accounted for in terms (i) of resonance effects, (ii) *via* intervention of nonclassical carbocations, (iii) by steric hindrance to initial ionisation, or (iv) by dramatic change in terms of perturbational molecular orbital (MO) theory. The first may be identified by satisfactory correlation with substituent constants in terms of the Yukawa-Tsuno equation.[222,223] The second is often either the first rationalisation used

or the last in desperation. The third is unlikely in terms of the small cone angles of the substituents employed here and their *para* positioning. For the last, it is improbable that the system experiences M→L back bonding as Zr^{4+} is d^0. In a π acceptor complex, for there to be a gain in the free energy, and thus stabilisation, both an empty ligand π* anti-bonding orbital of suitable symmetry and the presence of d electrons to occupy the resultant lower energy MO of the complex, are required.

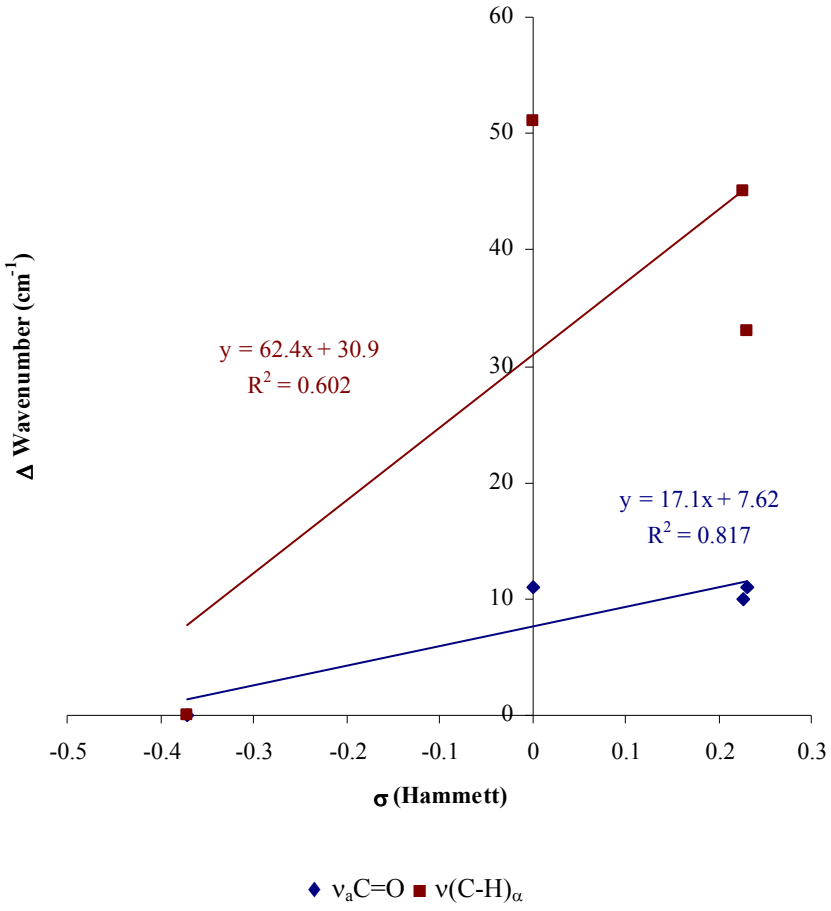

Figure 2.22: Plot of change in wavenumber versus conventional Hammett σ values for selected vibrations in zirconium *para* substituted mandelate complexes (ρ = 1).

L→M π bonding is more probable given the high oxidation state of the zirconium, and requires electrons in the HOMO ligand π bonding orbital to occupy the resultant lower energy MO of the π donor complex for there to be a gain in the free energy, and thus stabilisation. Both types of π bonding increase covalency and the degree of covalency is reflected in the frequency of ν_aC=O. This may be explained in terms of a conformational preference, which can be anticipated since chelation involving the α-OH (**Figure 2.18a**) requires a conformational change from that of the free ligand described above. However,

due to the limited number of mandelic acid derivatives available, the data does not provide a suitable basis for categorical proof. Confirmatory evidence for such conformational preference could be derived from a comparison of the crystal structures of the three substituents with the mandelate complex. XRPD (**Section 2.1.1.9**) were examined to determine whether the products were crystalline, and to see if they were isostructural. The fact that the materials are amorphous and soluble only at low pH leads to difficulties in successful single crystal growth. Nonetheless efforts are underway to grow single crystals.

Applicable to *para* substituents only, the equation of Yukawa and Tsuno is based on the substituent constants of the equations of Hammett (σ) and Brown-Okamoto (σ^+):

$$\log(k_X/k_H)_p = \rho[\sigma_p + r(\sigma^+ - \sigma_p)],$$

where r (resonance demand parameter) reflects the extent of resonance between the substituent X and the reaction centre.

The value of r ($r \leq 1$) implies conjugation of the positive charge within the ring is larger or smaller than that for the definitive system, and for $r = 0$ the classical Hammett equation is obtained. While r is generally positive, there is some debate in the literature regarding its theoretical significance. As a measure of the degree of π delocalisation of the negative charge into the substituent (X) at position 4, r increases linearly with decreasing electron affinity of the unsubstituted member.[224] Alternatively, the resonance demand parameter of solvolysis systems were linearly correlated with the resonance interaction, such as population, bond order and bond length, basicities in aqueous solution,[225] *etc.*, and accounted for in terms of polarisability[226,227] or in perturbational MO theory.[228]

A comparison of the Hammett and Yukawa-Tsuno plots for the free ligands (**Figures 2.21** and **2.23**) and complexes (**Figures 2.22** and **2.24**) indicates that inductive effects dominate within the benzene ring as the Hammett plots reflect better linearity for modes 8a, 8b, 19a and 19b. The relatively poor linearity of the 19b Wilson mode in general may be attributed to coupling with the 18b C-H bend ring vibration.[201]

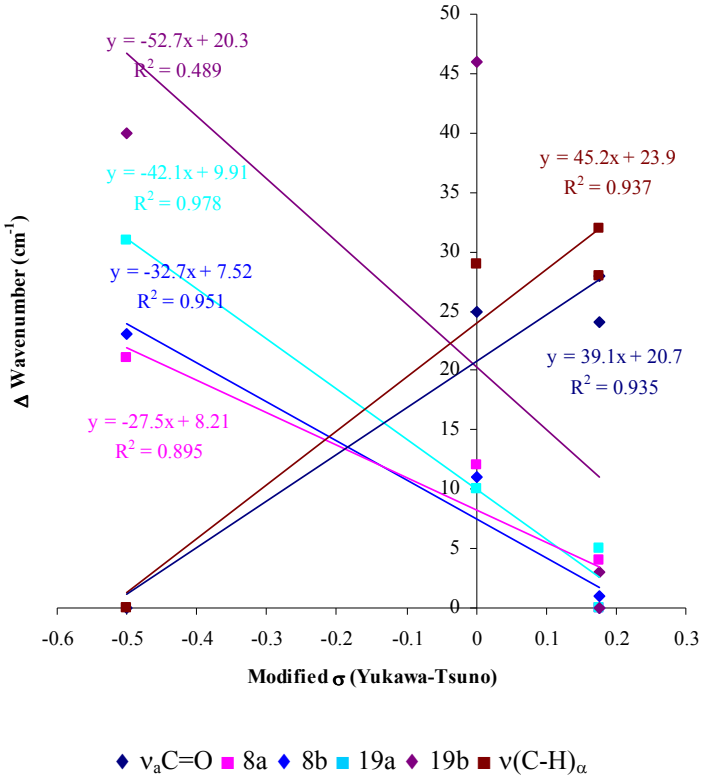

Figure 2.23: Plot of change in wavenumber versus modified Yukawa-Tsuno σ values for selected vibrations in *para*-substituted mandelic acid ligands (ρ = 1, r = 0.272).[214]

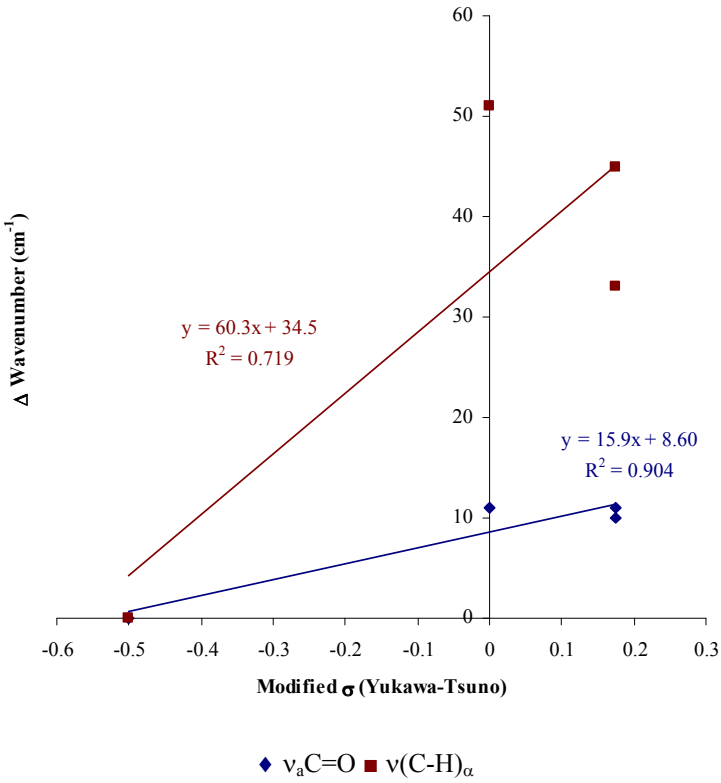

Figure 2.24: Plot of change in wavenumber versus modified Yukawa-Tsuno σ values for selected vibrations in zirconium *para*-substituted mandelate complexes (ρ = 1, r = 0.272).[214]

The zirconium α-hydroxymandelate to zirconium oxycarbonate decomposition endotherm peak temperatures of selected zirconium mandelates (**Section 2.2.3.2.3**) were similarly plotted versus Hammett and Yukawa-Tsuno modified σ values in an attempt to identify possible trends in thermal stability (**Figure 2.25**). Linearity of both plots is poor but the slope indicates that the stability of the 4-hydroxymandelate complex is the worst, followed by the mandelate, 4-chloromandelate and 4-bromomandelate complexes. This, however, does not necessarily imply that the Zr-O bond is weak, merely that *para* electron donating substituents may enhance an unknown decomposition mechanism.[120]

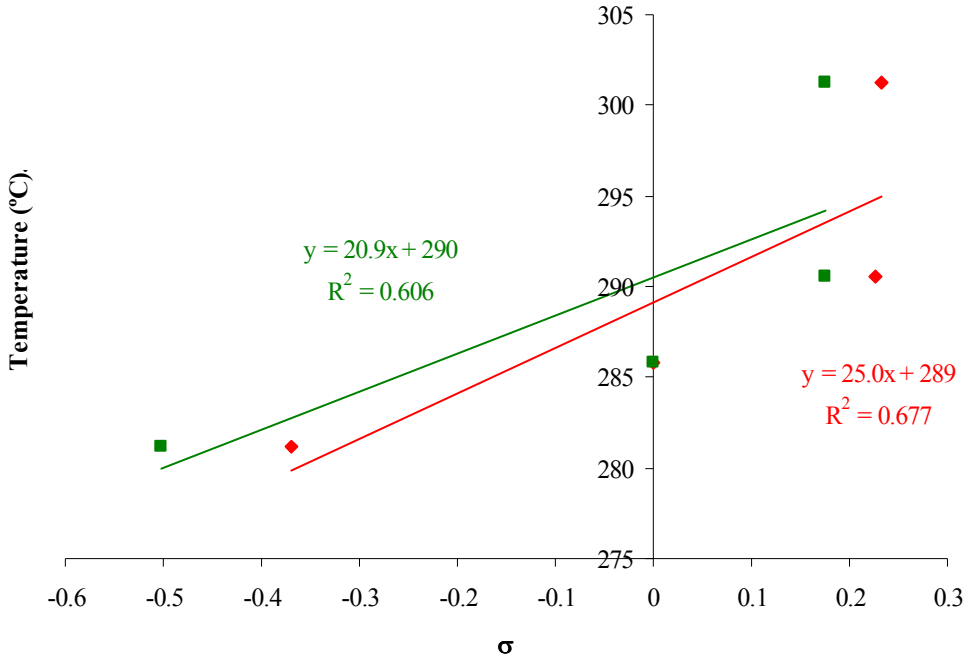

Figure 2.25: Plot of the decomposition endotherm peak temperature versus conventional Hammett (♦, ρ=1) and Yukawa-Tsuno (■, ρ = 1, r = 0.272) modified σ values for selected zirconium *para*-substituted mandelate complexes.

The ν_aC=O vibration for the zirconium 4-hydroxymandelate complex is the lowest of the mandelate series studied and suggests that the C=O bond has more single bond character. This in turn suggests a stronger Zr-O bond with more covalent character. The trends shown using the Hammett and Yukawa-Tsuno plots indicate that as electron donating effects of the *para* substituents increases, the double bond character of the carbonyl decreases and the L→M bonding increases, but the thermal stability of the complex decreases. The decrease in the slope of the ν_aC=O versus σ plots from free ligand to complex suggests an increase in stability and may be further evidence of L→M π bonding. The ν_aC=O vibration may thus be tentatively used as a diagnostic tool to determine if a complex is likely to be more ionic or covalent in nature.

In the synthesis of a substituted zirconium mandelate syntan, a more covalent Zr-O bond would be desirable for a permanently complexed syntan. Therefore, electron donating substituents should result in more C=O single bond character and a lower ν_aC=O wavenumber. A temporarily masked syntan would, however, require a more ionic bond, *i.e.*, more C=O double bond character and a higher ν_aC=O wavenumber.

CHAPTER 3:

THE GENERATION OF POTENTIAL ZIRCONIUM TANNING AGENTS AND THE TANNING OF HIDE POWDER AND GOATSKIN

In **Chapter 2** a range of potential zirconium masking agents were investigated and a series of α-hydroxycarboxylic acids were found to complex readily with zirconium. A range of synthesised and characterised zirconium α-hydroxycarboxylate complexes were discovered to dissolve at elevated pHs, suggesting they may prove suitable as syntans.

Chapter 3 covers the generation, *in situ*, of aqueous zirconium α-hydroxycarboxylate complexes (**Section 3.2.1**) and the investigation of their potential use as novel tanning agents with the aid of hide powder (**Section 3.2.2**) and goatskin pelt (**Section 3.2.3**).

3.1. EXPERIMENTAL

3.1.1. GENERAL METHODS

3.1.1.1. Differential Scanning Calorimetry (DSC)

DSC measurements were performed in a dry nitrogen atmosphere using a heat flux Mettler Toledo DSC 822e (BSLT, Northampton, UK). Approximately 20 mg samples of hide powder were weighed into medium pressure stainless steel pans and heated at a rate of 5°C.min^{-1}, with an empty pan as reference.

3.1.1.2. Inductively Coupled Plasma Mass Spectrometry (ICP-MS)

A Perkin-Elmer Sciex ELAN 6100 Inductively Coupled Plasma Mass Spectrophotometer (UPE, Port Elizabeth, South Africa) was used for quantitative zirconium measurements.

3.1.1.3. Attenuated Total Reflectance (ATR) Spectrometry

Hide powder and goatskin samples were analysed using a DurasamplIR™ horizontal configuration single reflection diamond ATR, with a zinc selenide crystal and 0.75 mm diameter sampling area, attached to a Shimadzu IR Prestige-21 FTIR-8400S spectrometer (BSLT, Northampton, UK). Spectra were obtained from 256 coadded and averaged scans with a resolution of 8 cm^{-1} using the Happ-Genzel apodization.

Single reflection diamond ATR hide powder spectra were compared to spectra from a Gateway™ six reflection horizontal ATR with a 45° angle zinc selenide crystal flat top plate attached to a Shimadzu IR Prestige-21 FTIR-8400S spectrometer (BSLT, Northampton, UK).

3.1.1.4. Scanning Electron Microscopy (SEM)

A Hitachi S-3000 N SEM (BSLT, Northampton, UK) was used for observation and evaluation of specimens prepared for SEM analysis.

3.1.1.5. Scanning Electron Microscopy (SEM) Energy Dispersive X-Ray Analysis (EDXA)

A Hitachi S-2500 SEM with a Link ISIS X-ray microanalysis system (BLC, Northampton, UK) was used for the energy dispersive X-ray mapping of zirconium in goatskin.

3.1.1.6. Analysis of Goatskin Leather

Tanned and dyed crust leather samples were conditioned at 65% RH and 20°C for 48 h according to SLP 3.[30]

Shrinkage temperatures of intact samples were measured using a shrinkage temperature apparatus according to SLP 18.[30]

The distension and strength of the grain was measured using a SATRA Lastometer (no. 5877) (BSLT, Northampton, UK) according to SLP 9.[30]

Tensile strength (MPa) and percent elongation at break were measured parallel and perpendicular to the backbone using an Instron 1122 (BSLT, Northampton, UK) according to SLP 6.[30]

The double-edge tear load (N) was also measured parallel and perpendicular to the backbone using the Instron 1122 (BSLT, Northampton, UK) according to SLP 7.[30]

Leather softness was measured using a RWD Bramley, BLC Research Softness Gauge (BSLT, Northampton, UK) and 25 mm aperture according to SLP 37.[30]

The leather thickness (SLP 4)[30] was measured using a Mitutoyo digital thickness gauge (BSLT, Northampton, UK).

Digestion of leather samples for analysis was achieved by adding 1 mL sulfuric acid (98%) and 5 mL of perchloric acid (60-70%) and heating to the boil over a moderate flame in a Kjeldahl flask. The solution was transferred quantitatively to a volumetric flask (100 mL or 250 mL) for analysis.

Goatskin samples were digested and the zirconium content was measured using ICP-MS (**Section 3.1.1.2**).

The chromium content of leather samples was measured according to SLC 8.[30]

Colour measurements and colour difference measurements were made using the hand-held reflected light Minolta Chroma Meter CR-210b colorimeter (BSLT, Northampton, UK). The measuring head uses a wide-area illumination, a 0° viewing angle geometry and a pulsed xenon arc lamp over the 50 mm diameter measuring area. The D_{65} illumination condition was used.

3.1.1.7. Analysis of Hide Powder

The hide powder utilised contained 18.9% moisture at 65% RH (SLC 125)[30] and 0.29% ash (SLC 128)[30] at pH 5.5 (SLC 129).[30]

Shrinkage temperatures of hide powder samples were measured using DSC according to **Section 3.1.1.1**.

Digestion of hide powder samples for analysis was achieved by adding 1 mL sulfuric acid (98%) and 5 mL of perchloric acid (60-70%) and heating to the boil over a moderate flame in a Kjeldahl flask. The solution was transferred quantitatively to a volumetric flask (100 mL or 250 mL).

Hide powder samples were digested and the zirconium content was measured using ICP-MS (**Section 3.1.1.2**).

The chromium content of leather samples was measured according to SLC 8.[30]

3.1.1.8. Chemicals

Chrome tanning salts (Chromosal® B) were obtained from Lanxess (Leverkusen, Germany) and are a 33% basified chromium sulfate salt with a chromium content of approximately 26% Cr_2O_3.

Zirconium tanning salts (Blancorol® ZB 33-N) were obtained from Lanxess (Leverkusen, Germany) and are a 0% basified zirconium sulfate salt with a zirconium content of approximately 33% ZrO_2.

The condensed vegetable tannin used was a modified wattle bark extract (Mimosa ME) obtained from Mimosa Central Co-operative Ltd (Pietermaritzburg, South Africa).

The hydrolysable vegetable tannin used (myrobalans) was an extract from the nuts of the myrobalan tree and was obtained from BSLT (Northampton, UK).

Zirconium oxychloride octahydrate was obtained from BDH Chemicals Ltd (Poole, UK). Airedale Brown DS from Hodgeson (Leeds, UK) is an anionic dyestuff used to dye leather.

All other chemicals were obtained from Sigma-Aldrich (St Louis, USA).

The use of the terms 1:2 and 1:4 throughout **Chapter 3** refer to the zirconium:ligand mole ratios used in the synthesis of the zirconium α-hydroxycarboxylate solutions and not the actual composition of zirconium:ligand complexes in solution.

3.1.2. TANNING OF HIDE POWDER

Dry hide powder was rehydrated for 24 hours using deionised water (20 mL). The hide powder was then stirred in a 6% salt solution for one hour and filtered using a Buchner funnel. Damp hide powder was sealed in a medium pressure pan and the onset of shrinkage measured (52 ± 1°C) using DSC. Tan offers were based on a percentage of the float volume and attempts were made to use industrially representative amounts. The 1:2 and 1:4 zirconium:ligand tanning solution offers were based on theoretical molecular masses of ZrL_2 and ZrL_4 respectively, where L is the monodeprotonated ligand.

3.1.2.1. Chromium Tanning Salts

In a typical experiment, chrome tanning salts (1.2 g, 3.1 mmol, 6% m/v) were dissolved in water (20 mL) with stirring. Sodium chloride (1.2 g) was added to ensure a 6%

solution (m/v), followed by formic acid (0.5 g) and the pH was measured (2.8). Dry hide powder (1.0 g), rehydrated according to **Section 3.1.2**, was added to the chrome/salt solution and stirred for two hours. Sodium formate (0.8 g) was added slowly and the solution was stirred for a further four hours (pH 3.9). The tanned hide powder was filtered using a Buchner funnel and washed with a little warm water (2 mL). Damp tanned hide powder was sealed in a medium pressure pan and the onset of shrinkage measured using DSC (97°C). Chromium content was measured at 3.3% Cr_2O_3 according to **Section 3.1.1.7**.

3.1.2.2. Zirconium Tanning Salts

In a typical experiment, zirconium tanning salts (2.0 g, 5.6 mmol, 10% m/v) were dissolved in water (20 mL) with stirring. Sodium chloride (1.2 g) was added to ensure a 6% solution (m/v), followed by formic acid (0.1 g) and the pH was measured (1.5). Dry hide powder (1.0 g), rehydrated according to **Section 3.1.2**, was added to the zirconium/salt solution and stirred for two hours. Sodium formate (1.2 g) was added slowly and the solution was stirred for a further four hours (pH 2.2). The tanned hide powder was filtered using a Buchner funnel and washed with a little warm water (2 mL). Damp tanned hide powder was sealed in a medium pressure pan and the onset of shrinkage measured (80°C) using DSC. The zirconium content based on dry hide powder mass was 0.85% (**Section 3.1.1.7**).

3.1.2.3. Glutaraldehyde

In a typical experiment, glutaraldehyde (0.5 g, 5.0 mmol, 2.5% m/v) was dissolved in water (20 mL) with stirring. Sodium chloride (1.2 g) was added to ensure a 6% solution (m/v), followed by formic acid (0.5 g) and the pH was measured (3.1). Dry hide powder (1.0 g), rehydrated according to **Section 3.1.2**, was added to the glutaraldehyde/salt solution and stirred for two hours. Sodium formate (0.7 g) was added slowly and the solution was stirred for a further four hours (pH 4.5). The tanned hide powder was filtered using a Buchner funnel and washed with a little warm water (2 mL). Damp tanned hide powder was sealed in a medium pressure pan and the onset of shrinkage measured (80°C) using DSC.

3.1.2.4. Mimosa Tanning Agent

In a typical experiment, Mimosa ME tannin (2.0 g, 10% m/v) was dissolved in water (20 mL) with stirring. Sodium chloride (1.2 g) was added to ensure a 6% solution (m/v) and the pH was measured (4.9). Dry hide powder (1.0 g), rehydrated according to **Section 3.1.2**, was added to the Mimosa/salt solution and stirred for two hours. Formic acid (0.5 g) was added slowly and the solution was stirred for a further four hours (pH 3.3). The tanned hide powder was filtered using a Buchner funnel and washed with a little warm water (2 mL). Damp tanned hide powder was sealed in a medium pressure pan and the onset of shrinkage measured (71°C) using DSC.

3.1.2.5. Myrobalan Tanning Agent

In a typical experiment, myrobalan tannin (2.0 g, 10% m/v) was dissolved in water (20 mL) with stirring. Sodium chloride (1.2 g) was added to ensure a 6% solution (m/v) and the pH was measured (3.2). Dry hide powder (1.0 g), rehydrated according to **Section 3.1.2**, was added to the Myrobalan/salt solution and stirred for two hours. Formic acid (0.1 g) was added slowly and the solution was stirred for a further four hours (pH 3.0). The tanned hide powder was filtered using a Buchner funnel and washed with a little warm water (2 mL). Damp tanned hide powder was sealed in a medium pressure pan and the onset of shrinkage measured (58°C) using DSC.

3.1.2.6. Zirconium Lactate (1:2)

In a typical experiment, zirconium oxychloride (2.40g, 7.42 mmol) was dissolved in water (5 mL) and concentrated hydrochloric acid (1 mL) was added with stirring. Lactic acid (1.34 g, 14.8 mmol) was dissolved in water (3 mL) and both solutions were warmed to approximately 80°C. The ligand solution was added to the zirconium slowly (5 min) and the precipitate was allowed to age for 48 h at RT. The zirconium lactate solution (10% m/v) was then treated with 2 ***M*** sodium hydroxide until the precipitate dissolved (pH 7.6). The solution was made up to 20 mL and sodium chloride (1.2 g) was added to ensure a 6% solution (m/v).

Dry hide powder (1.0 g), rehydrated according to **Section 3.1.2**, was added to the zirconium lactate/salt solution and stirred for two hours. Formic acid (1.0 g) was added slowly and the solution was stirred for a further four hours (pH 3.4). The tanned hide

powder was filtered using a Buchner funnel and washed with a little warm water (2 mL). Damp tanned hide powder was sealed in a medium pressure pan and the onset of shrinkage measured (73°C) using DSC. The zirconium content based on dry hide powder mass was 0.67% (**Section 3.1.1.7**).

3.1.2.7. Zirconium Lactate (1:4)

In a typical experiment, zirconium oxychloride (1.44 g, 4.48 mmol) was dissolved in water (5 mL) and concentrated hydrochloric acid (1 mL) was added with stirring. Lactic acid (1.61 g, 17.9 mmol) was dissolved in water (3 mL) and both solutions were warmed to approximately 80°C. The ligand solution was added to the zirconium slowly (5 min) and the precipitate was allowed to age for 48 h at RT. The zirconium lactate solution (10% m/v) was then treated with 2 ***M*** sodium hydroxide until the precipitate dissolved (pH 7.5). The solution was made up to 20 mL and sodium chloride (1.2 g) was added to ensure a 6% solution (m/v).

Dry hide powder (1.0 g), rehydrated according to **Section 3.1.2**, was added to the zirconium lactate/salt solution and stirred for two hours. Formic acid (1.0 g) was added slowly and the solution was stirred for a further four hours (pH 3.6). The tanned hide powder was filtered using a Buchner funnel and washed with a little warm water (2 mL). Damp tanned hide powder was sealed in a medium pressure pan and the onset of shrinkage measured (71°C) using DSC. The zirconium content based on dry hide powder mass was 0.40% (**Section 3.1.1.7**).

3.1.2.8. Zirconium Mandelate (1:2)

In a typical experiment, zirconium oxychloride (1.64 g, 5.08 mmol) was dissolved in water (5 mL) and concentrated hydrochloric acid (1 mL) was added with stirring. Mandelic acid (1.55 g, 10.2 mmol) was dissolved in water (3 mL) and both solutions were warmed to approximately 80°C. The ligand solution was added to the zirconium slowly (5 min) and the precipitate was allowed to age for 48 h at RT. The zirconium mandelate solution (10% m/v) was then treated with 2 ***M*** sodium hydroxide until the precipitate dissolved (pH 8.1). The solution was made up to 20 mL and sodium chloride (1.2 g) was added to ensure a 6% solution (m/v).

Dry hide powder (1.0 g), rehydrated according to **Section 3.1.2**, was added to the zirconium mandelate/salt solution and stirred for two hours. Formic acid (1.0 g) was added slowly and the solution was stirred for a further four hours (pH 3.7). The tanned hide powder was filtered using a Buchner funnel and washed with a little warm water (2 mL). Damp tanned hide powder was sealed in a medium pressure pan and the onset of shrinkage measured (70°C) using DSC. The zirconium content based on dry hide powder mass was 0.46% (**Section 3.1.1.7**).

3.1.2.9. Zirconium Mandelate (1:4)

In a typical experiment, zirconium oxychloride (0.926 g, 2.88 mmol) was dissolved in water (5 mL) and concentrated hydrochloric acid (1 mL) was added with stirring. Mandelic acid (1.75 g, 11.5 mmol) was dissolved in water (3 mL) and both solutions were warmed to approximately 80°C. The ligand solution was added to the zirconium slowly (5 min) and the precipitate was allowed to age for 48 h at RT. The zirconium mandelate solution (10% m/v) was then treated with 2 ***M*** sodium hydroxide until the precipitate dissolved (pH 8.3). The solution was made up to 20 mL and sodium chloride (1.2 g) was added to ensure a 6% solution (m/v).

Dry hide powder (1.0 g), rehydrated according to **Section 3.1.2**, was added to the zirconium mandelate/salt solution and stirred for two hours. Formic acid (1.0 g) was added slowly and the solution was stirred for a further four hours (pH 3.8). The tanned hide powder was filtered using a Buchner funnel and washed with a little warm water (2 mL). Damp tanned hide powder was sealed in a medium pressure pan and the onset of shrinkage measured (63°C) using DSC. The zirconium content based on dry hide powder mass was 0.26% (**Section 3.1.1.7**).

3.1.2.10. Zirconium Citrate (1:2)

In a typical experiment, zirconium oxychloride (1.36 g, 4.22 mmol) was dissolved in water (5 mL) and concentrated hydrochloric acid (1 mL) was added with stirring. Citric acid (1.62 g, 8.44 mmol) was dissolved in water (3 mL) and both solutions were warmed to approximately 80°C. The ligand solution was added to the zirconium slowly (5 min) and allowed to age for 48 h at RT. The zirconium citrate solution (10% m/v) was then

treated with 2 ***M*** sodium hydroxide until a pH of 7.5 was obtained. The solution was made up to 20 mL and sodium chloride (1.2 g) was added to ensure a 6% solution (m/v).

Dry hide powder (1.0 g), rehydrated according to **Section 3.1.2**, was added to the zirconium citrate/salt solution and stirred for two hours. Formic acid (1.0 g) was added slowly and the solution was stirred for a further four hours (pH 3.6). The tanned hide powder was filtered using a Buchner funnel and washed with a little warm water (2 mL). Damp tanned hide powder was sealed in a medium pressure pan and the onset of shrinkage measured (68°C) using DSC. The zirconium content based on dry hide powder mass was 0.38% (**Section 3.1.1.7**).

3.1.2.11. Zirconium Citrate (1:4)

In a typical experiment, zirconium oxychloride (0.754 g, 2.34 mmol) was dissolved in water (5 mL) and concentrated hydrochloric acid (1 mL) was added with stirring. Citric acid (1.70 g, 9.36 mmol) was dissolved in water (3 mL) and both solutions were warmed to approximately 80°C. The ligand solution was added to the zirconium slowly (5 min) and allowed to age for 48 h at RT. The zirconium citrate solution (10% m/v) was then treated with 2 ***M*** sodium hydroxide until a pH of 7.5 was obtained. The solution was made up to 20 mL and sodium chloride (1.2 g) was added to ensure a 6% solution (m/v).

Dry hide powder (1.0 g), rehydrated according to **Section 3.1.2**, was added to the zirconium citrate/salt solution and stirred for two hours. Formic acid (1.0 g) was added slowly and the solution was stirred for a further four hours (pH 3.7). The tanned hide powder was filtered using a Buchner funnel and washed with a little warm water (2 mL). Damp tanned hide powder was sealed in a medium pressure pan and the onset of shrinkage measured (64°C) using DSC. The zirconium content based on dry hide powder mass was 0.24% (**Section 3.1.1.7**).

3.1.2.12. Zirconium D-Gluconate (1:2)

In a typical experiment, zirconium oxychloride (1.34 g, 4.16 mmol) was dissolved in water (5 mL) and concentrated hydrochloric acid (1 mL) was added with stirring. D-Gluconic acid (1.62 g, 8.30 mmol) was dissolved in water (3 mL) and both solutions were warmed to approximately 80°C. The ligand solution was added to the zirconium slowly

(5 min) and allowed to age for 48 h at RT. The zirconium D-gluconate solution (10% m/v) was then treated with 2 ***M*** sodium hydroxide until a pH of 7.5 was obtained. The solution was made up to 20 mL and sodium chloride (1.2 g) was added to ensure a 6% solution (m/v).

Dry hide powder (1.0 g), rehydrated according to **Section 3.1.2**, was added to the zirconium D-gluconate/salt solution and stirred for two hours. Formic acid (1.0 g) was added slowly and the solution was stirred for a further four hours (pH 3.4). The tanned hide powder was filtered using a Buchner funnel and washed with a little warm water (2 mL). Damp tanned hide powder was sealed in a medium pressure pan and the onset of shrinkage measured (67°C) using DSC. The zirconium content based on dry hide powder mass was 0.36% (**Section 3.1.1.7**).

3.1.2.13. Zirconium D-Gluconate (1:4)

In a typical experiment, zirconium oxychloride (0.740 g, 2.30 mmol) was dissolved in water (5 mL) and concentrated hydrochloric acid (1 mL) was added with stirring. D-Gluconic acid (1.80 g, 9.18 mmol) was dissolved in water (3 mL) and both solutions were warmed to approximately 80°C. The ligand solution was added to the zirconium slowly (5 min) and allowed to age for 48 h at RT. The zirconium D-gluconate solution (10% m/v) was then treated with 2 ***M*** sodium hydroxide until a pH of 7.5 was obtained. The solution was made up to 20 mL and sodium chloride (1.2 g) was added to ensure a 6% solution (m/v).

Dry hide powder (1.0 g), rehydrated according to **Section 3.1.2**, was added to the zirconium D-gluconate/salt solution and stirred for two hours. Formic acid (1.0 g) was added slowly and the solution was stirred for a further four hours (pH 3.5). The tanned hide powder was filtered using a Buchner funnel and washed with a little warm water (2 mL). Damp tanned hide powder was sealed in a medium pressure pan and the onset of shrinkage measured (65°C) using DSC. The zirconium content based on dry hide powder mass was 0.22% (**Section 3.1.1.7**).

3.1.2.14. Zirconium 4-Hydroxymandelate (1:2)

In a typical experiment, zirconium oxychloride (1.51 g, 4.70 mmol) was dissolved in water (5 mL) and concentrated hydrochloric acid (1 mL) was added with stirring. 4-Hydroxymandelic acid (1.75 g, 9.40 mmol) was dissolved in water (3 mL) and both solutions were warmed to approximately 80°C. The ligand solution was added to the zirconium slowly (5 min) and the precipitate was allowed to age for 48 h at RT. The zirconium 4-hydroxymandelate solution (10% m/v) was then treated with 2 ***M*** sodium hydroxide until the precipitate dissolved (pH 6.3). The solution was made up to 20 mL and sodium chloride (1.2 g) was added to ensure a 6% solution (m/v).

Dry hide powder (1.0 g), rehydrated according to **Section 3.1.2**, was added to the zirconium 4-hydroxymandelate/salt solution and stirred for two hours. Formic acid (1.0 g) was added slowly and the solution was stirred for a further four hours (pH 3.3). The tanned hide powder was filtered using a Buchner funnel and washed with a little warm water (2 mL). Damp tanned hide powder was sealed in a medium pressure pan and the onset of shrinkage measured (80°C) using DSC. The zirconium content based on dry hide powder mass was 0.50% (**Section 3.1.1.7**).

3.1.2.15. Zirconium 4-Hydroxymandelate (1:4)

In a typical experiment, zirconium oxychloride (0.848 g, 2.64 mmol) was dissolved in water (5 mL) and concentrated hydrochloric acid (1 mL) was added with stirring. 4-Hydroxymandelic acid (1.96 g, 10.5 mmol) was dissolved in water (3 mL) and both solutions were warmed to approximately 80°C. The ligand solution was added to the zirconium slowly (5 min) and the precipitate was allowed to age for 48 h at RT. The zirconium 4-hydroxymandelate solution (10% m/v) was then treated with 2 ***M*** sodium hydroxide until the precipitate dissolved (pH 6.1). The solution was made up to 20 mL and sodium chloride (1.2 g) was added to ensure a 6% solution (m/v).

Dry hide powder (1.0 g), rehydrated according to **Section 3.1.2**, was added to the zirconium 4-hydroxymandelate/salt solution and stirred for two hours. Formic acid (1.0 g) was added slowly and the solution was stirred for a further four hours (pH 3.3). The tanned hide powder was filtered using a Buchner funnel and washed with a little warm water (2 mL). Damp tanned hide powder was sealed in a medium pressure pan and the

onset of shrinkage measured (68°C) using DSC. The zirconium content based on dry hide powder mass was 0.28% (**Section 3.1.1.7**).

3.1.2.16. Zirconium 4-Bromomandelate (1:4)

In a typical experiment, zirconium oxychloride (0.637 g, 1.98 mmol) was dissolved in water (5 mL) and concentrated hydrochloric acid (1 mL) was added with stirring. 4-Bromomandelic acid (1.83 g, 7.92 mmol) was dissolved in water (3 mL) and both solutions were warmed to approximately 80°C. The ligand solution was added to the zirconium slowly (5 min) and the precipitate was allowed to age for 48 h at RT. The zirconium 4-bromomandelate solution (10% m/v) was then treated with 2 ***M*** sodium hydroxide until the precipitate dissolved (pH 9.8). The solution was made up to 20 mL and sodium chloride (1.2 g) was added to ensure a 6% solution (m/v).

Dry hide powder (1.0 g), rehydrated according to **Section 3.1.2**, was added to the zirconium 4-bromomandelate/salt solution and stirred for two hours. Formic acid (1.0 g) was added slowly and the solution was stirred for a further four hours (pH 3.3). The tanned hide powder was filtered using a Buchner funnel and washed with a little warm water (2 mL). Damp tanned hide powder was sealed in a medium pressure pan and the onset of shrinkage measured (67°C) using DSC. The zirconium content based on dry hide powder mass was 0.20% (**Section 3.1.1.7**).

3.1.3. TANNING OF GOATSKIN SAMPLES

Goatskins were sourced locally and processed to pickled goatskin pelt (T_s = 63 ± 1°C) according to **Appendix 1**. Small samples (35-40 g) were then processed in experimental Wacker drums (20 x 30 cm). Tan offers were based on a percentage of the pelt mass with a float of 100% and attempts were made to use industrially representative amounts. The 1:2 and 1:4 zirconium:ligand tanning solution offers were based on theoretical molecular masses of ZrL_2 and ZrL_4 respectively, where L is the monodeprotonated ligand.

3.1.3.1. Chromium Tanning Salts

In a typical experiment, pickled goatskin (38 g), 100% float (38 g) and sodium chloride (2.3 g) were placed in a Wacker drum and drummed (10 min) before the pH was

measured (3.0). Chrome tanning salts (2.31 g, 2.89 mmol, 6% m/m) were added and drummed for two hours. Small additions of sodium bicarbonate were added over two hours until a pH of 4.0 was reached. The goatskin was left to drum for a further six hours before the liquor was drained and the skin was washed using 100% warm water (38 g, 40°C). The skin was sealed in a plastic bag and stored overnight. The shrinkage temperature of the damp tanned skin was measured (98°C) according to **Section 3.1.1.6**. The chromium content was measured at 3.8% Cr_2O_3 according to **Section 3.1.1.6**.

3.1.3.2. Zirconium Tanning Salts

In a typical experiment, pickled goatskin (35 g), 100% float (35 g) and sodium chloride (2.1 g) were placed in a Wacker drum and drummed (10 min) before the pH was measured (2.9). Zirconium tanning salts (3.50 g, 9.86 mmol, 10% m/m) were added and drummed for six hours. Small additions of sodium bicarbonate were added over two hours until a pH of 2.5 was reached. The goatskin was left to drum for a further six hours before the liquor was drained and the skin was washed using 100% warm water (35 g, 40°C). The skin was sealed in a plastic bag and stored overnight. The shrinkage temperature of the damp tanned skin was measured (91°C) according to **Section 3.1.1.6**. The zirconium content based on dry goatskin mass was 4.6% (**Section 3.1.1.6**).

3.1.3.3. Zirconium Lactate (1:2)

In a typical experiment, zirconium oxychloride (4.19 g, 13.0 mmol) was dissolved in water (8 mL) and concentrated hydrochloric acid (1 mL) was added with stirring. Lactic acid (2.34 g, 26.0 mmol) was dissolved in water (8 mL) and both solutions were warmed to approximately 80°C. The ligand solution was added to the zirconium slowly (15 min) and the precipitate was allowed to age for 48 h at RT. The zirconium lactate solution (10% m/m) was then treated with 2 ***M*** sodium hydroxide until the precipitate dissolved (pH 6.3). The solution was made up to 35 mL and sodium chloride (2.1 g) was added to ensure a 6% solution (m/v).

The zirconium lactate/salt solution was placed in a Wacker drum and goatskin added (35 g) and drummed for four hours (pH 5.2-5.5). Formic acid was added slowly (30 min) until a pH of 3.5 was reached. The skin was drummed for a further twelve hours, the float was drained and the skin was sealed in a plastic bag and stored overnight. The

shrinkage temperature of the damp tanned skin was measured (82°C) according to **Section 3.1.1.6**. The zirconium content based on dry goatskin mass was 4.0% (**Section 3.1.1.6**).

3.1.3.4. Zirconium Lactate (1:4)

In a typical experiment, zirconium oxychloride (2.88 g, 8.94 mmol) was dissolved in water (8 mL) and concentrated hydrochloric acid (1 mL) was added with stirring. Lactic acid (3.22 g, 35.7 mmol) was dissolved in water (8 mL) and both solutions were warmed to approximately 80°C. The ligand solution was added to the zirconium slowly (15 min) and the precipitate was allowed to age for 48 h at RT. The zirconium lactate solution (10% m/m) was then treated with 2 ***M*** sodium hydroxide until the precipitate dissolved (pH 6.5). The solution was made up to 40 mL and sodium chloride (2.4 g) was added to ensure a 6% solution (m/v).

The zirconium lactate/salt solution was placed in a Wacker drum and goatskin added (40 g) and drummed for four hours (pH 5.2-5.5). Formic acid was added slowly (30 min) until a pH of 3.5 was reached. The skin was drummed for a further twelve hours, the float was drained and the skin was sealed in a plastic bag and stored overnight. The shrinkage temperature of the damp tanned skin was measured (75°C) according to **Section 3.1.1.6**. The zirconium content based on dry goatskin mass was 3.0% (**Section 3.1.1.6**).

3.1.3.5. Zirconium Mandelate (1:2)

In a typical experiment, zirconium oxychloride (3.11 g, 9.66 mmol) was dissolved in water (8 mL) and concentrated hydrochloric acid (1 mL) was added with stirring. Mandelic acid (2.94 g, 19.3 mmol) was dissolved in water (8 mL) and both solutions were warmed to approximately 80°C. The ligand solution was added to the zirconium slowly (15 min) and the precipitate was allowed to age for 48 h at RT. The zirconium mandelate solution (10% m/m) was then treated with 2 ***M*** sodium hydroxide until the precipitate dissolved (pH 8.5). The solution was made up to 38 mL and sodium chloride (2.3 g) was added to ensure a 6% solution (m/v).

The zirconium mandelate/salt solution was placed in a Wacker drum and goatskin added (38 g) and drummed for four hours (pH 6.0-6.5). Formic acid was added slowly (30 min) until a pH of 3.5 was reached. The skin was drummed for a further twelve hours, the float was drained and the skin was sealed in a plastic bag and stored overnight. The shrinkage temperature of the damp tanned skin was measured (78°C) according to **Section 3.1.1.6**. The zirconium content based on dry goatskin mass was 3.8% (**Section 3.1.1.6**).

3.1.3.6. Zirconium Mandelate (1:4)

In a typical experiment, zirconium oxychloride (1.71 g, 5.32 mmol) was dissolved in water (8 mL) and concentrated hydrochloric acid (1 mL) was added with stirring. Mandelic acid (3.24 g, 21.3 mmol) was dissolved in water (10 mL) and both solutions were warmed to approximately 80°C. The ligand solution was added to the zirconium slowly (15 min) and the precipitate was allowed to age for 48 h at RT. The zirconium mandelate solution (10% m/m) was then treated with 2 ***M*** sodium hydroxide until the precipitate dissolved (pH 8.3). The solution was made up to 37 mL and sodium chloride (2.2 g) was added to ensure a 6% solution (m/v).

The zirconium mandelate/salt solution was placed in a Wacker drum and goatskin added (37 g) and drummed for four hours (pH 6.0-6.5). Formic acid was added slowly (30 min) until a pH of 3.5 was reached. The skin was drummed for a further twelve hours, the float was drained and the skin was sealed in a plastic bag and stored overnight. The shrinkage temperature of the damp tanned skin was measured (67°C) according to **Section 3.1.1.6**. The zirconium content based on dry goatskin mass was 1.8% (**Section 3.1.1.6**).

3.1.3.7. Zirconium Citrate (1:2)

In a typical experiment, zirconium oxychloride (2.45 g, 7.60 mmol) was dissolved in water (8 mL) and concentrated hydrochloric acid (1 mL) was added with stirring. Citric acid (2.92 g, 15.2 mmol) was dissolved in water (8 mL) and both solutions were warmed to approximately 80°C. The ligand solution was added to the zirconium slowly (15 min) and the mixture was allowed to age for 48 h at RT. The zirconium citrate solution (10% m/m) was then treated with 2 ***M*** sodium hydroxide until a pH of 6.5 was obtained. The

solution was made up to 36 mL and sodium chloride (2.2 g) was added to ensure a 6% solution (m/v).

The zirconium citrate/salt solution was placed in a Wacker drum and goatskin added (36 g) and drummed for four hours (pH 5.5-6.0). Formic acid was added slowly (30 min) until a pH of 3.5 was reached. The skin was drummed for a further twelve hours, the float was drained and the skin was sealed in a plastic bag and stored overnight. The shrinkage temperature of the damp tanned skin was measured (75°C) according to **Section 3.1.1.6**. The zirconium content based on dry goatskin mass was 2.4% (**Section 3.1.1.6**).

3.1.3.8. Zirconium Citrate (1:4)

In a typical experiment, zirconium oxychloride (1.39 g, 4.32 mmol) was dissolved in water (8 mL) and concentrated hydrochloric acid (1 mL) was added with stirring. Citric acid (3.32 g, 17.3 mmol) was dissolved in water (8 mL) and both solutions were warmed to approximately 80°C. The ligand solution was added to the zirconium slowly (15 min) and the mixture was allowed to age for 48 h at RT. The zirconium citrate solution (10% m/m) was then treated with 2 ***M*** sodium hydroxide until a pH of 6.5 was obtained. The solution was made up to 37 mL and sodium chloride (2.2 g) was added to ensure a 6% solution (m/v).

The zirconium citrate/salt solution was placed in a Wacker drum and goatskin added (37 g) and drummed for four hours (pH 5.5-6.0). Formic acid was added slowly (30 min) until a pH of 3.5 was reached. The skin was drummed for a further twelve hours, the float was drained and the skin was sealed in a plastic bag and stored overnight. The shrinkage temperature of the damp tanned skin was measured (75°C) according to **Section 3.1.1.6**. The zirconium content based on dry goatskin mass was 1.8% (**Section 3.1.1.6**).

3.1.3.9. Zirconium D-Gluconate (1:2)

In a typical experiment, zirconium oxychloride (2.54 g, 7.89 mmol) was dissolved in water (8 mL) and concentrated hydrochloric acid (1 mL) was added with stirring. D-Gluconic acid (3.10 g, 15.8 mmol) was dissolved in water (8 mL) and both solutions were

warmed to approximately 80°C. The ligand solution was added to the zirconium slowly (15 min) and the mixture was allowed to age for 48 h at RT. The zirconium D-gluconate solution (10% m/m) was then treated with 2 ***M*** sodium hydroxide until a pH of 6.5 was obtained. The solution was made up to 38 mL and sodium chloride (2.3 g) was added to ensure a 6% solution (m/v).

The zirconium D-gluconate/salt solution was placed in a Wacker drum and goatskin added (38 g) and drummed for four hours (pH 5.5-6.0). Formic acid was added slowly (30 min) until a pH of 3.5 was reached. The skin was drummed for a further twelve hours, the float was drained and the skin was sealed in a plastic bag and stored overnight. The shrinkage temperature of the damp tanned skin was measured (75°C) according to **Section 3.1.1.6**. The zirconium content based on dry goatskin mass was 2.5% (**Section 3.1.1.6**).

3.1.3.10. Zirconium D-Gluconate (1:4)

In a typical experiment, zirconium oxychloride (1.40 g, 4.36 mmol) was dissolved in water (8 mL) and concentrated hydrochloric acid (1 mL) was added with stirring. D-Gluconic acid (3.41 g, 17.4 mmol) was dissolved in water (8 mL) and both solutions were warmed to approximately 80°C. The ligand solution was added to the zirconium slowly (15 min) and the mixture was allowed to age for 48 h at RT. The zirconium D-gluconate solution (10% m/m) was then treated with 2 ***M*** sodium hydroxide until a pH of 6.5 was obtained. The solution was made up to 38 mL and sodium chloride (2.3 g) was added to ensure a 6% solution (m/v).

The zirconium D-gluconate/salt solution was placed in a Wacker drum and goatskin added (38 g) and drummed for four hours (pH 5.5-6.0). Formic acid was added slowly (30 min) until a pH of 3.5 was reached. The skin was drummed for a further twelve hours, the float was drained and the skin was sealed in a plastic bag and stored overnight. The shrinkage temperature of the damp tanned skin was measured (76°C) according to **Section 3.1.1.6**. The zirconium content based on dry goatskin mass was 1.8% (**Section 3.1.1.6**).

3.1.3.11. Zirconium 4-Hydroxymandelate (1:2)

In a typical experiment, zirconium oxychloride (2.65 g, 8.23 mmol) was dissolved in water (8 mL) and concentrated hydrochloric acid (1 mL) was added with stirring. 4-Hydroxymandelic acid (3.06 g, 16.5 mmol) was dissolved in water (8 mL) and both solutions were warmed to approximately 80°C. The ligand solution was added to the zirconium slowly (15 min) and the precipitate was allowed to age for 48 h at RT. The zirconium 4-hydroxymandelate solution (10% m/m) was then treated with 2 ***M*** sodium hydroxide until the precipitate dissolved (pH 6.8). The solution was made up to 35 mL and sodium chloride (2.1 g) was added to ensure a 6% solution (m/v).

The zirconium 4-hydroxymandelate/salt solution was placed in a Wacker drum and goatskin added (35 g) and drummed for four hours (pH 6.0-6.5). Formic acid was added slowly (30 min) until a pH of 3.5 was reached. The skin was drummed for a further twelve hours, the float was drained and the skin was sealed in a plastic bag and stored overnight. The shrinkage temperature of the damp tanned skin was measured (92°C) according to **Section 3.1.1.6**. The zirconium content based on dry goatskin mass was 3.3% (**Section 3.1.1.6**).

3.1.3.12. Zirconium 4-Hydroxymandelate (1:4)

In a typical experiment, zirconium oxychloride (1.57 g, 4.87 mmol) was dissolved in water (8 mL) and concentrated hydrochloric acid (1 mL) was added with stirring. 4-Hydroxymandelic acid (3.63 g, 19.5 mmol) was dissolved in water (8 mL) and both solutions were warmed to approximately 80°C. The ligand solution was added to the zirconium slowly (15 min) and the precipitate was allowed to age for 48 h at RT. The zirconium 4-hydroxymandelate solution (10% m/m) was then treated with 2 ***M*** sodium hydroxide until the precipitate dissolved (pH 6.8). The solution was made up to 37 mL and sodium chloride (2.2 g) was added to ensure a 6% solution (m/v).

The zirconium 4-hydroxymandelate/salt solution was placed in a Wacker drum and goatskin added (37 g) and drummed for four hours (pH 6.0-6.5). Formic acid was added slowly (30 min) until a pH of 3.5 was reached. The skin was drummed for a further twelve hours, the float was drained and the skin was sealed in a plastic bag and stored overnight. The shrinkage temperature of the damp tanned skin was measured (86°C)

according to **Section 3.1.1.6**. The zirconium content based on dry goatskin mass was 1.8% (**Section 3.1.1.6**).

3.1.3.13. 4-Hydroxymandelate

In a typical experiment, 4-hydroxymandelic acid (3.50 g, 18.8 mmol, 8.75% m/m) was dissolved in water (8 mL) and then treated with 0.2 ***M*** sodium hydroxide until a pH of 5.0-5.5 was obtained. The solution was made up to 40 mL and sodium chloride (2.4 g) was added to ensure a 6% solution (m/v).

The 4-hydroxymandelate/salt solution was placed in a Wacker drum and goatskin added (40 g) and drummed for two hours (pH 5.0-5.5). Formic acid was added slowly (15 min) until a pH of 3.5 was reached. The skin was drummed for a further twelve hours, the float was drained and the skin was removed and sealed in a plastic bag and stored overnight. The shrinkage temperature of the damp "tanned" skin was measured (45°C) according to **Section 3.1.1.6**.

3.1.4. Optimisation of the Zirconium 4-Hydroxymandelate (1:2) Tanning Process using Goatskin

Goatskins were sourced locally and processed to pickled goatskin pelt (T_s = 63 ± 1°C) according to **Appendix 1**. Two "pickle" pHs were investigated: High = pH 7.5-8.0 and Low = pH 5.0-5.5. Two floats were investigated: High = 200% and Low = 100%. The tanning and fixing process times were investigated: Long Tan (12 h)/Short Fix (2 h) and Short Tan (2 h)/Long Fix (12 h). After fixation, the samples were investigated to determine if washing influenced the shrinkage temperature. Tanning offers of 15%, 10%, 7.5%, 5% and 2.5% based on pelt mass were investigated. The 1:2 and 1:4 zirconium:ligand tanning solution offers were based on theoretical molecular masses of ZrL_2 and ZrL_4 respectively, where L is the monodeprotonated ligand.

3.1.4.1. Zirconium 4-Hydroxymandelate (1:2)
Low Pickle pH, Low Float, Long Tan/Short Fix and 10% Offer

In a typical experiment, zirconium oxychloride (2.65 g, 8.23 mmol) was dissolved in water (8 mL) and concentrated hydrochloric acid (1 mL) was added with stirring. 4-Hydroxymandelic acid (3.06 g, 16.5 mmol) was dissolved in water (8 mL) and both

solutions were warmed to approximately 80°C. The ligand solution was added to the zirconium slowly (15 min) and the precipitate was allowed to age for 48 h at RT. The zirconium 4-hydroxymandelate solution was then treated with 2 ***M*** sodium hydroxide until the precipitate dissolved (pH 6.8) and aged overnight before the pH was lowered to pH 5.0-5.5 using formic acid. The solution was made up to 35 mL and sodium chloride (2.1 g) was added to ensure a 6% solution (m/v).

The zirconium 4-hydroxymandelate/salt solution was placed in a Wacker drum and goatskin added (35 g) and drummed for twelve hours (pH 5.0-5.5). Formic acid was added slowly (30 min) until a pH of 3.5 was reached. The skin was drummed for a further two hours, the float was drained and a sample of skin was removed and sealed in a plastic bag and stored overnight. The remaining skin was washed using warm water (40°C) before being sealed in a plastic bag and stored overnight. The shrinkage temperature of the damp tanned skin was measured without a final wash (95°C) and then with a final wash (86°C) according to **Section 3.1.1.6**. The zirconium content based on dry goatskin mass was 1.80% (**Section 3.1.1.6**).

3.1.4.2. Zirconium 4-Hydroxymandelate (1:2)
High Pickle pH, Low Float, Long Tan/Short Fix and 10% Offer

In a typical experiment, zirconium oxychloride (3.03 g, 9.40 mmol) was dissolved in water (8 mL) and concentrated hydrochloric acid (1 mL) was added with stirring. 4-Hydroxymandelic acid (3.50 g, 18.8 mmol) was dissolved in water (10 mL) and both solutions were warmed to approximately 80°C. The ligand solution was added to the zirconium slowly (15 min) and the precipitate was allowed to age for 48 h at RT. The zirconium 4-hydroxymandelate solution was then treated with 2 ***M*** sodium hydroxide until the precipitate dissolved (pH 6.9) and aged overnight before the pH was raised to pH 7.5-8.0 using sodium hydroxide. The solution was made up to 40 mL and sodium chloride (2.4 g) was added to ensure a 6% solution (m/v).

The zirconium 4-hydroxymandelate/salt solution was placed in a Wacker drum and goatskin added (40 g) and drummed for twelve hours (pH 7.5-8.0). Formic acid was added slowly (30 min) until a pH of 3.5 was reached. The skin was drummed for a further two hours, the float was drained and the skin was removed and sealed in a plastic bag and stored overnight. The shrinkage temperature of the damp tanned skin was

measured (91°C) according to **Section 3.1.1.6**. The zirconium content based on dry goatskin mass was 3.36% (**Section 3.1.1.6**).

3.1.4.3. Zirconium 4-Hydroxymandelate (1:2) Low Pickle pH, High Float, Long Tan/Short Fix and 10% Offer

In a typical experiment, zirconium oxychloride (2.88 g, 8.93 mmol) was dissolved in water (8 mL) and concentrated hydrochloric acid (1 mL) was added with stirring. 4-Hydroxymandelic acid (3.33 g, 17.9 mmol) was dissolved in water (10 mL) and both solutions were warmed to approximately 80°C. The ligand solution was added to the zirconium slowly (15 min) and the precipitate was allowed to age for 48 h at RT. The zirconium 4-hydroxymandelate solution was then treated with 2 ***M*** sodium hydroxide until the precipitate dissolved (pH 7.0) and aged overnight before the pH was lowered to pH 5.0-5.5 using formic acid. The solution was made up to 76 mL and sodium chloride (4.6 g) was added to ensure a 6% solution (m/v).

The zirconium 4-hydroxymandelate/salt solution was placed in a Wacker drum and goatskin added (38 g) and drummed for twelve hours (pH 5.0-5.5). Formic acid was added slowly (30 min) until a pH of 3.5 was reached. The skin was drummed for a further two hours, the float was drained and the skin was removed and sealed in a plastic bag and stored overnight. The shrinkage temperature of the damp tanned skin was measured (85°C) according to **Section 3.1.1.6**. The zirconium content based on dry goatskin mass was 1.78% (**Section 3.1.1.6**).

3.1.4.4. Zirconium 4-Hydroxymandelate (1:2) Low Pickle pH, Low Float, Short Tan/Long Fix and 10% Offer

In a typical experiment, zirconium oxychloride (2.65 g, 8.23 mmol) was dissolved in water (8 mL) and concentrated hydrochloric acid (1 mL) was added with stirring. 4-Hydroxymandelic acid (3.06 g, 16.5 mmol) was dissolved in water (10 mL) and both solutions were warmed to approximately 80°C. The ligand solution was added to the zirconium slowly (15 min) and the precipitate was allowed to age for 48 h at RT. The zirconium 4-hydroxymandelate solution was then treated with 2 ***M*** sodium hydroxide until the precipitate dissolved (pH 6.8) and aged overnight before the pH was lowered to pH 5.0-5.5 using formic acid. The solution was made up to 35 mL and sodium chloride (2.1 g) was added to ensure a 6% solution (m/v).

The zirconium 4-hydroxymandelate/salt solution was placed in a Wacker drum and goatskin added (35 g) and drummed for two hours (pH 5.0-5.5). Formic acid was added slowly (30 min) until a pH of 3.5 was reached. The skin was drummed for a further twelve hours, the float was drained and the skin was removed and sealed in a plastic bag and stored overnight. The shrinkage temperature of the damp tanned skin was measured (98°C) according to **Section 3.1.1.6**. The zirconium content based on dry goatskin mass was 3.81% (**Section 3.1.1.6**).

3.1.4.5. Zirconium 4-Hydroxymandelate (1:2) Low Pickle pH, Low Float, Short Tan/Long Fix and 15% Offer

In a typical experiment, zirconium oxychloride (4.20 g, 13.0 mmol) was dissolved in water (8 mL) and concentrated hydrochloric acid (1 mL) was added with stirring. 4-Hydroxymandelic acid (2.80 g, 26.0 mmol) was dissolved in water (15 mL) and both solutions were warmed to approximately 80°C. The ligand solution was added to the zirconium slowly (15 min) and the precipitate was allowed to age for 48 h at RT. The zirconium 4-hydroxymandelate solution was then treated with 2 ***M*** sodium hydroxide until the precipitate dissolved (pH 7.2) and aged overnight before the pH was lowered to pH 5.0-5.5 using formic acid. The solution was made up to 37 mL and sodium chloride (2.2 g) was added to ensure a 6% solution (m/v).

The zirconium 4-hydroxymandelate/salt solution was placed in a Wacker drum and goatskin added (37 g) and drummed for two hours (pH 5.0-5.5). Formic acid was added slowly (30 min) until a pH of 3.5 was reached. The skin was drummed for a further twelve hours, the float was drained and the skin was removed and sealed in a plastic bag and stored overnight. The shrinkage temperature of the damp tanned skin was measured (100°C) according to **Section 3.1.1.6**. The zirconium content based on dry goatskin mass was 5.15% (**Section 3.1.1.6**).

3.1.4.6. Zirconium 4-Hydroxymandelate (1:2) Low Pickle pH, Low Float, Short Tan/Long Fix and 7.5% Offer

In a typical experiment, zirconium oxychloride (2.04 g, 6.33 mmol) was dissolved in water (8 mL) and concentrated hydrochloric acid (1 mL) was added with stirring. 4-Hydroxymandelic acid (2.36 g, 12.7 mmol) was dissolved in water (8 mL) and both

solutions were warmed to approximately 80°C. The ligand solution was added to the zirconium slowly (15 min) and the precipitate was allowed to age for 48 h at RT. The zirconium 4-hydroxymandelate solution was then treated with 2 ***M*** sodium hydroxide until the precipitate dissolved (pH 6.7) and aged overnight before the pH was lowered to pH 5.0-5.5 using formic acid. The solution was made up to 36 mL and sodium chloride (2.2 g) was added to ensure a 6% solution (m/v).

The zirconium 4-hydroxymandelate/salt solution was placed in a Wacker drum and goatskin added (36 g) and drummed for two hours (pH 5.0-5.5). Formic acid was added slowly (30 min) until a pH of 3.5 was reached. The skin was drummed for a further twelve hours, the float was drained and the skin was removed and sealed in a plastic bag and stored overnight. The shrinkage temperature of the damp tanned skin was measured (88°C) according to **Section 3.1.1.6**. The zirconium content based on dry goatskin mass was 2.10% (**Section 3.1.1.6**).

3.1.4.7. Zirconium 4-Hydroxymandelate (1:2)
Low Pickle pH, Low Float, Short Tan/Long Fix and 5% Offer

In a typical experiment, zirconium oxychloride (1.36 g, 4.22 mmol) was dissolved in water (8 mL) and concentrated hydrochloric acid (1 mL) was added with stirring. 4-Hydroxymandelic acid (1.58 g, 8.46 mmol) was dissolved in water (8 mL) and both solutions were warmed to approximately 80°C. The ligand solution was added to the zirconium slowly (15 min) and the precipitate was allowed to age for 48 h at RT. The zirconium 4-hydroxymandelate solution was then treated with 2 ***M*** sodium hydroxide until the precipitate dissolved (pH 6.7) and aged overnight before the pH was lowered to pH 5.0-5.5 using formic acid. The solution was made up to 36 mL and sodium chloride (2.2 g) was added to ensure a 6% solution (m/v).

The zirconium 4-hydroxymandelate/salt solution was placed in a Wacker drum and goatskin added (36 g) and drummed for two hours (pH 5.0-5.5). Formic acid was added slowly (30 min) until a pH of 3.5 was reached. The skin was drummed for a further twelve hours, the float was drained and the skin was removed and sealed in a plastic bag and stored overnight. The shrinkage temperature of the damp tanned skin was measured (84°C) according to **Section 3.1.1**. The zirconium content based on dry goatskin mass was 1.77% (**Section 3.1.1.6**).

3.1.4.8. Zirconium 4-Hydroxymandelate (1:2)
Low Pickle pH, Low Float, Short Tan/Long Fix and 2.5% Offer

In a typical experiment, zirconium oxychloride (0.426 g, 2.29 mmol) was dissolved in water (8 mL) and concentrated hydrochloric acid (1 mL) was added with stirring. 4-Hydroxymandelic acid (0.853 g, 4.58 mmol) was dissolved in water (8 mL) and both solutions were warmed to approximately 80°C. The ligand solution was added to the zirconium slowly (15 min) and the precipitate was allowed to age for 48 h at RT. The zirconium 4-hydroxymandelate solution was then treated with 2 ***M*** sodium hydroxide until the precipitate dissolved (pH 6.8) and aged overnight before the pH was lowered to pH 5.0-5.5 using formic acid. The solution was made up to 39 mL and sodium chloride (2.4 g) was added to ensure a 6% solution (m/v).

The zirconium 4-hydroxymandelate/salt solution was placed in a Wacker drum and goatskin added (39 g) and drummed for two hours (pH 5.0-5.5). Formic acid was added slowly (30 min) until a pH of 3.5 was reached. The skin was drummed for a further twelve hours, the float was drained and the skin was removed and sealed in a plastic bag and stored overnight. The shrinkage temperature of the damp tanned skin was measured (78°C) according to **Section 3.1.1**. The zirconium content based on dry goatskin mass was 0.94% (**Section 3.1.1.6**).

3.1.5. TANNING OF GOATSKIN SIDES

Three goatskins were sourced locally and processed in Dose (Lichtenau, Germany) experimental tanning drums (35 x 60 cm) through to the bated stage according to **Appendix 1**. The skins were sided and labelled 1-6. One side of each skin (Sides 1, 3 and 5) was tanned using conventional chrome tanning salts. The corresponding sides were tanned with (a) conventional zirconium tanning salts (Side 2) (b) zirconium 4-hydroxymandelate (1:2) with zirconium oxychloride as the source of zirconium (Side 4), and (c) zirconium 4-hydroxymandelate (1:2) with zirconium sulfate as the source of zirconium (Side 6). Tan offers were based on a percentage of the pelt mass and attempts were made to use industrially representative amounts. The 1:2 and 1:4 zirconium:ligand tanning solution offers were based on theoretical molecular masses of ZrL_2 and ZrL_4 respectively, where L is the monodeprotonated ligand.

The sides were divided further into matched pairs of shoulders and butts. The shoulders were not treated further and the butts were processed through to crust leather for further comparison.

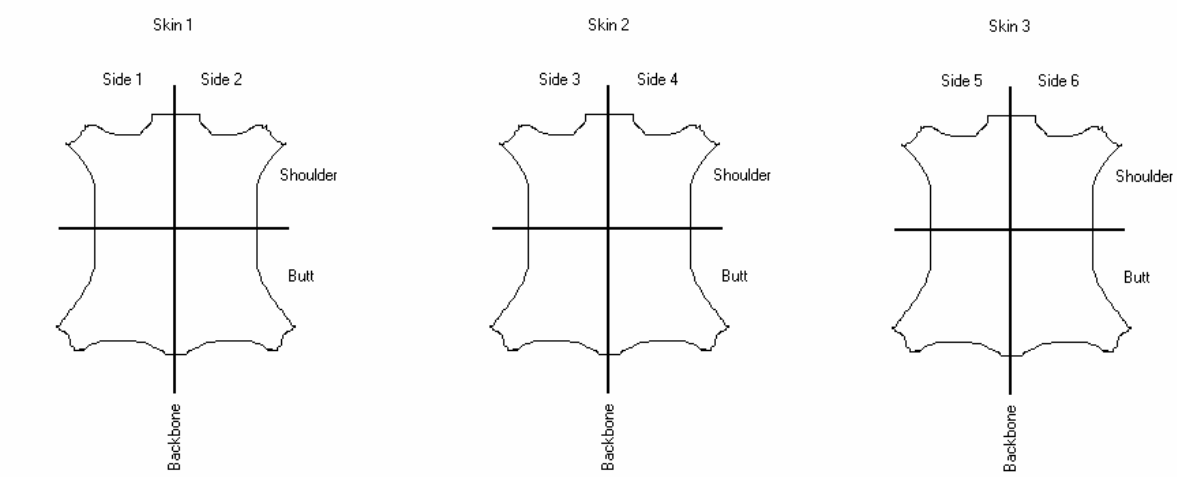

Figure 3.1: Division of goatskins into six sides for the physical and aesthetic comparison of chromium tanned goatskin (Sides 1, 3 and 5) with (a) conventional zirconium salt tanned goatskin (Side 2), (b) zirconium oxychloride - 4-hydroxymandelate (1:2) tanned goatskin (Side 4), and (c) zirconium sulphate – 4-hydroxymandelate (1:2) tanned goatskin (Side 6).

3.1.5.1. Conventional Chromium Tanning Process

Bated pelt (3.70 kg, Sides 1, 3 and 5) was placed into a stainless steel drum and float added (3.7 kg, 100% m/m). Sodium chloride (222 g, 6% m/v) and sodium formate (37 g, 1% m/v) were added and drummed (10 min) until a Baumé of six was obtained. Concentrated sulfuric acid (55.5 g, 1.5% m/v) was diluted (1:10) and added through the hollow axle of the drum while the drum was turning. The material was drummed (90 min) and the skin cross-section checked with bromocresol green indicator to confirm acid penetration (pH 2.6). Chromium tanning salts (222 g, 0.566 mol, 6% m/m) were added and drummed until penetration was complete (pH 2.5). Sodium bicarbonate was added in small aliquots (7.4 g, 0.2% m/v) until a pH of 4.0 was obtained. Drumming was continued (8 h) before the float was drained. The tanned material was washed (3.70 kg, 100% float, 40°C), covered in plastic and aged overnight before the shrinkage temperature was measured (>100°C).

3.1.5.2. Conventional Zirconium Tanning Process

Bated pelt (730 g, Side 2) was placed into a stainless steel drum and float added (730 g, 100% m/v). Sodium chloride (43.8 g, 6% m/v) and sodium formate (7.3 g, 1% m/v) were added and drummed (10 min) until a Baumé of six was obtained. Concentrated sulfuric acid (11 g, 1.5% m/v) was diluted (1:10) and added through the hollow axle of the drum while the drum was turning. The material was drummed (90 min) and the skin cross-section checked with bromocresol green indicator to confirm acid penetration (pH 2.7). Zirconium tanning salts (73.0 g, 0.206 mol, 10% m/m) were added and drummed intermittently for twenty-four hours (pH 1.4). Sodium bicarbonate was added in small aliquots (1.5 g, 0.2% m/v) until a pH of 2.5 was obtained. Intermittent drumming was continued (12 h) before the float was drained. The tanned material was washed (3.7 kg, 100% float, 40°C), covered in plastic and aged overnight before the shrinkage temperature was measured (94°C).

3.1.5.3. Zirconium Oxychloride - 4-Hydroxymandelate (1:2) Tanning Process

Zirconium oxychloride (30.3 g, 94.0 mmol) was dissolved in water (80 g) and concentrated hydrochloric acid (5 mL) was added with stirring. 4-Hydroxymandelic acid (35.0 g, 188 mmol) was dissolved in water (100 g) and both solutions were warmed to approximately 80°C. The ligand solution was added to the zirconium slowly (45 min) and the precipitate was allowed to age for 48 h at RT. The zirconium 4-hydroxymandelate solution (10% m/m) was then treated with 2 ***M*** sodium hydroxide until the precipitate dissolved (pH 6.8) and aged overnight before the pH was lowered to pH 5.0-5.5 using formic acid. The solution was made up to 400 mL and sodium chloride (24 g) was added to ensure a 6% solution (m/v).

Bated pelt (400 g, Side 4) was placed into a stainless steel drum and the zirconium 4-hydroxymandelate/salt solution was added and the pH adjusted to 5.2 using formic acid. The material was drummed for two hours and then formic acid was added slowly (30 min) until a pH of 3.5 was reached. The skin was drummed for a further twelve hours, the float was drained and the skin was covered in plastic and aged overnight and the shrinkage temperature measured (92°C).

3.1.5.4. Zirconium Sulfate - 4-Hydroxymandelate (1:2) Tanning Process

Zirconium sulfate (55.1 g, 155 mmol) was dissolved in water (200 g) and concentrated hydrochloric acid (15 mL) was added with stirring. 4-Hydroxymandelic acid (57.8 g, 310 mmol) was dissolved in water (200 g) and both solutions were warmed to approximately 80°C. The ligand solution was added to the zirconium slowly (45 min) and the precipitate allowed to age for 48 h at RT. The zirconium 4-hydroxymandelate solution (10% m/m) was then treated with 2 ***M*** sodium hydroxide until the precipitate dissolved (pH 7.2) and aged overnight before the pH was lowered to pH 5.0-5.5 using formic acid. The solution was made up to 660 mL and sodium chloride (40 g) was added to ensure a 6% solution (m/v).

Bated pelt (660 g, Side 6) was placed into a stainless steel drum and the zirconium 4-hydroxymandelate/salt solution was added and the pH adjusted to 5.2 using formic acid. The material was drummed for two hours and then formic acid was added slowly (30 min) until a pH of 3.5 was reached. The skin was drummed for a further twelve hours, the float was drained and the skin was covered in plastic and aged overnight and the shrinkage temperature measured (90°C).

3.1.5.5. Production of Goatskin Crust Leather

The chromium tanned butts of Sides 1, 3 and 5 and zirconium tanned butts of sides 2, 4 and 6 (**Section 3.1.5**) were processed through to crust leather using a conventional garment-type process (**Appendix 2**). The crust material was analysed according to **Section 3.1.1.6**.

3.2. RESULTS AND DISCUSSION

3.2.1. GENERATION OF ZIRCONIUM α-HYDROXYCARBOXYLATE TANNING AGENTS

Zirconium α-hydroxycarboxylate complexes were synthesised according to **Section 2.1.5**. The pH of the solutions was raised until the complex dissolved or the desired pH was reached, using approximately 2 ***M*** sodium hydroxide. The use of dilute sodium hydroxide (approximately 0.2 ***M***) generated tanning solutions with volumes that were too large for comparative use, and the use of more concentrated sodium hydroxide solutions (5 ***M***) resulted in the precipitation of zirconium and was not utilised.

The use of the terms 1:2 and 1:4 throughout **Chapter 3** refer to the zirconium:ligand mole ratios used in the synthesis of the zirconium α-hydroxycarboxylate solutions. These ratios, therefore, also reflect the zirconium:ligand ratios present in solution after the solubilisation of the complexes. In the tanning experiments the tanning agents are generated *in situ* and are not necessarily the same species as the precipitates characterised in **Chapter 2**.

According to Mukherji[128] and Hahn and Weber,[129] the zirconium α-hydroxycarboxylate precipitates dissolve at high pH due to deprotonation of the acidic α-OH hydrogen and the ligand (H_2L) exists as L^{2-} as opposed to HL^{1-}. Electron withdrawing substituents and the coordination of the α-OH oxygen were proposed to weaken the O-H bond and increase the acidity of the α-OH hydrogen. Larsen and Homeier[121] questioned this and suggested that the dissolution involved the attack by alkalis on the hydrogen bonds of a polymeric structure. Hahn, using titration studies, also suggested that treatment of the complexes with excess alkali produced a non-stoichiometric mixture of seven, $ZrL_3(HL)^{3-}$, and eight coordinate, ZrL_4^{4-}, zirconium salts. This was supported by the work of Kapoor and Mehrotra.[127]

Potentiometric and spectroscopic studies of oxovanadium(IV) α-hydroxcarboxylate complexes[229] showed that aryl substituents increase the acidity of the α-OH hydrogen and encourage $–COO^-$ and $–O^-$ complexation with the metal. This was supported by the current study and work done by Reeder and Rieger.[230] Mandelate complexes were shown

by them to complex with deprotonated carboxylate and hydroxy groups which is likely to limit hydrolysis and impart stability to the complex in aqueous solution.

Micera *et al.*[229] introduced, using oxovanadium(IV), a general change in speciation with an increase in pH (2 – 7) for α-hydroxycarboxylate ligands (H_2L) according to:

$$[VO(H_2O)_5]^{2+} \rightarrow [VO(H_2O)_2HL]^{+} \rightarrow [VO(HL)_2] \rightarrow [VO(H_2O)_2L]$$
$$\rightarrow [VO(HL)L]^{-} \rightarrow [VO(L)_2]^{2-}$$

Pecsok and Sandera[231] investigated iron(III) D-gluconate (HGH_4) systems and proposed the following species progression as pH was increased:

$$[HFeGH_3]^{2+} \rightarrow [HFeGH] \rightarrow [FeGH]^{-} \rightarrow [FeGH(OH)]^{2-}$$

Kostromina[232] proposed six lanthanum(III) D-gluconate species as the pH was increased, including:

$$[LaGH_3]^{2+} \rightarrow [La(GH_4)_2]^{+} \rightarrow [LaGH_3]^{+} \rightarrow [LaGH_2] \rightarrow [La(GH_4)(GH_3)] \rightarrow [LaGH_3]^{2-}$$

.

$[Zr(H_2Cit)]^{3+}$ was identified from an aqueous solution[233] containing HNO_3, citric acid (H_3Cit) and $LiNO_3$, while a complex, $K[ZrO(Cit)]\cdot 2.5H_2O$ was identified[234] after treating zirconium carbonate with citric acid. Warner and Weber[235] also showed that the α-OH hydrogen is more easily displaced than the third –COOH hydrogen in some citrate-ferric complexes.

Table 3.1 shows a theoretical selection of monomeric zirconium α-hydroxycarboxylate species possible in solution if the α-OH is either protonated (HL^-) or deprotonated (L^{2-}) with a maximum coordination number of eight (coordination numbers of six and seven are also common) and excluding all other possible ligands in the current study (O^{2-}, OH^-, H_2O and Cl^-). The table only includes bidentate monomeric complexes for simplicity as monodentate and bridging ligands are also possible which could give rise to polymeric structures. The species shown are predominantly cationic, however, in aqueous solution the complex ions are highly likely to be hydroxylated, hydrated and polymerised to produce predominantly anionic species.[128]

Table 3.1: Theoretically possible monomeric zirconium - α-hydroxycarboxylic acid (H_2L) species (excluding all other ligands) with a maximum coordination number of eight.

$Zr(HL)_4$	→	$Zr(HL)_3^+$	→	$Zr(HL)_2^{2+}$	→	$ZrHL^{3+}$
↓		↓		↓		↓
$Zr(HL)_3L^-$	→	$Zr(HL)_2L$	→	$Zr(HL)L^+$	→	ZrL^{2+}
↓		↓		↓		
$Zr(HL)_2L_2^{2-}$	→	$Zr(HL)L_2^-$	→	ZrL_2		
↓		↓				
$Zr(HL)L_3^{3-}$	→	ZrL_3^{2-}				
↓						
ZrL_4^{4-}						

Table 3.1 shows only a small sample of the large number of zirconium species possible in aqueous solution and serves to indicate how complex aqueous zirconium chemistry can be. An increase in pH may be represented by: (i) moving from left to right along a row, where α-hydroxcarboxylate ligands may be sequentially substituted by an hydroxyl group, (ii) by moving down a column, which results in the deprotonation of the α-OH, or (iii) a combination of (i) and (ii).

Aqueous zirconium - α-hydroxycarboxylic acid solutions form precipitates at pH below 3[229] and all evidence indicated that complexation was bidentate with a deprotonated carboxyl group and a protonated hydroxyl group (**Figure 2.18a**).[121,177] An increase in electron donation through inductive effects towards the R–CH(OH)CO_2H moiety results in more stable ZrL_4 complexes and this may be illustrated by the complexes isolated in **Chapter 2** for glycolic acid (R = H), lactic acid (R = CH_3) and mandelic acid (R = C_6H_5):

$$Zr_2O(OH)_2(\text{glycolate})_4 \rightarrow ZrOH(\text{lactate})_3 \rightarrow Zr(\text{mandelate})_4$$

4-Hydroxy-, 4-chloro- and 4-bromo-substituted phenyl groups are electron donating functional groups and all three substituted mandelic acids produced stable unhydroxylated ZrL_4 complexes. The relatively weak electron donating, glycolate and lactate ligands are expected to form hydroxylated or complex polymeric zirconium:ligand solutions when dissolved at elevated pH. Ligands that coordinate strongly to zirconium are not readily hydrolysed and encourage the deprotonation of the ligand as they solubilise, *e.g.*, mandelates and substituted mandelates. They are more likely to produce mixed ligand (HL^- and L^{2-}) species in solution as intermediates according to **Table 3.1**.

D-gluconic and citric acids also coordinate strongly with metals and have been shown to dissolve by deprotonation of OH groups as pH is increased.[231-233,235] The D-gluconate ligand was shown to lose the α-OH hydrogen as well as an additional OH hydrogen, [$LaGH_2$], without hydroxylation occurring when bound to lanthanum(III) and mixed ligand species were also observed, [$La(GH_4)(GH_3)$].[232] The additional OH and COOH groups of D-gluconic, citric and 4-hydroxymandelic acid appear to be instrumental in assisting the water solubility of the zirconium complexes, and the D-gluconate and citrate complexes are permanently soluble and the 4-hydroxymandelate complex soluble at pH below that of the zirconium lactate complexes (**Table 2.6**).

The low solubility of the zirconium mandelate complex resulted in its use in gravimetric determinations and Belcher *et. al.*[236] calculated the solubility of zirconium mandelate to be 0.1569 g/L (surprisingly high for use in gravimetric determinations). The desire for better reagents (lower solubility) prompted the investigation of bromo- and chloro-substituted mandelates as replacements and Oesper and Klingenberg[237] found them to be superior to the parent acid.

Much of the work done on zirconium sulfate tanning salts by Ranganathan and Reid[154] showed a mixture of cationic (~39%), anionic (~11%) and non-ionic (~50%) species at pH 2 in the absence of a masking agent. The addition of two moles of citric acid per mole of zirconium resulted in approximately 95% and 5% anionic and non-ionic species only. A decrease in acidity caused the ratio of ligand to zirconium to decrease which was ascribed to hydrolysis and the ratio of ligand to metal could be manipulated by varying the conditions.[238] From the evidence above, the zirconium complex tanning species generated *in situ* would likely be predominantly anionic.

Reacidification, according to Mukherji,[178] does not necessarily result in the reprecipitation of the original complex. Experimentally, reprecipitation of the zirconium α-hydroxcarboxylates varied for each ligand, and the relatively soluble glycolate and 4-hydroxymandelate complexes took longer and produced less precipitate than the 4-bromomandelate, mandelate and lactate zirconium complexes. These precipitates were not characterised.

ZrL_4 species, generated in the 1:4 mole ratio solutions, are coordinatively saturated and the strong coordination of the α-hydroxcarboxylate anions to zirconium resists hydrolysis. It is unlikely that the zirconium would be able to coordinate directly to collagen and the tanning ability of these complexes would likely be related to the available functional groups of the ligand. The use of 1:2 mole ratio solutions, however, is likely to produce more soluble ZrL_2Y_n complexes (Y = O^{2-}, OH^-, H_2O or Cl^-) that are likely to possess different chemical reactivities to the ZrL_4 species. The ability of the high pH, polymerised zirconium α-hydroxcarboxylate complexes to depolymerise as the pH is lowered, creates the potential for the zirconium in the (1:2) complexes to bind directly with collagen. Shrinkage temperatures close to or better than conventional zirconium tannins may be possible without the properties associated with conventional zirconium leather.

In order to investigate the effect the above behavior would have on hide powder (**Section 3.2.2**) and goatskin (**Section 3.2.3**), samples were treated with a range of zirconium α-hydroxcarboxylate complexes and conventional tanning agents.

3.2.2. HIDE POWDER EXPERIMENTS

The literature[9] indicates that conventional zirconium tanning with sulphate salts reaches a T_s of 95°C at a ZrO_2 content of 10%. A zirconium tanning agent offer of 10% relative to the tanning volume (float) was therefore chosen for hide powder experiments and 10% relative to the pelt mass for goatskin tannages. Calculations were based on ZrL_2 for the 1:2 tanning solutions and ZrL_4 for the 1:4 tanning solutions (where L represents the monodeprotonated ligand). It must be noted that the amount of zirconium offered decreases with increased molecular weight of the ligands and that 1:4 complexes offer a lower amount of zirconium than the corresponding 1:2 complexes.

Hide powder samples were tanned (**Section 3.1.2**) and analysed according to **Section 3.1.1.7**. The results of the experiments may be found in **Table 3.2**.

Table 3.2: Table of zirconium tannages of hide powder in order of increasing shrinkage temperature (T_s).

Tannage	T_s (°C)	ΔT_s (°C)	Zr (%)	Zr Uptake (%)
None	52	0	0	-
Zr Mandelate (1:4)	63	11	0.259	50.7
Zr Citrate (1:4)	64	12	0.235	47.4
Zr D-Gluconate (1:4)	65	13	0.212	43.0
Zr 4-Bromomandelate (1:4)	67	15	0.198	60.4
Zr D-Gluconate (1:2)	67	15	0.367	43.0
Zr 4-Hydroxymandelate (1:4)	68	16	0.279	59.6
Zr Citrate (1:2)	68	16	0.383	44.4
Zr Mandelate (1:2)	70	18	0.464	51.5
Zr Lactate (1:4)	71	19	0.419	53.0
Zr Lactate (1:2)	73	21	0.660	50.3
Zr 4-Hydroxymandelate (1:2)	80	28	0.509	60.9
Conventional Zr Sulfate	80	28	0.862	86.8

The results show a correlation between the shrinkage temperature measured by DSC, and the amount of zirconium in the hide powder for all the tannages except for the 4-hydroxymandelate series. **Figure 3.2** indicates that the stabilisation of the zirconium 4-hydroxymandelate tanned hide powder to heat is enhanced by the use of the 4-hydroxymandelate ligand relative to zirconium content. This is expected as the ligand contains a phenolic group, which is known to have an affinity for collagen (**Section 1.3.1.2** and **1.3.1.3**), and the likely result is the synergistic interaction of the zirconium and 4-hydroxymandelic acid with collagen, analagous to combination tannages. The solubility and/or stability of these complexes in water may also play a role in the uptake of the complex by collagen.

The D-gluconate ligand possesses four hydroxy groups in addition to the α-OH but the complexes did not raise the shrinkage temperature as much as the equivalent 4-hydroxymandelate complexes. This may be explained by Covington's postulation[38] that a rigid matrix is necessary for the effective stabilisation of collagen. D-Gluconic acid has a flexible aliphatic side-chain, compared to the rigid aromatic side-chain of 4-hydroxymandelic acid, and consequently would not reduce the rotational degrees of freedom within the collagen structure.

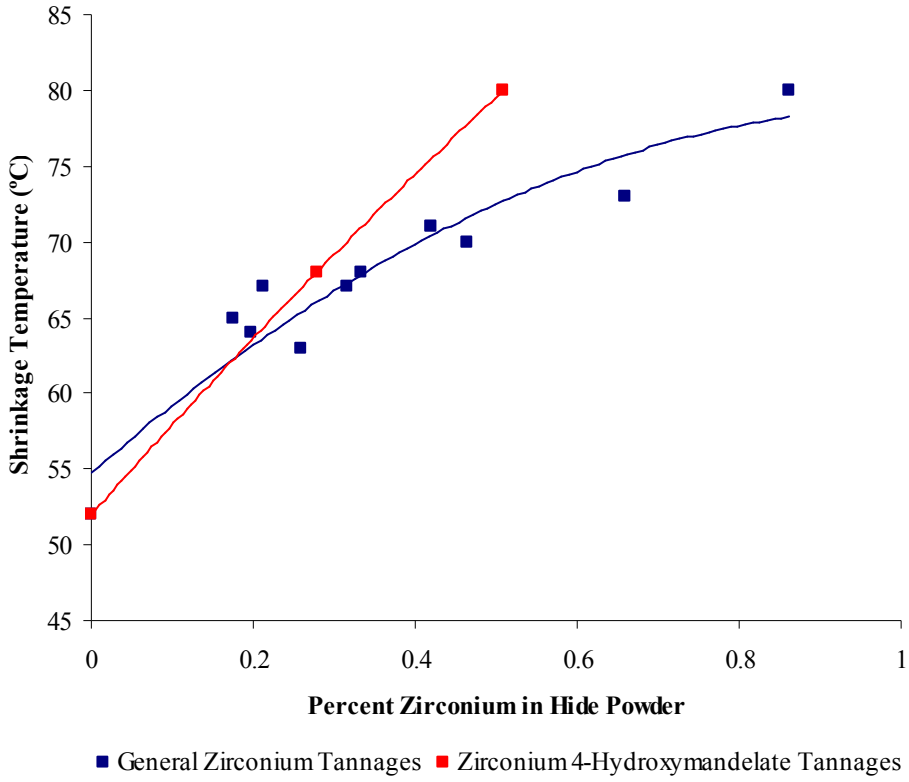

Figure 3.2: Graph showing the correlation between shrinkage temperature and the zirconium content of tanned hide powder.

Combination tanning (**Section 1.3**) refers to the tanning of leather with two or more tanning agents.[1] Currently, combination tannages are the main avenue of investigation for replacements for chromium tanned leather.[16] There are many combination tannages possible but focus has shifted to combination tannages that are synergistic, *i.e.*, the effect of the combination tannage is greater than the sum of the individual tannages. Mineral-free combination tannages include the crosslinking of vegetable tanned material with oxazolidines[239,240] and mineral combination tannages include the use of aluminium,[44,45,50,71] zirconium,[50] zinc[69] and titanium[241] tanning/retanning of vegetable pretanned/tanned material. Kallenberger and Hernandez[70] also performed preliminary studies on the use of cobalt, lead, manganese, nickel, molybdenum and iron, and Goldfarb[72] reinvestigated the use of chromium.

Combination tanning is not a new concept and vegetable-aluminium combination tannage predates chromium tanning.[31] The aluminium is thought to complex with the hydroxyl groups of bound vegetable tannins which is improved at elevated pH. Shrinkage

temperatures of 117°C were measured by Slabbert[50] compared to 76 and 84°C for Mimosa and aluminium tanned material, respectively.

A plot of shrinkage temperature versus the type of tannage in **Figure 3.3** shows to what extent the different tannages investigated in this work (**Section 3.1.2**) stabilise the collagen structure. Tanning offers of 10% (based on float) were used for the myrobalan, Mimosa ME, conventional zirconium sulfate and Zr 4-hydroxymandelate (1:2) tannages, and 6% and 2.5% for the chromium and glutaraldehyde tannages, respectively. Vegetable tannages frequently require 20 to 25% tanning agent[55] and the low shrinkage temperature values could be significantly improved with higher tannin offers.

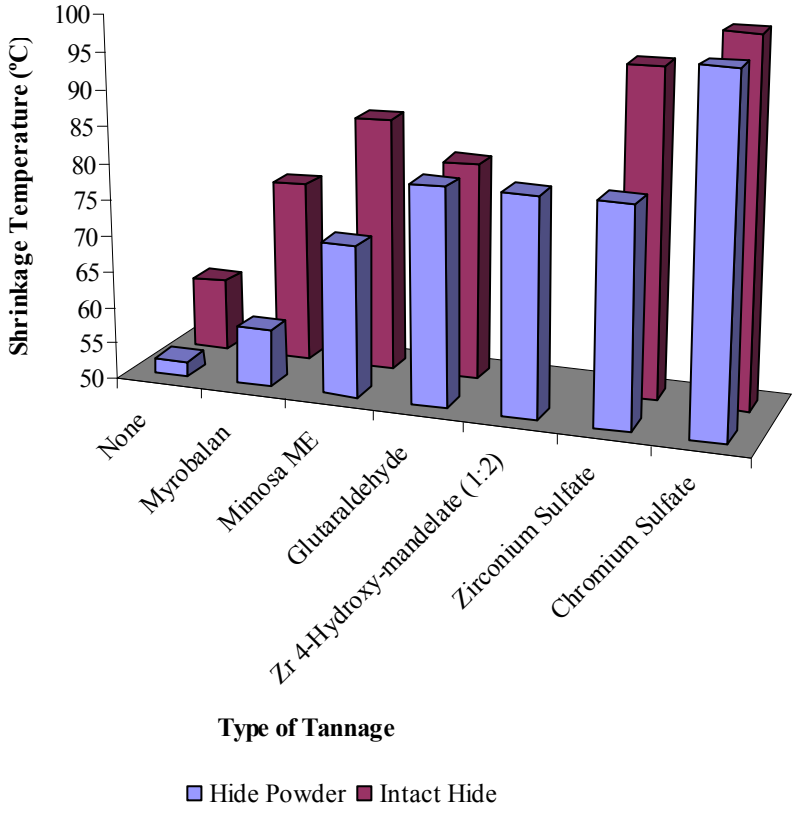

Figure 3.3: Graph of shrinkage temperature values for different tannages of hide powder and intact hide.

The shrinkage temperature values for the different tannages (intact hides) are generally higher than those of the hide powder tannages as the quaternary structure of the collagen hierarchy is lost in hide powder, *e.g.*, the shrinkage temperature for soluble collagen may be as low as 42°C.[242]

The values obtained for chromium and glutaraldehyde tanned material closely match the values obtained for the hide powder samples and reflect the effectiveness of these tanning agents and that optimum tan offers were used. The Zr 4-hydroxymandelate (1:2) tanned material is comparable with the hide powder tanned with conventional zirconium tanning salts even though it only contains approximately 60% of the amount of zirconium. **Figure 3.2** indicates that zirconium 4-hydroxymandelate (1:2) tannages could potentially reach shrinkage temperatures of 90-100°C if the zirconium content could be increased to that of conventionally tanned zirconium leathers.

3.2.2.1. Attenuated Total Reflectance (ATR) Investigations

FTIR spectroscopy has been used to study collagen, collagen crosslinking, denaturation, and thermal self-assembly, as well as gelatin and gelatin melting.[243] The dominant bands in collagen include the amide A (3300 to 3200 cm^{-1}), amide I (1661 to 1636 cm^{-1}), amide II (1558 to 1549 cm^{-1}) and the amide III (1300 to 1200 cm^{-1}). The amide A band represents the ν(NH) stretching vibration and is expected to be a strong band, which may be broad if hydrogen bonded. A weaker band due to overtones of the amide II may appear at approximately 3100 cm^{-1}. The amide I band corresponds to the coupled ν_a(C=O) carbonyl stretch, which absorbs strongly in the mid infrared region. The in-plane NH bending frequency and the CN stretching frequency fall close together and interact to produce the highly coupled amide II band, which is due predominantly, to the C-N-H bending vibration and the highly coupled amide III band, predominantly the CN stretch. A broad out-of-plane NH wag may be observed near 700 cm^{-1} although this is not likely to be seen using a zinc selenide ATR crystal.[197]

ATR spectrometry is a widely employed technique for examining surfaces of materials. When a beam of radiation enters a prism it is reflected internally if the angle of incidence is greater than the critical angle, which is a function of refractive index of the prism. On internal reflection, all the energy is reflected, however, the beam does penetrate slightly beyond the reflecting surface and then return (the depth of penetration is approximately one wavelength of the incident beam, typically ~ 1μm). When a material is placed in contact with the reflecting surface, the beam loses energy at those wavelengths where the material absorbs due to an interaction with the penetrating beam (**Figure 3.4**). This

attenuated radiation, when measured and plotted as a function of wavelength is similar to a conventional infrared spectrum with variation in the band intensity since the depth of penetration into the sample material is dependent on the wavelength. The major advantages of this approach are the convenience, speed of use and the ability to measure solids in their gross form without the need for grinding and mulls.[197]

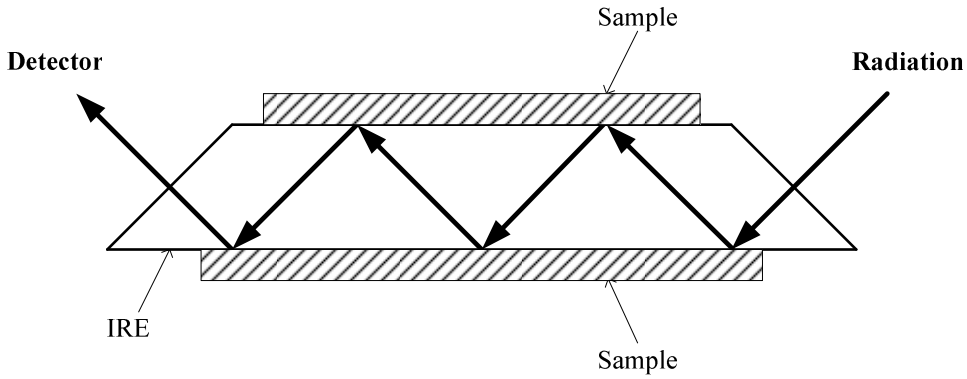

Figure 3.4: Multiple internal reflection attenuated total reflectance (ATR) plate showing path of radiation through the internal reflection element (IRE), *e.g.*, zinc selenide.

Untanned hide powder spectra were recorded using a multiple reflectance horizontal ATR (**Figure 3.4**) and compared to a single reflectance horizontal diamond ATR. **Figure 3.5** shows that the single reflectance ATR generated far superior spectra for the material analysed.

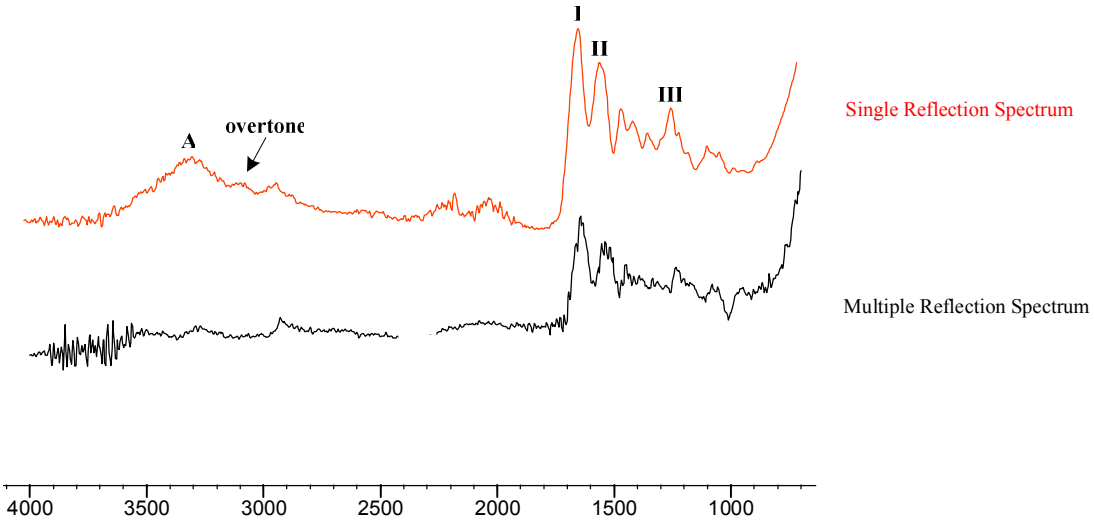

Figure 3.5: Hide powder ATR spectra using multiple and single reflectance equipment showing the amide A and I to III bands.

Radiation absorption using ATR generally increases with an increase in sample to IRE contact. The fibrous nature of the hide powder results in a poor surface contact area and

pressure must be applied to improve this. The large size of the IRE in multiple reflectance equipment limits the ability to apply pressure and results in relatively poor spectra. The single reflectance ATR equipment has a small sampling area (small amount of sample required) and controlled compression clamp to improve sample contact, which yielded superior spectra.

ATR spectra of hide powder, zirconium complexes and tanned hide powder samples were obtained according to **Section 3.1.1.3** and are summarised in **Figures 3.5-3.11**. A comparison between hide powder, zirconium lactate (1:2) tanned hide powder, and the $Zr(OH)L_3$ complex (**Figure 3.6**) shows that the spectrum of tanned hide powder is more similar to that of the complex.

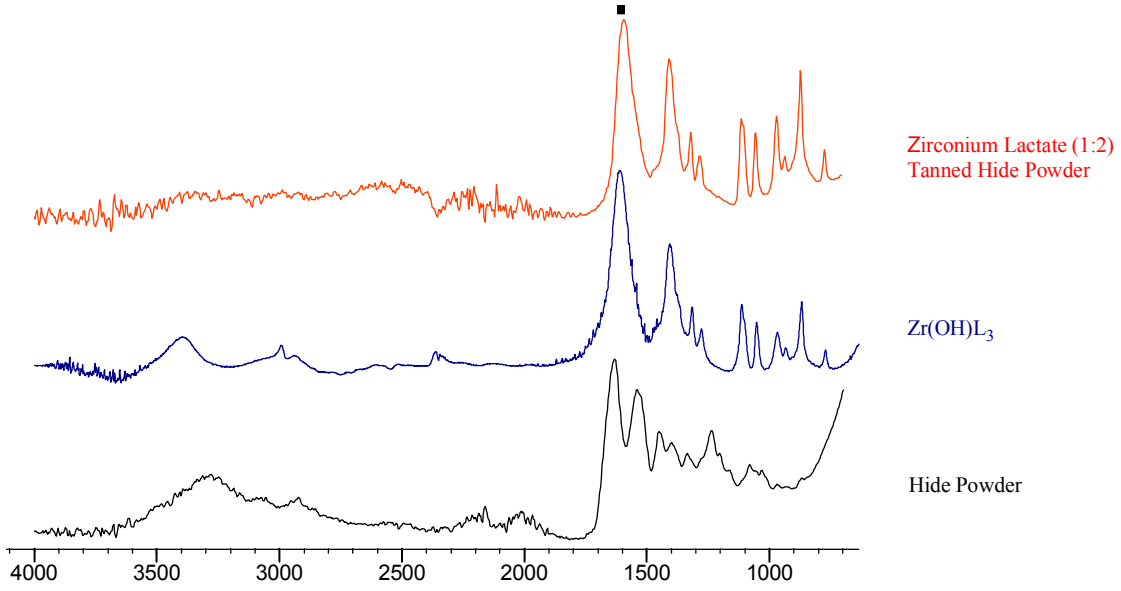

Figure 3.6: ATR spectra of hide powder, zirconium lactate complex and zirconium lactate (1:2) tanned hide powder.

The main difference observed between the zirconium lactate (1:2) tanned hide powder and $Zr(OH)L_3$ complex spectra is a shift in the $\nu_a C{=}O$ band (■) of 20 cm^{-1}. This is likely to be due to interaction with collagen and indicates that the complex is not merely precipitated on the surface of the hide powder. This may be supported by the apparent loss of νO-H in comparing the tanned hide powder with that of the complex. That the tanned hide powder is more similar to the lactate complex does, however, indicate the complex is principally located on the surface of the hide powder. In contrast, the various

substituted mandelate tanned hide powder shows the appearance of hide powder bands in addition to the dominant complex bands (**Figures 3.7 - 3.9**).

The ZrM_4 and zirconium mandelate (1:2) tanned hide powder spectra (**Figure 3.7**) were similar except for the notable development of a shoulder (§) at ~1560 cm^{-1} to the right of the $\nu_a C{=}O$ peak.

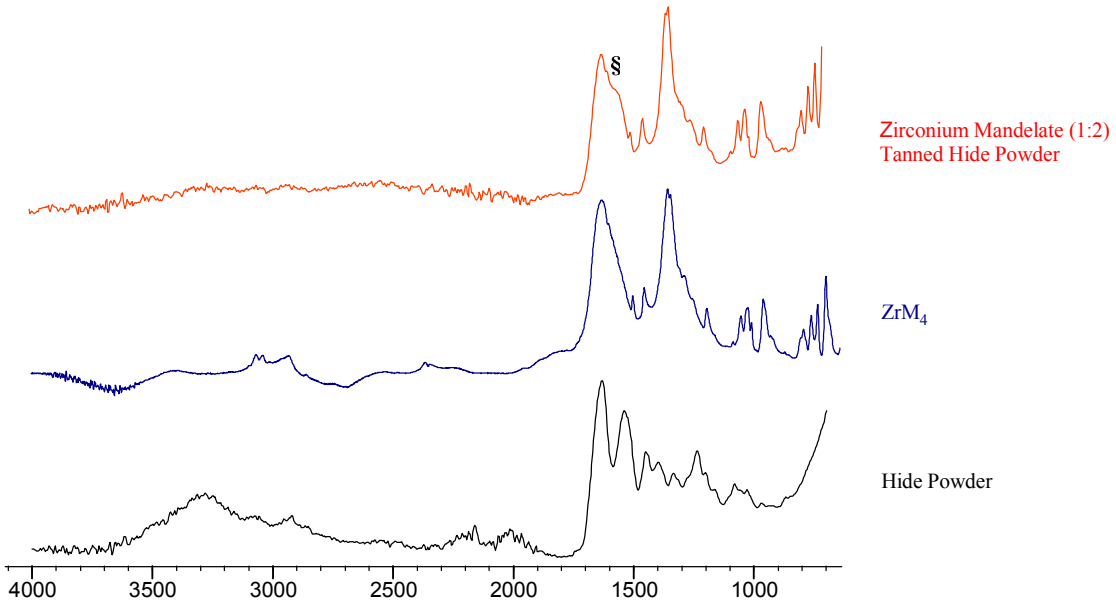

Figure 3.7: ATR spectra of hide powder, zirconium mandelate complex and zirconium mandelate (1:2) tanned hide powder.

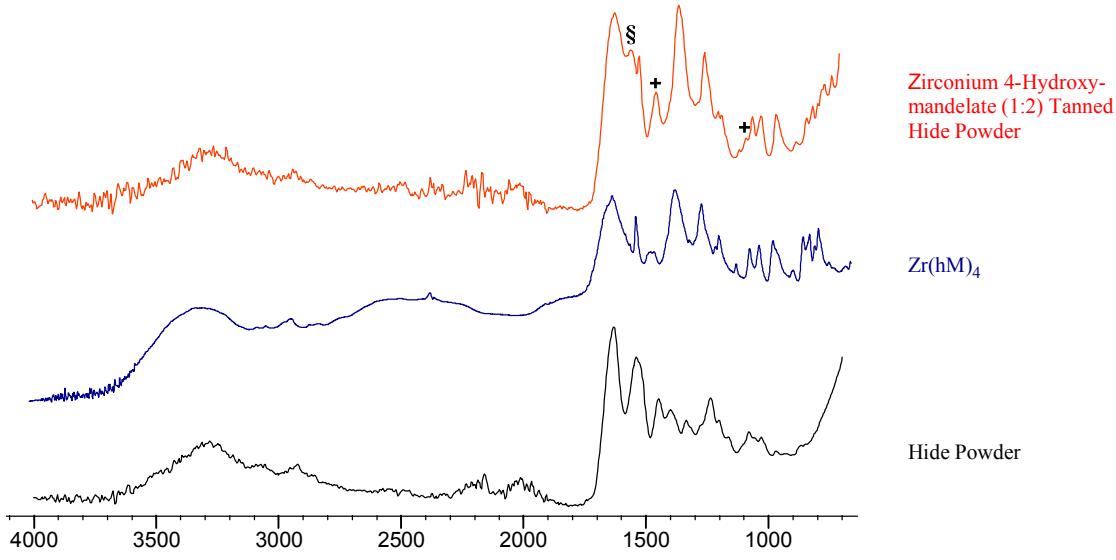

Figure 3.8: ATR spectra of hide powder, zirconium 4-hydroxymandelate complex and zirconium 4-hydroxymandelate (1:2) tanned hide powder.

The zirconium 4-hydroxymandelate (1:2) tanned hide powder ATR spectrum (**Figure 3.8**) also shows the development of a shoulder (§) at 1551 cm^{-1} which appears to be indicative of the interaction of the zirconium mandelates with collagen as it also appears in the spectrum of the zirconium 4-bromomandelate (**Figure 3.9**). Peaks attributed to the hide powder have been denoted by (+).

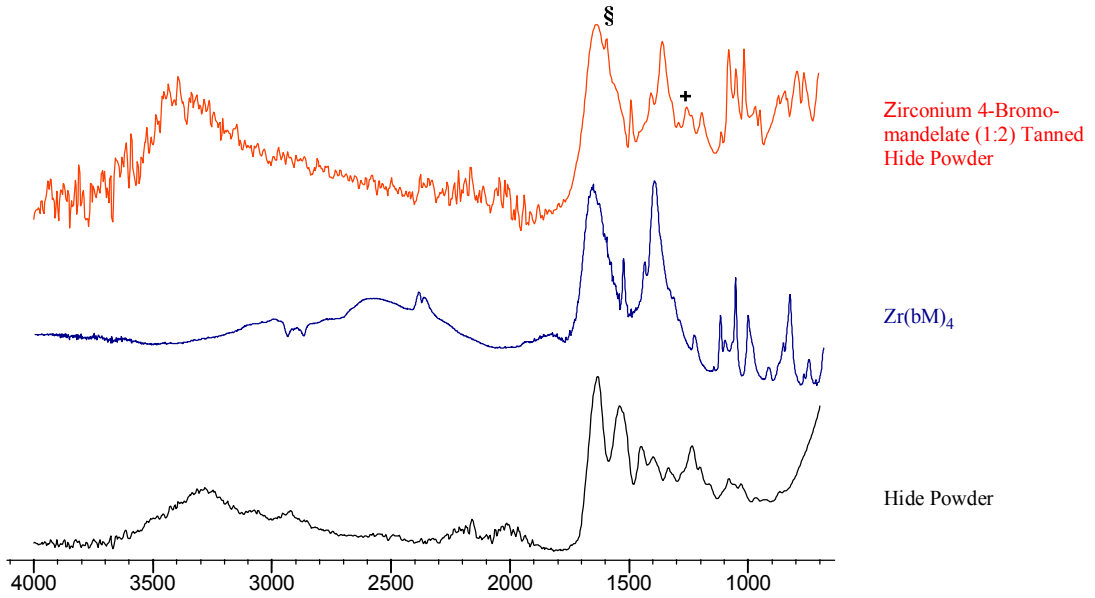

Figure 3.9: ATR spectra of hide powder, zirconium 4-bromomandelate complex and zirconium 4-bromomandelate (1:2) tanned hide powder.

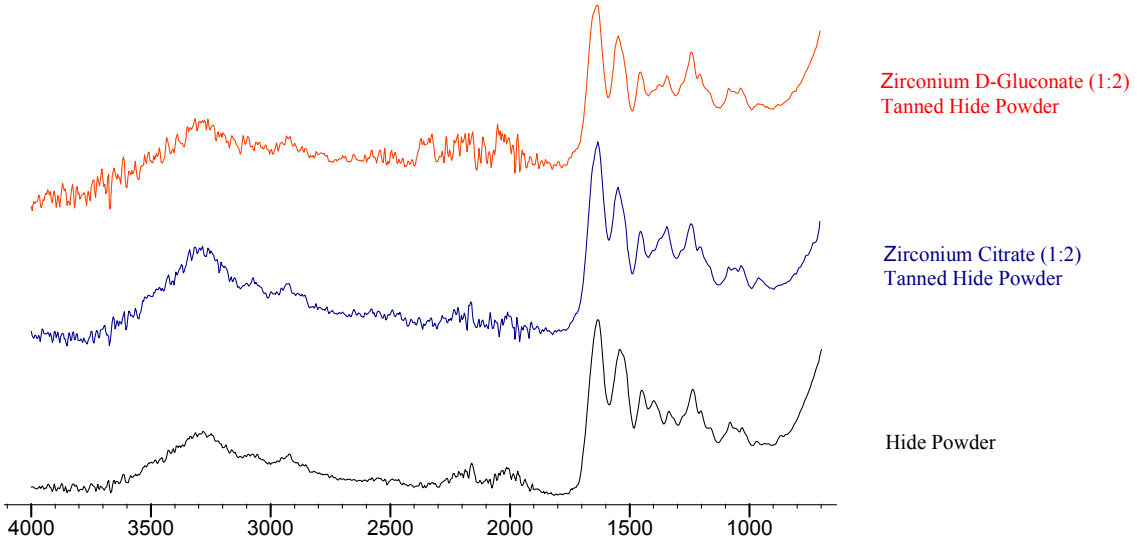

Figure 3.10: ATR spectra of hide powder, zirconium citrate (1:2) tanned hide powder, and zirconium D-gluconate (1:2) hide powder.

The soluble zirconium citrate and D-gluconate complexes were not characterised and therefore spectra were not available for comparison, however, what is evident (**Figure 3.10**) is that the tanned hide powder closely resembles untanned hide powder. This would imply that these complexes do not coat the fibres but penetrate into the collagen matrix.

SEM pictures of selected tanned hide powder (**Figure 3.11**) supported the idea that precipitated tanning agent coated the hide powder fibres. Chromium tanned material, used as a reference, appears similar to untanned hide powder whereas the zirconium mandelate (1:4) and 4-hydroxymandelate (1:2) tanned hide powders clearly show coated fibres.

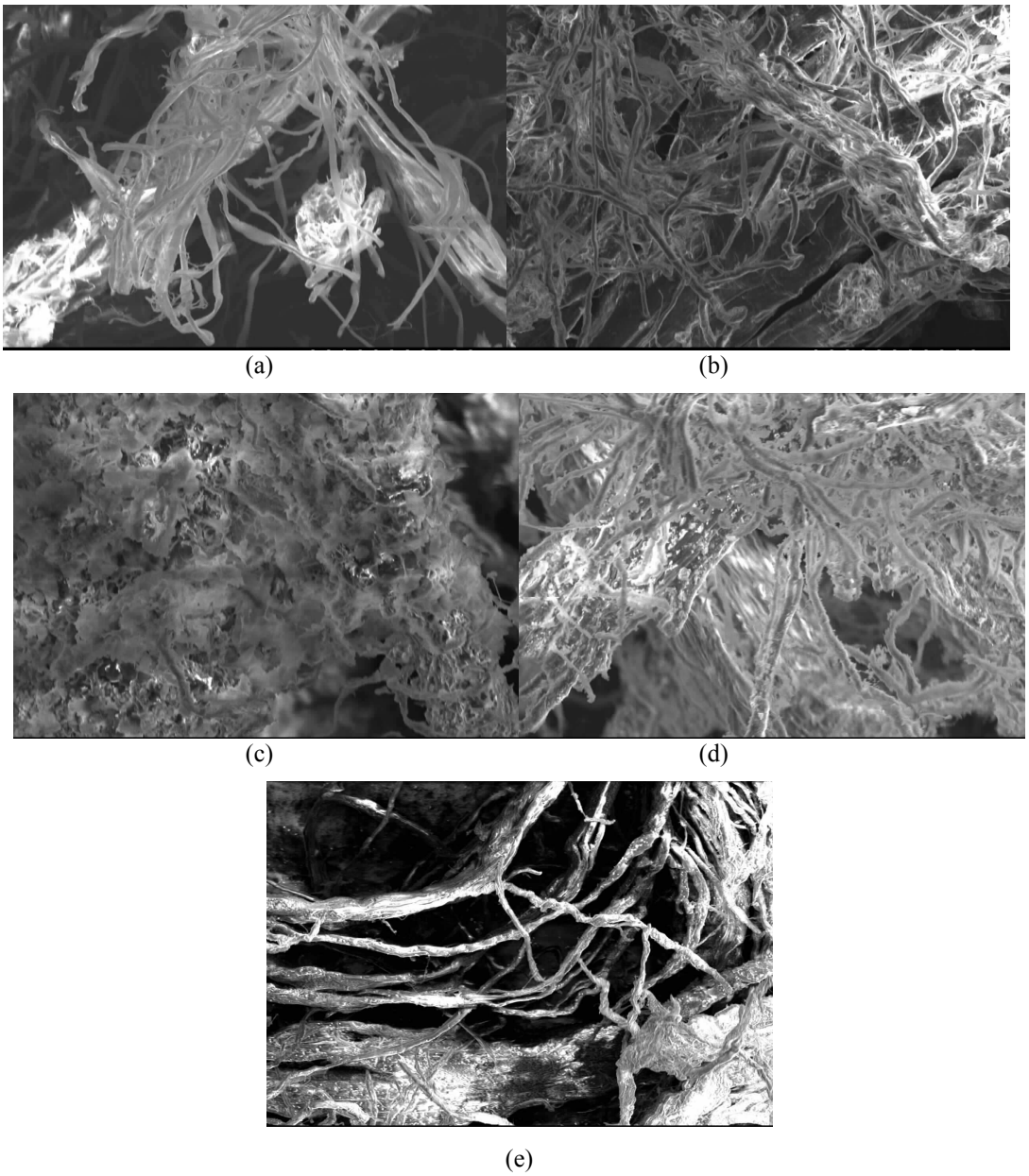

Figure 3.11: Selected SEM images (x400 magnification) of hide powder (a) untanned, (b) chromium tanned, (c) zirconium mandelate (1:4) tanned, (d) zirconium 4-hydroxymandelate (1:2) tanned, and (e) zirconium D-gluconate (1:2) tanned.

The increase in shrinkage temperature of collagen is commonly associated with an increase in the hydrophobicity of the fibres.[38] This may account for the increase in shrinkage temperature shown by the majority of the α-hydroxycarboxylate complexes

(**Table 3.2**). This, however, does not account for the increase in shrinkage temperature for the D-gluconate tanned hide powder which shows no precipitate formation on the fibres. The zirconium D-gluconate (1:2) complex is highly water soluble and is therefore able to penetrate deeply into the collagen fibre. Once "fixed," however, it would not provide hydrophobicity to the fibre and is hydrophilic to such an extent that it is still water soluble and may be washed out. The hydroxy substituent of the 4-hydroxymandelate ligand is envisaged to provide sufficient solubility to the complex to encourage a degree of penetration into the fibre structure and still maintain enough hydrophobicity to increase the shrinkage temperature. The phenolic moiety is likely to provide a tanning ability and fix the complex to the collagen fibre through hydrogen bonding similarly to the polyphenolic structures of vegetable tannins (**Section 1.3.1.2**).

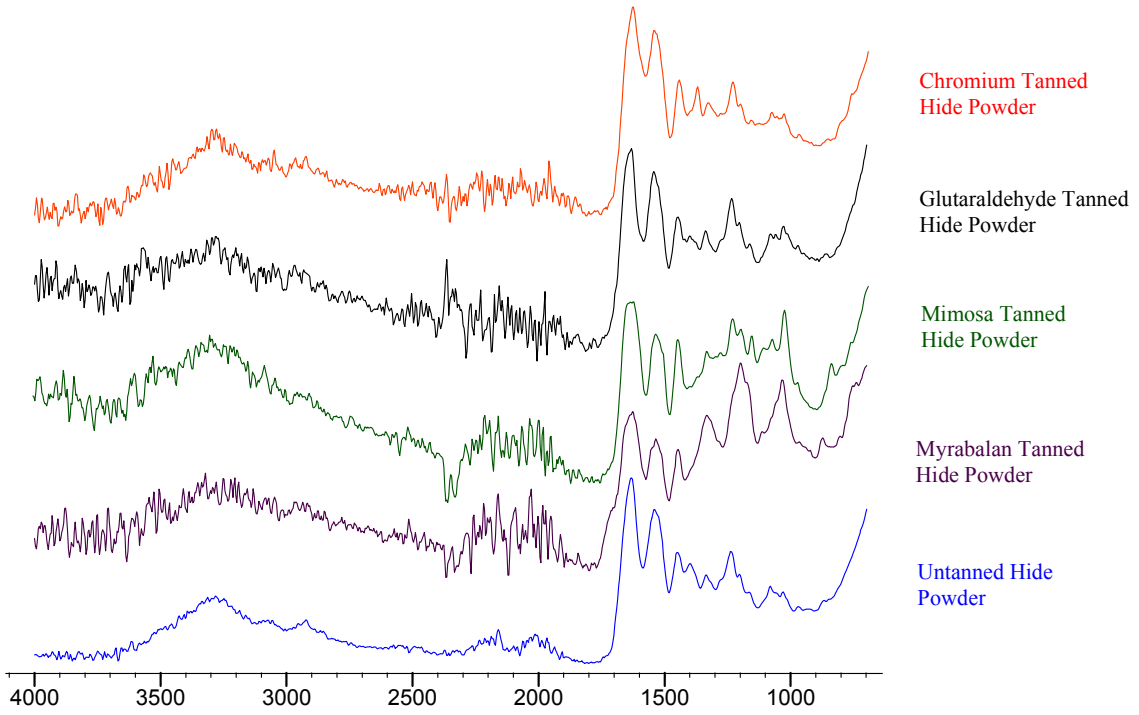

Figure 3.12: ATR spectra of conventionally tanned hide powder samples.

Figure 3.12 shows a series of ATR spectra for hide powder tanned with selected conventional tanning agents. The spectra serve to show the similarity between tanned and untanned hide powder with the retention of the amide A, I and II bands for all the samples. The vegetable tanned material, however, show a significant increase in peak intensity and broadening in the vibrationally rich fingerprint region due to the presence of hydrogen bonded aromatic tannins. The glutaraldehyde and chromium tanned hide powder closely resembles untanned hide powder.

3.2.3. TANNING OF GOATSKIN

The tanning of goatskin was divided into three parts: (a) a comparative study of tannages using intact goatskin samples (**Section 3.2.3.1**), (b) optimisation of a small-scale tanning process using the complex identified in (a) which showed the greatest tanning potential (**Section 3.2.3.2**), and (c) the tannage, retannage, dyeing and fatliqouring of matched samples for a tentative comparison of physical and aesthetic properties between the complex identified in (a) and chromium tanned material (**Section 3.2.3.2**).

3.2.3.1. Shrinkage Temperature of Tanned Goatskin Samples

A range of tanning agents was used to tan goatskin samples (**Section 3.1.3**). **Figure 3.13** shows the plot of shrinkage temperatures measured versus the quantity of zirconium in the skin and includes results from **Section 3.2.3.2**.

Chromium tanned material (3.5% Cr_2O_3) produced a shrinkage temperature of 100°C (illustrated in **Figure 3.13** by ●). The conventional zirconium tannages reached a maximum shrinkage temperature of 95°C with a zirconium content close to 7.5%. The zirconium 4-hydroxymandelate tannages showed a similar decrease in slope as the zirconium content of the skin increased although the maximum shrinkage temperature reached was higher and with a lower zirconium content (100-101ºC at 5% zirconium). Extrapolation of this curve indicates that shrinkage temperatures well in excess of 100°C are theoretically possible as the zirconium content approaches that of conventionally tanned zirconium leathers. The remaining zirconium α-hydroxycarboxylate tannages resulted in shrinkage temperatures similar to conventional tannages.

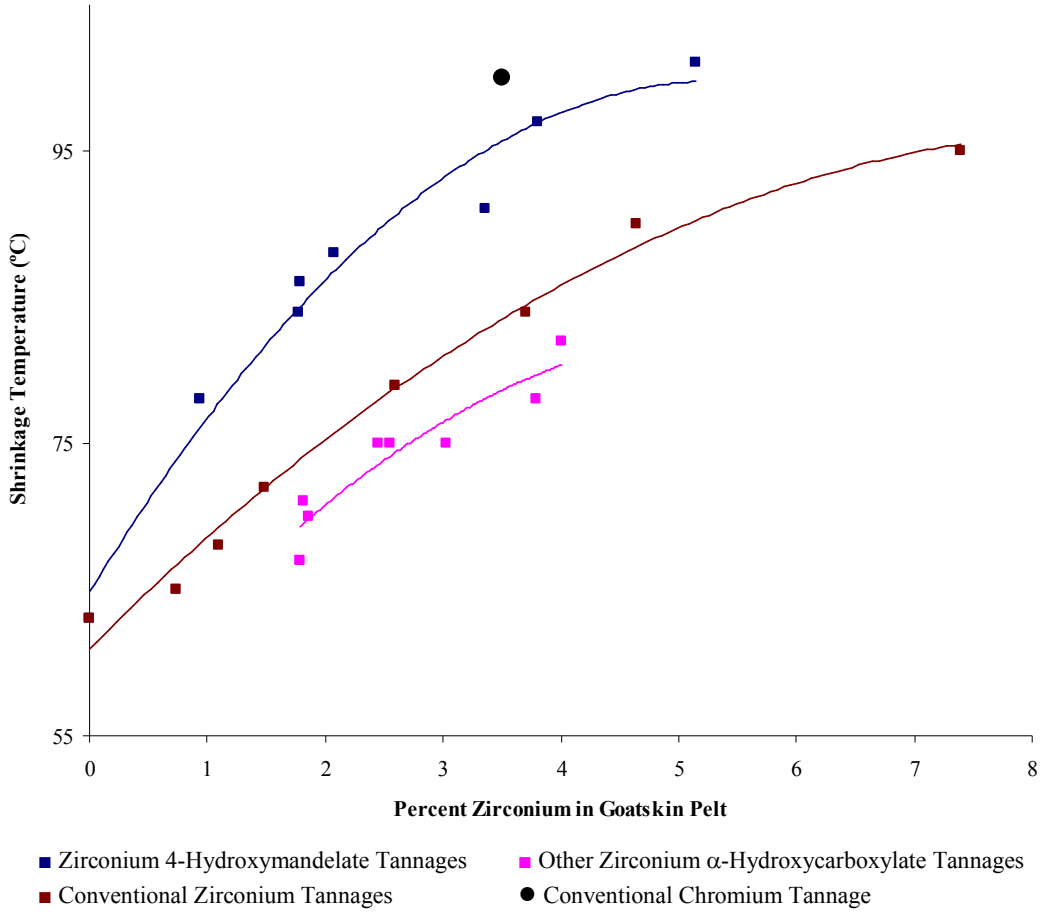

Figure 3.13: Graph showing the correlation between shrinkage temperature and the zirconium content of tanned goatskin samples (includes a conventional chromium tanned sample for comparison).

The percentage zirconium found in hide powder (**Table 3.2**) was significantly lower than the amount of zirconium found in goatskin (**Table 3.3**). This may be explained by a number of factors: (i) the goatskin samples were aged after tanning which allows the tanning agents time to fix and the hide powder was not, (ii) the goatskin is a "closed" matrix structure and washing would only remove superficial complex which is unbound. The hide powder, on the other hand, is an "open" fibrous material and washing may remove significant amounts of material, and (iii) if, as previously suggested, fixing of the complex occurs *via* precipitation, then an insoluble complex within the goatskin structure would not be removed easily, whereas, a largely superficial deposition of complex on hide powder may be readily removed.

The zirconium 4-hydroxymandelate tannages improved dramatically when used on goatskin with ΔT_s of 23 and 34ºC *cf.* 16 and 21ºC for hide powder, respectively.

Table 3.3: Table of zirconium tannages of goatskin in order of increasing shrinkage temperature (T_s).

Tannage	T_s (°C)	ΔT_s (°C)	Zr (%)	Zr Uptake (%)
None	63	0	0	-
Zr Mandelate (1:4)	67	4	1.78	77.8
Zr Citrate (1:4)	70	7	1.86	58.0
Zr D-Gluconate (1:4)	71	8	1.82	55.6
Zr D-Gluconate (1:2)	75	12	2.54	70.7
Zr Citrate (1:2)	75	12	2.45	67.0
Zr Lactate (1:4)	75	12	3.02	78.5
Zr Mandelate (1:2)	78	15	3.79	87.1
Zr Lactate (1:2)	82	19	4.00	63.2
Zr 4-Hydroxymandelate (1:4)	86	23	1.78	77.4
Conventional Zr Sulfate	90	27	4.64	97.4
Zr 4-Hydroxymandelate (1:2)	97	34	3.81	94.7

It was evident after shrinkage temperatures were measured that many of the zirconium α-hydroxycarboxylate tanned goatskin samples were not tanned throughout the cross-section. The heated samples showed that the collagen fibres close to the surface of the skin remained intact and those found in the inner zones of the cross-section were denatured. This was confirmed using SEM and is illustrated using zirconium mandelate (1:4) tanned material (**Figure 3.14**), which showed the poorest penetration of the "new" zirconium tanning agents investigated.

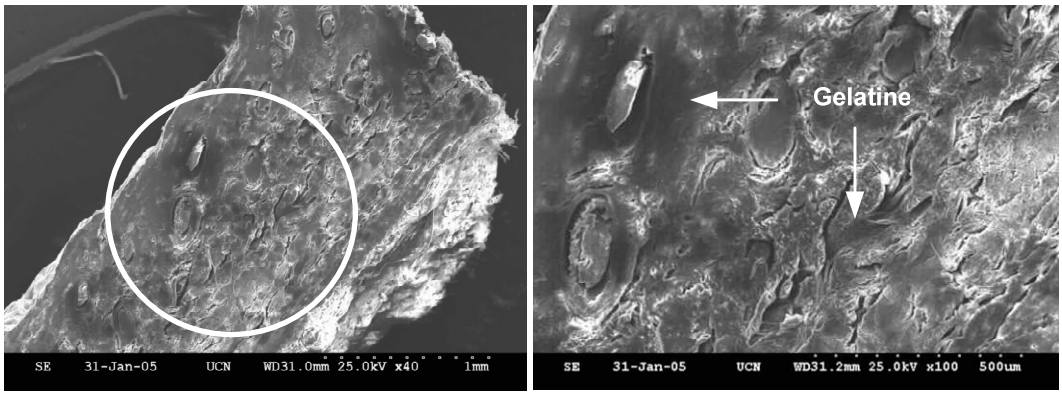

(a) (b)

Figure 3.14: View of the cross-section of goatskin samples after shrinkage has occurred for zirconium mandelate (1:4), with magnification (a) x40 and (b) x100.

The cross section of zirconium 4-hydroxymandelate (1:2) tanned samples, however, showed a less distinct loss of structure upon shrinkage (**Figure 3.15**).

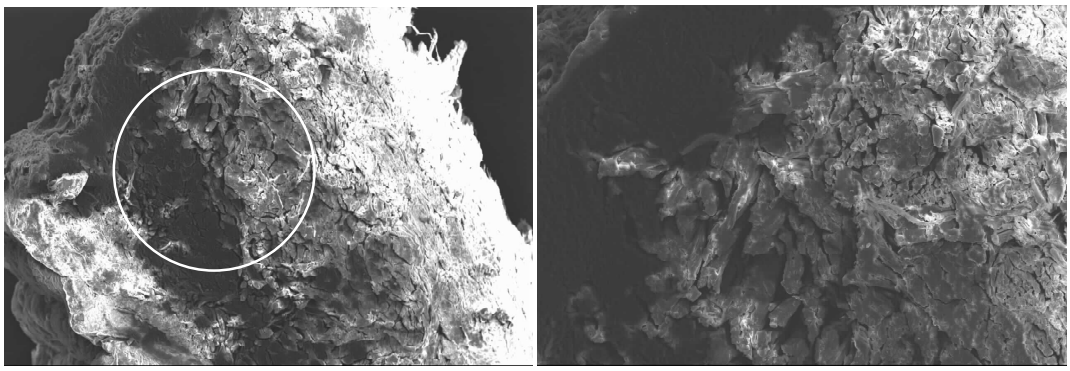

(a) (b)

Figure 3.15: View of the cross-section of goatskin samples after shrinkage has occurred for zirconium 4-hydroxymandelate (1:2), with magnification (a) x40 and (b) x100.

SEM EDXA (**Section 3.1.1**) indicated that this difference was likely to have been the result of a difference in penetration of the tanning complexes. Zirconium was measured and mapped through the cross section of tanned samples and **Figure 3.16** shows a representative comparison of the zirconium mandelate (1:4) and 4-hydroxymandelate (1:2) tanned samples.

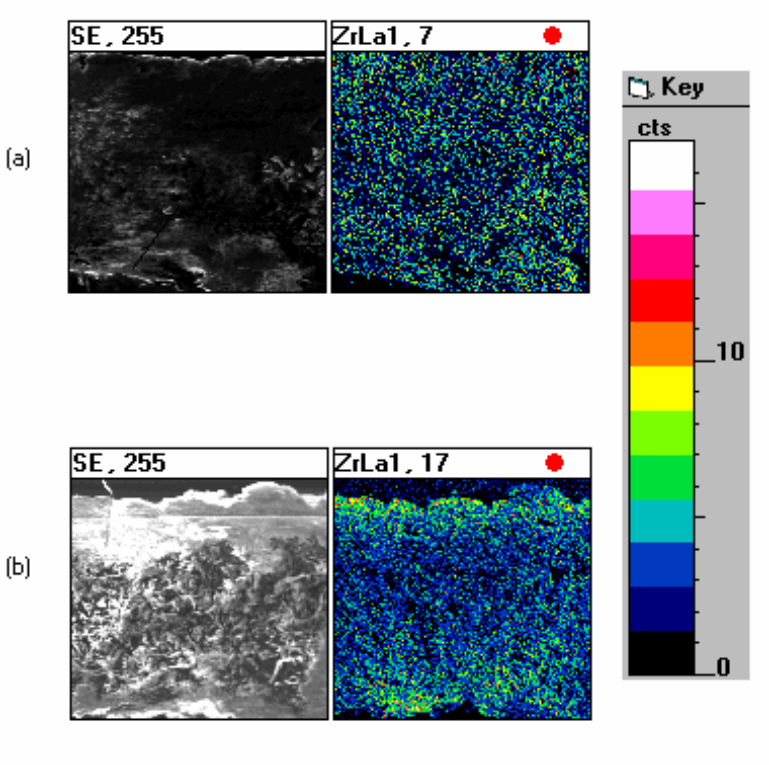

Figure 3.16: SEM EDXA scan showing the distribution of zirconium within the skin cross-section of (a) zirconium 4-hydroxymandelate (1:2), and (b) zirconium mandelate (1:4) tanned samples.

Figure 3.16b shows an accumulation of zirconium (green and yellow) in the grain (upper) and flesh (lower) layers for the material tanned with zirconium mandelate (1:4). On the other hand, the cross-section of the skin tanned with zirconium 4-hydroxymandelate (1:2) (**Figure 3.16a**) shows a more uniform distribution of zirconium throughout the skin structure and this is likely to contribute to higher shrinkage temperatures. The mandelate, 4-bromomandelate and lactate complexes all resulted in the superficial deposition of zirconium. These complexes are not readily soluble in water and may be expected to precipitate with relative ease. Similarly to chromium tanned material, the citrate and D-gluconate complex tanned material showed a relatively uniform distribution of zirconium throughout the cross section.

The 4-hydroxymandelate ligand with the *para* hydroxyl group appears to provide sufficient water solubility and stability to the complex without generating highly crosslinked polymeric complexes at elevated pHs and favours penetration of the complex under the conditions utilised. The zirconium and phenolic moieties are both potentially able to stabilise collagen and increase: (i) the ease of penetration, or (ii) the variety of possible binding to the collagen. These factors or their cumulative effect are likely to result in an increase of the shrinkage temperature.

A goatskin sample was tanned with only 4-hydroxymandelic acid at a level equivalent to 10% in a 1:2 ratio synthetic procedure (**Section 3.1.3.13**). A shrinkage temperature of 45°C was measured and indicates that 4-hydroxymandelic acid alone acts as a hydrogen bond breaker. Covington[38] postulated four tanning zones based on shrinkage temperature (**Table 1.9**). The only tannage investigated which falls into the negative tannage zone was the 4-hydroxymandelic acid tannage described above. Tanning using the ligand alone destabilises the collagen structure and highlights the importance of the use of zirconium in the tanning complexes. The α-hydroxycarboxylate group is likely to be instrumental in destabilising the collagen and requires the metal ion to mask this negative interaction. The majority of the zirconium α-hydroxycarboxylate tannages investigated in this work fall into the zone of moderate stability tannages and only zirconium 4-hydroxymandelate (1:2) falls into the combination tannage zone. Zirconium 4-hydroxymandelate (1:4) falls on the border of the moderate stability and combination tannage zones.

In the synthesis of conventional syntans, charge distribution density within the ring is important and hydroxyl groups must be distributed to maximise conjugation and resonance structures. The presence of hydroxyl groups in the *para* and *ortho* position is expected to improve hydrogen bonding and therefore tanning through resonance effects.[9] 4-Hydroxymandelic acid fulfils these requirements. Future optimisation studies of related zirconium α-hydroxycarboxylate complexes are required to confirm this. However, preliminary chemical considerations can be noted.

Section 2.2.3.2.4 identified that 4-hydroxymandelic acid and its zirconium complexes had the lowest ν_aC=O vibration of the mandelate series. This was attributed to resonance stabilisation from the strongly activating, electron-donating *para* hydroxyl functional group (**Section 2.2.4**). The bromo group is electron-withdrawing and weakly deactivating, however, it still results in resonance stabilisation but to a lesser degree than its hydroxy equivalent. The shrinkage temperatures of goatskin tanned with zirconium α-hydroxycarboxylates correlate well with the infrared ν_aC=O vibration values for the mandelate series. An increase in shrinkage temperature appears to be favoured by a lowering of the ν_aC=O vibration due to a combination of inductive and resonance effects and their effect on the α-OH (**Table 3.4**). Lactic acid does not exhibit resonance effects due to an aromatic ring and the methyl group attached to the α-hydroxycarboxylic acid moiety is a relatively weak electron donor. Tanning ability appears to be favoured by electron donation and strong resonance stabilisation of the group attached to the α-hydroxycarboxylic acid moiety.

Citric and D-gluconic acid appear to complex strongly with zirconium and the complexes have a mild tanning ability. Rehydration (stirring for 24 hours in deionised water) of tanned goatskin samples showed that these tannages were reversible as the shrinkage temperature was reduced to that of raw material. The stability and water solubility of the complexes hinders interaction with collagen and the tanning effect may be attributed to the deposition of the zirconium complexes within the fibre structure upon drying. Citric and D-gluconic acid are strong, effective chelating agents and not suitable as masking agents under the conditions utilised.

Table 3.4: Correlation between shrinkage temperature, $\nu_a C=O$ and the effect of the R substituent of selected α-hydroxycarboxylic acids.

Ligand R-CH(OH)CO_2H	Goatskin T_s (ºC)		$\nu_a C=O$ (cm^{-1})		Effect of R
	1:2	1:4	Ligand	Complex	
Lactic acid R=CH_3	82	75	1717	1610	Electron donating
Mandelic acid R=C_6H_5	78	67	1720	1623	Electron withdrawing Moderate resonance stabilisation
4-Hydroxymandelic acid R=*p*-HOC_6H_4	97	86	1671	1612	Electron withdrawing Good resonance stabilisation Strongly activating
4-Bromomandelic acid R=*p*-BrC_6H_4	80	71	1718	1620	Electron withdrawing Moderate resonance stabilisation Weakly deactivating

The greatest tanning potential exhibited by the hide powder and goatskin tanning experiments was shown by the zirconium 4-hydroxymandelate (1:2) complexes and all further studies were limited to this complex. Tanning with the zirconium 4-hydroxymandelate mineral syntan yielded leathers which fall in the combination tannage zone, but require one step only, without the need for low pickle pHs and retanning.

3.2.3.2. Optimisation of the Zirconium 4-Hydroxymandelate (1:2) Tanning Process using Goatskin

It was identified in **Section 3.2.3.1** that the penetration of the zirconium complexes into the skin matrix was a potential problem. In order for a tanning agent to be effective in tanning hides or skins it must be able to enter the hide or skin structure prior to, or in conjunction with, fixation. The major factors that affect the penetration of tanning agents into the collagen matrix are temperature, diffusion gradient, mechanical action, pH and time.[39]

An increase in temperature increases the average energy of molecules and therefore improves diffusion (penetration) but it also increases the rate of reaction and therefore improves fixation.

The diffusion gradient is directly proportional to the concentration of tanning agents in the tanning float. An increase in float and/or decrease in the amount of tanning agent used, results in a lower diffusion gradient and therefore a poorer penetration of tanning agents. Penetration and fixation of tanning agents are improved by an increase in diffusion gradient. This factor's influence can be minimised by the introduction of mechanical action.[2]

Mechanical action improves tanning liquor exchange between the collagen matrix and drum liquor by flexing, compressing, relaxing and stretching of the skin. A vigorous mechanical action provides a more effective chemical distribution, and improved penetration and fixation of the tanning material. Mechanical action is affected by: (i) the type and design of the process vessel, (ii) the rotation or mixing speed of the process vessel, (iii) the float length, and (iv) the total volume of the load.[7]

The influence of pH on the penetration of tanning agents is dependent on the nature of the tanning agent. As mentioned in **Section 1.2**, collagen is cationic in nature at pHs below its isoelectric point and anionic above this. Generally speaking, if the tanning agent is cationic in nature it will penetrate better at low pH and if anionic will penetrate better at higher pH. The isoelectric point of collagenic material is a contentious issue but limed and pickled pelt is commonly accepted to have an isoelectric point in the region of 5.[2,16] Neutral tanning species are also likely to be affected by pH as pH dictates the nature of possible reactive sites on the collagen itself, *e.g.*, glutaraldehyde is a neutral tanning agent but reacts with deprotonated amine groups at elevated pH and therefore penetrates at low pH.[2] A change in pH is commonly utilised to fix chemicals to collagen and leather and is usually opposite to the pH required for penetration.

Naturally, time will affect the penetration and fixation of tanning chemicals with longer times favouring better penetration and fixation. There is a limit that is dependent on process, raw material and chemicals, to the length of time after which physical and chemical damage to the skin is likely to occur.

The variables investigated in this work include, tanning float length, "pickle" pH, tan offer, tanning and fixation times, and washes. The tanning apparatus utilised was not equipped with temperature control and experiments were run at room temperature (20 to

25°C). All samples were processed in similar process vessels at a fixed speed to minimise variations in mechanical action. Samples were tanned according to **Section 3.1.4** and a summary of the processes and results may be found in **Table 3.5**.

Table 3.5: A summary of the optimisation of zirconium 4-hydroxymandelate (1:2) tanning.

Exp.	Pickle pH	Float (%)	Tan Offer (%)	Tanning Time (h)	Fixation Time (h)	Wash	Shrinkage Temp. (°C)
1	5.0-5.5	100	10	12	2	Yes	86
2	5.0-5.5	100	10	12	2	No	95
3	7.5-8.0	100	10	12	2	No	91
4	5.0-5.5	200	10	12	2	No	86
5	5.0-5.5	100	10	2	12	No	97
6	5.0-5.5	100	15	2	12	No	100
7	5.0-5.5	100	7.5	2	12	No	88
8	5.0-5.5	100	5	2	12	No	84
9	5.0-5.5	100	2.5	2	12	No	78

Experiments 1-5 (**Table 3.5**) indicate that the two main factors found to decrease shrinkage temperature were the wash after tanning (Experiment 1) and the use of a high tanning float (Experiment 4). Washing the leather is likely to remove tanning agent before the leather has had a chance to age and high floats result in a low diffusion gradient and poorer penetration and fixation of tanning material.

A pickle pH of 5.0-5.5 as opposed to the higher pH of 7.5-8.0, combined with a preference for a shorter tanning and longer fixation time results in efficient tannages. These factors are likely to be related as the zirconium 4-hydroxymandelates are likely to polymerise as the pH is increased, thus hindering their penetration. It was evident after measuring the shrinkage temperatures of Experiments 3 and 4 and from naked observations of the cross-section of the tanned samples that the tanning agents did not penetrate the pelt properly. The cross-sections showed a sandwich type effect where the grain and flesh surfaces remained white and intact with a gelatinous denatured centre similar to zirconium mandelate (1:4) tanned samples (**Figure 3.14**).

The highest shrinkage temperatures were obtained using the process conditions of Experiment 5 and were used for the optimisation of tanning agent offer (Experiments 6-

9). An offer of 15% resulted in a higher shrinkage temperature than an offer of 10% but there is only a moderate increase in shrinkage temperature (4°C) and tanning agent offers of 10% were deemed most efficient.

All subsequent tanning processes using zirconium 4-hydroxymandelate (1:2) were based on the parameters of Experiment 5 (**Table 3.5**).

3.2.3.3. Pilot-Scale Tanning of Goatskin and Evaluation of Leather

Goatskins were sided and tanned in matched-skin trials according to **Section 3.1.5**. The leathers produced provide an indicative comparison of the tanning agents, however, an extensive full-scale trial would be required for definitive results.

The tanned leathers had shrinkage temperatures comparable to conventional values **(Table 3.6)**. The scale-up from processing small pieces of goatskin (~40 g, **Section 3.1.3**) to goatskin sides (~800 g) proceeded without incident.

Table 3.6: Shrinkage temperatures (T_s) of tanned goatskin sides.

Skin	Tannage	T_s (°C)
1	Conv. Cr	>100
	Conv. Zr	94
2	Conv. Cr	>100
	Zr(hM) (1:2) $ZrOCl_2.8H_2O$	92
3	Conv. Cr	>100
	Zr(hM) (1:2) $Zr(SO_4)_2.4H_2O$	90

3.2.3.3.1. Physical Evaluation of Leathers

The strength of a skin varies with fibre thickness and density and the butt is expected to have superior physical properties to the shoulder or belly areas as they are thicker and more tightly interwoven.[9] Directional properties were considered, as the average fibre length is longer parallel to the backbone than perpendicular and the relevant test results were expressed as the average of parallel and perpendicular sample values.

Each side was divided further into shoulders and butts (**Figure 3.1, page 120**). Tensile strength, percent elongation at break, double-edge tear load, grain crack load and distension, and softness were measured for the tanned shoulder samples (according to **Section 3.1.1.6**) and a summary of the results may be found in **Table 3.7**.

A general chromium tanned leather retanning, dyeing and fatliquoring process for sheepskin garment leathers (**Appendix 2**) was selected for the crusting of the goatskin butts. The tanned leathers were processed in one lot in an attempt to minimise *in situ* process variations. The process was not particularly suited to the goatskin structure but was designed to introduce softness and flexibility to the leather without excessive filling; properties that are not common to conventionally tanned zirconium leather.

Table 3.7: Results of the physical evaluation of tanned goatskin samples.

Skin	Tannage	Tensile Strength (MPa)	Percent Elongation at Break (%)	Double-Edge Tear Load (N)	Grain Crack Load (kgf)	Distension at Grain Crack (mm)	Softness (mm)
1	**Conv. Cr**	27.5	40.0	77.0	51	9.84	12
	Conv. Zr	25.9	43.3	92.7	48	8.17	4
2	**Conv. Cr**	17.2	61.7	86.4	40	9.44	9
	Zr(hM) (1:2) $ZrOCl_2.8H_2O$	23.5	25.0	51.1	30	7.68	10
3	**Conv. Cr**	24.2	55.0	91.3	60	11.49	6
	Zr(hM) (1:2) $Zr(SO_4)_2.4H_2O$	21.0	38.3	89.6	40	7.72	8

A single neutralising syntan (Coralon® OT powder, Clariant) was chosen to minimise the influence on the properties of the main tannage. The syntan is a naphthalene sulfonate auxiliary syntan and does not increase the shrinkage temperature but assists with the penetration and even distribution of dyestuff and fatliquors. Fatliquors lubricate the collagen fibres and improve the stretch, tear, tensile strength and comfort of retanned leather.[39] A blend of fatliquors was used as the sulfited Derminol® OS-1 liquid (Clariant) provides excellent softening combined with good penetration and the Trupon® DB (Trumpler) produces exceptional softness, coupled with a waxy, slightly wet handle. Tensile strength, percent elongation at break, double-edge tear load, grain crack load and

distension, and softness were measured for each crusted butt sample (according to **Section 3.1.1.6)** and a summary of the results may be found in **Table 3.8**.

Table 3.8: Results of the physical evaluation of crust goatskin samples.

Skin	Tanage	Tensile Strength (MPa)	Percent Elongation at Break (%)	Double-Edge Tear Load (N)	Grain Crack Load (kgf)	Distension at Grain Crack (mm)	Softness (mm)
1	**Conv. Cr**	28.1	68.3	123.0	65	12.04	24
	Conv. Zr	30.4	50.0	160.3	56	11.63	15
2	**Conv. Cr**	33.7	70.0	111.5	39	10.44	25
	Zr(hM) (1:2) $ZrOCl_2.8H_2O$	48.6	70.0	122.9	34	9.20	25
3	**Conv. Cr**	34.8	66.7	162.2	72	12.43	22
	Zr(hM) (1:2) $Zr(SO_4)_2.4H_2O$	39.9	53.3	140.2	66	10.06	23

The results from **Table 3.8** cannot be compared directly to the results from **Table 3.7** due to the expected intra-skin variation between the shoulder and butt. Also, due to inter-skin variations, results from Skin 1 cannot be compared directly to Skin 2 or 3.[4] General trends may, however, be identified as each zirconium tannage was compared to a matched chromium tannage.

Tensile strength is an important concept in the field of material science and is one of the most fundamental tests for leather performance even though it is not directly applicable to use.[4] Tensile strength is the maximum amount of "pulling" (tensile) stress that a material can be subjected to before it breaks. Tensile strength is measured in units of force per unit area and was expressed in megapascals (MPa). The tensile strength of the zirconium and chromium tanned material is similar in magnitude, however, values for the zirconium crust leathers were found to be marginally greater than the chromium crust leathers.

Elongation and strain are important for a number of applications and are usually measured in conjunction with tensile strength. Strain expresses itself as a change in shape or size and is the geometrical expression of deformation caused by the action of a stress on a material. Elongation in leather testing is commonly expressed as a percentage of the increase in length relative to its starting length whereas strain is the ratio of change in

length to the original nondeformed length. Percent elongation values measured for the conventionally tanned zirconium samples yield results similar to the conventional chromium tanned material, however, values for the zirconium 4-hydroxymandelate (1:2) tanned leathers are particularly low. Crusting reversed this trend, yielding lower elongation for the conventional zirconium crust and values similar to the chromium crust for the zirconium 4-hydroxymandelate (1:2) leathers.

Tearing tests relate well to performance in use and the measurement of tearing load is common. The double-edge tear test measures the maximum stress, in Newtons (N), obtained from the propagation of two simultaneous tears, as a slit punched into the leather is torn in a tensile tester. Results were mixed but higher values for the conventional zirconium tanned and crust leathers were evident.

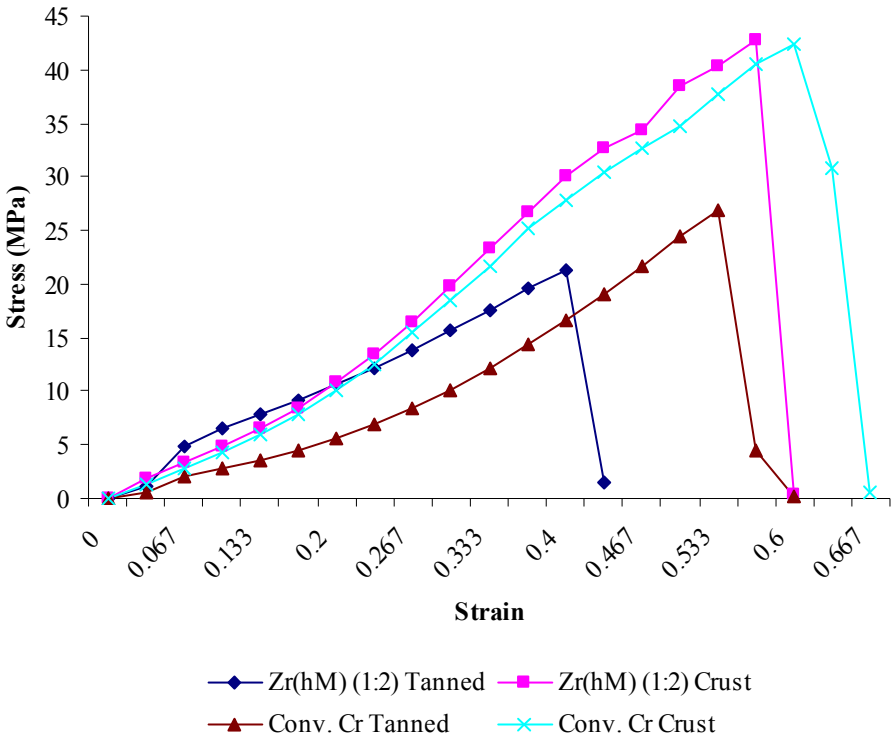

Figure 3.17: A representative stress versus strain graph comparing zirconium 4-hydroxymandelate (1:2) tanned and crust leathers (using $ZrOCl_2.8H_2O$) to conventional chromium tanned and crust leathers summarising the similarity between the crust leathers and difference between tanned leathers. Results shown were measured parallel to the backbone.

The lastometer test is a popular test and is widely used on footwear leathers. A ball on a rod is pressed against the flesh side of a clamped piece of leather with increasing pressure

until a crack is seen on the leather surface. The extension (mm) and load (kgf) are recorded at grain crack. Chromium tanned and crust leathers proved consistently superior to the zirconium leathers in grain crack load and distension.

Softness of leather samples is measured by the distension (mm) of the leather as a cylindrical rod of defined mass is lowered onto a securely clamped area of leather. Apertures of varying diameter may be used for softer or firmer leathers. The use of a 25 mm aperture showed that the zirconium 4-hydroxymandelate (1:2) tanned and crust material is similar in softness to the chromium tanned material. The conventional zirconium tanned and crusted material produces leathers that are firmer than the corresponding chromium tanned material.

3.2.3.3.2. Aesthetic Evaluation of Leathers

Leather grading is not performed using physical testing alone and personnel trained in inspecting leathers will also judge leathers based on aesthetic properties such as touch and grain quality. These properties and others may be impossible to assess using equipment and subjective inspection still forms a large part of leather inspection.

The conventional chromium tanned material was uniform in grain quality, appearance, feel and colour. The leather felt dry, empty and slightly boardy. The crust leathers were also consistent and showed complete dye penetration through the cross-section, a slightly darker flesh colour and felt slightly tinny, dry and empty.

The conventional zirconium tanned leather was full, firm and more boardy than the corresponding chromium tanned material. The leather was white on the grain and flesh sides. The conventional zirconium crust showed incomplete dye penetration. This was expected as conventional zirconium tanned material is highly cationic with a high isoelectric point and fixation of anionic chemicals (*e.g.* dyestuffs) is favoured. The grain colour was uneven and is another indicator of the astringent nature of conventional zirconium leathers to anionic chemicals. The syntan and fatliquors are also anionic and the dye acts as a tentative visual indicator of the penetration and distribution of these chemicals. The leather had a slightly empty feel.

The zirconium 4-hydroxymandelate (1:2) tanned leather (using $ZrOCl_2.8H_2O$) produced an even coloured, slightly yellow, off-white leather. The crust had a pleasing handle with a cool, slightly "wet" and waxy feel to it. The crust, felt full without roundness and showed a marked difference between the grain and flesh colour. The grain was a pale yellow-brown colour and the flesh a darker red-brown. A pale grain and large grain/flesh colour difference is a common feature when large amounts of syntan are taken up in the grain.[16]

The zirconium 4-hydroxymandelate (1:2) tanned leather (using $Zr(SO_4)_2.4H_2O$) produced a slightly transparent, thin, dry, bony material similar in appearance and texture to parchment and dry raw pelt. The crust was empty, dull and boardy with a slightly waxy surface. The grain surface colour was uneven and a large grain/flesh colour difference, similar to the previous samples, was observed.

To better represent the colours and colour variations described above, colour was measured according to the Commision Internationale de I'Eclairage (CIE) 1976 L*a*b* (CIELab) chromatic system using a colorimeter (**Section 3.1.1.6**). CIELab is a widely used, internationally accepted coordinate system for the three-dimensional expression of the colour of an object (**Figure 3.18**). The Euclidean distance, ΔE, was measured using the same system and is a measure of the difference in colour as determined by eye.[244]

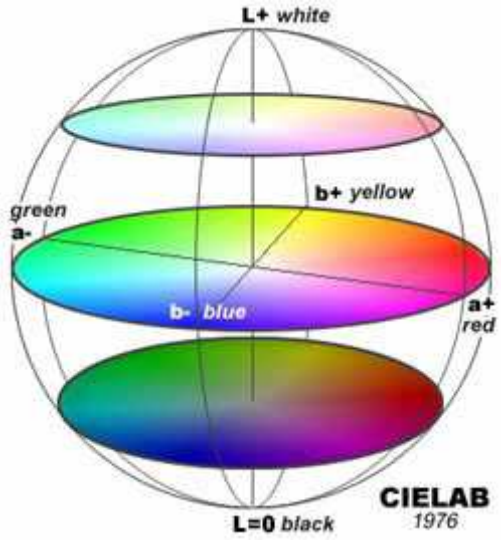

Figure 3.18: A representation of CIE 1976 (L*a*b*) three-dimensional colour space.

The a* axis represents the red (+) and green (-) component, the b* axis represents the yellow (+) and blue (-) axis, and the L* axis represents the light (100) to dark (0) scale.

ΔL*, Δa* and Δb* values were calculated from the average of three absolute colour measurements (*Equations 1-3*) and ΔE values were calculated from the ΔL*, Δa* and Δb* values according to *Equation 4*.[245]

$$\Delta L^* = L^*_{sample} - L^*_{reference} \qquad \textit{Equation 1}$$

$$\Delta a^* = a^*_{sample} - a^*_{reference} \qquad \textit{Equation 2}$$

$$\Delta b^* = b^*_{sample} - b^*_{reference} \qquad \textit{Equation 3}$$

$$\Delta E = [(\Delta L^*)^2 + (\Delta a^*)^2 + (\Delta b^*)^2]^{½} \qquad \textit{Equation 4}$$

Table 3.9: True CIE 1976 (L*a*b*) colour values of chromium and zirconium tanned and crust leathers measured using a colorimeter and calculated colour differences between grain and flesh (ΔL*, Δa*, Δb* and ΔE) using grain colour as reference.

Skin	Tannage	Surface	L*	a*	b*	Δ L*	Δ a*	Δ b*	ΔE
1	Conv. Cr Tanned	Grain	79.5	-0.6	-1.2	-2.8	0.1	-0.6	2.89
		Flesh	76.7	-0.5	-1.8				
	Conv. Cr Crust	Grain	41.6	22.2	33.1	-8.6	-1.7	-11.9	14.8
		Flesh	33.0	20.5	21.2				
	Conv. Zr Tanned	Grain	82.7	1.1	10.2	-0.1	-0.2	-0.3	0.3
		Flesh	82.6	0.9	9.9				
	Conv. Zr Crust	Grain	33.2	22.0	19.0	-7.6	-7.1	-8.3	13.3
		Flesh	25.6	14.8	10.7				
2	Conv. Cr Tanned	Grain	78.3	-0.7	-0.9	-2.4	0.5	-0.4	2.5
		Flesh	75.9	-0.2	-1.3				
	Conv. Cr Crust	Grain	38.3	23.1	28.7	-6.6	-2.8	-8.8	11.4
		Flesh	31.7	20.2	20.0				
	Zr(hM) (1:2) $ZrOCl_2.8H_2O$ Tanned	Grain	86.3	-0.9	11.9	-0.8	0.9	-2.5	2.8
		Flesh	85.6	0.0	9.4				
	Zr(hM) (1:2) $ZrOCl_2.8H_2O$ Crust	Grain	52.0	27.8	47.8	-24.4	-14.0	-36.3	45.9
		Flesh	27.6	13.7	11.5				
3	Conv. Cr Tanned	Grain	80.4	-0.8	0.0	-2.7	0.3	-1.9	3.3
		Flesh	77.7	-0.5	-1.9				
	Conv. Cr Crust	Grain	42.5	23.1	33.1	-8.2	-2.1	-10.3	13.6
		Flesh	34.3	21.0	22.7				
	Zr(hM) (1:2) $Zr(SO_4)_2.4H_2O$ Tanned	Grain	77.2	2.0	22.3	1.7	-1.4	-6.4	6.8
		Flesh	79.0	0.6	15.9				
	Zr(hM) (1:2) $Zr(SO_4)_2.4H_2O$ Crust	Grain	41.4	26.6	32.8	-12.0	-10.4	-18.4	24.2
		Flesh	29.4	16.2	14.4				

Euclidean distance (ΔE) values in **Table 3.9** indicate the dramatic colour variation between the grain and flesh of the zirconium 4-hydroxymandelate (1:2) crust samples (45.9 and 24.2) compared to chromium tanned crust (14.8, 11.4 and 13.6). The conventionally tanned zirconium crust shows a grain/flesh colour variation similar to chromium crust leather (13.3).

The colour of the zirconium sulphate based zirconium 4-hydroxymandelate (1:2) crust grain was closest in colour to its chromium crust reference (**Table 3.10**). The conventional zirconium tanned crust and zirconium oxychloride based zirconium 4-hydroxymandelate (1:2) crust were significantly different in colour to their corresponding chromium crust leathers. The zirconium oxychloride based zirconium 4-hydroxymandelate (1:2) grain was lighter (ΔL* = +13.7), more red (Δa* = +4.7) and more yellow (Δb* = 19.0) than its chromium crust reference.

Table 3.10: Calculated CIE 1976 (L*a*b*) colour differences (ΔL*, Δa*, Δb* and ΔE) between the grain of zirconium tanned crust and the grain of the matched chromium crust using the chromium crust as reference.

Skin	Tannage	Δ L*	Δ a*	Δ b*	ΔE
1	Conv. Zr	-8.4	-0.3	-14.1	16.4
2	Zr(hM) (1:2) $ZrOCl_2.8H_2O$	13.7	4.7	19.0	23.9
3	Zr(hM) (1:2) $Zr(SO_4)_2.4H_2O$	-1.2	3.6	-0.3	3.76

The distribution of dye is indicative of the distribution of anionic retanning and fatliquor chemicals introduced. Dark colours may indicate surface fixation, uneven dyeing may indicate poor neutralisation and an uneven surface astringency, and incomplete penetration of dye may indicate a high surface astringency (sometimes desirable). The penetration and distribution of retanning agents and fatliquors dictates the final physical properties of the leather and dyestuff distribution and colour was used to gauge the effect of the tanning agent on all anionic chemicals.

3.2.4. SUMMARY OF THE IDENTIFICATION OF A ZIRCONIUM TANNING COMPLEX AND THE EVALUATION OF THE LEATHER PRODUCED

Chapter 2 identified the importance of the α-hydroxycarboxylic acid moiety in complex formation with zirconium(IV) in aqueous solution. The identification of a suitable zirconium masking agent was abandoned in favour of the generation of a zirconium α-hydroxycarboxylate syntan as precipitated zirconium complexes generated were found to dissolve at elevated pHs.

Six ligands were selected for investigation in **Chapter 3** and included lactic acid, mandelic acid, 4-hydroxymandelic acid and 4-bromomandelic acid, which formed precipitates when complexed; and D-gluconic acid and citric acid which produced soluble complexes at all pHs. Tanning experiments using 1:2 and 1:4 zirconium:ligand aqueous solutions on hide powder and goatskin were utilised to identify 4-hydroxymandelic acid as the ligand best suited for a zirconium syntan at a zirconium to ligand ratio of 1:2.

Initial optimisation studies showed that zirconium 4-hydroxymandelate (1:2) tanning favours a pickle pH of 5.0-5.5, a short tanning time followed by a long fixation time and no wash after tanning. Tanning agent offers of 10% with a low float (100%) were deemed most efficient and produced a creamy white leather.

Chromium tanned leathers and processes were used as a benchmark and only the tanning process parameters and chemicals were tentatively optimised for the zirconium tanned leathers. Poor results, therefore, serve only to indicate the necessity for further trials and optimisation that was beyond the scope of the current investigation.

The conventional zirconium tanned leathers were full, round and firm as expected. The uneven colour and lack of dye penetration may be directly attributed to process parameters and the high astringency of conventional zirconium tanned leather.

The difference in results between the zirconium 4-hydroxymandelates can be attributed to the source of zirconium in the generation of the tanning agent. The results clearly indicate the superiority of zirconium oxychloride as the source of zirconium. A small amount of precipitate was evident in the zirconium sulphate based 4-hydroxymandelate

(1:2) tanning solution prior to use and indicated that a complete pH stabilisation of the zirconium had not occurred. This was not unexpected as the sulphate anion has been reported to interfere with the complexation of zirconium (**Section 2.2.1**). The tanned leather produced was empty and tinny and resembled raw pelt. The crust leather produced was also of poor quality relative to the chromium and zirconium 4-hydroxymandelate (1:2) (using $ZrOCl_2.8H_2O$).

CHAPTER 4:
CONCLUSIONS

The present study, involving an investigation of over thirty ligands, reaffirmed the importance of oxygen as the donor atom of choice in complexing zirconium. The type, position and combination of oxygen containing donor groups proved significant with the overall dominance of the α-hydroxycarboxylic acid moiety as a chelator of choice.

Initial attempts to identify a new effective masking agent to allow the use of zirconium(IV) salts in aqueous solution between pH 2.5 and 6.7 were unsatisfactory. Ligands produced zirconium "complexes" which were either ineffective at preventing hydrolysis, or so effective that (i) hydrolysis was prevented completely, or (ii) insoluble precipitates were formed.

Selected α-hydroxycarboxylic acid ligands generated precipitates with zirconium. Glycolic acid, lactic acid, mandelic acid, 4-hydroxymandelic acid, 4-chloromandelic acid and 4-bromomandelic acid, were employed in zirconium:ligand ratios of 1:2 and 1:4. The products were isolated at low pH and characterised using inductively coupled plasma mass spectrometry, microanalysis, differential scanning calorimetry, thermogravimetric analysis and infrared and Raman spectroscopy. The precipitates from the 1:2 and 1:4 syntheses were indistinguishable and fitted three types, *viz*., $Zr_2O(OH)_2L_4$ with glycolic acid, $Zr(OH)L_3$ with lactic acid, and ZrL_4 for the mandelate series, where L=ligand. The zirconium α-hydroxycarboxylates chelate *via* unidentate coordination of the carboxylic acid and α-OH moieties.

The insoluble precipitates with the α-hydroxycarboxylic acids, synthesised at low pH, were discovered to redissolve as the pH was elevated over an approximate pH range of 5.0 to 10.0. Dissolution of the strongly coordinated mandelate series precipitates was identified to favour the deprotonation of the α-OH and the polymeric hydrolysis of the

zirconium ion by ligand substitution. Reacidification and depolymerisation of these dissolved zirconium species in the presence of a coordinating collagen matrix was proposed as a possible mechanism for the direct binding of zirconium to collagen. The focus of the research was therefore directed to investigate zirconium α-hydroxycarboxylates as possible suitable mineral syntans.

Considering the limitations of conventional "wet white" tannages - the labile aluminium tannages and the leather plumpness associated with zirconium sulfate tannages - linear free energy relationships were used to optimise selection criteria for stabilising the zirconium complex and controlling the fixing pH. Lactic acid, mandelic acid, 4-hydroxymandelic acid, 4-bromomandelic acid, citric acid and D-gluconic acid were selected as the ligands to be extended to tanning studies. The tanning ability of 1:2 and 1:4 zirconium:ligand solutions was assessed using hide powder and intact goatskin. Tanning solutions were generated *in situ* by raising the pH of the synthesis solution using 2 ***M*** sodium hydroxide. Precipitation of the zirconium complex was found to occur, coating the collagen fibres, however, spectroscopic studies, high pHs, and elevated shrinkage temperatures indicate a direct interaction with collagen was achieved.

Most of the zirconium α-hydroxycarboxylates fall in the zone of moderate stability tannages, with the zirconium 4-hydroxymandelate (1:2 metal:ligand ratio) in the combination tannage zone, while the zirconium 4-hydroxymandelate (1:4) is borderline. Zirconium complexes with citrate, D-gluconate, and 4 hydroxymandelate ligands show the greatest penetration into hide powder or goatskin necessary for potential as syntans. Rehydration studies of the citrate and D-gluconate tannages show reversibility, indicating similar behaviour to aluminium tannages.

The zirconium 4-hydroxymandelate (1:2) tanning solution was shown to be the most effective at tanning hide powder and goatskin with respectable shrinkage temperatures of 80 and 97ºC respectively. Provisional optimisation of the tanning process identified a tan offer of 10%, a 100% float, a two hour tanning process followed by a twelve hour fixation, and no final wash as the most effective parameters.

Pilot scale tanning of matched goatskin sides was successfully performed using the optimised zirconium 4-hydroxymandelate (1:2) process. The process is simple and convenient to use and would slot into any conventional tanning process with relative ease. Zirconium oxychloride and zirconium sulphate were utilised as the source of zirconium in the syntan and the leathers were compared to conventionally tanned chromium and conventionally tanned zirconium leathers. Zirconium oxychloride proved to be instrumental in the generation of an effective tanning agent and the tanned and crust leathers produced were physically and aesthetically comparable to the chromium tanned material.

With a fixation pH of 5 and a shrinkage temperature of 97ºC, the zirconium 4-hydroxymandelate (1:2) process may provide an alternative to the Organozir process (fixation pH of 5, shrinkage temperature of 90ºC).

Several areas of future investigation are open. The first is a full comparative study of the zirconium 4-hydroxymandelate (1:2) and the Organozir process. The second is a detailed investigation of the use of zirconium 4-hydroxymandelate (1:2) as a retanning agent in combination tannages. A third possible area is the introduction of α-hydroxycarboxylic acid groups onto the collagen matrix as a zirconium chelating moiety. Finally, a detailed evaluation of the tanning mechanism of zirconium 4-hydroxymandelate can be made in light of conventionally proposed mechanisms. To this end, the need to grow crystals of the complexes, and the use of DFT calculations should prove valuable in examining L→M bonding through conformational preferences. In addition, we have identified that the behaviour of the ν_aC=O vibration of α-hydroxycarboxylate complexes may provide a useful diagnostic tool in the search for mineral syntans.

REFERENCES

1. International Glossary of Leather Terms, International Council of Tanners, London, England, 1968, pp. 1-47.

2. J. H. Sharphouse, *Leather Technician's Handbook*, Leather Producer's Association, Northampton, England, 1995, Chapters 1-4, 8-13, 15, 16, 20-22, and 27-31

3. S. Dasgupta, *J. Soc. Leath. Tech. Chem.*, 2004, **88**, pp. 116-119.

4. M. K. Leafe (Ed.), *Leather Technologists Pocket Book*, Society of Leather Technologists and Chemists, Withernsea, UK, 1999, Chapters 1-10.

5. J. Buljan, G. Reich and J. Ludvik, *J. Leder & Haeutemarkt*, 1998, **4**, pp. 30-37.

6. T. Ramasami, J. Raghava Rao, N. K. Chandra Babu, K. Parthasarathi, P. G. Rao, S. Saravanan, R. Gayathri and K. J. Sreeram, *J. Soc. Leath. Tech. Chem.*, 1999, **83**, pp. 39-45.

7. K. T. Sarkar, *Theory and Practice of Leather Manufacturing*, Published by The Author, Madras, India, 1995, 5th Ed., Chapters V and X.

8. R. Daniels, *Back to Basics: Leather Manufacture*, World Trades Publishing Limited, Liverpool, UK, 2003, pp. 8-18.

9. K. Bienkiewicz, *Physical Chemistry of Leather Making*, Robert E. Krieger Publishing Company, Malabar, Florida, USA, 1983, Chapters 2-5, 10, 12 and 14-19.

10. W. Landmann, *The Machines in the Tannery, a Review of Leather Producing Machinery and Equipment in the Tannery*, World Trades Publishing, Dewsbury, UK, 2003.

11. Anonymous, *Tanning, Dyeing Finishing*, Bayer AG, Leverkusen, Germany, 1994, 6th Ed., Chapters 1-3.

12. Anonymous, *Pocket Book for the Leather Technologist*, BASF, Ludwigshafen, Germany, 1997, 3rd Ed., pp. 85-128.

13. G. John, *Possible Defects in Leather Production, Definitions, Causes, Consequences, Remedies and Types of Leather*, Druck Partner Rubelmann, GmbH, Hemsbach, Germany, 1996, pp. 294-346.

14. H. Lodish, D. Baltimore, A. Berk, S. L. Zipursky, P. Matsudaira, and J. Darnell, *Molecular Cell Biology*, Scientific American Books, New York, USA, 1995, 3rd Ed., pp. 1130-1135.

15. L. Stryer, *Biochemistry*, W. H. Freeman and Company, New York, USA, 1981, pp. 195-197.

16. E. Heidemann, *Fundamentals of Leather Manufacturing*, Eduard Roether KG, Darmstadt, Germany, 1993, pp. Chapters 4, 9-12 and 17.

17. A. J. Bailey, *J. Soc. Leath. Tech. Chem.*, 1992, **76**, pp. 111-127.

18. P. L. Kronick and S. Iandola, *J. Am. Leath. Chem. Ass.*, 1997, **92**, pp. 172-178.

19. E. M. Brown, G. King and J. M. Chen, *J. Am. Leath. Chem. Ass.*, 1997, **92**, pp. 1-5.

20. D. Buttar, R. Docherty and R. M. Swart, *J. Am. Leath. Chem. Ass.*, 1997, **92**, pp. 185-199.

21. C. K. Matthews and K. E. van Holde, *Biochemistry*, The Benjamin/Cummings Publishing Company Inc., Redwood City, USA, 1990, pp. 183-184.

22. T. E. Creighton, *Protein: Structures and Molecular Properties*, W. H. Freeman and Company, New York, USA, 1993, 2nd Ed., pp. 194-197.

23. W. Freiss, *Eur. J. of Pharm. and Biopharm.*, 1998, **45**, pp. 113-136.

24. L. H. H. Olde Damink, P. J. Dijkstra, M. J. A. van Luyn, P. B. van Wachem, P. Nieuwenhuis and J. Feijen, *Biomaterials*, 1996, **17**, pp. 765-773.

25. K. J. Bienkiewicz, *J. Am. Leath. Chem. Ass.*, 1990, **85**, pp. 305-325.

26. I. G. Mogilner, G. Ruderman, J. R. Grigera, *J. Mol. Graph. Model.*, 2002, **21**, pp. 209-213.

27. J. Kopp, M. Bonnet and J. P. Renou, *Matrix*, 1989, **9**, pp. 443-450.

28. S. K. Holmgren, K. M. Taylor, L. E. Bretscher and R. T. Raines, *Nature*, 1998, **392**, pp. 666-667.

29. G. Reich, *J. Soc. Leath. Tech. Chem.*, 1999, **83**, pp. 63-79.

30. Anonymous, *Official Methods of Analysis*, Society of Leather Technologists and Chemists, The Charlesworth Group, Huddersfield, UK, 1996.

31. K. H. Gustavson, *The Chemistry and Reactivity of Collagen*, Academic Press Inc., New York, USA, 1956, Chapters 4-8.

32. T. Bosch, A. M. Manich, J. Carilla, J. Cot, A. Marsal, H-J Kellert and H-P Germann, *J. Am. Leath. Chem. Ass.*, 2002, **97**, pp. 441-450.

33. A. Rochdi, L. Foucat and J-P Renou, *Food Chem.*, 2000, **69**, pp. 295-299.

34. S. Jeyapalina, Ph.D. Thesis, *Studies on the Hydro-Thermal and Viscoelastic Properties of Leather*, University of Leicester, Leicester, 2004.

35. A. M. Manich, T. Bosch, J. Carilla, J. Cot, A. Marsal, J. Sala and P. J. Celma, *J. Am. Leath. Chem. Ass.*, 2003, **98**, pp. 279-284.

36. R. Dong, X. Yan, X. Pang and S. Liu, *Spectrochim. Acta, Part A*, 2004, **60**, pp. 557-561.

37. G. J. Maffia, M. A. Seltzer, P. H. Cooke, and E. M. Brown, *J. Am. Leath. Chem. Ass.*, 2004, **99**, pp. 164-169.

38. A. D. Covington, *J. Soc. Leath. Tech. Chem.*, 2001, **85**, pp. 24-34.

39. T. C. Thorstensen, *Practical Leather Technology*, Krieger Publishing Company, Malabar, USA, 1993, 4th Ed., Chapters 4 and 7.

40. S. Wren, and M. Saddington, *J. Am. Leath. Chem. Ass.*, 1995, **90**, pp. 146-153.

41. S. Das Gupta, *J. Soc. Leath. Tech. Chem.*, 1980, **64**, pp. 16-23.

42. A. D. Covington, *J. Am. Leath. Chem. Ass.*, 1987, **82**, pp. 1-14.

43. P. M. Pojer, E. L. S. Chin and R. N. Reddie, *J. Soc. Leath. Tech. Chem.*, 1993, **77**, pp. 78-81.

44. R. L. Sykes and C. W. Cater, *J. Soc. Leath. Tech. Chem.*, 1980, **64**, pp. 29-31.

45. R. L. Sykes, R. A. Hancock and S. T. Orszulik, *J. Soc. Leath. Tech. Chem.*, 1980, **64**, pp. 32-37.

46. A. D. Covington, G. S. Lampard and M. Pennington, *J. Soc. Leath. Tech. Chem.*, 1998, **82**, pp. 78-80.

47. S. Gangopadhyay, S. Lahiri and P. K. Gangopadhyay, *J. Soc. Leath. Tech. Chem.*, 2000, **84**, pp. 88-93.

48. C. Gaidau, F. Platon and N. Badea, *J. Soc. Leath. Tech. Chem.*, 1998, **82**, pp. 143-146.

49. P. Thanikaivelan, V. Geetha, J. Raghava Rao, K. J. Sreeram and B. Unni Nair, *J. Soc. Leath. Tech. Chem.*, 2000, **84**, pp. 82-87.

50. N. P. Slabbert, *Das Leder*, 1980, **31**, pp. 79-82.

51. B. Madhan, V. Subramanian, J. Raghava Rao, B. Unni Nair and T. Ramasami, *J. Am. Leath. Chem. Ass.*, 2003, **98**, pp. 273-278.

52. N. P. Slabbert, *J. Am. Leath. Chem. Ass.*, 1999, **94**, pp. 1-7.

53. B. Madhan, J. Raghava Rao, V. Subramanian, B. Unni Nair and T. Ramasami, *J. Am. Leath. Chem. Ass.*, 2004, **99**, pp. 157-163.

54. A. D. Covington, *Chem. Soc. Rev.*, 1997, pp. 111-126.

55. J. C. Bickley, *J. Soc. Leath. Tech. Chem.*, 1992, **76**, pp. 1-5.

56. W. C. Prentiss, C. R. Sigafoos, H. A. Tetreault, *J. Am. Leath. Chem. Ass.*, 1978, **73**, pp. 30-31

57. J. C. Bickley, *J. Soc. Leath. Tech. Chem.*, 1986, **70**, pp. 143-147.

58. E. Staisny, 50 Years: Synthetic Tannins, BASF, Ludwigshafen, Germany, 1962, pp. 1-45.

59. V. S. Sundara Rao, K. K. Reddy and Y. Nayudamma, *Leather Science*, 1971, **18**, pp. 8-16.

60. V. S. Sundara Rao, K. K. Reddy and Y. Nayudamma, *Leather Science*, 1971, **18**, pp. 43-50.

61. H. Traeubel and K. H. Rogge, *J. Am. Leath. Chem. Ass.*, 1988, **83**, pp. 193-205.

62. P. Thenikaivelan, M. Kanthimathi, J. Raghva Rao, B. Unni Nair, *J. Am. Leath. Chem. Ass.*, 2002, **97**, pp. 127-136.

63. E. M. Filachione, M. L. Fein and E. H. Harris, Jr., *J. Am. Leath. Chem. Ass.*, 1964, **59**, pp. 281-292.

64. D. T. Cheung, N. Perelman, E. C. Ko and M. E. Nimni, *Connective Tissue Research*, 1985, **13**, pp. 109-115.

65. A. Gunasekaran and K. Balasubramanian, *J. Soc. Leath. Tech. Chem.*, 1988, **72**, pp. 25-26.

66. S. Das Gupta, *J. Soc. Leath. Tech. Chem.*, 1977, **61**, pp. 97-105.

67. F. J. D. Shortland and W. C. Prentiss, *J. Soc. Leath. Tech. Chem.*, 1980, **64**, pp. 60-64.

68. S. Das Gupta, *J. Soc. Leath. Tech. Chem.*, 1979, **63**, pp. 49-54.

69. J. M. Morera, E. Bartoli, M. D. Borras and A. Marsal, *J. Soc. Leath. Tech. Chem.*, 1996, **80**, pp. 120-122.

70. W. E. Kallenberger and J. F. Hernandez, *J. Am. Leath. Chem. Ass.*, 1983, **78**, pp. 217-222.

71. N. P. Slabbert, *J. Am. Leath. Chem. Ass.*, 1981, **76**, pp. 231-244.

72. J. Goldfarb, *J. Am. Leath. Chem. Ass.*, 1999, **94**, pp. 79-83.

73. A. D. Covington, *J. Am. Leath. Chem. Ass.*, 1998, **93**, pp. 168-182.

74. W. T. Astbury, *J. Soc. Leath. Tech. Chem.*, 1940, **24**, pp. 69-92.

75. A.J. Bailey and C.A. Miles, *Chimica Sciences*, 1999, **111**, pp. 71-80.

76. C. E. Weir and J. Carter, *J. Res. Natl. Bus. Stand.*, 1950, **44**, pp. 599-609.

77. J. H. Sharphouse, *J. Soc. Leath. Tech. Chem.*, 1985, **69**, pp. 29-43.

78. T. Ramasami, *J. Am. Leath. Chem. Ass.*, 2001, **96**, pp. 290-304.

79. A. D. Covington, G. S. Lampard, R. A. Hancock and I. A. Ioannidis, *J. Am. Leath. Chem. Ass.*, 1998, **93**, pp. 107-120.

80. B. Madhan, N. N. Fathima, J. Raghava Rao, V. Subramanian, B. U. Nair and T. Ramasami, *J. Am. Leath. Chem. Ass.*, 2003, **98**, pp. 263-272.

81. G. S. Hammond, *J. Am. Chem. Soc.*, 1955, **77**, pp. 334-338.

82. W. B. Blumenthal, *The Chemical Behaviour of Zirconium*, D. Van Nostrand Company, Inc., Princeton, USA, 1958, Chapters 1 and 4-9.

83. N. N. Greenwood and A. Earnshaw, *Chemistry of the Elements*, Pergamon Press, Oxford, UK, 1984, Chapter 21.

84. http://minerals.usgs.gov/minerals/pubs/commodity/zirconium/

85. H. G. Hira, *Zirconium and Hafnium*, In: *The Mineral Resources of South Africa Handbook*, M. G. C. Wilson and C. R. Anhaeusser (Eds), Council for Geoscience **16**, 1998, pp. 682-685.

86. W. J. Verwoerd, *Mineral Deposits of Southern Africa*, C. R. Anhaeusser and S. Maske (Eds), Geological Society of South Africa, **1** and **2**, 1986, pp. 2173-2191.

87. S. G. Ampian, *Zirconium and Hafnium*, In: *Mineral Facts and Problems*. Biocentennial Edition, Bureau of Mines, Bulletin 667, United States Department of the Interior, 1975 Ed., pp. 1243-1259.

88. C. Skidmore, *Zirconium Oxides/Chemicals: A Review of Raw Materials, Markets and Future Prospects*, The 2nd South African Industrial Minerals Conference, Johannesburg, South Africa, October 1998.

89. A. Clearfield, *Rev. Pure and Appl. Chem.*, 1964, **14**, pp. 91-108.

90. W. S. Hummers, S. Y. Tyree, Jr. and S. Yolles, *Inorg. Synth.*, 1953, **4**, pp. 121-127.

91. R. C. Fay, *Zirconium and Hafnium*, In: *Comprehensive Coordination Chemistry: The Synthesis, Reactions, Properties and Applications of Coordination Compounds*, G. Wilkinson (Ed.), Pergamon Press, Oxford, UK, 1987, **3**, Chapter 32.

92. D. C. Bradley and P. Thornton, *Zirconium and Hafnium*, In: *Comprehensive Inorganic Chemistry*, A.F. Trotman-Dickenson, Pergamon Press, Oxford, UK, 1973, **3**, Chapter 33.

93. P. Woodman, P. B. Hitchcock and P. Scott, *Chem. Commun.*, 1996, pp. 2735-2736.

94. N. A. H. Male, M. Thornton-Pett and M. Bochmann, *J. Chem. Soc., Dalton. Trans.*, 1997, pp. 2487-2494.

95. A. J. Rogers, E. Solari, C. Floriani, A. Chiesi-Villa and C. Rizzoli, *J. Chem. Soc., Dalton. Trans.*, 1997, pp. 2385-2386.

96. L. Singh, A. K. Manglik and N. P. Dhaka, *Asian J. Chem.*, 1997, **9**, pp. 831-836.

97. G. I. Nikonov, A. J. Blake and P. Mountford, *Inorg. Chem.*, 1997, **36**, pp. 1107-1112.

98. M. T. H. Tarafder and A. R. Khan, *J. Indian Chem. Soc.*, 1997, **74**, pp. 489-491.

99. J. A. Cronin, S. M. Palmer and R. D. Archer, *Inorg. Chim. Acta*, 1996, **251**, pp. 81-87.

100. B-J. Deelman, P. B. Hitchcock, M. F. Lappert, H-K Lee and W-P Leung, *J. Organomet. Chem.*, 1996, **513**, pp. 281-285.

101. H. Mack and M. S. Eisen, *J. Organomet. Chem.*, 1996, **525**, pp. 81-87.

102. F-C Wu and S-C Yu, *J. Mater. Sci.*, 1990, **25**, pp. 970-976.

103. T. E. Macdermott, *Coord. Chem. Rev.*, 1973, **11**, pp. 1-20.

104. R. P. Planalp and R. A. Andersen, *J. Am. Chem. Soc.*, 1983, **105**, pp. 7774-7775.

105. V. A. Potyomkin and Y. I. Sukharev, *Chem. Phys.*, 2003, **371**, pp. 626-633.

106. A. Veyland, L. Dupont, J. C. Pierrard, J. Rimbault and M. Aplincourt, *Eur. J. Inorg. Chem.*, 1998, pp. 1765-1770.

107. L. M. Zaitsev, *Russ. J. Inorg. Chem.*, 1966, **11**, pp. 900-904.

108. S. Hannane, F. Bertin and J. Bouix, *Bull. Soc. Chim. Fr.*, 1990, **127**, pp. 43-49.

109. D. H. Devia and A. G. Sykes, *Inorg. Chem.*, 1981, **20**, pp. 910-913.

110. J. R. Fryer, J. L. Hutchison and R. Paterson, *J. Colloid Interface Sci.*, 1970, **34**, pp. 238-248.

111. M. A. K. Ahmed, H. Fjellvåg and A. Kjekshus, *Acta Chem. Scand.*, 1999, **53**, pp. 24-33.

112. F. G. R. Gimblett, A. Hussain and K. S. W. Sing, *J. Therm. Anal.*, 1988, **34**, pp. 1001-1013.

113. L. A. Pospelova and L. M. Zaitsev, *Russ. J. Inorg. Chem.*, 1966, **11**, pp. 995-1004.

114. M. Y. Reza, H. Matsushima, M. Koikawa, N. Nakashima and T. Tokii, *Bull. Chem. Soc. Jpn*, 1998, **71**, pp. 155-160.

115. D. C. Bradley, R. C. Mehrotra and W. Wardlaw, *J. Chem. Soc.*, 1952, pp. 2027-2032, pp. 4204-4209, pp. 5020-5023.

116. F. Rubio, J. Rubio and J. L. Oteo, *J. Mater. Sci. Lett.*, 1998, **17**, pp. 1839-1842.

117. G. Kickelbick and U. Schubert, *J. Chem. Soc., Dalton Trans.*, 1999, pp. 1301-1305.

118. B. P. Straughan, W. Moore and R. McLaughlin, *Spectrochim. Acta, Part A*, 1986, **42**, pp. 451-456.

119. C. M. Stables and H. Sutcliffe, *J. Therm. Anal.*, 1988, **34**, pp. 963-973.

120. P. Spacu, M. Brezeanu, L. Patron, A. Contescu, D. Crisan and E. Segal, *Thermochim. Acta*, 1991, **178**, pp. 231-239.

121. E. M. Larsen and E. H. Homeier, *Inorg. Chem.*, 1972, **11**, pp. 2687-2692.

122. J-L Tosan, B. Durand, M. Roubin, F. Chassagneux and F. Bertin, *J. Non-Cryst. Solids*, 1994, **168**, pp. 23-32.

123. G. R. Willey, T. J. Woodman and M. Fisher, *Transition Met. Chem.*, 1998, **23**, pp. 467-471.

124. W. Brzyska and P. Sadowski, *Pol. J. Chem.*, 1984, **58**, pp. 669-674.

125. J. Etienne, A. Larbot, C. Guizard, L. Cot and J. A. Alary, *J. Non-Cryst. Solids*, 1990, **125**, pp. 224-229.

126. L. M. Zaitsev and G. S. Bochkarev, *Russ. J. Inorg. Chem.*, 1962, **7**, pp. 802-806.

127. R. N. Kapoor and R. C. Mehrotra, *J. Am. Chem. Soc.*, 1958, **80**, pp. 3569-3573.

128. A. K. Mukherji, *Analytical Chemistry of Zirconium and Hafnium*, In: *International Series of Monographs in Analytical Chemistry*, R. Belcher and M. Frieser (Eds), Pergamon Press, Oxford, UK, 1970, **40**, Chapters 1 and 4-7.

129. R. B. Hahn and L. Weber, *J. Am. Chem. Soc.*, 1955, **77**, pp. 4777-4779.

130. W. J. Evans, M. A. Ansari and J. W. Ziller, *Polyhedron*, 1998, **17**, pp. 299-304.

131. T. J. Pinnavaia and R. C. Fay, *Inorg. Chem.*, 1968, **7**, pp. 502-507.

132. R. C. Fay and T. J. Pinnavaia, *Inorg. Chem.*, 1968, **7**, pp. 508-514.

133. Y. Chi, J-W Lan, W-L Ching, S-M Peng and G-H Lee, *J. Chem. Soc., Dalton Trans.*, 2000, pp. 2923-2927.

134. D. M. Palmer, B. P. Straughan and J. A. Treverton, *Appl. Surf. Sci.*, 1993, **68**, pp. 243-250.

135. S. Katsuta and H. Yanagihara, *Solvent Extr. Ion Exch.*, 1997, **15**, pp. 577-589.

136. L. M. Zaitsev and G. S. Bochkarev, *Russ. J. Inorg. Chem.*, 1962, **7**, pp. 411-414.

137. C. E. Holloway, I. M. Walker and M. Melnik, *Rev. Inorg. Chem.*, 1986, **8**, pp. 169-219.

138. L. A. Zeiss and E. W. Giesekke, *S. Afr. J. Chem.*, 1997, **50**, pp. 136-143.

139. M. Chatterjee, J. Ray, A. Chatterjee and D. Ganguli, *J. Mater. Sci. Lett.*, 1989, **8**, pp. 548-550.

140. E. E. Platero, M. P. Mentruit, C. O. Arean and A. Zecchina, *J. Catal.*, 1996, **162**, pp. 268-276.

141. F. Farnworth, S. L. Jones and I. McAlpine, *Spec. Pub. - R. Soc. Chem.*, 1981, **40**, pp. 248-284.

142. B. W. Wolff, *J. Korea Tappi.*, 1995, **27**, pp. 92-97.

143. L. B. Cohen, *Polym. Paint Colour J.*, 1987, **177**, pp. 868-899.

144. I. C. Somerville, *J. Am. Leath. Chem. Ass.*, 1942, **37**, pp. 381-390.

145. H. G. Turley and I. C. Somerville, *J. Am. Leath. Chem. Ass.*, 1942, **37**, pp. 391-397.

146. I. C. Somerville and H. G. Turley, *J. Am. Leath. Chem. Ass.*, 1943, **38**, pp. 326-332.

147. I. C. Somerville and H. G. Turley, *J. Am. Leath. Chem. Ass.*, 1948, **43**, pp. 345-351.

148. I. C. Somerville and W. J. Rau, *J. Am. Leath. Chem. Ass.*, 1949, **44**, pp. 784-795.

149. I. C. Somerville and J. Wendkos, *J. Am. Leath. Chem. Ass.*, 1952, **47**, pp. 687-700.

150. I. C. Somerville and W. J. Rau, *J. Am. Leath. Chem. Ass.*, 1956, **51**, pp. 542-555.

151. K. H. Gustavson, *Sven. Kem. Tidskr.*, 1958, **70**, pp. 367-378.

152. T. S. Ranganathan and R. Reed, *J. Soc. Leath. Tech. Chem.*, 1958, **42**, pp. 59-62.

153. T. S. Ranganathan and R. Reed, *J. Soc. Leath. Tech. Chem.*, 1958, **42**, pp. 351-359.

154. T. S. Ranganathan and R. Reed, *J. Soc. Leath. Tech. Chem.*, 1958, **42**, pp. 205-210.

155. J. P. Lassere, *Bull. Ass. Franc. Chim. Ind. Cuir*, 1950, **12**, pp. 143-160.

156. B. A. J. Lister, and L. A. McDonald, *J. Chem. Soc.*, 1952, pp. 4315-4330.

157. A. L. Hock, *J. Soc. Leath. Tech. Chem.*, 1975, **59**, pp. 181-188.

158. D. A. Williams-Wynn, *J. Soc. Leath. Tech. Chem.*, 1958, **42**, pp. 360-368.

159. D. A. Williams-Wynn, *J. Soc. Leath. Tech. Chem.*, 1959, **43**, pp. 76-82.

160. D. A. Williams-Wynn, *J. Phys. Chem.*, 1959, **63**, pp. 2065-2066.

161. D. A. Williams-Wynn and R. L. Sykes, *J. Soc. Leath. Tech. Chem.*, 1960, **44**, pp. 23-32.

162. D. A. Williams-Wynn, *J. Soc. Leath. Tech. Chem.*, 1960, **44**, pp. 405-418.

163. R. L. Sykes and D. A. Williams-Wynn, *J. Soc. Leath. Tech. Chem.*, 1961, **45**, pp. 83-92.

164. A. R. Babich and Y. G. Shapilskaya, *Kosk. Obuv. Prom.*, 1970, **12**, pp. 26-30.

165. K. C. Montgomery, *J. Soc. Leath. Tech. Chem.*, 1992, **76**, pp. 39-46.

166. I. F. Poletaev, V. I. Sokolov, V. S. Smukovich, N. A. Shostenko, L. I. Romanova and S. V. Pichugin, *Russian Patent. (SU 90-4836680 19900611)*, Abstract cited in *J. Am. Leath. Chem. Ass.*, 1994, **89**, pp. 147.

167. C. Gaidau, F. Platon and M. Popescu, *IULTCS Congress Proceedings*, 1997, pp. 328-335.

168. A. Sundarrajan, B. Madhan, J. Raghava Rao, and B. Unni Nair, *J. Am. Leath. Chem. Ass.*, 2003, **98**, pp. 101-106.

169. B. Madhan, A. Sundarrajan, J. Raghava Rao and B. U. Nair, *J. Am. Leath. Chem. Ass.*, 2003, **98**, pp. 107-114.

170. N. N. Fathima, M. Balaraman, J. Raghava Rao and B. Unni Nair, *J. Inorg. Biochem.*, 2003, **95**, pp. 47-54.

171. J. Holmes, *J. Soc. Leath. Tech. Chem.*, 1996, **80**, pp. 133-135.

172. K. J. Sreeram, M. Kanthimathi, J. Raghava Rao, R. Sundaram, B. Unni Nair and T. Ramasami, *J. Am. Leath. Chem. Ass.*, 2000, **95**, pp. 324-332.

173. K. J. Sreeram, J. Raghava Rao, B. Unni Nair and T. Ramasami, *J. Am. Leath. Chem. Ass.*, 2000, **95**, pp. 359-367.

174. B. B. Corson, R. A. Dodge, S. A. Harris and J. S. Yeaw, *Org. Synth., Collective Volume I*. H. Gilman and A. H. Blatt (Eds), John Wiley and Sons Inc., New York, 1944, 2nd Ed., pp. 336-340.

175. D. D. Perrin and W. L. F. Armarego, *Purification of Laboratory Chemicals*, Pergamon Press, Oxford, 1988, 3rd Ed., pp. 60-61.

176. J. March, *Advanced Organic Chemistry: Reactions, Mechanisms and Structure*, Wiley-Interscience, New York, USA, 1992, 4th Ed., pp. 327-330.

177. T. J. Collopy and J. J. Klingenberg, *J. Inorg. Nucl. Chem.*, 1961, **18**, pp. 184-191.

178. A. K. Mukherji, *Anal. Chem.*, 1964, **36**, pp. 1064-1066.

179. J. D. Roberts and M. C. Caserio, *Basic Principles of Organic Chemistry*, W. A Benjamin, Inc., New York, USA, 1979, 2nd Ed., Chapters 15, 18 and 26.

180. R. Lanzetta, A. Mancino, B. Naviglio, M. Parrili, M. Tomaselli and G. Tortora, *Cuoio Pelli, Materie Concianti*, 2000, **76**, pp. 325-334.

181. F. A. Cotton and G. Wilkinson, *Advanced Inorganic Chemistry*, Wiley-Interscience, New York, USA, 1980, 4th Ed., pp. 824-831.

182. H. Iwahashi, *Biochem. J.*, 2000, **346**, pp. 265-273.

183. J. L. Domingo, A. Ortega, J. M. Llobet and J. Corbella, *Fundam. Appl. Toxicol.*, 1990, **14**, pp. 88-95.

184. H. T. F. Rhodes, *Chemistry & Industry*, 1940, **59**, pp. 143-145.

185. K. Nakamoto, *Infrared and Raman Spectra of Inorganic and Coordination Compounds*, Wiley-Interscience, New York, USA, 1986, 4th Ed.

186. P. Schwendt, P. Švančárek, I. Smatanová and J. Marek, *J. Inorg. Biochem.*, 2000, **80**, pp. 59-64.

187. R. B. Hahn and P. T. Joseph, *J. Am. Chem. Soc.*, 1957, **79**, pp. 1298-1301.

188. M. Kurosu and M. Lorca, *J. Org. Chem.*, 2001, **66**, pp. 1205-1209.

189. H. Itoh, N. Itoh and Y. Suzuki, *Bull. Chem. Soc. Jpn*, 1984, **57**, pp. 716-718.

190. P. Peralta-Zamora and J. W. Martins, *Talanta*, 1999, **49**, pp. 937-941.

191. S. P. Arya and V. Slathia, *Indian J. Chem., Sect. A*, 1988, **27**, pp. 463-464.

192. S. Kalyanaraman and T. Fukasawa, *Anal. Chem.*, 1983, **55**, pp. 2239-2241.

193. T. V. Ramakrishna and M. S. Subramanian, *Bull. Chem. Soc. Jpn*, 1983, **56**, pp. 321-325.

194. H. H. Willard, L. L. Merritt, Jr, J. A. Dean and F. A Settle, Jr, *Instrumental Methods of Analysis*, Wadsworth Publishing Company, Belmont, USA, 1988, 7th Ed., pp. 224-255.

195. L. J. Stephens, *J. Soc. Leath. Tech. Chem.*, 1987, **71**, pp. 10-11.

196. E. S. Pilkington and W. Wilson, *Anal. Chim. Acta*, 1965, **33**, pp. 577-585.

197. N. B. Colthup, L. H. Daly and S. E. Wiberley, *Introduction to Infrared and Raman Spectroscopy*, Academic Press Inc., Boston, USA, 1964, 3rd Ed.

198. H. Gunzler and H-U Gremlich, *Infrared Spectroscopy: An Introduction*, Wiley-VCH, Weinheim, Germany, 2002.

199. F. R. Dollish, W. G. Fateley and F. F. Bentley, *Characteristic Raman Frequencies of Organic Compounds*, John Wiley and Sons, New York, USA, 1974.

200. N. L. Alpert, W. E. Keiser and H. A. Szymanski, *Infrared Theory and Practice of Infrared Spectroscopy*, Plenum Press, New York, USA, 1964, 2nd Ed.

201. G. Varsányi and S. Zöke, *Vibrational Spectra of Benzene Derivatives*, Academic Press, New York, USA, 1969.

202. K. Nakamoto and J. P. McCarthy, *Spectroscopy and Structure of Metal Chelate Compounds*, John Wiley and Sons, New York, USA, 1968.

203. A. Fischinger, A. Sarapu and A. Companion, *Can. J. Chem.*, 1969, **47**, pp. 2629-2637.

204. G. B. Deacon and R. J. Phillips, *Coord. Chem. Rev.,* 1980, **33**, pp. 227-250.

205. P. V. Khadikar, R. L Ameria, M. G. Kekre and S. D. Chauhan, *J. Inorg. Nucl. Chem.,* 1973, **35**, pp. 4301-4304.

206. G. B. Deacon, F. Huber and R.J. Phillips, *Inorg. Chim. Acta*, 1985, **104**, pp. 41-45.

207. J. D. S. Goulden, *Spectrochim. Acta, Part A*, 1960, **16**, pp. 715-720.

208. K. Nakamoto, P. J. McCarthy and B. Miniatas, *Spectrochim. Acta,Part A*, 1965, **21**, pp. 379-388.

209. D. W. Herlocker, R. S. Drago and V. I. Meek, *Inorg. Chem.*, 1966, **5**, pp. 2009-2015.

210. H. Shindo, *Chem. Pharm. Bull.*, 1958, **6**, pp. 117-129.

211. S. I. Shupack and M. Orchin, *J. Am. Chem. Soc.*, 1973, **95**, pp. 103-104.

212. S. Ehrenson, R. T. C. Brownlee and R. W. Taft, *Prog. Phys. Org. Chem.*, 1973, **10**, pp. 1-80.

213. C. G. Swain and E. C. Lupton, Jr., *J. Am. Chem. Soc.*, 1968, **90**, pp. 4328-4337.

214. Y. Yukawa, Y. Tsuno and M. Sawada, *Bull. Chem. Soc. Jpn*, 1966, **39**, pp. 2274-2286.

215. T. Auf der Heyde, G. A. Foulds, D. A. Thornton and G. M. Watkins, *Spectrosc. Lett.*, 1981, **14**, pp. 455-462.

216. J. J. MacDougall, L. C. Nathan and J. H. Nelson, *Inorg. Chim. Acta*, 1976, **17**, pp. 243-246.

217. J. M. Haigh and D. A. Thornton, *J. Mol. Struct.*, 1971, **8**, pp. 351-361.

218. G. C. Percy and D. A. Thornton, *Inorg. Nucl. Chem. Lett.*, 1971, **7**, pp. 599-604.

219. D. A. Thornton, *Chem. Rev.*, 1990, **104**, pp. 173-249.

220. P. Vassileva, I. Binev and I. Juchnovski, *Spectrochim. Acta, Part A*, 1983, **39**, pp. 709-712.

221. N. Mori, Y. Asano, T. Irie and Y. Tsuzuki, *Bull. Chem. Soc. Jpn*, 1969, **42**, pp. 482-487.

222. F. van Meurs, J. M. A. Baas and W. van Bekkum, *J. Organomet. Chem.*, 1977, **129**, pp. 347-360.

223. B. M. Wepster, *J. Am. Chem. Soc.*, 1973, **95**, pp. 102-104.

224. C. Huh, C. H. Kang, H. W. Lee, H. Nakamura, M. Mishima, Y. Tsuno and H. Yamataka, *Bull. Chem. Soc. Jpn*, 1999, **72**, pp. 1083-1091.

225. M. Mishima, M. Fujio and Y. Tsuno, *Bull. Chem. Soc. Jpn*, 1996, **69**, pp. 2009-2018.

226. R. W. Taft, J. L. M. Abboud, F. Anvia, M. Berthelot, M. Fujio, J-C. Gal, A. D. Headley, W. G. Henderson, I. Koppel, J. H. Qian, M. Mishima, M. Taagepera and S. Ueji, *J. Am. Chem. Soc.*, 1988, **110**, pp. 1797-1800.

227. J. L. M. Abboud, J. Catalan, J. Elguero and R. W. Taft, *J. Org. Chem.*, 1988, **53**, pp. 1137-1140.

228. C. D. Johnson, *J. Org. Chem.*, 1978, **43**, pp. 1814-1815.

229. G. Micera, D. Sanna, A. Dessi, T. Kiss and P. Buglyo, *Gazz. Chim. Ital.*, 1993, **123**, pp. 573-577.

230. P. H. Rieger and R. R. Reeder, *Inorg. Chem*., 1971, **10**, pp. 1258-1264.

231. R. L. Pecsok and J. Sandera, *J. Am. Chem. Soc.*, 1955, **77**, pp. 1489-1494.

232. N. A. Kostromina, *Zh. Neorg. Khim.*, 1966, **11**, pp. 2340-2346, CAN 66:6077.

233. B. N. Zaitsev, V. M. Nikolaev and V. V. Shalimov, *Radiokhimiya*, 1975, **17**, pp. 284-287, CAN 83:489800.

234. L. N. Sheronov and B. V. Ptitsyn, *Zh. Neorg. Khim.*, 1959, **4**, pp. 367-371, CAN 53:93474.

235. R. C. Warner and I. Weber, *J. Am. Chem. Soc.*, 1953, **75**, pp. 5086-5094.

236. R. Belcher, A. Sykes and J. C. Tatlow, *Anal. Chim. Acta*, 1954, **10**, pp. 34-47.

237. R. E. Oesper and J. J. Klingenburg, *Anal. Chem.*, 1949, **21**, pp. 1509-1511.

238. R. B. Hahn and E. S. Baginski, *Anal. Chim. Acta*, 1956, **14**, pp.45-47.

239. A. D. Covington and B. Shi, *J. Soc. Leath. Tech. Chem.*, 1998, **82**, pp. 64-71.

240. A. D. Covington and B. Shi, *J. Soc. Leath. Tech. Chem.*, 1999, **83**, pp. 8-13.

241. J. J. Van Benschoten, D. G. Tasset, R. Eversole and W. E. Kallenberger, *J. Am. Leath. Chem. Ass.*, 1985, **80**, pp. 237-242.

242. G. Goissis, E. Marcantonio, Jr., R. A. C. Marcantonio, R. C. C. Lia, D. C. J. Cancian and W. M. de Carvalho, *Biomaterials*, 1999, **20**, pp. 27-34.

243. J. H. Muyonga, G. C. B. Cole and K. G. Duodu, *Food Chem.*, 2004, **86**, pp. 325-332.

244. R. McDonald (Ed.), *Colour Physics for Industry*, Society of Dyers and Colourists, Bradford, UK, 1997, Chapter 4.

245. D. L. Randall, *J. Am. Leath. Chem. Ass.*, 1994, **89**, pp. 309-319.

APPENDIX 1:

BEAMHOUSE PROCESSING OF DRIED GOATSKIN

Raw Material: Dry salted goatskin
Soaking and Liming: Masses based on dry weight
All following processes: Masses based on limed weight
_____ Indicates to drain float

Process	%	Chemical	Time	Temp	Comments
Static Soak	400 0.2	water soaking aid	 4 hr	RT	ensure skins are covered
Main Soak	200	water soaking aid	 4 hr	RT	 drum 1 hr (3 rpm) drum 15' every hr (3 rpm)
Liming	100 1 3 3 100	water liming aux. lime sod. sulfide water	 15 min 1 hr 15 hr	RT RT	 (3 rpm) (3 rpm) drum 15' every hr (3 rpm)
Wash	150	water	15 min	RT	(3 rpm)
Flesh Wash	150	water	15 min	35ºC	(8 rpm)
Delime	3 0.5	amm. sulfate sod. metabisulfite	 90 min		 (8 rpm) phenolphthalein
Bate	50 1	water pancreatic bate	 4 hr	38ºC	 (8 rpm)
Pickle	50 6 1 2	water salt sod. formate sulfuric acid	 15 min 2 hr	RT	 Bé = 6 dilute 1:10 (8 rpm) bromocresol green

APPENDIX 2:

CRUSTING PROCESS OF TANNED MATERIAL

Raw Material: Wet blue and zirconium tanned goatskin
All masses are based on weight of tanned material
_____ Indicates to drain float

Process	%	Chemical	Time	Temp	Comments
Wet Back	300	water		40ºC	
	0.5	wetting aid	15 min		check rehydration (10 rpm)
Neutralisation	150	water		40ºC	
	1.5	Coralon® OT	15 min		
	1	amm. bicarb.	30 min		pH 5.5-6.0 bromocresol green
Dye	4	acid dye	30 min		check cut
	80	water		60ºC	
Fatliquor	5	Derminol® OS-1			
	5	Trupon® DB	60 min		dilute (1:4) and blend pH 5.5-6.0
Fix	1.5	formic acid	30 min		3 additions of 0.5 pH 3.6-3.8
Wash	300	water	5 min	60ºC	horse-up slick and allow to dry